

This item was submitted to [Loughborough's Research Repository](#) by the author.
Items in Figshare are protected by copyright, with all rights reserved, unless otherwise indicated.

Effects of physical parameters in mashing on lautering performance

PLEASE CITE THE PUBLISHED VERSION

PUBLISHER

© T.M. Buhler

PUBLISHER STATEMENT

This work is made available according to the conditions of the Creative Commons Attribution-NonCommercial-NoDerivatives 4.0 International (CC BY-NC-ND 4.0) licence. Full details of this licence are available at:
<https://creativecommons.org/licenses/by-nc-nd/4.0/>

LICENCE

CC BY-NC-ND 4.0

REPOSITORY RECORD

Buhler, Thomas M.. 2015. "Effects of Physical Parameters in Mashing on Lautering Performance". figshare.
<https://hdl.handle.net/2134/16925>.

BLDSC no: - 0X231428



Pilkington Library

Author/Filing Title BUHLER, T.M.

Accession/Copy No.

040129839

Vol. No.

Class Mark

11 JUL 2000

LOAN COPY

0401298396



Effects of Physical Parameters in Mashing on Lautering Performance

by

Thomas Martin Bühler

A Doctoral Thesis


Submitted in partial fulfilment of the requirements

for the award of

Doctor of Philosophy of Loughborough University

1. October 1996

© by T.M. Bühler 1996

 Loughborough University	
Date: <u>Apr 97</u>	
Class:	
Acc	
No.	040129839

99103463

Table of Contents.....	i
Abstract.....	vi
Acknowledgement.....	vii
1. Introduction.....	1
1.1. Background	1
1.2. Introduction and Objectives.....	1
2. Literature Survey	3
2.1. Introduction.....	3
2.2. Brewhouse Operations.....	3
2.2.1. Raw Materials and their Influence on Lautering	3
2.2.2. Milling.....	5
2.2.3. Mashing in Procedure (Pre masher design)	7
2.2.4. Mashing	9
2.2.4.1. Effects of Proteins on Lautering Performance.....	10
2.2.4.2. Effects of Polyphenols on Lautering Performance.....	14
2.2.4.3. Carbohydrate Material and Influences on Filterability of Mash	14
2.2.5. Lautering Technique	17
2.2.5.1. The Lauter Tun Operation - Effects on Performance.....	18
2.2.5.2. Lauter Tun Operation - Influences on Beer Quality	20
2.3. Mechanical Forces and their Effects on Mashing and Lautering	21
2.4. The Impact of Agitation on Oxygen Uptake.....	22
2.5. Effects of Increased Stirring Rates.....	23
2.6. Unit Operations in the Brewhouse.....	27
2.6.1. Theory of Mashing	27
2.6.1.1. Reaction Kinetics	27
2.6.1.2. Mixing and Agitation.....	28
2.6.1.3. Shear in Fluids	31
2.6.2. Aspects of Filtration	32
2.6.3. Sedimentation.....	33
2.6.3.1. Sedimentation Curve	34

2.6.3.2. Reduced Settling in Closed Systems.....	35
2.6.3.3. Sedimentation Model	36
2.6.3.4. Compaction of Sediment.....	37
2.6.4. Cake Filtration.....	38
2.6.4.1. Compressible Cake Filtration.....	43
2.6.4.2. Compressible Cake Filtration with Simultaneous Sedimentation.....	45
2.6.5. Blockage Filtration	46
2.6.6. Washing of the Spent Grains Cake	47
2.7. Discussion.....	51
3. Materials and Methods	54
3.1. Raw Materials.....	54
3.1.1. Malt	54
3.1.2. Water	56
3.2. Equipment and Plants	57
3.2.1. Pilot Mashing Equipment.....	57
3.2.1.1. Mashing-In	61
3.2.2. Pilot Lautering Rig	62
3.2.2.1. Design Specification	64
3.2.2.2. Calibration Procedure	66
3.2.3. Bench Scale Mashing	67
3.2.3.1. Torque Measurement in Laboratory Scale Mashing Trials.....	69
3.2.3.2. Data Processing.....	70
3.2.3.3. Calculation of Shear Rates	71
3.2.4. Bench Scale Mash Filterability Test.....	72
3.2.4.1. Background.....	73
3.2.4.2. Information Content	73
3.2.4.3. Apparatus/Material.....	74
3.2.4.4. Operation	75
3.2.4.5. Processing of Results	75
3.2.4.6. Accuracy of Analysis.....	76
3.3. Brewing Procedures	77
3.3.1. Milling.....	77
3.3.2. Mashing	77
3.3.2.1. Process Routine.....	79
3.3.3. Lautering.....	80

3.3.3.1. Process Routine.....	81
3.4. Analyses.....	83
3.4.1. Viscosity Analysis	83
3.4.1.1. Measuring Principle	83
3.4.1.2. Calibration Constant of the Glass Ball:	84
3.4.1.3. Analysis Procedure	85
3.4.2. Filtrate Turbidity Analysis	85
3.4.3. Coulter Counter, LS130	86
3.4.3.1. Diffraction Sizing	86
3.4.3.2. Measurement.....	86
3.4.3.3. Determining the Size Distribution.....	87
3.4.3.4. PIDS Sizing.....	88
3.4.3.5. Data Processing.....	89
3.4.3.6. Sample Preparation for the Laser Sizer	90
3.4.4. Coulter Multisizer II	90
3.4.5. Statistical Evaluation of Data	91
3.4.6. Wet Sieving of Mash.....	92
3.4.7. Scanning Electron Micrographs.....	92
3.4.8. Other Physical and Chemical Analyses	92
3.5. Conclusion.....	93
4. Results and Discussion	95
4.1. Initial Trials	95
4.1.1. Adjusting the Gap Setting of the Laboratory Mill	95
4.1.2. Effect of Different Grinding Systems on Fine Malt Particles.....	99
4.1.3. Comparability of Different Particle Sizing Methods.....	100
4.1.4. Properties of Spent Grains Cake Layers	103
4.1.4.1. Particles and Size Distributions in the Spent Grains Cake	104
4.1.4.2. Permeability of the Spent Grains Cake Layers	106
4.1.5. Change of Particle Size Distribution of the Fines during Mashing	108
4.1.6. Density of Fine Mash Particles	110

4.1.7. Viscosity of Mash	111
4.1.7.1. Viscosity Change During Mashing	111
4.1.7.2. Effect of Temperature on Viscosity	113
4.1.8. Industrial Scale Power Input	114
4.2. Agitation Pilot Scale Trials	117
4.2.1. Valve Trials	117
4.2.1.1. Introduction - Aims	117
4.2.1.2. Results	118
4.2.1.3. Conclusions	125
4.2.2. Orifice Trials	126
4.2.2.1. Aims	126
4.2.2.2. Results	128
4.2.2.3. Conclusion	128
4.2.2.4. Reproducibility Test	129
4.2.3. Effect of Stirring on Mash Filtration Performance - Laboratory Scale Trials	131
4.2.3.1. Introduction	131
4.2.3.2. Aims	132
4.2.3.3. Results	132
4.2.3.4. Conclusion	140
4.3. Effects of Final Mashing Temperatures on Lautering Performance	141
4.3.1. Introduction	141
4.3.1.1. Aims	142
4.3.1.2. Experimental	143
4.3.1.3. Results	143
4.3.1.4. Conclusion	154
4.3.1.5. Applicability to Lautering and Practical Mashing	155
4.4. Particle Size Changes in the Fine Fraction of Mash and the Effects on Lautering Performance	157
4.4.1. Aim	157
4.4.2. Results and Discussion	157
4.5. Overall Conclusions	160
5. Modelling of the Lautering Process	161
5.1. Description of the Process	161
5.1.1. The Effect of Temperature on MPS	161

5.1.2. Effect of Temperature on Viscosity of the Liquid Phase of Mash	162
5.1.3. Sedimentation - The Cake Height after Settling	165
5.1.4. Final Permeability of the Cake	167
5.1.5. Effect of Pressure on the Final Cake Height.....	169
5.1.6. Compaction of the Cake over Filtrate Volume	171
5.1.7. Effects of Cake Height on Permeability	173
5.1.8. Change of Extract with Time - Cake Washing	176
5.2. A Computer Model describing Lautering	182
5.2.1. Development of the Computer Model	182
5.2.2. Predicting Lautering Performance with the Model	190
5.3. Conclusions.....	195
6. Conclusion.....	195
6.1. General Comments and Overall Conclusions	195
6.2. Implications on Industrial Brewing Practice	196
7. Appendix.....	198
7.1. Nomenclature	198
7.2. References	206
7.3. Glossary of Brewing Terms	215
7.4. Table of Figures	221
7.5. Pictures and Electron Micrographs.....	229
7.6. Publications	245

Abstract

This thesis investigates performance parameters of unit operations in the brewery. It describes effects of the parameters temperature and agitation during mashing on mash properties. Mainly two properties are influenced by these parameters, the viscosity and the particle size distribution in the fines. It could be shown that both factors have significant influence on filterability of mash.

In pilot scale and laboratory trials particle size effects in mash were investigated systematically. The importance of fine particles for lautering performance could be confirmed and quantified.

The precipitation and aggregation of fine particles with increasing temperatures in the mash could be monitored for the first time. It could be shown that this parameter is not malt dependent. Mashes from different malts react in the same way. In laboratory trials it could be proved that the particle size parameter is more important than viscosity for filterability of mash.

The parameters described above have been quantified and correlated with mash filtration parameters. This work provided a basis for the development of a computer model which describes mash separation in a lauter tun.

Acknowledgement

This thesis was carried out at the Process Innovation Department of BRF International, Nutfield, England. I would like to thank all staff at BRF International for their support during the experimental phase of this work and the Director General for his permission to register and the financial support. Special thanks to Steve Garland and Graham Gasson who manufactured and assembled the pilot scale mashing and lautering plant.

I would also like to thank Dr Malcolm McKechnie, Head of Process Innovation, who waved many of the practical difficulties during this thesis and Professor Charlie Bamforth, Director of Research, who made it possible to register for a part time PhD. It was on Dr McKechnie's recommendation that Professor Wakeman accepted the supervisory task.

Further, I would like to thank Professor Wakeman for his excellent supervision and guidance during the various phases of this thesis. The meetings with Professor Wakeman and Dr McKechnie at Exeter and Loughborough enabled to re-focus on the aims of this thesis and made it possible to develop solutions to various scientific and practical problems.

Last-but-not-least I wish to thank my wife Almut for all the patience and understanding she has shown during our separation, and particularly during the write-up at Unna.

Unna, September 1996

1. Introduction

1.1. Background

This PhD Thesis was conducted as a part time research programme and was supervised by Prof. Richard Wakeman (Exeter University and later Loughborough University) and Dr. Malcolm McKechnie, Head of Process Innovation was the external supervisor at BRF International (Brewing Research Foundation). The experimental part of the programme was carried out in part as a core research project of the Process Innovation Department at BRF International, Nutfield, Great Britain. The basic subject of this thesis was proposed by industrial members of the Process Innovation panel meeting in April 1992. The main objective of the project was to investigate effects of agitation during mashing on wort filtration.

With the support of the Head of Department, Dr McKechnie, it was possible to register with this project for a part time PhD at the School of Engineering at Exeter University. The objectives of this work were adapted by Professor Wakeman and Dr McKechnie to make it suitable for a postgraduate research subject. In summer 1995 Prof. Wakeman moved to Loughborough University to take a Chair of Chemical Engineering. At this time, registration was transferred to Loughborough University.

1.2. Introduction and Objectives

This work investigates the effects of processing conditions during mashing on lautering performance. In beer brewing these two operations are important for obtaining a suitable wort for good fermentation and for a high quality beer. Both steps have crucial influence on the yield of the total brewing process and on the overall performance in the brewhouse. Due to this importance there has always been great interest in the brewing industry to improve the knowledge base for these unit operations.

The following objectives were determined for this thesis:-

1. Investigation of effects of agitation on mash properties. Agitation due to stirring and pumping could have various effects on the composition of a mash. Soluble material from malt grist could be extracted to different extents due to variations in mass transfer, due to forces

acting on the particles or due to enhanced enzymatic reactions. The leaching of such soluble material could affect viscosity in a mash. Particle attrition, due to mechanical forces would result in reduction of the particle size distribution of a mash.

Both parameters, viscosity and particle size distribution, would influence the filtration process in the lauter tun. The extent to which these effects are combined in mashing and lautering and which of these effects would be predominant should be clarified.

To make this work relevant for industry, the agitation levels in industrial mashing should be determined and trials should use similar range agitation levels.

This work should determine the influence of temperature on a change of particle size distribution due to precipitation. Temperature in mashing and lautering varies and this variation could affect the precipitation of proteinaceous material.

2. It was also planned to develop a model for lautering. This would require experimental data which is suitable for scale-up. Therefore, it would be necessary to develop a pilot scale system which works under similar conditions as the large scale plant.

In a computer model the different variables and effects on lautering should be combined and quantified to enable prediction of these process parameters.

As a starting point, a literature search should help to select suitable experimental process conditions and to develop a suitable experimental programme for the thesis.

2. Literature Survey

2.1. Introduction

The first part of this literature survey describes the operational steps in the brewhouse such as milling, mashing and lautering. Parameters known to affect the performance of the filtration step will be described. This will help to establish standardised conditions during the experimental phase of this study. In addition, influences of preceding processing steps (milling and mashing) and other effects (such as raw materials) on mash separation performance will be determined and described.

As it will be part of this work to investigate the role of agitation on filtration performance, the effects which could play a role will be explored in detail. The biochemistry of these operations is a major factor in this. However, little information on mechanical and particle size effects on filtration performance has been found in published literature. In the second part of the survey, the theory of mashing and lautering will be described from an engineering point of view.

In order to improve the understanding of the operations in the brewhouse, the following flow diagram gives an overview and describes the functions of each step (Figure 2.1). The special terminology used in brewing is explained in the glossary, at the end of this work.

2.2. Brewhouse Operations

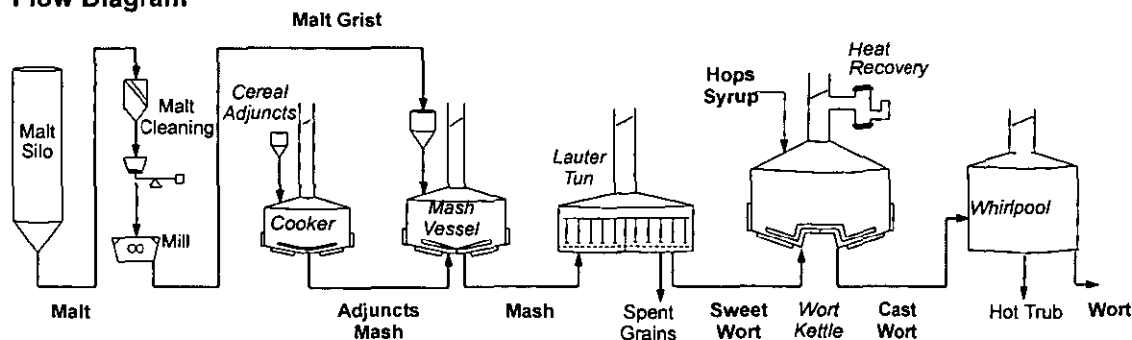
This chapter describes the operations milling, mashing and lautering with a detailed view of their effects on filtration performance. A short discussion on the effects derived from raw materials is presented first.

2.2.1. Raw Materials and their Influence on Lautering

Malt modification and use of adjuncts are very important for mash composition and run off rate. Webster (1981) found that poorly modified malts give high wort viscosities and produce large amounts of fine particles. Different concentrations of β -glucans and proteins in the mash

were observed for varying modifications of the malt (Home et al. 1993, Narziß, 1985).

Flow Diagram



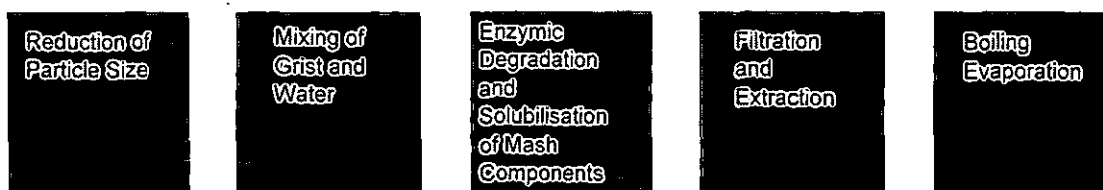
Operation



Equipment



Function



2.1: Flow Diagram and Functions of Brewhouse Operations

The calcium content of water can influence protein precipitation and pH level of the mash; both have an effect on the filterability of the mash. Laing and Taylor (1984) found a direct improvement of the run off rate with increasing Ca content. This effect was thought to be mainly due to the influence of lower pH-levels on the rate of proteolysis. Lower pH-values improve the enzymatic action, and levels of total soluble nitrogen and the ratio of FAN (free α -Amino Nitrogen) to TSN (Total Soluble Nitrogen) in wort increase. The amount of fine particles in the filter bed is reduced, which is the main reason for improved filterability. Lewis and Wahnon (1984) also investigated this influence and found a near linear relationship between Ca^{2+} addition and pH decrease. Calcium reacts with phosphates, which affects the pH change.

2.2.2. Milling

This operation should prepare a grist composition, making suitable for the succeeding stages of mash conversion and filtration. Milling is undertaken by means of hammer or roller mills. For the separation of the mash with lauter tuns a 6 roller mill is most commonly used. Figure 2.2 shows the working principle of such a mill (Bühler, 1993).

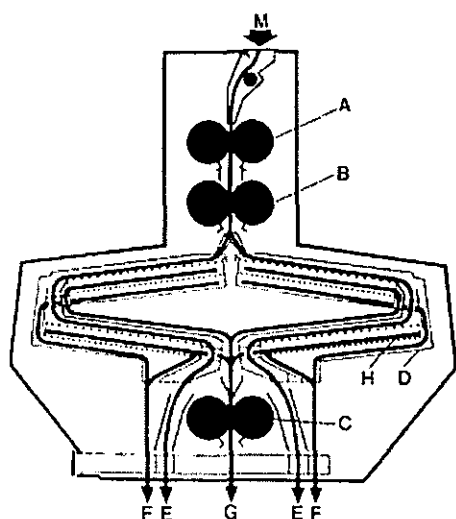


Figure 2.2: Roller Mill (Bühler, 1993)

- A: Precrushing roller cylinders
- B: Husk removing roller cylinders
- C: Grits milling roller cylinders
- D: Screen box
- E: Husks
- F: Flour
- G: Grits
- H: Set of screens
- M: Malt inlet

The coarser the milling, the higher will be the run off rate (Webster, 1981). For the use of grist for lauter tuns, a compromise has to be achieved between fineness of the grist and the preservation of the entire barley husk. Fine milling, achieved in hammer mills, is advantageous for fast enzyme reaction and solubilization of the extract in the malt (Wackerbauer et al., 1992). Muts and Pesman (1986) described this optimisation problem as being between, on the one hand, the need for optimal accessibility of the starch to amylolytic attack during mashing, and, on the

other, the improved solubility of unwanted materials like cell wall components.

Richter (1993) examined different particle size distributions of the malt grist on the rate of solubilization of extract. Extract increase is mainly caused by hydrolysis of starch to lower molecular sugars, due to the actions of α -amylase and β -amylase. He found that finer milling did not increase the reaction rate. The initial levels of extract in solution are higher with finer milled grain, and these levels stay higher during the entire mashing procedure. Finer grist enhances physical solubilization and water absorption. The same observations were made for the concentration of α -amino nitrogen in the liquid phase of the mash. Meddings and Potter (1977) also examined the influence of particle size on mashing: according to Richter (1993), the rate of water uptake (absorption) and the rate of solubilization of the malt extract increase with finer milling. The rate of increase in "reducing power" (a measure for reducible compounds from malt) also increases with fineness of the grist. The above factors are favoured by fine milling, however, the husk fraction, with particle sizes bigger than 1.25 mm is required as a filter aid in lauter tun operations. This fraction assists to increase the permeability of the filter bed. These conditions led to the use of 6 roller mills with 3 passages and screening sieve sets (see Figure 2.2), which enables the production of large amounts of fine grits (particle diameter bigger than 0.5 mm) with reduced damage to the husk fraction. Further improvements can be achieved by employing a conditioning stage: warm water or steam is used to increase the water content of the malt by 1 - 2 % leading to reduced friability of the husk and increased grist volume (Kraus et al., 1973).

A different system for milling uses steeping of the malt before grinding it in a two roller mill. In this wet milling procedure, the malt is in contact with water for 60 seconds, which increases the water content in the husks to about 20%. This can reduce the damage to the husk fraction (Herrmann, 1991), and the specific volume of the spent grains can reach 320 ml/100 g malt.

Greffin et al. (1978) compared the recommended particle size distributions (dry grist) of grist from various authors. In conclusion, and according to MEBAK (Mittel-Europäische Brautechnische Analysen Kommission, 1987)

the distribution in Table 2.1 seems to be adequate for modern lauter tun operation.

Table 2.1: Recommended particle size distribution of lauter tun grist

Sieve Fractions	Particle size	Weight [%]
Husks	>1.27 mm	18
Coarse grits	>1.01 mm	8
Fine grits I	>0.54 mm	35
Fine grits II	>0.25 mm	21
Grits flour	>0.15 mm	7
Powder flour	<0.15 mm	11

With milling of conditioned malt, the percentage of grist below 0.54 mm and, in particular, the amount of the powder flour fraction can be reduced. The fraction of fine grits I is increased. The specific grist volume changes from 280ml/100g malt to 320ml/100g, which causes an increase of the voidage of the spent grains filter cake (in the lauter tun) and consequently a higher permeability (Narziß, 1990).

2.2.3. Mashing in Procedure (Pre masher design)

In order to obtain a homogenous distribution of the malt grist in water and to minimise the risk of balling and dust formation, specially designed pre-mashers are used. Mashing in from the top into the mash conversion vessel is the conventional method; the grist and the water-grist mixture is fed by gravitation. Fig. 2.3 shows a recent design based on this principle (McFarlane, 1993).

Designs for low oxygen uptake have been developed more recently, as oxygen has been considered, to have a negative effect on the brewing process and on the beer quality. Such premashers use screw conveyors in combination with static in-line mixers and positive displacement mono-pumps (see Fig. 2.4).

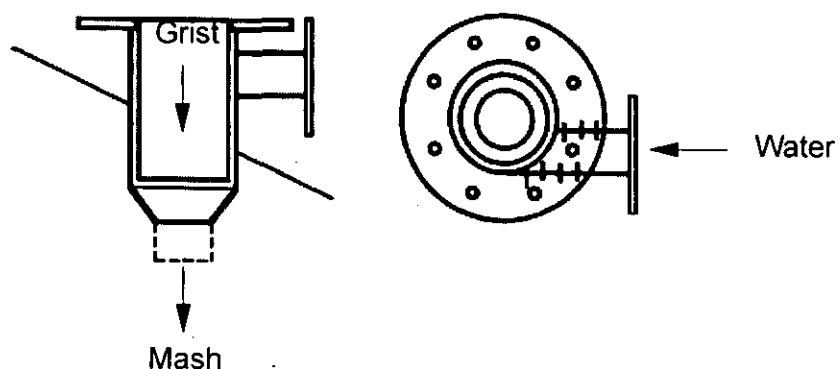


Figure 2.3: Vortex Pre-masher, (McFarlane, 1993)

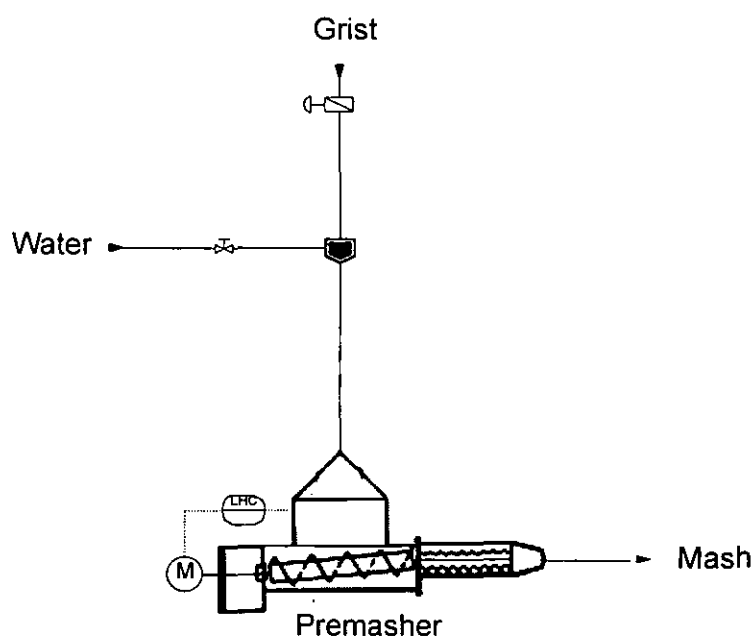


Figure 2.4: Premasher System (Stippler, 1988)

The mash is fed into the mashing vessel from a bottom-entry inlet to keep the mash surface in the vessel as smooth as possible. The agitator speed is controlled by the liquid level. This technique minimises the oxygen uptake by avoiding splashing of the mash. However, Lie et al. (1977) found that the mashing in procedure has little effect on oxygen uptake, as compared to the uptake in the mashing, lautering and boiling stages. It is an additional advantage of this newer pre-mashing system, that mash

concentrations can be very high. Liquor to grist ratios of 2.3 : 1, which allow the addition of hot water (for infusion mashing) during the mashing process, can be easily achieved (Narziß, 1992, Heyse, 1993).

2.2.4. Mashing

Mashing is basically an enzymatic conversion and extraction process. Insoluble components in the malt are solubilised by physical and enzymatic action. In addition, high molecular weight molecules are degraded into smaller molecules. There are several different mashing procedures in use, which can be categorised by the application of temperature:

1. The simplest procedure is the so called "Infusion Mashing". Malt grist and water are mashed at single temperature. A temperature of between 65 and 68°C is kept constant during the entire process. This allows the use of unheated vessels, and is mainly employed for well modified malt. It was also very often used for experimental purposes, because it allows easier modelling and gives better repeatability.
2. Another variation of the infusion mash is a temperature programmed procedure, employing temperature rests between 40 and 78°C. The advantage is an enhanced enzymatic conversion, resulting in higher extraction yields. This method is most commonly used in breweries world wide.
3. Slightly more complicated is the so called "Decoction Mashing". During the mashing process, parts of the mash are boiled, in order to obtain physical degradation of the malt grist. The so treated mash-parts are pumped back to the remaining mash and heat it up. Enzymes from the remaining, un-boiled mash are then degrading material which was solubilised during the boiling stage. Up to three mash parts can be boiled. This procedure is mainly used for less well modified malt. Figure 2.5 shows a flow sheet for a typical mashing vessel.

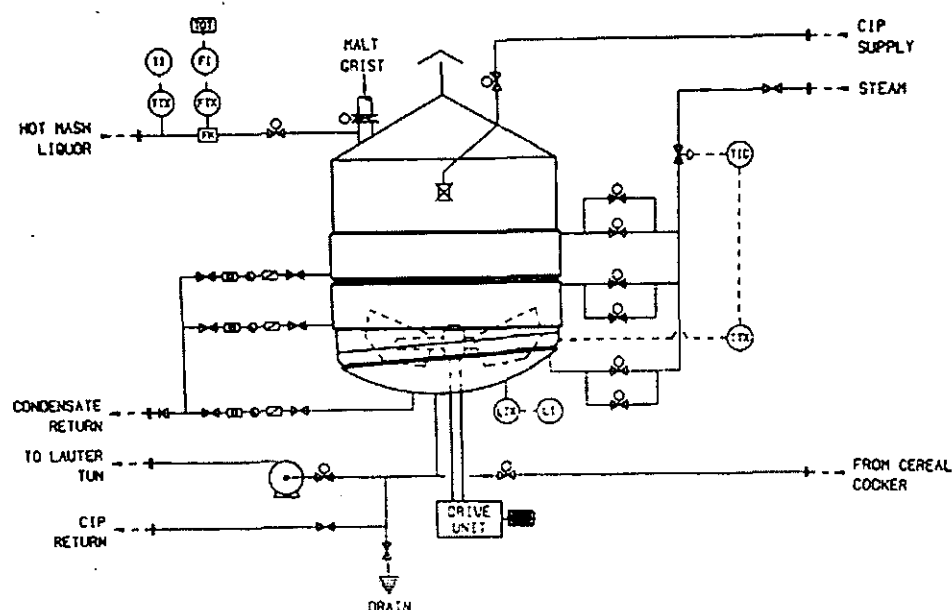


Figure 2.5: Flow sheet of a mashing vessel (Briggs, 1993)

For a close examination of the consequential effects of mashing on lautering performance, it will be necessary to describe the reactions of different chemical groups in detail.

2.2.4.1. Effects of Proteins on Lautering Performance

Proteinaceous material has major effects in mashing and subsequent lautering. It is generally agreed, that proteins can affect filterability of mash in a negative way. Most effects have been explained using chemical mechanisms. Malt contains a wide range of different protein compounds. The most important group of proteins for the lautering process contain sulphur-aminoacids like cysteine or cystine as a dipeptide. The reaction of these sulphuric compounds in proteins, in malting and in mashing has been reported by various authors.

Baxter and Wainwright (1979) examined the hordein fraction of barley and its behaviour in malting and mashing. They showed that a part of these hordeins have a relatively high sulphur content (extractable with 70% ethanol containing mercaptoethanol). Hordeins are broken down during malting to smaller peptides and aminoacids by the action of enzymes, but hordeins with higher sulphur content are broken down to a lesser extent. Their proportion in the malt is therefore higher. During mashing, lower

molecular weight hordeins are extracted but large molecules remain insoluble.

As large proteins contain a higher level of disulphide bonds, the total amount of cystine in the spent grains is increased. Baxter and Wainwright (1979) concluded that, during mashing, a rearrangement of disulphide bonds occurs, forming more cross-linked material which precipitates and accumulates in the spent grains. This protein material reduces the filterability of mash in the lauter tun. They proved this theory by using reducing agents (like metabisulphide, mercaptoethanol, cysteine, ascorbic acid), which could improve the filtrate flux substantially. These reducing agents help to keep the thiol groups unlinked. This work showed that sulphur containing hordeins participate in protein-protein interactions and that disulphide bonds play an important role in these reactions. It also demonstrates the importance of the redox status of the mash.

Gel-proteins, another class of proteinaceous material, were investigated by van den Berg et al (1981). Their name is derived from the gelatinous layer they form after extraction with SDS-solution (Sodium Dodecyl Sulphate) and centrifugation. Graveland et al (1979) found this fraction in wheat flour and described it as a group of glyco-proteins. They have very high molecular weights up to 10^6 Daltons. The gel-proteins consist of sub-units with different molecular weight, which are linked to each other by inter-molecular disulphide bonds. These bonds can be broken during the reducing phase of the malting process, when oxygen is used by the germinating barley. Another part of these gel-proteins is broken down by enzymatic action, during the malting and the mashing process, into smaller peptides and aminoacids.

Muts et al. (1984) reported a direct correlation between gel-protein concentration in malt and the filtration rate in a lauter tun (see Figure 2.6). The correlation coefficient for these trials was 0.854. They analysed the top layer of the lauter tun filter cake and found 60% proteins, 20% polysaccharides, 12% lipids and 8% residual material.

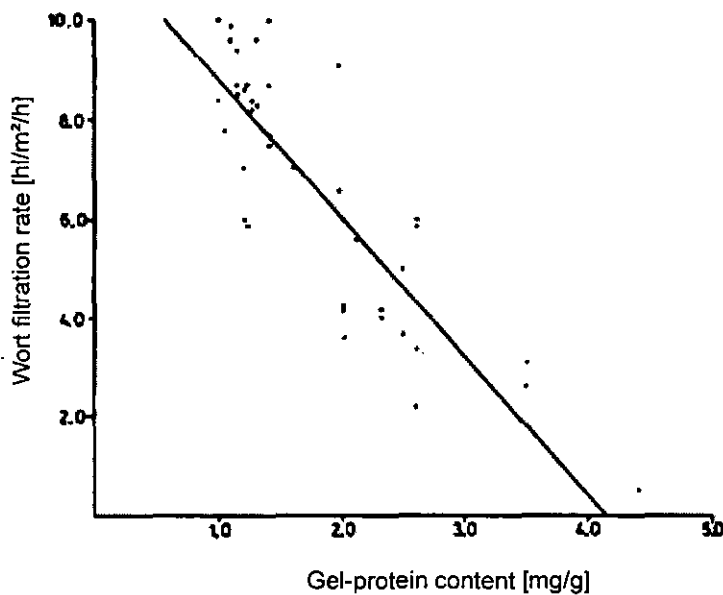


Figure 2.6: Concentration of gel-proteins and effects on lautering performance

As described earlier, the mashing process, with its possible oxidative environment can lead to re-formation of disulphide bonds with resultant increasing molecular weights. These disulphide crosslinks of gel-proteins lead to the formation of large protein complexes. They can also be linked with gluteline or albumin fractions, either by molecular interchanges or by enclosure. Due to their hydrophobic character this protein-fraction can easily adsorb lipids. β -glucan, pentosans and small starch granules linked to proteins can also become part of these complexes (Barett et al. 1975). Van den Berg et al (1981) found that the amount of fine material in the spent grains cake and the filterability are linked, with the filtration rate being dependent on the amount of gel-protein in the fine fraction of the cake.

The precipitation and aggregation of proteins causes the formation of a sediment on the filter bed in the lauter tun (the so called "fines layer"). How this formation of fines is influenced by the mashing process has been described by several authors.

Ferenczy and Bendek (1991) analysed this upper layer on the filter cake and found, among carbohydrates and polyphenols, a protein content of more than 60%. They observed that, in temperature programmed infusion mashing, the total nitrogen content reduces with mashing time. The higher

molecular weight protein fraction is reduced to the greatest extent. These authors describe two reasons for this reduction. For the first the degradation, due to enzymatic work, and secondly the precipitation with increasing temperatures while heating up from 50 to 70°C. In pure malt they found a reduction of over 50% of protein with molecular weights greater than 5000 Daltons. The precipitation and removal of proteins was found to occur in two steps: the proteins precipitate, and then an aggregation with polyphenols takes place.

Lewis and different co-workers also investigated the reduction of proteins during mashing. Lewis and Oh (1985) state that the formation of proteinaceous precipitate in mash appears to be unique to temperature programmed mashing. This protein material dissolves during the protein rest temperature (40 - 55°C) and precipitates even at low mashing temperatures. Their studies showed that up to 10 % (w/w) of this precipitate could be found in the spent grains. The effect of the amount of protein particles was studied in a model lautering system, with glass beads instead of mash spent grain. It was shown that added protein material had a negative effect on the run off rate and that the aggregation of these particles induced clogging of the filter bed.

Lewis and Wahnnon (1984) observed, that the final amount of higher molecular weight proteins (< 5000 Daltons) in solution, after different infusion mashing procedures, were the same. Proteins dissolved during low temperature rests at 25 or 40°C, but were precipitated with increasing temperatures. A single temperature stand infusion mash at 70°C did not show this effect of release of high amounts of proteins into solution.

As proposed by various other authors (Narziß, 1985, Ferenzcy and Bendek, 1991), the reduction in higher molecular weight proteins could be partially accounted for by enzymatic degradation. However, Lewis and Wahnnon (1984) prove in a mass balance, that the amount of protein recovered from a specially prepared model lauter bed (glass beads without spent grains) was equal to the reduction of proteins in the liquid phase of the mash. That meant that the entire reduction of higher proteins could be explained by precipitation. The size of proteinaceous particles can have major impact on the filterability of the mash. Therefore factors influencing formation and size of flocs will also influence filterability.

2.2.4.2. Effects of Polyphenols on Lautering Performance

Lewis and Serbia (1984) investigated the influences of polyphenols on aggregation of proteinaceous particles, and found that this effect was dependent on the presence of low molecular sized polyphenols. This fraction, consisting of proanthocyanidins and tannoids, is described as sensitive to oxygen, as Narziß claims in several articles (Narziß, 1987, Narziß, 1992, Narziß et al., 1986). Hug et al. (1986) also confirm this influence on the oxidation of polyphenols. Lewis and Serbia (1984) found that polyphenols react with protein only at comparatively high temperature (i.e. 70°C) and only after an initial aggregation occurred. By inactivating the polyphenols with PVP (Polyvinyl Pyrrolidone) in mash, a reduced precipitation was observed. The oxidation due to addition of hydrogen peroxide with peroxidase had a similar effect on the floc formation. The haze which formed at 70°C, without a subsequent aggregation, made the mashes unfilterable. Sodium-metabisulphite, a reducing agent, had a reverse effect. It increased removal of protein. This again shows the importance of the redox status in different circumstances.

2.2.4.3. Carbohydrate Material and Influences on Filterability of Mash

Barrett et al. (1973) found influences of particle size, and especially of fine particulate materials, on the filterability of mash. The addition of wheat flour caused an increased amount of fines on top of the spent grains bed. The composition of this sediment is given with 30 - 70% carbohydrate and 30% protein, depending on the composition of the raw materials. The carbohydrate fraction was found to consist mainly of glucose with significant amounts of xylose, arabinose and galactose. The fines examined by electron microscopy showed aggregates of small starch granules, enclosed in a "matrix of amorphous material". Kano and Karakawa (1979) also described the impact of starch granules in the spent grains bed on wort run off. They considered small starch granules to be implicated with lautering difficulties.

Barrett et al. (1975) analysed the composition of fine material in more detail. In an all-malt mash they found the following fractions as percent dry weight: aggregates of protein 42%, starch 29%, bound polar lipids 17%, ether soluble, free lipids 5%, pentosane (arabinoxylane) 5% and β -glucan

3%. These concentrations vary with different raw materials. However, these results correlate well with the analyses described previously.

Carbohydrates are the main soluble fraction which produces extract. These water soluble substances could cause changes in viscosity. Barrett et al. (1973) demonstrated that the change in viscosity due to different extract concentrations is negligible. Changes in extract (analysed as specific gravity in the liquid) also seemed to have a very small effect on run-off rate at lautering temperatures.

Lewis and Oh (1985) stated that "small differences in specific gravity, especially at high temperature, had only a small effect on run off rate". It is important to mention this, because different mashing intensities and grist particle sizes can cause variations in extract levels.

More critical in their influence on filterability are higher molecular weight carbohydrate compounds in the form of β -glucan or pentosane. These substances, also called gums, are originally located in the cell walls of barley as a support material and they are partially soluble in water (Schuster et al. 1967, Bamforth 1982). In addition to the soluble fraction there are further amounts of insoluble β -glucans in the hemicellulose fraction of malt.

These components can have two effects on filterability of the mash. They can increase the viscosity of the liquid phase of the mash (the wort) and they can, due to their stickiness, change the composition of the filter bed and reduce the pore size of the cake. Barrett et al. (1973) examined the influences of β -glucan on the filtration rate and found the particle size effect to be more important than the viscosity effect (see also Eyben and Huipe, 1980). They also reported that aggregation of macromolecules of β -glucan and pentosane with the protein of small starch granules result in an impermeable deposit which blinds the filter bed and impedes wort run off. These bonds with proteinaceous material are possible if, as Pierce (1980) reports, glucan contains small amounts of proteinaceous material. The work of Pierce also found increasing viscosity of β -glucan combined with wort as compared to water. Eyben and Huipe (1980) state that viscosity and β -glucan content have no significant value in predicting the filtration rate. They also mention, that the filtration depended closely on the nature and size of particles present in the mash bed.

With improvement of β -glucan analysis-techniques it became clear that not only is the total amount of β -glucan important, but also the molecular weight of the components. Aastrup and Erdal (1987) carried out a mass balance of β -glucan with the calcofluor analysis in the mashing and lautering stage. This method detected molecules bigger than 50 000 Da (Wainwright, 1990). They found about 50% of this high molecular weight β -glucan in the wort and about 30% in the spent grains, irrespective of the malt modification. With a single temperature infusion mash (65°C), the release of β -glucan into solution was constant over the mashing time and the final amount was similar to other mashing procedures. Narziß et al. (1990) observed a rapid increase in high molecular weight (>90 000 Da) fractions with lower modification of the malt and increasing mashing in temperatures. The change of the particle size with fine milling increased both total and high molecular weight β -glucan content; the high molecular weight pentosanes were increased as well. Fine ground grist allowed the release of more cell wall polysaccharides. In the case of undermodified malt, higher amounts of β -glucans were released. The α -glucan content was found to be independent of the grist particle size. The improved solubilization of finer grist changes the composition of wort, as these components go into solution but are often not degraded during the mashing process.

The relation between viscosity of the wort in laboratory analysis and the β -glucan content was investigated by Neumann and Zaake (1980). They found a poor correlation coefficient of 0.37. This study also showed that an improved modification of the malt is an important condition for a low content of cell wall components such as β -glucan.

Similar results were published by Muts et al. (1984), who found the malt modification to be a decisive factor for the mash filterability. Large amounts of undegraded, high molecular weight β -glucans and gel-proteins were found the most important factor in determining beer filterability. However, with lautering the gel-proteins were thought to play the more important role, because the influence of β -glucans on viscosity at lautering temperatures (75 - 78°C) is very low.

Stirring can have a great impact on the solubilization of β -glucan, especially if the malt modification is very low (Jäger et al. 1977). With all malt worts these authors found higher viscosities in sweet wort of stirred

mashes. A correlation between viscosity of the first runnings and the total lautering time was also found.

2.2.5. Lautering Technique

The lautering procedure separates wort from spent grains. This filtration technique is carried out as follows.

Mash slurry is pumped from the mash conversion vessel into the lauter tun (see Figure 2.7, describing a typical lauter tun). The mash is fed vertically from bottom inlets. This allows the solids in the mash to distribute evenly and settle on top of the false bottom without compacting. The bulk of the particles sediment very quickly, in about 10 minutes under normal, practical conditions. Smaller particulate material forms a layer of fines on top of the spent grains cake. Filtration is started when all the slurry is transferred into the lauter tun. The first turbid filtrate is recirculated to the top of the filter bed, until an acceptable clarity of the filtrate stream is reached. This recirculation helps in forming a suitable filter cake which is able to restrain even small particles in the range of 5 to 10 μm .

After the recirculation phase, the wort is drained until the liquid level is just above the filter bed. This measure helps to maintain the buoyancy of the spent grains cake. Hot water is then added on top of the filter cake to wash it (sparging).

In order to increase permeability of the bed, the cake is raked by means of knives. This procedure ensures that new channels are created in the cake. The level (height) of the rake-knives in the bed is controlled by the filter resistance. If high resistance occurs, the cutting is carried out at a very small distance (about 3 cm) above the support bottom. During the washing procedure the rake works continuously. The amount of water used for sparging is predetermined by the extract content desired in the wort. However, the cake has to be washed carefully enough to gain high extraction yields.

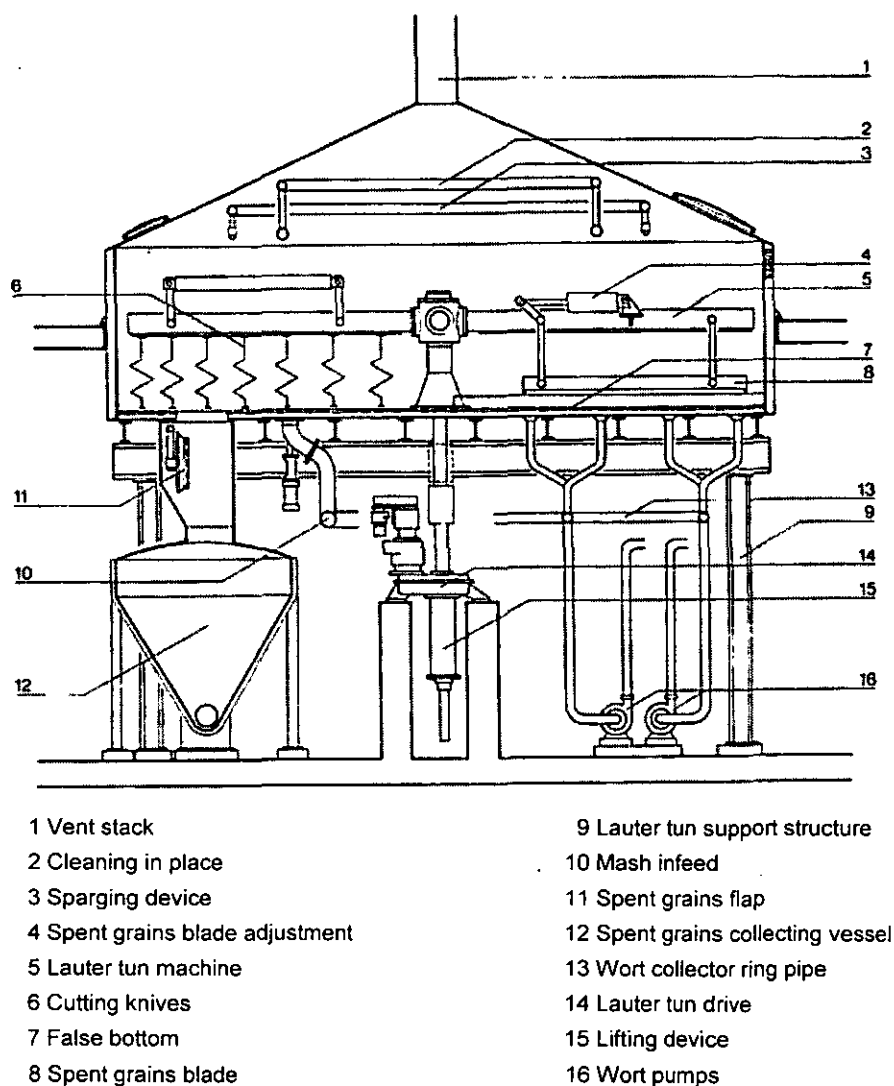


Figure 2.7: Typical lauter tun with additional equipment (Ziemann, 1993)

The flow of the filtrate is maintained by the hydrostatic pressure difference and the active suction of a filtrate pump. The pressure drop across the filter cake increases with filtration time as the filter cake compacts. By employing the raking procedure (which increases the porosity of the bed) the filter resistance in the bed can be reduced.

2.2.5.1. The Lauter Tun Operation - Effects on Performance

Trials from Jäger et al. (1977) showed, that the run off rate not only depends on viscosity, but also on the structure of the cake. The ratio of malt to adjuncts and milling regimes seem to be very important. Even with worts of high β -glucan content normal run off times can be obtained,

whereas maize as an adjunct (which is relatively glucan-free) reduced the lautering time. This was reported to be influenced by the structure of the bed.

With increasing depth, due to higher loading of the filter, the filtration rate gets reduced (Webster 1978, 1981). During the filtration, the bed tends to compact or tighten. This reduces the permeability with lower filterability as a consequence. Raking is most commonly used to lift and open up the bed.

In modern lauter tun operation, the mash is pumped in from the bottom of the lauter tun (see Fig. 3.7). This accelerates stratification of particles (formation of the bed) and reduces the oxygen uptake. Herrmann et al. (1990) found this improvement to be due to the absence of mechanical sedimentation forces. Compaction of the cake is avoided and the permeability of the bed is much higher.

De Clerck (1957) described the sedimentation of the spent grains and the formation of the bed. It is possible to identify three different layers. The largest particles sediment fast and form a thin layer on the false bottom. On top of that a mixture of husks and coarse particles settle, the main part of the cake. The upper layer consists of very fine, light particles.

Huige and Westerman (1975) reported that with increasing initial flow rates the permeability decreases further. This effect was already observed empirically by De Clerck (1957).

In general, it is necessary to control the suction on the bed, not only at the beginning of the filtration, because this influences the compaction of the bed. Too high a suction could lead to a premature plugging of the filter cake. The first runnings are recirculated on top of the filter bed until an acceptable clarity is reached. If the wort gets too cloudy during lautering, recirculation can be applied again.

Further steps which include raking, sparging and the removal of wort and weaker wort are carried out continuously.

The raking machine is started, if the spent grains resistance reaches 80 - 100 mm water column (0.008 - 0.01 bar). At this point it is then lowered according to the spent grains resistance to a minimal level of 3 cm above the false bottom. The raking is used over the remaining period of lautering,

with an average speed of the rake of 0.8 - 2.5 m/min (Stippler, 1988, Johnstone, 1992).

The addition of sparge liquor (hot water) of 75 - 76°C is started if the liquid level is 1 - 2 cm above the spent grains cake. This is necessary to keep the spent grains floating and avoid oxygenation of the spent grains (Narziß, 1985). The flow rate of the wash water is controlled by the run off rate. This procedure allows the level in the lauter tun to be kept constant. Oxygen uptake and a disturbance of the upper layer of the bed can be avoided. Measures to ensure low oxygen uptake influence the design of lauter tuns; the recirculated wort is fed into the vessel from underneath the liquid level, and the sparge inlets are very close to the surface of the wort.

The wort is removed from below the false bottom by means of "extractor pipes". The pipe diameter is designed to allow wort velocities of 0.1 - 0.3 m/s. A bottom area of 0.9 m² is covered by one pipe (Herrmann et al. 1990).

Currently, for the false bottom mainly stainless steel in the shape of segmented plates is used. These plates have slots of 0.8 - 0.9 mm width, providing a free area for the filtrate flow of 10%. Wedge wire constructions are also used with the advantage of a higher open area (of 20%) and higher mechanical strength. Salzgeber (1976) found that the free area had little effect on the filtration rate. His investigation used slotted plates and wedge wires with free areas of 10.7 - 31%. Wider gaps produced worts with higher solids concentrations and didn't show improved filtration rate.

2.2.5.2. Lauter Tun Operation - Influences on Beer Quality

The lautering procedure has a major impact on the clarity of the wort (Leedham et al., 1975). The opinions concerning clarity of the sweet wort are very different, and the influence of haze on quality of the final beer is manifold, but the following aspect is most important:

Lipids from malt get into solution during the mashing process. In the mash separation stage most of the lipids should be restrained. The lipids content is closely related with turbidity of the wort. The higher the turbidity, the higher the level of long-chain fatty acids (Dufour et al. 1986). Linolic acid and palmitic acid have very high concentrations in the mash and are therefore found in increasingly high levels in turbid wort (Narziß 1885).

These compounds can affect the flavour stability of beer (Nielsen, 1973; Zangrando, 1978). Ahvenainen et al. (1983) describes 50 mg/l as a normal level, above the critical limit of 100 mg/l negative effects on flavour and head retention value can occur. High amounts of haze can also have negative effects on beer filterability. Below a lipids level of 5 mg/l, fermentation may be slower.

In practice, haze, solids content and lipids level show a good correlation for one filtration system. Modern lauter tuns, for example, can contain levels of 20 mg/l of solids in the sweet wort. Englmann and Wasmuht (1993) postulated that the solids content in sweet wort should be below 150 mg/l for good quality beers. Older lauter tuns produced solids levels of 100 - 200 mg/l or even higher.

2.3. Mechanical Forces and their Effects on Mashing and Lautering

The effects of malt quality and mashing on resultant filterability in lauter tuns have been studied intensively. The influence of shear is very often cited as being deleterious to the filterability. However, only few investigations have been carried out on the effects of mechanical forces. Most effects were described and quantified using chemical analyses. No detailed information was found on effects such as particle attrition, aggregation or precipitation.

Milling is the first step in the brewhouse, where mechanical forces are acting on the process stream. This affects the particle size distribution of the grist, which determines the permeability of the filter bed and consequently the run off rate (Webster, 1981).

In the mash conversion stage, mechanical forces can be induced with stirring or with pumping (Leedham et al., 1975; Schur et al., 1981). It has been generally accepted that the agitation should be as low as possible. However, a certain amount is unavoidable to achieve sufficient mixing to establish a uniform temperature and an acceptable mass transfer rate. This applies especially to the mashing in and heating up procedures. Temperature stands can be carried out without or with intermittent stirring.

The design of mashing vessels and stirrers is based on establishing gentle mixing conditions, viz. folding the mash with low speeds, providing mixing

without splashing and minimal surface movement. All brewhouse suppliers fit their mashing vessels with specially designed paddle stirrers and dished bottoms. The stirrers are fitted immediately above the bottom of the vessel. Inclined blades are used to move the mash in a specific flow pattern: In the centre of the vessel the mash is pushed downwards against the heating pads. At the periphery the upward stream is also forced by the stirrer, for better heat transport and suspension of the particles. A typical mash stirrer is shown in Figure 2.8. Designs of different brewhouse manufacturers vary slightly.

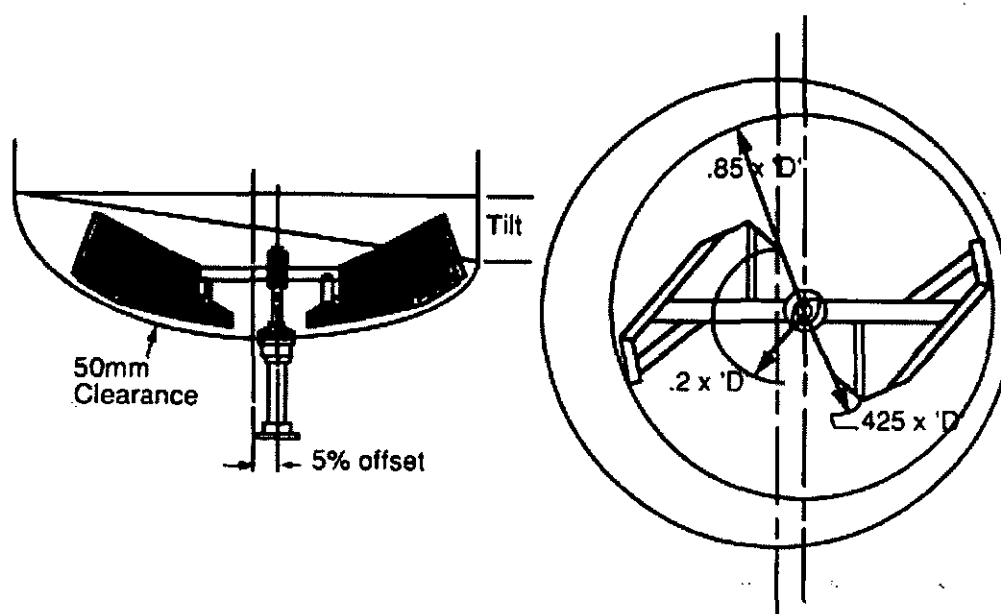


Figure 2.8: Mash Stirrer (Briggs, 1993)

Herrmann (1991) recommends the use of circumferential stirrer speeds below 3 m/s. A speed of 3 to 4 m/s is also used by Briggs (Robertson, 1990). The stirrer speed should be adjusted to follow the liquid level in the vessel, in order to avoid vortices (Narziß, 1992). Stippler (1988) recommends using a diameter of the stirrer (D_R) of 0.7 times the vessel diameter.

2.4. The Impact of Agitation on Oxygen Uptake

In industrial use, intensive stirring is always associated with an increased oxygen uptake (Schur et al, 1981). Lie et al. (1977) investigated the influence of stirring on oxygen uptake, using a sulphite solution to monitor

the reaction of oxygen with the solution. They found that both brewhouse design, and especially stirring, determine the oxygen uptake. Surface movement caused by stirring or convection causes the transfer of the oxygen saturated top layer into the liquid. Even with infusion mashing procedures, where no mash transfer takes place, this could lead to high oxygen uptake. Heating periods and periods with higher temperatures (above 60°C) are sensitive to oxygen uptake. In addition, transfer of mash (with decoction mashing or during transfer to the filtration unit) has a further deleterious impact on the oxygen uptake. The absolute values of oxygen consumption in mash were difficult to determine, because of different rheological properties of the diluted sulphite solution used in these trials. However, relative values permitted comparability of different systems and procedures.

Schöffel (1978) describes the stirring of the mash and its influence on oxygen uptake. Mass transfer between air and mash is marginally increased with higher stirrer speeds, because the surface boundary area is increased compared to a quiescent surface. This is due to both the vortex in the stirred vessel and waves. Extreme aeration of the vortex can occur if the air phase reaches down to the stirrer blades. Air is then dispersed into the liquid. This effect is mainly dependent upon on the liquid level above the stirrer and the stirrer speed. The influence of the stirrer speed on oxygen uptake was also reported by Schur et al. (1981) and Zürcher and Gruß (1989).

2.5. Effects of Increased Stirring Rates

The impact of shear due to stirring of mash is often quoted in literature (Narziß 1985; Leberle and Schuster, 1956, van Waesberge 1988) but only a few researchers have quantitatively investigated the effect of mechanical forces in mashing on lautering performance. All investigations in this field imply that it is very difficult to induce shear without getting oxygen uptake (Van Waesberghe, 1988). Van Waesberghe found shear forces to be more important than oxygen uptake for negative effects on filterability of the mash. Combined effects were regarded most deleterious for lautering.

Some work has been carried out in applying different agitation levels to the mash. Laing and Taylor (1984) used different speeds (0 - 80 rpm) of a stirrer with 50 mm diameter. With increased mixing, the mash bed

permeability decreased (see Figure 2.9). At stirrer speeds above 60 rpm, the permeability showed a strong and rapid decrease. This was explained as the production of fines and husk breakage. Above a critical level, the particles were broken up, rather than displaced. The influence of oxygen in these trials has not been considered.

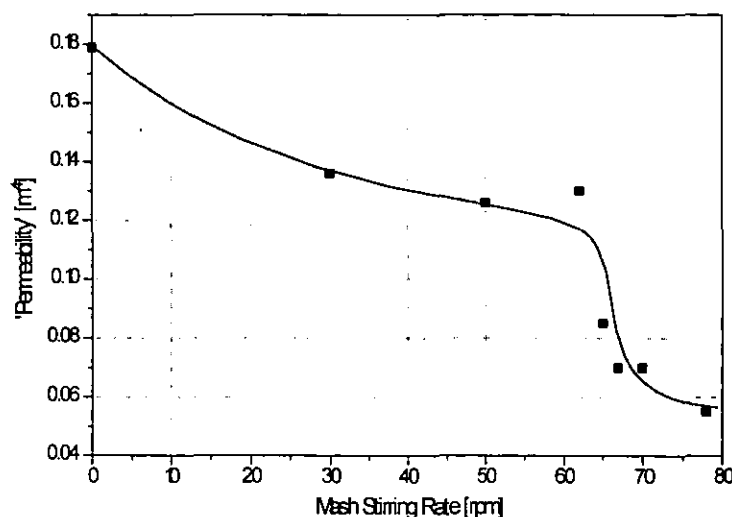


Figure 2.9: Influence of stirring of mash on 'permeability'. The permeability displayed in Laing and Taylor (1984) is not related to the filter area. Hence, the absolute figures are not comparable with other cake permeabilities.

Jäger et al. (1977) also analysed the influence of agitation (determined as stirrer speed) on mash filterability and wort composition. These trials, carried out in a pilot size brewhouse used stirrer speeds of 4.0 rpm in the mash conversion vessel and 5.5 in the mash copper. For "extreme" conditions stirrer speeds of 6.5 and 9.0 were employed. The authors used three different malt modifications, adjuncts and enzymes in their trials. Analyses such as extract, viscosity, polyphenols, total soluble nitrogen, α -amino nitrogen showed no significant changes for the two different agitation rates. Only the β -glucan level in the sweet wort of undermodified malt showed a dramatic increase (7 - 14 fold) with the higher agitation regimes. More interesting than results from these analyses are the influences of different malt modifications, different amounts of adjuncts and different stirring rates on viscosity, run off rate and spent grains bed permeability.

Viscosities of all-malt worts showed no significant changes with increased stirring. Maize and rice dosage resulted in a reduction of viscosity with increasing concentrations, whereas higher amounts of barley caused a rise in viscosity. Undermodified malt treated with higher agitation resulted in a longer lautering time. The use of maize and rice reduced the volume of the spent grains cake in all cases. Increased agitation had similar effects and caused a further reduction of the filter bed volume. Maize, in particular, produced high amounts of fines on top of the cake and showed an impaired filterability. Raw barley increased the filter bed volume and showed, despite the higher wort-viscosity, an improved filterability.

These results define the importance of the particle size distribution of the mash solids as a key factor for the permeability of the filter bed in the lauter tun. They also highlight the effect of viscosity with its interdependence on malt modification and the use of adjuncts and agitation in mashing. In comparison, the effect of agitation on changes in the particle size distribution seems to be more important than the changes in viscosity. It has to be noted that oxidation effects were not mentioned and that oxygen uptake was not controlled.

Arndt and Linke (1979) determined the amount of stirring required for a sufficient conversion (extraction) of the raw materials in a laboratory mashing unit. This work has been carried out with an adjunct concentration of 30% raw barley and enzymes for the degradation of gums.

They used different stirrer speeds and analysed the change in extract, nitrogen content, viscosity, pH, colour and the time for saccharification. They found no substantial influence of agitation on extract level and saccharification time. The amount of protein and α -amino-nitrogen was found to increase with increasing stirrer speed. The viscosity values had the lowest levels at 500 - 600 rpm in the laboratory mash tun; these values were proposed to be suitable for scale-up. Details about the amount of shear induced into the mash are not given. However, they reported that excessive stirrer speeds influence the downstream processes (without giving more details about oxygen uptake or particle size changes).

Uhlig and Vasquez (1992) proposed a method to measure the influence of shear forces in the mash. With this method they assessed the amount of non-hydrolysed fines and found increasing amounts with mashing time

and higher stirrer revolution rate. They also found that at temperatures above approx. 60°C the higher speed of the stirrer blades had a negative effect on the production of fines. This indicates that a component in the mash which develops at this temperature level reacts very sensitively to shear and is broken down into fine particles.

Leedham et al. (1975) and Curtis (1979) investigated the input of mechanical forces into the mash with stirring or recirculation, by comparing two breweries. They observed changes in particle size distribution, filterability, viscosity, and β -glucan content: Higher forces produced more particles below 2.5 μm diameter in beer, they reduced filterability by membrane filtration and caused a release of more, higher molecular weight β -glucan. Mash subjected to higher shear produced higher pressure drops in the lautering stage and beer filtration was negatively affected as well. These findings are confirmed by the results reported by Uhlig and Vasques (1992).

2.6. Unit Operations in the Brewhouse

The second part of this survey describes the theoretical background for the two main operations in the brewhouse, mashing and lautering. The unit operations are mixing (agitation), sedimentation, filtration and washing of filter cakes. These principles are described, using information from brewing literature and related areas, as well as literature about unit operations in chemical engineering.

2.6.1. Theory of Mashing

The mashing process extracts water soluble material from the malt grist. Lower molecular malt components like sugars and peptides are instantly soluble, but a transport from the grain into the liquid is required. Enzymatic hydrolysis of higher molecular mass, insoluble components into soluble components are a decisive part of this extraction. Therefore the malt particles must be in aqueous suspension, where mixing assists quick reaction rates.

2.6.1.1. Reaction Kinetics

Starch hydrolysis is the most important reaction in mashing. Due to the action of α - and β -amylase, insoluble starch is degraded into soluble sugars. Physical factors are the dissolution of hydrolysed carbohydrates, the dissolution of malt enzymes and the gelatinization of starch at a temperature of 55 °C (Marc et al., 1982). In summary these reactions lead to the formation of soluble extract, consisting of dextrans and sugars with up to three molecular units.

Schur et al. (1975) investigated the formation of extract and fermentable sugars as a summary reaction of several, different hydrolysis enzymes. They describe the kinetics of formation of soluble material (extract) by a first order reaction:

$$E = E_{\infty}(1 - e^{-kt}) \quad 2.1$$

Where E is the extract level in the resulting wort for the reaction time t , E_{∞} the resulting extract level for $t = \infty$, and k is the reaction rate constant. By

plotting equation 3.1 in a logarithmic scale, it is possible to derive the reaction rate constant k from the slope of the line.

$$\ln \frac{E_{\infty} - E}{E} = -kt \quad 2.2$$

Schur et al. (1975) obtained a maximum k value of $2.52 \times 10^{-2} \text{ min}^{-1}$ for a reaction temperature of 60°C .

The activation energy A for the production of extract in mashing can be calculated from the Arrhenius equation:

$$k = ce^{\frac{A}{RT}} \quad 2.3$$

For a temperature range of 50 to 55°C an activation energy of $A = 4.7 \text{ kcal.mol}^{-1}$ results, for 55 to 60°C the activation energy is $A = 7.2 \text{ kcal.mol}^{-1}$. From these findings Schur et al. derived that for coarse ground grist diffusion is the rate limiting step. For higher temperatures, above 60°C , they observed negative values for the activation, which they found was due to heat inactivation of enzymes. However, remaining enzyme activities seemed to be high enough to transfer starch granules (which do not gelatinise until temperatures higher than 60°C are reached) into soluble extract. This explains why the maximum extract yield was reached at 67°C .

2.6.1.2. Mixing and Agitation

The agitation of mash has two main aims:

1. to improve mass transfer by providing a homogeneous particle distribution in the suspension. This improves extraction of malt grist by transfer of extract from the particle surface into the liquid. An improved mass transfer also provides better enzymatic reaction rates by reducing local high concentrations of product in the solution (Arndt and Linke, 1979)
2. to provide an even temperature distribution in the mash, keeping its variation as little as possible (in practice: $\Delta t < 0.5^{\circ}\text{C}$). It is also important to prevent the development of fouling and stagnant layers, because these layers have low thermal conductivities, reducing the rate of heat transmission into the liquid.

Mash is normally heated using steam jacketed vessels. Heating areas and steam pressures have to be designed to provide heating up rates in the mash of at least $1\text{ }^{\circ}\text{C}\cdot\text{min}^{-1}$. The overall heat transfer coefficient from the heating medium to the mash is influenced by the convection on the steam side, the conduction in the vessel wall and forced convection in the mash (see Figure 2.10). The natural convection in the mash is supported by the agitation, which is, especially during heating, very necessary.

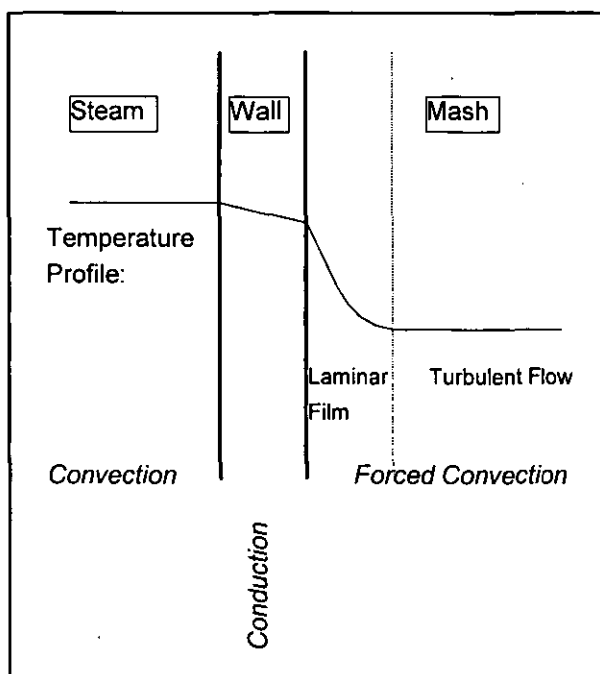


Figure 2.10: Heat transfer in a mashing vessel

The heat transfer from the wall of a vessel into the mash can be described, using the equation formulated by McCabe et al. (1985), for heat transfer with anchor stirrers:

$$\frac{h_j D_t}{k} = K Re^a \left(\frac{c_p \eta}{k} \right)^{0.33} \left(\frac{\eta}{\eta_w} \right)^{0.18} \quad 2.4$$

The heat transfer coefficient h_j for the heater-liquid surface is obviously dependent on the Reynolds number defined by

$$Re = \frac{D_a^2 n \rho}{60 \eta} \quad 2.5$$

in stirred containers. In addition, the coefficient K and the exponent a are also dependent on the Re number. This indicates the importance of the

flow regime in the vessel for the heat transfer from the inner wall of the vessel into the mash. McFarlane (1993) mentions the heat transfer on the mash side being "proportional to the Reynolds number raised to the power of 0.8 under turbulent flow conditions".

However, Schöffel's (1978) experiments showed the heat transfer from the wall was not the dominant process in determining temperature use in the mash. For a stirrer speed increase of 50%, the transfer coefficient is increased by 30%, whereas the time to attain the desired temperature is cut just by 15%. The influence of the diameter of the stirrer is regarded as more important than the stirrer speed, for improved mixing and heat transfer (Schöffel 1978).

Suspending the malt grist in the liquor, described as the second task of agitation, is as important as the heat transfer. Stirring should provide good transport conditions for transfer of solubles from the particle into the liquid phase. Without mixing, the mass transfer from the malt particles into the liquid can be described by molecular diffusion. The force creating a mass flow into the liquid phase is the difference in concentration. Fick's Law describes this situation:

$$\dot{m} = -D \frac{\Delta c}{\Delta L} \quad 2.6$$

The application of turbulent flow increases the mass transfer significantly: in addition to the molecular diffusion coefficient D , a coefficient E , describing the transport created by turbulence, can be added to the equation:

$$\dot{m} = -(D + E) \frac{\Delta c}{\Delta L} \quad 2.7$$

High mass transfer rates \dot{m} are obtained, if all particles are in direct contact to the surrounding liquid. This state is reached if *all* particles are whirled up in the liquid by a turbulent flow. Einkenkel and Mersmann (1977) defined the minimal stirrer speed required to comply with this criterion:

$$\left(Fr \frac{\rho_{fl} v}{\Delta \rho v_0 c_v} \right)^{\frac{1}{3}} = K Re^m \quad 2.8$$

with

$$Fr = \frac{\left(\frac{n}{60}\right)^2 d}{g} \quad 2.9$$

K and m can be derived from experiment, by keeping similar geometries between small and big scale.

2.6.1.3. Shear in Fluids

The shear created by stirring or pumping in mash can be determined as loss of energy (Camp and Stein, 1943). In general, the mean shear G_m dissipated in the liquid is determined by the power input P per volume of liquid V depending on the viscosity η (Koglin, 1984).

$$G_m = \sqrt{\frac{P}{\eta V}} \quad 2.10$$

For flow in tubes, the internal work per time per unit volume, lost in the fluid can be determined as:

$$W_m = \frac{Av(\rho g h)}{AL} = \frac{v(\rho g h)}{L} \quad 2.11$$

The mean velocity gradient or shear in a pipe can then be expressed as:

$$G_m = \sqrt{\frac{W_m}{\eta}} = \sqrt{\frac{Q \Delta p}{V \eta}} \quad 2.12$$

(Camp and Stein, 1943).

It has to be mentioned that this approach is limited to laminar flow conditions. In turbulent flow regimes, internal velocity gradients can be much higher. However, this calculation of the mean shear could be useful to assess the shear effects of a stirrer. Mixing in a vessel can be accomplished with stirring or by pumping in external circulation loops. Both methods create an energy input in the vessel content. The stirrer movement creates a drag force.

$$F_d = C_d A_p \frac{\rho v^2}{2} \quad 2.13$$

The work done by a stirrer is (Vauck and Müller, 1974):

$$W_m = \frac{C_d A_p v^3}{V} \quad 2.14$$

The mean shear induced in the liquid in a vessel is then:

$$G_m = \sqrt{\frac{C_d A_p v^3 \rho}{V}} \quad 2.15$$

Modern mash-stirrers follow the requirements for low shear input into the mash: they are built with large diameters, using low rotation velocities and small projectional areas of the blades. For practical assessment of stirrers, the work input for any kind of stirrer device may be computed from the torque measurements made on the rotating shaft.

2.6.2. Aspects of Filtration

The unit operation of cake filtration can be divided into individual processes which describe and structure the wide range of influences on filtration performance (Klotz and Dallmann, 1984). The following lays out the different influences on the filter cake.

Processes in the filter cake:-

- *Cake formation*

Cake structure is dependent on properties of particles in the slurry such as particle size distribution, differential density between liquid and solid phase, shape of particles, solids concentration in the slurry and differential pressures throughout the cake.

- *Fluid flow through the cake*

This most important micro-process contains the flow regimes inside the cake at a given cake structure.

- *Cake compression*

This effect describes the strength of the cake and its consolidation behaviour during filtration. It covers the change of pore shape distribution due to the liquid flow, which results in a reduction of voidage.

- *Blockage*

This determines the change of the filter cake structure due to transport

of small particles into the cake. Such particles can attach to the walls of filter pores or seal filter pores of the cake. Both principal mechanisms cause an increase in resistance of the cake.

Processes in the slurry:-

- *Particle sedimentation*

Particles with different density to the surrounding liquid sediment due to gravitational forces. As described in section 2.6.3 sedimentation can have significant influence on the formation and structure of the filter cake.

- *Particle transport due to fluid flow*

This microprocess describes the change of particle concentrations in time and place due to laminar or turbulent flow patterns, induced by the filtrate flow, sedimentation or raking of the cake.

2.6.3. Sedimentation

Solids in the mash slurry settle on the false bottom plate of the lauter tun, forming the active filter material. The false bottom is mainly designed as a support, only restraining particles bigger than the slot diameter of about 0.6 mm.

Solids concentrations in the mash are typically greater than 20%. The size of particles ranges from approximately 5 μm to 2 mm with a mean particle size of 1.6 mm (Chládek, 1977). However, this varies with milling conditions and previous operational steps. The density of the particles can also be expected to be different. These conditions make it inaccurate to use sedimentation models, derived from Stokes law, which assume uniform particle sizes and dilute suspensions.

Fitch (1962) found that sedimentation with high particle concentrations and solids of different density, size and shape settle in zones (bands) with mixed distribution (sludge line settling). This leads to sedimentation behaviour in separate bands. If the range of particle size is not more than about 6:1, the interface between the band of the suspension and the particle free liquid zone is very distinctive (Coulson et al. 1985). In a mash the particle range is about 400:1, which means the separation of bands is

less distinct, but sludge line settling could still be appropriate for describing this behaviour.

For activated sludge some interesting aspects of sedimentation behaviour have been reported. Similarities with mash sedimentation are evident and therefore some aspects are listed below.

Lower layers of activated sludge reduce the sedimentation velocity by supporting upper layers. The reduction can be substantial, especially with higher concentrations and for liquid levels below 2 m height (Dick and Ewing, 1967).

For the same medium, diameters of cylindrical vessels greater than 90 cm were necessary to avoid influences from walls. Smaller diameter cylinders gave higher sedimentation velocities. This was caused by the lower drag force on the walls (Horn, 1988).

2.6.3.1. Sedimentation Curve

Concentrated suspensions which settle in concentration bands can be described by a sedimentation curve (see Figure 2.11).

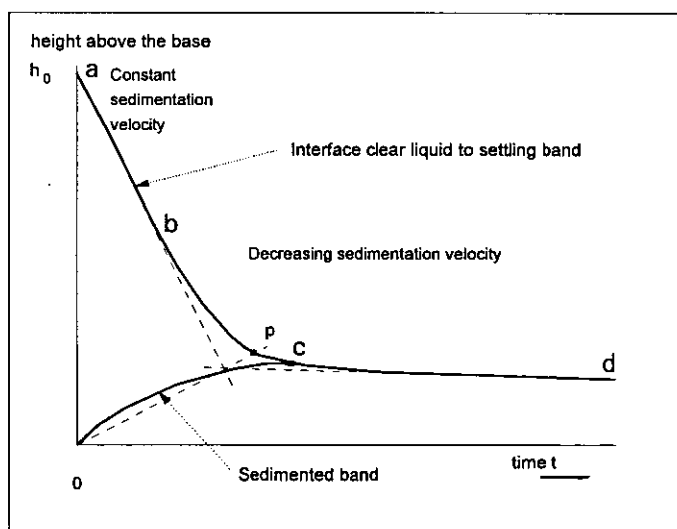


Figure 2.11: Sedimentation curve (after Horn, 1988)

The height of the falling clear liquid/slurry interface is plotted against time. Three different areas can be determined:

1. The interface settles at the beginning at a constant rate and sediment is accumulated on the bottom of the container. (a-b)
2. The sedimentation rate decreases because the increasing particle concentrations hinder the settling (b-c).
3. When the sedimented band and the settling band meet each other, the rate of fall decreases further. (This point is called "critical settling point" (point c)). Subsequent sedimentation (c-d) results in a consolidation (compaction) of the sediment. Liquid is forced upwards and the particles contact one another, forming a bed.

2.6.3.2. Reduced Settling in Closed Systems

Sedimenting particles in closed systems cause a liquid flow opposite to the sedimentation direction. This counterflow reduces the sedimentation velocity.

It can be seen from a balance of the volume flow over a differential area in vertical direction, (see Figure 2.12)

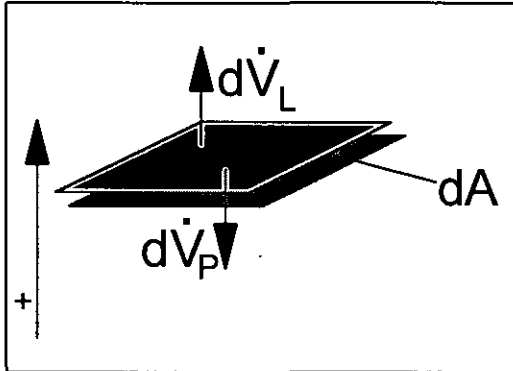


Figure 2.12: Settling of particles in closed systems

$$-d\dot{V}_p + d\dot{V}_L = 0 \quad 2.16$$

that the volume flow of particles $d\dot{V}_p$ replaces the liquid flux $d\dot{V}_L$.

This can be written as

$$dA_p w_{PR} = dA_L w_L \quad 2.17$$

with w_{PR} , the sedimentation velocity of particles in a closed system and w_L , the average liquid velocity over the cross section.

With the porosity ε the fraction of the differential element taken by the particles can be expressed as

$$\frac{dA_p}{dA} = 1 - \varepsilon \quad 2.18$$

and the fraction used by the liquid as

$$\frac{dA_L}{dA} = \varepsilon \quad 2.19$$

Combining equations 3.17, 3.18 and 3.19 results in:

$$\frac{w_L}{w_{PR}} = \frac{1 - \varepsilon}{\varepsilon} \quad 2.20$$

The free particle velocity w_p is reduced by the upwards streaming liquid:

$$w_{PR} = w_p - w_L \quad 2.21$$

Hence, it is possible to express the ratio of the two different sedimentation velocities:

$$\frac{w_p}{w_{PR}} = \frac{1}{\varepsilon} \quad 2.22$$

This shows that, for low porosities (or high particle concentrations), the sedimentation velocity is considerably reduced.

In the lautering procedure the filtrate recycling on top of the bed is started at the beginning of the settling, which minimises or avoids an upwards flow and increases the sedimentation rate.

2.6.3.3. Sedimentation Model

If the sedimentation velocity is only dependent on the concentration of the suspension, it is possible to determine the characteristics of the sedimentation velocity from different slurry concentrations.

Using a mathematical model for the sedimentation process (Kynch, 1952), the characteristics of the sedimentation velocity for a range of concentrations can be extrapolated from just one sedimentation curve (Talmage and Fitch, 1955).

For the application of this model the following basic assumptions have to be correct (Coulson et al., 1985):

1. particle concentration is uniform across any horizontal layer
2. wall effects can be ignored
3. there is no difference in settling as a result of differences in particle shape, size or composition
4. the velocity of the falling particles depends on the local concentration of particles
5. the initial concentration is either uniform or increases towards the bottom of the suspension, and,
6. the sedimentation velocity tends to zero as the concentration approaches a limiting value corresponding to that of the sediment layer deposited at the bottom of the container."

From brewhouse practice, it is well known that in lautering differentials in settling occur due to the size or shape of the particles (see 2.2.5.1). Therefore the use of this sedimentation model would be restricted, or even inappropriate.

2.6.3.4. Compaction of Sediment

Higher concentrations of slurry or sedimented particles in lower layers close to the bottom behave differently from the way described above. The particles are touching each other and are supported from the bottom of a container. The weight of the particles causes a compression of the sediment. For a limited particle concentration the sedimentation behaviour can be described by compression.

For the determination of the sedimentation rate from the sedimentation curve, it is necessary to know the point when compression of the entire

sediment occurs. The compression point is reached when the interface liquid/suspension reaches the consolidated sediment layer.

If this point can't be detected visually or directly from the graph, it is possible to determine this point by a geometrical construction (see Figure 2.11, Horn, 1988).

A balance of the static forces acting in this bed can be described as follows (Horn, 1988), (see Figure 2.13):

$$0 = -F_G + F_A + F_W - \frac{dp_s}{dx} V \quad 2.23$$

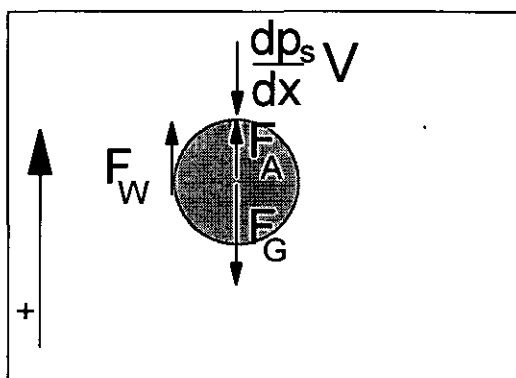


Figure 2.13: Forces exerted on particles in compacted beds

In comparison with band sedimentation, (where the pressure p_s is zero) the pressure exerted by the solids p_s reaches high values, which makes it impossible to neglect these forces in modelling.

It could also be an important factor that bridging of the solid aggregates increases the influence of wall effects (Michaels and Bolger, 1962).

2.6.4. Cake Filtration

This section describes basic theory of cake filtration. Operations relevant for lautering are described in more detail.

Flow through the cake

The fluid flow through a filter cake can be visualised as a flow of liquid through a packed bed of solid bodies with regular pores.

Darcy's basic equation relates the average flow velocity u of a filtrate of viscosity η through a filter bed with thickness L to the driving pressure Δp .

$$u = K \frac{\Delta p}{\eta L} \quad 2.24$$

The permeability of the bed K can be expressed as cake resistance R with:

$$R = \frac{L}{K} \quad 2.25$$

With this relationship the Darcy equation can be written in the form:

$$u = \frac{\Delta p}{\eta R} \quad 2.26$$

Under experimental conditions the superficial velocity u will be determined as filtrate volume per unit time and unit filter area

$$u = \frac{1}{A} \frac{dV}{dt} \quad 2.27$$

Equation 3.26 becomes

$$\frac{dV}{dt} = \frac{\Delta p A}{\eta R} \quad 2.28$$

The overall resistance R can be divided into individual resistances, the resistance of the medium R_m and the cake R_c (Ruth, 1946). Equation 2.26 becomes:

$$u = \frac{\Delta p}{\eta (R_m + R_c)} \quad 2.29$$

The medium resistance is usually assumed to stay constant over the filtration time, however, compression of the medium or particle penetration into the pores could increase this parameter.

The cake resistance is expected to increase throughout the filtration run, because additional material settles on top of the filter cake. The flow paths through the filter get longer. This increase is proportional to the mass of dry solids deposited on the cake. The proportionality constant α is defined as the specific cake resistance. The dimensions of α are $[\text{m.kg}^{-1}]$ representing a fictional pore length per unit mass of cake.

$$R_c = \alpha \frac{W}{A} = \alpha w \quad 2.30$$

with the total mass of dry cake deposited W or w the mass per unit area.

W is related to the filtrate volume V by a material balance.

If V volumes of filtrate have been filtered, a dry mass W has been deposited as filter cake. This cake has a moisture content m defined by the mass ratio:

$$m = \frac{\text{mass of wet cake}}{\text{mass of dry cake}} \quad 2.31$$

The mass fraction of solids in the feed slurry (mash) is:

$$s = \frac{\text{mass of solids}}{\text{mass of slurry}} \quad 2.32$$

With these relations, the ratio of the volume of filtrate to the dry mass of cake can be expressed as:

$$\frac{\rho V}{w A} = \frac{1-s}{s} - (m-1) \quad 2.33$$

This can be rearranged to express the cake dry solids mass by the filtrate volume.

$$W = \frac{\rho s}{1-m s} V = c V \quad 2.34$$

Where c is the concentration dry solids in the slurry, corrected for the presence of liquid in the cake.

With equation 2.30 and 2.34 equation 2.29 can be rearranged to:

$$u = \frac{\Delta p}{\eta \alpha c \frac{V}{A} + \eta R_m} \quad 2.35$$

This equation relates the filtrate flow velocity to the pressure drop and the resistances of the medium and the cake. The change of the cake resistance is expressed by the filtrate volume and the corrected dry solids concentration.

The flow velocity is related to the filtrate rate dV/dt by:

$$u = \frac{1}{A} \frac{dV}{dt} \quad 2.36$$

Inserting 2.36 in 2.35 gives the basic filtration equation:

$$\frac{1}{A} \frac{dV}{dt} = \frac{A \Delta p}{\eta(\alpha c V + A R_m)} \quad 2.37$$

Carman and Kozeny

In Darcys law (see equation 2.24) the characteristics of the filter bed with regard to fluid flow are described by only one parameter, the permeability K .

Carman and Kozeny's model specifies this permeability further, by introducing geometric properties of the packing.

The laminar flow through a porous bed explained by Darcy's Law is closely analogous to the laminar flow through a capillary tube described by Poiseuille's law (Carman, 1937).

$$u = \frac{d^2}{32 \eta L} \frac{\Delta p}{L} \quad 2.38$$

where L is the length of a straight circular capillary with a diameter, d .

Kozeny introduced the porosity of a packed bed in Darcy's equation. He expressed the permeability using porosity ε , particle surface per unit volume of packed space S and the Kozeny constant K_0 . Carman replaced the surface area S using the following relationship for spherical particles with a diameter d .

$$S = \frac{6(1-\varepsilon)}{d} \quad 2.39$$

in Kozeny's equation

$$u = \frac{d^2 \varepsilon^3}{K_0 36(1-\varepsilon)^2} \frac{\Delta p}{\eta L} \quad 2.40$$

which is known as the Carman-Kozeny equation, a more detailed form of Darcy's law. It can be written in a more general form as follows:

$$u = \frac{\varepsilon^3}{K_0 S_0^2 (1-\varepsilon)^2} \frac{\Delta p}{\eta L} \quad 2.41$$

It shows the influencing factors such as particle size, porosity and particle shape on the permeability of a filter cake.

Porosity is the most important factor on the permeability. It is largely dependent on the packing structure of the bed. That is the arrangement of particles in relation to each other.

Particle size effects on cake permeability can be explained by two influences:

1. permeability increases with the square of the particle diameter (as shown, for spherical shaped particles, in equation 2.40)
2. in particle distributions with a wide dispersity, smaller particles will reduce the porosity by occupying the voids between larger particles, thus reducing porosity of the cake due to denser packing.

The specific resistance of the cake can be related to the porosity by combining equations 2.41, with 2.35:

$$\alpha = \frac{S_0^2 K_0}{\rho_s} \frac{(1-\varepsilon)}{\varepsilon^3} \quad 2.42$$

It shows that the specific resistance is very sensitive to changes in porosity.

Relationship between cake thickness and filtrate volume

The mass of dry solids deposited on a unit area of filter can be related to the thickness using the average porosity of the cake ε_{av} and the density ρ_s of the solids

$$w = \rho_s (1 - \varepsilon_{av}) L \quad 2.43$$

The filtrate volume is related to the thickness by:

$$V = \frac{1 - m s}{s} \frac{\rho_s}{\rho} (1 - \varepsilon_{av}) A L \quad 2.44$$

The ratio of wet to dry cake mass is related to the porosity by:

$$m = 1 + \frac{\rho \varepsilon_{av}}{\rho_s (1 - \varepsilon_{av})} \quad 2.45$$

Using equation 2.45 in 2.44 leads to:

$$V = \frac{\frac{\rho_s}{\rho} (1 - m s)}{s \left\{ \frac{\rho_s}{\rho} (1 - m) + 1 \right\}} A L \quad 2.46$$

2.6.4.1. Compressible Cake Filtration

For compressible cakes, the porosity is affected by the pressure drop across the cake. The influence of different pressures have been investigated using a compression permeability cell in which a cake in a cylindrical tube is subjected to mechanical pressure by a piston. The change of ε or α are recorded for different pressures. From these investigations empirical relationships like the Lewis equation

$$\alpha = \alpha_0 \Delta p^n \quad 2.47$$

were proposed (Tiller and Crump, 1985) to relate the specific resistance to the pressure drop. With α_0 and ε_0 specific resistance and porosity at unit applied pressure drop and the compressibility index n and λ . The porosity relation can be expressed in a similar way:

$$\varepsilon = \varepsilon_0 \Delta p^{-\lambda} \quad 2.48$$

n and λ are zero for non compressible cakes, for compressible cakes values range between 0 and 1, sometimes up to 2. α_0 and ε_0 have a mathematical meaning but no physical significance.

As a practical working relationship to describe compressible cake filtration it is possible to replace α in equation 3.37 by the average specific resistance over the cake α_{av} with

$$\alpha_{av} = \alpha_0(1-n)\Delta p_c^n \quad 2.49$$

With this functional relationship equation 3.37 can be written as:

$$\frac{1}{A} \frac{dV}{dt} = \frac{A \Delta p}{\eta(\alpha_{av}cV + AR_m)} \quad 2.50$$

Constant pressure operation

When Δp is maintained constant during filtration equation 3.37 may be integrated (with limits 0 to t and 0 to V ; c , R_m , α are constant)

$$\frac{V}{t} = \frac{2A^2 \Delta p}{\alpha c \eta V + 2A\eta R} \quad 2.51$$

For the practical evaluation of filtration performance in constant pressure experiments it can be useful to transfer equation 3.50 to the reciprocal form:

$$\frac{dt}{dV} = \frac{\eta \alpha c}{A^2 \Delta p} V + \frac{\eta R_m}{A \Delta p} = K_1 V + K_2 \quad 2.52$$

or in the integrated form

$$\frac{t}{V} = \frac{\eta \alpha c}{2 A^2 \Delta p} V + \frac{\eta R_m}{A \Delta p} = \frac{K_1}{2} V + K_2 \quad 2.53$$

It can be seen that if K_1 and K_2 are constant (basic assumptions for the integration) a straight line can be obtained by plotting t/V versus V or dt/dV vs. V , with K_1 the slope of the line and K_2 the intersection on the ordinate. If the medium resistance K_2 is zero or negative a simpler relationship can be obtained.

$$\frac{t}{V} = \frac{K_1}{2} V \quad 2.54$$

Filterability can be defined as

$$F = \frac{1}{K_1} \quad 2.55$$

Hermia and Eyben (1983) described the lautering process as compressible cake filtration. They present values for the specific filter resistance of spent grains with $\alpha_{av} = 1 \times 10^{10}$ m/kg. The influence of the filter cake support (medium resistance) was assumed negligible. For the compressibility of the spent grains cake in relation to pressure they quote the Lewis law with values for n of 0.9 to 1.0. That means the filter cake compressibility is linearly related to pressure.

In 1990 Hermia and Rahier quote the Lewis equation to be applicable for spent grains filtration. The value of n is described as 'slightly greater than one'.

They conclude that with such a highly compressible cake, filtration should be carried out under moderate pressure. Optima of around 1 bar (Hermia and Rahier, 1990) were found by experiments. It has to be mentioned that their trials have been carried out with finely milled grist. Hence particle size distribution is narrower and differs significantly from grist used in lauter tuns.

Baluais et al. (1986) fits the following Lewis equation $\alpha_{av} = 1.6 \times 10^7 \times \Delta p^{1.05}$ m/kg (in a range from $0.5 - 1.5 \times 10^5$ Pa) to describe the change of the specific resistance of the lauter tun cake with pressure. Trials were carried out in a compression cell. He gives values for the specific resistance of $1.25 - 1.4 \times 10^{10}$ m/kg.

2.6.4.2. Compressible Cake Filtration with Simultaneous Sedimentation

The lauter tun filtration procedure was described by Bockstal et al. (1985) as a constant pressure filtration with a compressible cake and simultaneous sedimentation. These authors also used Ruth's equation for constant pressure (equation 2.52) as a basis:

The first term of this equation increases with the increasing mass W of cake deposited per unit area of filter medium. As Bockstal et al. (1985) found, the mass of cake is not only dependent on the volume of filtrate, but particle sedimentation affects the increase of deposit on the filter cake to a further extent. Therefore the absolute mass deposited on the cake is:

$$W = m_1 A + W_2 \quad 2.56$$

The mass of particles, W_2 , sedimenting is (for a constant slurry concentration and a constant settling velocity):

$$W_2 = c A v_s t \quad 2.57$$

Where v_s is the settling velocity of the particles derived from Stokes law (Bockstal et al., 1985).

With this additional term, equation 2.52 becomes:

$$\frac{dt}{dV} = \frac{\alpha \eta c}{A^2 \Delta p} V + \frac{\eta R_m}{A \Delta p} + \frac{\alpha \eta c v_s}{A \Delta p} \quad 2.58$$

and after integration:

$$\frac{t}{V} = \frac{\eta \alpha c}{2A^2 \Delta p} V + \frac{\eta R_m}{A \Delta p} + \frac{(\eta \alpha c)^2 v_s}{6A^3 (\Delta p)^2} V^2 \quad 2.59$$

This equation describes constant pressure filtration combined with sedimentation. Bockstal et al. (1985) found good correlation with hammer milled grist experiments. Typical values obtained in his experiments were:

$$\frac{K_1}{2} = \frac{\eta \alpha c}{2A^2 \Delta p} = 4 \times 10^3 \left[\text{s.m}^{-6} \right] \quad 2.60$$

with $A = 2 \times 10^{-3} \text{m}^2$. R_m was assumed to be negligible.

2.6.5. Blockage Filtration

The complete blocking filtration model assumes that each particle reaching a filter medium seals a filter pore. With this assumption each volume of filtrate filtered through a filter area causes a certain proportion of the filter area to block.

The proportion blocked, per unit volume of filtrate, is dependent on the volumetric concentration of solid particles and the projectional area of the particles.

There are filtration models between the two extremes of the blockage filtration and the cake filtration model: the standard blocking filtration model for example assumes that the pore volume in a filter cake decreases with the volume of liquid filtered, as particles deposit on the pore walls. In this instance particles are not directly blocking the pores, but reduce the pore's cross sectional area.

Poiseuille's equation for flow in capillaries explains the importance of the cross sectional diameter d as a parameter for the flow and pressure loss relationship:

$$u = \frac{d^2 \Delta p}{32 \mu L} \quad 2.61$$

In the case of lautering it is easy to imagine that if fine particles settle on top of a coarse spent grains cake, these fine particles could be drawn into the capillaries of the cake. These particulates could then reduce the size of the cross sectional area of pores in the cake or even block individual pores.

2.6.6. Washing of the Spent Grains Cake

The washing of non-dewatered filter cakes is very important as the spent grains retain about 50% of soluble sugars. Sparging in the lauter tun operation is carried out by displacement. In practice about 4ℓ of hot water (of temperatures between 72 and 80°C) per kg of malt are used to sparge the filter cake and to leach the residual extract out of the solids. This liquor is applied evenly on top of the spent grains surface and permeates through the voids of the bed. Care has to be taken not to disturb the filter cake structure. The formation of cracks or channels in the cake can be avoided by raking.

A suitable way of presenting the washing performance can be the so called washing curve (see Figure 2.14). In this curve the normalised wash

fluid concentration $\frac{c}{c_0}$ on the exit of the filter is plotted as a dimensionless function versus the number of void volumes of wash liquor W .

$$W = \frac{Q t}{\varepsilon A L}$$

2.62

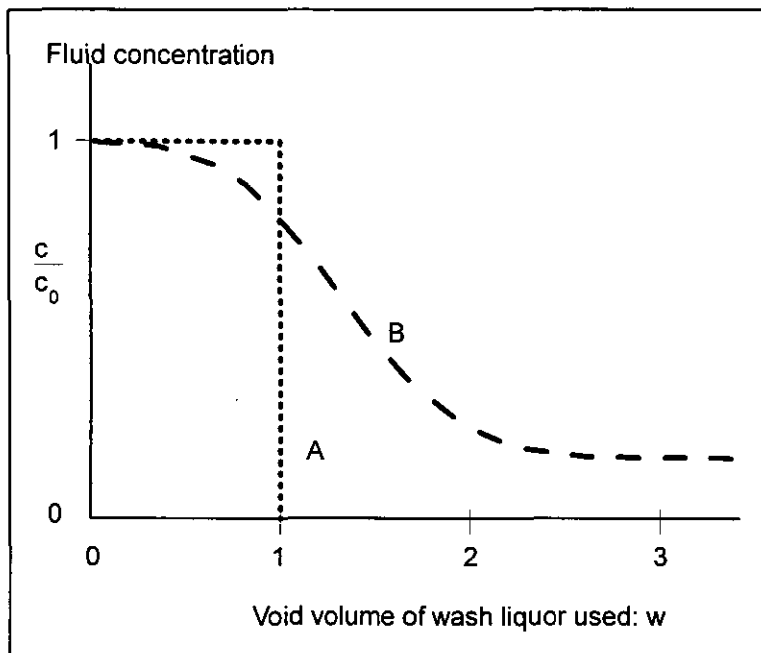


Figure 2.14: Washing curve

Wakeman (1981) divided the washing curve into two main stages. In the first phase a quantity of filtrate is displaced hydraulically by the wash fluid. The optimum washing by pure displacement would result in a plug flow through the filter bed (see Figure 2.14, Curve A). The volume of wash liquor required would be equal to the void volume of the cake.

In real filter cakes (e.g. a spent grains cake), however, pores with a wide distribution of sizes are present. Sparge water travels quicker in wide than in small pores, which causes a breakthrough of wash liquor prior to the use of one void volume (Curve B in Figure 2.14).

Between the two main phases of cake washing an intermediate phase can be identified where the fluid from smaller pores is still high in extract concentration. Effluent from larger pores dilutes the fluid from the smaller pores.

The second stage is dominated by mass transfer mechanisms. Extract is 'attached' to the surface of particles and held in interstices between particles. In addition porous structural material for example from plant cells can contain high extract within the pores. In this stage the following fundamental mechanisms can be identified (Wakeman, 1981):

- "internal diffusion in the solid;
- transfer to the liquid phase in the pores of the solid
- diffusion in the particle micropores to the particle exterior
- diffusion in the liquid surrounding the particles
- eddy mixing in the inter-particle voids".

This shows the complexity of the phenomena influencing the washing process. In addition, changes in the cake structure can affect the washing process further. In lautering, for example, raking will enhance mixing effects and disturb the original filter cake structure.

Washing of spent grains (from finely ground malt grist) filter cake without raking was explained with the axial dispersion model (Moll et al., 1991, Hermia and Rahier, 1990). This model describes the displacement of liquor in the bed by a wash fluid with the same density and viscosity during laminar flow. Application of the dispersion model is suitable for washing cakes with fine particles, if the cake consists of fully saturated pores before washing starts (Wakeman, 1981). Hydrodynamic dispersion is caused by two mass transport phenomena:

1. the mechanical dispersion due to a flow through the pores and
2. molecular diffusion caused by concentration gradients.

The dispersion model gives a good description of a wide variety of washings (Purchas and Wakeman, 1986). It can be written as:

$$\frac{c - c_w}{c_0 - c_w} = 1 - \frac{1}{2} \left\{ \operatorname{erfc} \left[\frac{1 - \lambda W}{2\sqrt{\lambda W}} \right] \sqrt{\frac{uL}{D_L}} + \exp \left(\frac{uL}{D_L} \right) \operatorname{erfc} \left[\frac{1 + \lambda W}{2\sqrt{\lambda W}} \sqrt{\frac{uL}{D_L}} \right] \right\}$$

2.63

where

$$\lambda = \left\{ 1 + K \left(\frac{1}{\varepsilon} - 1 \right) \right\} \quad 2.64$$

When there are no sorption effects $K=0$ and $\lambda=1$.

The term $\left(\frac{uL}{D_L} \right)$ is characterised as a combination of two dimensionless groups, the Reynolds number $Re = \rho u d \eta^{-1}$ for the wash liquor flow through the cake and the Schmidt number $Sc = \frac{\eta}{\rho D}$, which describes the ratio of molecular diffusivity of momentum to the molecular diffusivity of mass.

$$\frac{uL}{D_L} = Re Sc \frac{L}{d} \frac{D}{D_L} \quad 2.65$$

$$\frac{ud}{D} = Re Sc \quad 2.66$$

The effective particle size, d is calculable with (Wakeman, 1986)

$$d = 13.4 \sqrt{\frac{1-\varepsilon}{\bar{\alpha} \rho_s \varepsilon^3}} \quad 2.67$$

The axial dispersion coefficient D_L and the molecular diffusion coefficient D can be related quantitatively. The relationship is dependent on the tortuosity of the cake. For granular material and $Re Sc < 1$, a factor of $\sqrt{2}$ was found (Wakeman, 1975).

$$\frac{D_L}{D} = 0.707 \quad 2.68$$

for $Re Sc > 1$ and a bed thickness greater than 10 cm the following correlation was found (Perkins and Johnston, 1963, in: Wakeman, 1981):

$$\frac{D_L}{D} = 0.707 + 1.75 Re Sc \quad 2.69$$

Hermia and Rahier (1990) applied the following simplification of the dispersion model for washing of the spent grains cake with pure water:

$$\frac{c}{c_0} = \frac{1}{2} \left[1 + \operatorname{erf} \left(\frac{1-W}{2\sqrt{W}} \sqrt{\frac{uL}{D_L}} \right) \right] \quad 2.70$$

2.7. Discussion

The literature survey describes effects from the raw materials and the process on lautering performance. It also presents literature describing mashing and lautering from an engineering point of view.

Analysis of the literature suggests that the influence of the fines layer on lautering performance is dominant. Research focussed on the analysis of the fine fraction of the spent grains cake and possible influences from raw materials and processing. Substances in this layer and their change with variables such as malt modification, or oxygen uptake and temperature regimes during mashing were described. The impact of the status of these substances on lautering performance was measured.

The sulphur bonds of proteins can crosslink and hence increase in size. Gel-proteins can, due to their large size and stickiness, reduce the permeability of a filter bed. These compounds were found to be mainly raw material dependent. Proteins also precipitate already at "normal" mashing temperatures (50-78°C). Polyphenols, also present in mash, can act as finings and support aggregation of proteins to larger flocs. Small starch granules, a group of carbohydrates, were determined in the lautertun bed as one reason for reduced lautering performance. The amount of granules is raw material dependent.

Many of the articles quoted above mention particle size or particle size distribution, without actually measuring it, as the main reason for effects on lautering. In most cases no direct investigation of the size of these small particles was possible as suitable analysis was not available. Most of the effects were described and quantified using chemical analyses.

Hence, a relationship from particle size distribution of the fines fraction of mash to lautering performance is missing. Such a relationship should be able to explain the different chemical effects mentioned above.

Another effect on lautering mentioned in the literature is the viscosity of the liquid phase of the mash. The viscosity of the mash will be affected by concentration of the extract and higher molecular mass carbohydrates such as β -glucan and pentosanes. The influence of extract on viscosity is limited and can be predicted, whereas the release of high molecular mass carbohydrates can cause viscosity changes which are raw material and

process dependent. For an investigation which focuses on particle size changes during processing, it will therefore be beneficial to use one source of raw materials with a low concentration of such carbohydrates, as these substances could mask relationships related to size change.

Several researchers report the negative influence of stirring on the production of fine particles. In most cases fines are not analysed quantitatively and details of particle size distribution changes and the relationship to lautering performance are not available. None of the research results found in the literature tried to correlate and predict the lautering performance from particle size distributions using a systematic approach.

Most research work used the stirrer speed as a measure for shear rates. Power input of a stirrer, which would give a more detailed picture of the shear stress acting in the mash, was not measured.

Only a few parts of the unit operations in the brewhouse are described in the literature with models. Amongst these, only those related to the processes in the lauter tun were found relevant for this work. No comments were found in the literature describing the sedimentation behaviour of mash in the lauter tun. Lautering was described as compressible cake filtration under constant pressure. However, under practical conditions in the lauter tun, the suction of the wort flow varies with time and with change of the extract concentration of the wort during washing. The washing of the spent grains cake was described using the dispersion model.

From this literature search, the following conclusions can be derived to provide a guide for the experimental work.

1. As both water and malt affect the composition of a mash these parameters should be kept constant.
2. Particle size distributions in the mash, especially in the fine fraction, seem important for the clarity and the filtration performance in the lauter tun. It would therefore be appropriate to find a suitable procedure to characterise the sizes of these fines.
3. There are various parameters in the mashing process which could influence the particle size distribution in the fines. In the main, two

parameters could be very important and therefore especially interesting to investigate: the temperature of the mash and the agitation regimes in the mash vessel.

4. The role of oxygen on lautering performance and the relationship to agitation is unclear, therefore the trials should separate oxygen and agitation effects in mashing.
5. It would be interesting to measure power input into mash as a function of the shear stress acting on the mash particles.
6. For suitable modelling of the lautering process, the pilot scale lauter tun should be wide enough to avoid wall effects. Filtration should be carried out under variable pressure to make the results more realistic. Cake washing should be incorporated into the process.

3. Materials and Methods

3.1. Raw Materials

The two raw materials involved in the experiments for this thesis are malt and water. The properties of both materials were defined using analyses recommended by the Analysis Committee of the European Brewery Convention (EBC). As mentioned in the discussions of the literature survey it was found important to limit the raw material variables. Both water and malt can have influences on lautering performance: Water can affect the pH levels in mash due to ion concentrations; different pH levels and ion concentrations would then affect the enzyme activities in mash. With changes in pH levels different components from malt (polyphenols, proteins) would be water soluble and leached from the malt grist.

Malt is processed barley which can vary in composition due to the processing, the growth conditions and the barley variety. This can have a wide range of influences on the mashing and lautering process.

3.1.1. Malt

Standard malt

The malt for all "agitation" trials was taken from one batch. This batch was stored at the maltings at BRFI.

The barley variety used for this malt is "Blenheim", harvested 1992.

The following malt analysis (see Table 3.1) was carried out at the Brewing Services Department at BRFI after arrival of the first part (22. 7. 93).

This analysis describes the malt as very well modified. The extract difference in the mash between fine and coarse ground malt (0.2 mm, 1.0 mm) is very low. Therefore the influence of milling conditions on extract formation is expected to be reduced. The ratio of total soluble nitrogen to total nitrogen in the malt sample is relatively high. Nearly half of the total nitrogen is soluble (46%) under normal mashing conditions. This malt does not require any enhanced protein degradation during the mash

conversion. Therefore, the mashing procedure can be designed without a protein rest.

Table 3. 1: Well modified malt from "Blenheim" barley

Analysis	Result
Moisture	3.9 % (W/W)
Hot Wort Extract (0.2 mm)	82.0 % (W/W)
Hot Wort Extract (1.0 mm)	81.6 % (W/W)
Fine Coarse Difference	0.4 % (W/W)
Colour	4.4 EBC
Total Soluble Nitrogen	0.73 % (W/W)
Total Nitrogen	1.57 % (W/W)
Soluble Nitrogen Rate (Kolbachzahl)	46 %
Free Amino Nitrogen	150 mg/l
pH	5.88
Viscosity	1.50 mPas

About 20% of the total soluble nitrogen consists of free amino nitrogen (FAN). This value shows that a simple mashing procedure with a single temperature stand will be sufficient to provide enough FAN for yeast nutrition.

The pH-value is normal. The viscosity of the laboratory wort is low, showing that the cytolytic modification of this malt is very good.

Undermodified malt

In one trial the effect of heat on particle size distribution of fines in the mash was investigated. To verify that effects are relevant over a range of different malt modifications, a less modified malt was used to compare it with the well modified malt. The malt analysis is shown in Table 3.2.

Table 3. 2: Analysis of less modified malt

Analysis	Result
Moisture:	4.5 % (W/W)
Hot Wort Extract (0.2 mm)	81.3 % (W/W)
Hot Wort Extract (1.0 mm)	78.3 % (W/W)
Fine Coarse Difference	3.0 % (W/W)
Colour	2.9 EBC
Total Soluble Nitrogen	0.66 % (W/W)
Total Nitrogen	1.71 % (W/W)
Soluble Nitrogen Rate (Kolbachzahl)	39 %
Free Amino Nitrogen	0.12 mg/l
pH	6.00
Viscosity	2.00 mPas

3.1.2. Water

Water used for brewing purposes has to have a suitable ionic composition. As mentioned above, enzymatic reactions, extraction and precipitation reactions are dependent on ionic composition and pH levels in the malt. The quality of the water used for these trials was improved and standardised by the use of a reverse osmosis filter cartridge. After treatment by reverse osmosis the concentration of minerals, such as Mg^{2+} and Ca^{2+} , is reduced. Softer water creates a lower pH level in the mash, a prerequisite for suitable mash conversion and a good beer quality.

The following analysis results (Table 3.3) were obtained from reverse osmosis water taken at the beginning of the experiments (Jan. 1994).

The remaining alkaline level, RA, defined by Kolbach (Narziß, 1985) as a measure for the influence of water ions on the mash pH value, can be calculated from the above analyses. It relates the pH reducing ions in the water to the pH increasing ions and is expressed in °d (German degrees of hardness), with CaH (calcium hardness), MgH (magnesium hardness) and total alkaline level which is related to the hydrogen-carbonate concentration) :

$$RA = \text{Total alkaline level} - \frac{CaH + 0.5 \times MgH}{3.5} \quad 3.1$$

$$RA = 0.39 - \frac{0.046^\circ d + 0.5 \times 0.27^\circ d}{3.5} = 0.34^\circ d$$

The remaining alkaline level (RA) is only slightly positive. Kolbach found that $-10^\circ d$ reduces the pH in the mash by 0.3 units, compared to distilled water. This shows that a value close to zero (as found above) won't effect a pH change. This water will behave neutral in the mashing process.

Table 3. 3: Water analysis of reversed osmosis water

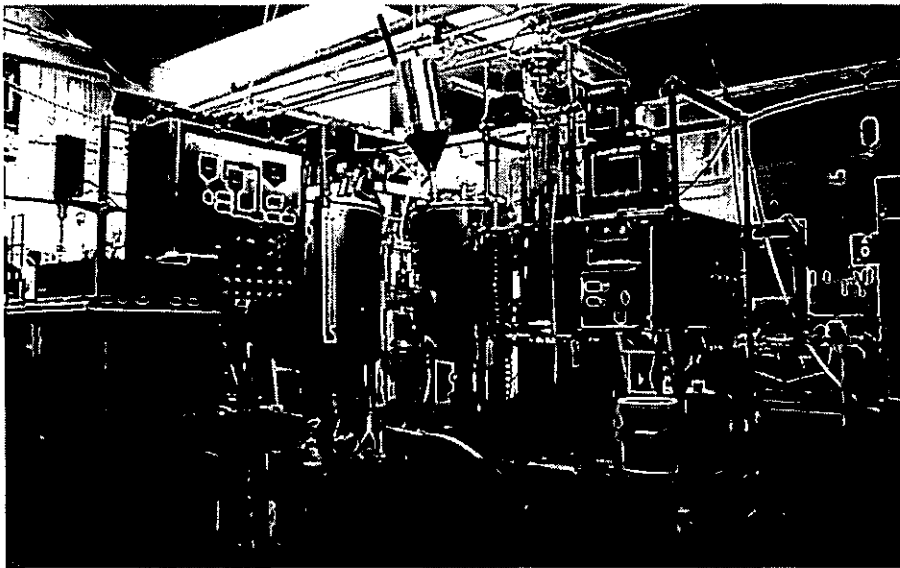
Parameter	Result
Hydrogen-carbonate, HCO_3^-	8.54 mg/l
Magnesium	<0.2 mg/l
Calcium	1.9 mg/l

3.2. Equipment and Plants

This section describes the equipment used for pilot and bench scale trials.

3.2.1. Pilot Mashing Equipment

Mashing was carried out in a pilot rig built by APV Rosista, Rochester, UK. This plant was modified for the requirements of these investigations. Figure 3.1 shows the arrangement of all parts of the rig. All pipework and vessels are manufactured in 316 stainless steel with a sand blasted surface finish. Mashing is carried out in a 100 l jacketed vessel with electrical heating pads in the conically (45° to the vertical axis) shaped bottom section. The heating pads provide a thermal energy input of approx. $3 \times 0.7 \text{ kW} = 2.1 \text{ kW}$. The heating elements are controlled by a Cal 9000 Temperature controller (Controls & Automation Ltd. Hitchin, UK) combined with a PT100 thermocouple inserted in the mash vessel.



Picture 3.1: Mashing and lautering pilot plant

The bottom outlet of the vessel is directly flanged to the inlet of a progressing cavity mono pump (Robbins & Myers, London, UK). This pump delivers a flow through a loop with an internal pipe diameter of 47 mm.

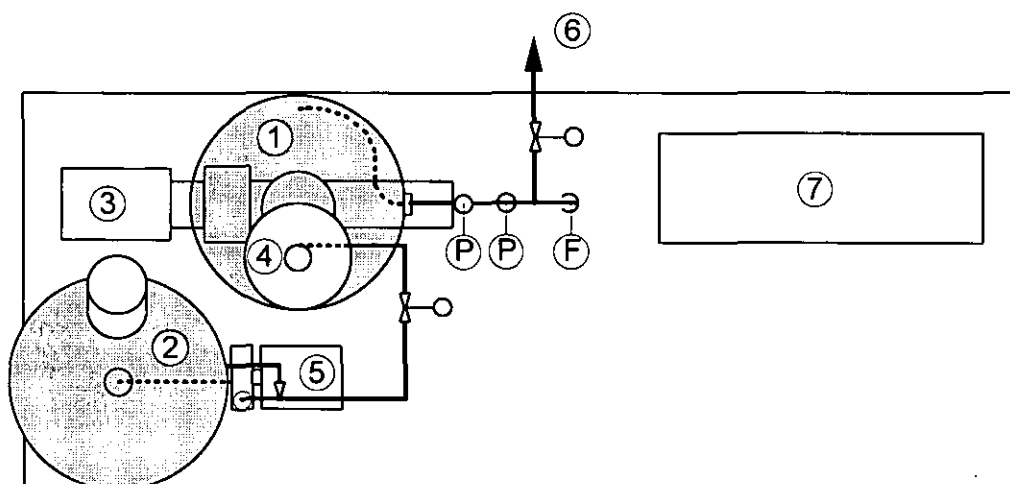


Figure 3.1: Top view of the mashing rig with:

- 1: Mash vessel
- 2: Hot Water Tank
- 3: Mono Pump
- 4: Mashing-in Unit
- 5: Hot Water Mashing-in Pump
- 6: Outlet to the Lauter tun Rig
- 7: Control Unit with Frequency Inverter

The motor of this pump is frequency controlled, which allows to adjust pressure-flowrate combinations over the entire flow range. The setting of the frequency controller was calibrated against the flow rate of mash through the pump loop. Figure 3.2 shows this relationship. The flow rate was measured using a pre-calibrated electromagnetic flow meter, type Variomag (Endress + Hauser, Manchester, UK) in the mash loop. This flow meter was also used during some of the trials. The flow rate of the pump was fixed at a level suitable to create sufficient mixing in the mash vessel. It must be mentioned that flow rate of the pump is constant over different pressure drops up to pressure losses of 4 bar created at a valve. The frequency controller was set to '4.0' equivalent to a flow rate of 26.6 l min^{-1} .

A loop from the mono pump into the mash conversion vessel was fitted, to control the mixing in the vessel. An inductive flow meter, pressure transducers and an adjustable single seat valve were fitted in the loop (see Figure 3.3). The total hold up volume in the loop, from the mono pump outlet to the inlet in the mashing vessel has been calculated to:

$$V = \frac{d_i^2}{4} \pi l = \frac{(4.7 \text{ cm})^2}{4} \pi 108 \text{ cm} = 1874 \text{ cm}^3 \quad 3.2$$

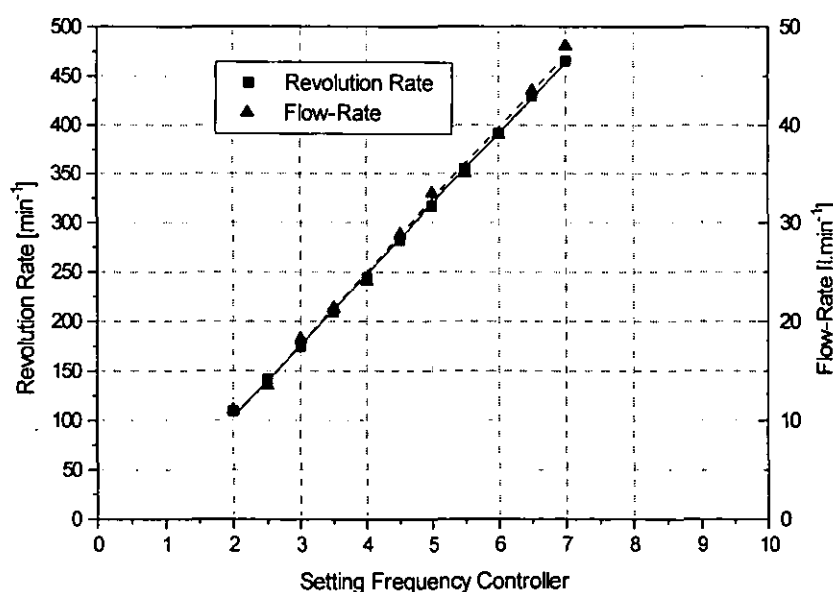


Figure 3.2: Flow rate and revolution rate vs. setting of the frequency controller

The pressure in the flow loop was measured using two different methods: Small pressure differences in the loop were measured using a U-tube manometer, large pressure losses, induced at the valve, were measured by electronic pressure transducers (Wika, Croydon, UK).

For trials in the small power input range (small differential pressures), orifices were inserted in a straight section of the loop, which replaced the inductive flow-meter. The pressure loss across the orifice was measured at two tappings before and after the orifice (see Figure 3.3).

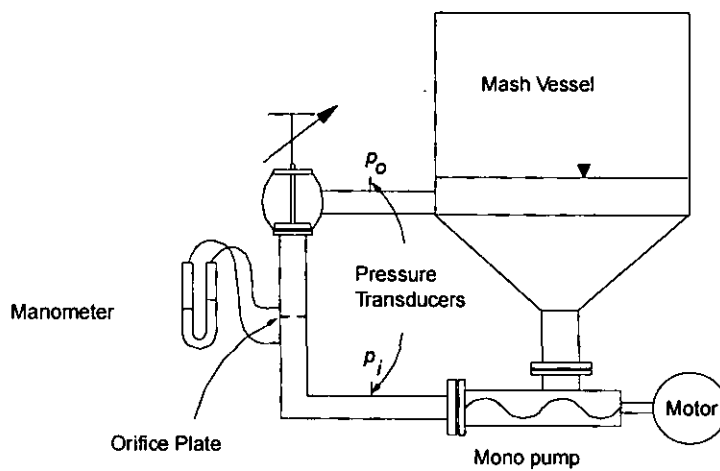


Figure 3.3: Pressure measurement at the mashing flow-loop

The orifice plates and tappings were manufactured according to BS 1042. Figure 3.4 shows the design.

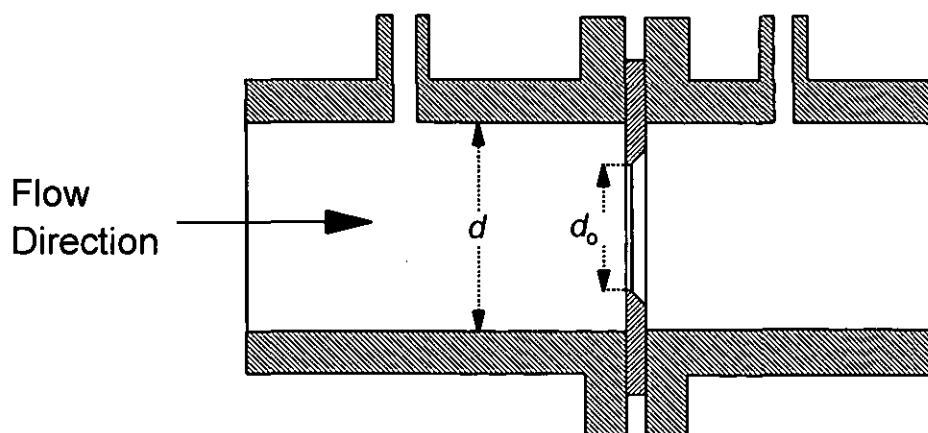


Figure 3.4: Orifice plate with pressure tappings at a distance of $0.5 \times d$ and $1 \times d$ from the plate. Discs with a diameter d_o of 0.5, 0.6, 0.7, 0.8, $0.9 \times d$ were available.

3.2.1.1. Mashing-In

Malt grist was stored in a 'hopper' container, directly above the mash vessel. During mashing-in, the malt grist dropped into the mash vessel and was mixed with water, which was continuously inserted tangentially into the vertical pipe. The setup is shown in Figure 3.5

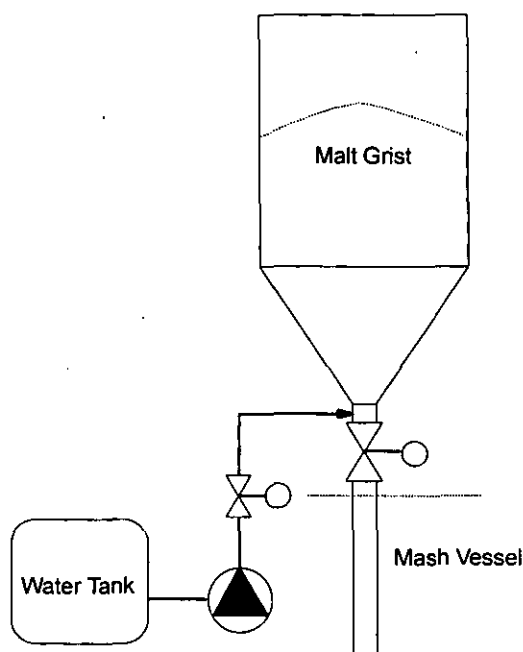


Figure 3.5: Mashing-in unit

The amount of water added to the grist has to be controlled in order to achieve a constant water to grist ratio. The hot water from the liquor tank is pumped into the hopper's vertical pipe by a centrifugal pump through pipework with 1 inch internal diameter. Control of the mass of water pumped in could be achieved by timing the opening time of a pneumatic butterfly valve which was fitted in the pipework.

The following calibration curve, shown in Figure 3.6, was obtained for water at 70°C.

To get 17.5 kg of hot water into the mash vessel, the pneumatic valve has to be opened for 82 s. This mass of water is required for 5 kg of grist at a water to grist ratio of 3.5 to 1. This time was found long enough to get all the dropping grist wetted with water.

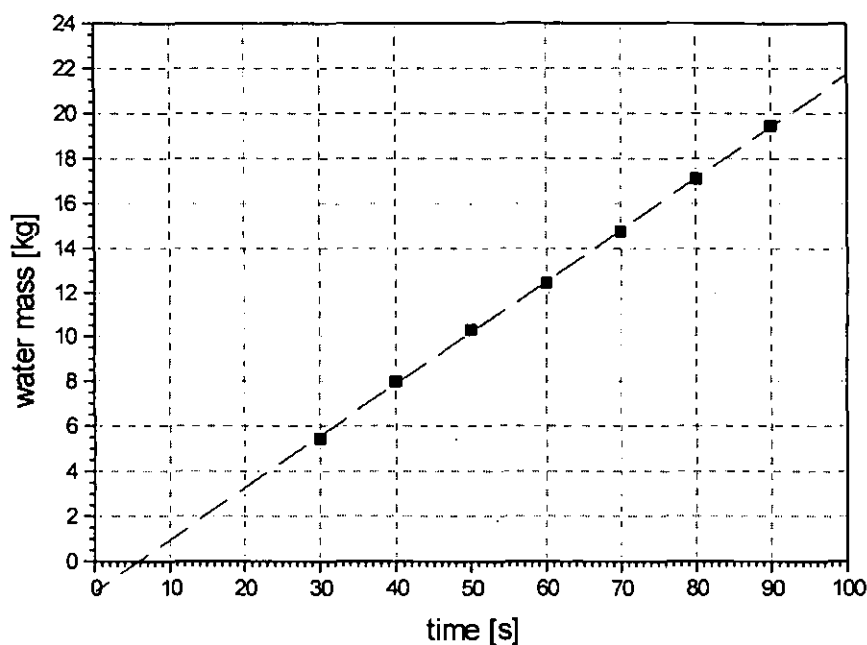


Figure 3.6: Calibration curve for the premasher timed water dosage

3.2.2. Pilot Lautering Rig

The pilot scale lautering rig was designed to assess the filterability of mash under circumstances which allow scale-up of the results to large industrial scale lauter tuns. Therefore the following requirements had to be fulfilled:

1. specific load of the lauter tun floor area in the same range as industrial scale equipment .
2. specific filtrate flow rates in the same range as industrial scale equipment
3. pilot lauter tun should be wide enough to avoid wall effects during settling of the fines and with filtration.

To meet these requirements, a jacketed glass column (Schott, Mainz, Germany) with an internal diameter of 15 cm and a height of 1.5 m was

used. Bottom and top plates were machined at BRFI's workshops from stainless steel plates. The entire rig was assembled at BRFI.

The pipework supplying hot water for cake washing and for the filtrate line was made from 1/4 inch o.d. stainless steel pipes (Swagelock, Ohio, USA) and silicon tubing (3.2 mm i.d., WT 1.6 mm, Watson-Marlow, UK). The two media (water and wort) were pumped by two coupled peristaltic pump heads (see Figure 3.7, Watson Marlow, Falmouth, UK). This ensures that the same volumes of liquid removed from the lauter column by filtration are replaced with water.

Two pressure transmitters (range 0 - 1000 mbar, Sensor Technics GmbH, Waldkirchen, Germany) were fitted to monitor the pressure loss across the filter cake and to control the flow rate of a peristaltic pump.

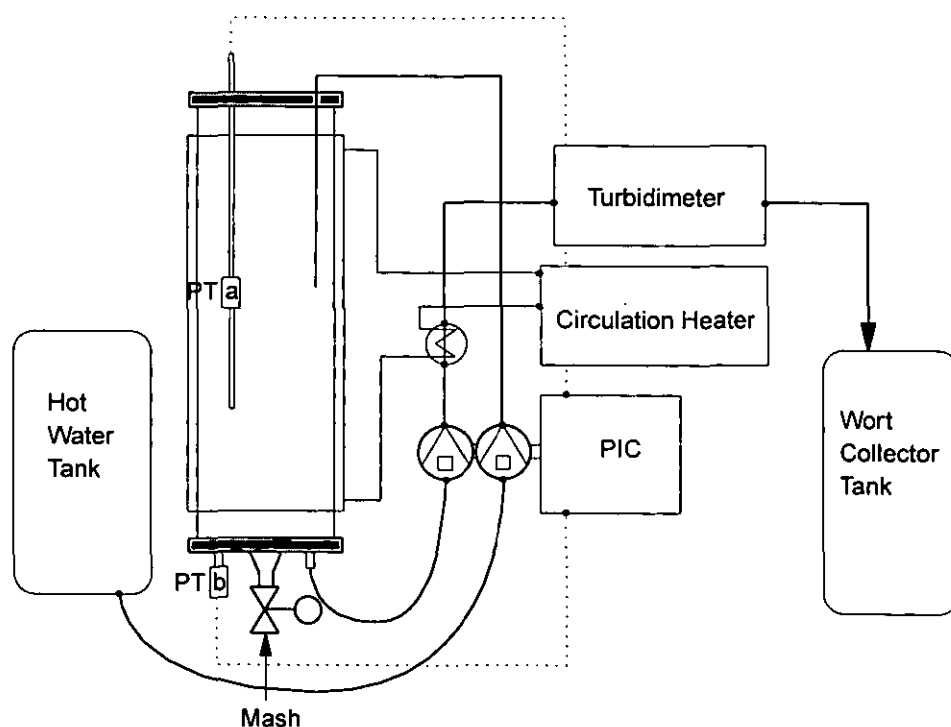


Figure 3.7: Lauter Tun Setup

The turbidity of the filtrate is analysed in-line with a nephelometer type turbidity meter. As turbidity of wort changes with temperature, the filtrate needs to be kept at a constant temperature under different flow rates. This was accommodated by a laboratory glass shell and tube heat exchanger,

installed ahead of the turbidimeter. After turbidity measurement, the filtrate is collected in a 12 ℓ graduated glass aspirator bottle.

The bottom plate of the lauter tun which includes the false bottom was made of a stainless steel plate with a mash inlet in the centre and two tappings below the false bottom for the filtrate outlet and for the bottom pressure transducer. Figure 3.8 shows the details of the design. A stainless steel wire mesh (BOPP, Zurich, Switzerland) with an aperture size of 600 μm was inserted into the solid bottom plate as false bottom and clamped into position in the centre and at the outer circle by rings. The active filter area of the false bottom was calculated to be 0.0134 m^2 .

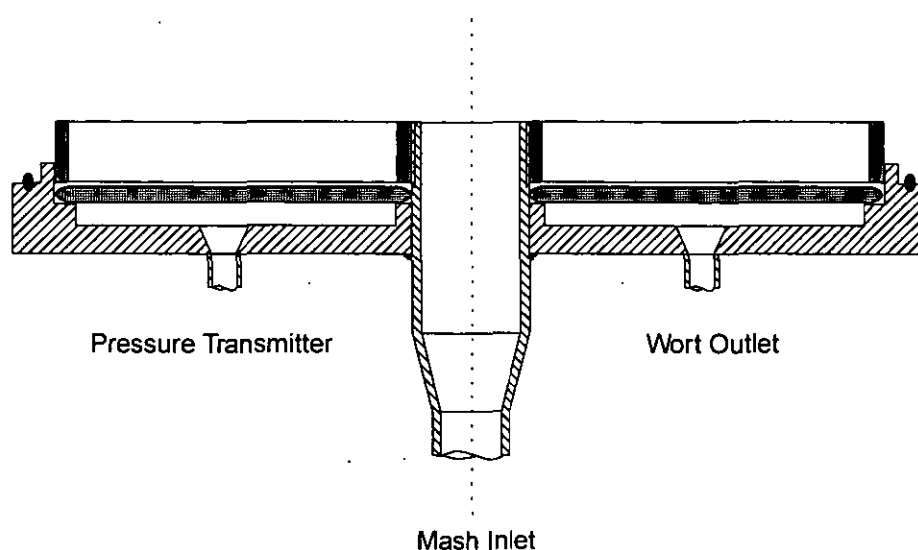


Figure 3.8: Bottom plate for the lauter tun

3.2.2.1. Design Specification

The specific load for a lauter tun is typically in the range from 150 to 250 kg m^{-2} . For the pilot scale trials, a load of 170 kg m^{-2} dry malt grist was selected. This represents a good value for normal lauter tun operation.

To achieve this value with the floor area in the pilot lauter tun 2.27 kg m^{-2} are required. At a water to grist ratio of 3.5 to 1, 7.95 litres of water will be in the mash. Malt grist requires a volume of 0.7 ℓ per kg of grist. Thus the total volume of mash in the lauter tun will be:

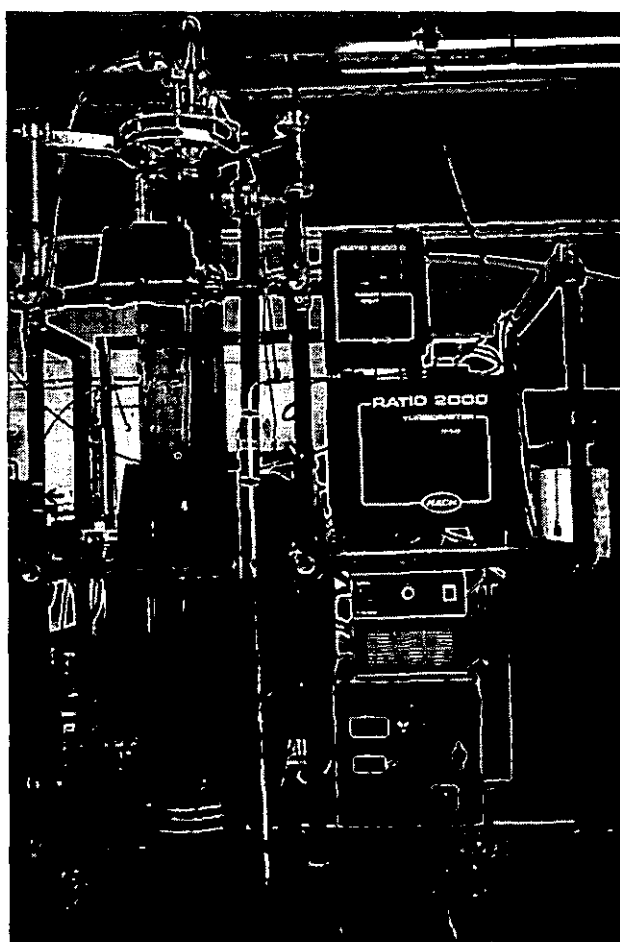
$$7.95\ell + \left(0.7 \frac{\ell}{\text{kg}} \times 2.27\text{kg}\right) = 9.5\ell \quad 3.3$$

This volume of mash requires a height in the lauter tun of 0.527 m.

Maximum flow rate in the lauter tun should be set to $0.12 \ell \text{ m}^{-2} \text{ s}^{-1}$. This specific flow rate requires a pump which delivers:

$$0.12 \frac{\ell}{\text{m}^2 \text{ s}} \times 0.0134 \text{ m}^2 = 1.608 \times 10^{-3} \frac{\ell}{\text{s}} = 96.5 \frac{\text{ml}}{\text{min}} \quad 3.4$$

To achieve this flow rate, a peristaltic pump (Watson-Marlow, Falmouth, UK) with 3.2 mm i.d. silicone tubing and speed control was used. The peristaltic pump revolution rate was controlled by the differential pressure between the two pressure transmitters (PT a and PT b at the column, Figure 3.7).



Picture 3.2: Pilot lauter column with peristaltic pump, control equipment and turbidimeter

3.2.2.2. Calibration Procedure

The pump control was set up to reduce the flow rate with increasing suction across the bed. This condition simulates practical conditions of large scale equipment very well, where neither differential pressure nor filtrate flow rate are constant. Transmitter 'a' was calibrated to read zero at atmospheric pressure. Transmitter 'b', below the bottom plate, was adjusted with hot water (75°C) in the column filled to the level of transmitter 'a', to give a zero reading at the differential pressure output dp . The slope of the flow rate versus the differential pressure of the pump was then calibrated by changing the water level in the column. This allows to simulate differential pressure conditions. Figure 3.9 shows four possible calibration points. The flow rate was adjusted (for a defined pipe dimension) to maximum flow at $dp = 0$ mbar. This maximum flow is set at $0.16 \text{ l m}^{-2} \text{ s}^{-1}$, with the variable potentiometer setting of the pump at 4.0. The second condition for the pump speed is $dp = 30$ mbar. At this pressure the pump speed should be zero.

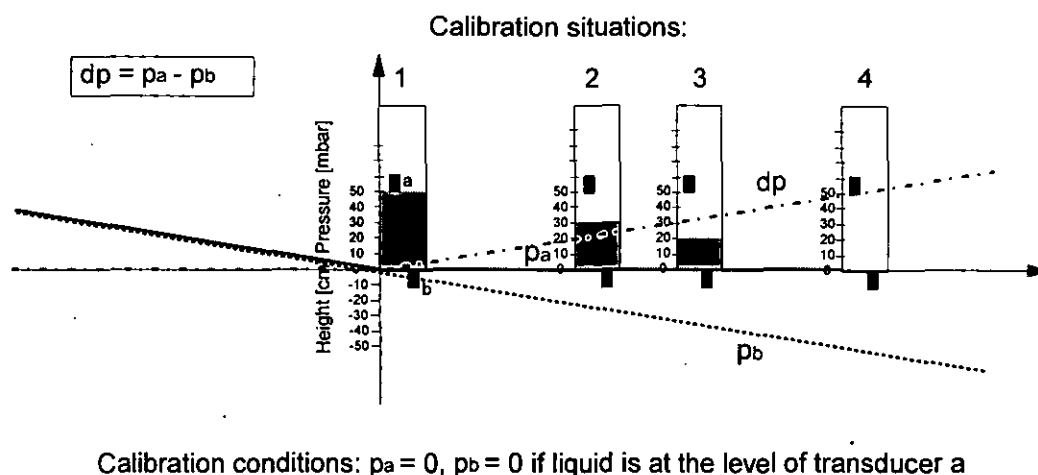


Figure 3.9: Calibration procedure for the lauter tun pump control unit

Figure 3.10 shows the calibration curve a potentiometer setting of 4.0. The relationship between flowrate and pressure drop can be described by a second order polynomial equation. A direct correlation between rotation speed (min^{-1}) and flow rate (g min^{-1}) was found for the silicon tubing. The flow rate at 0 mbar is 98 g min^{-1} which is equal to a specific flux of $0.12 \text{ l m}^{-2} \text{ s}$.

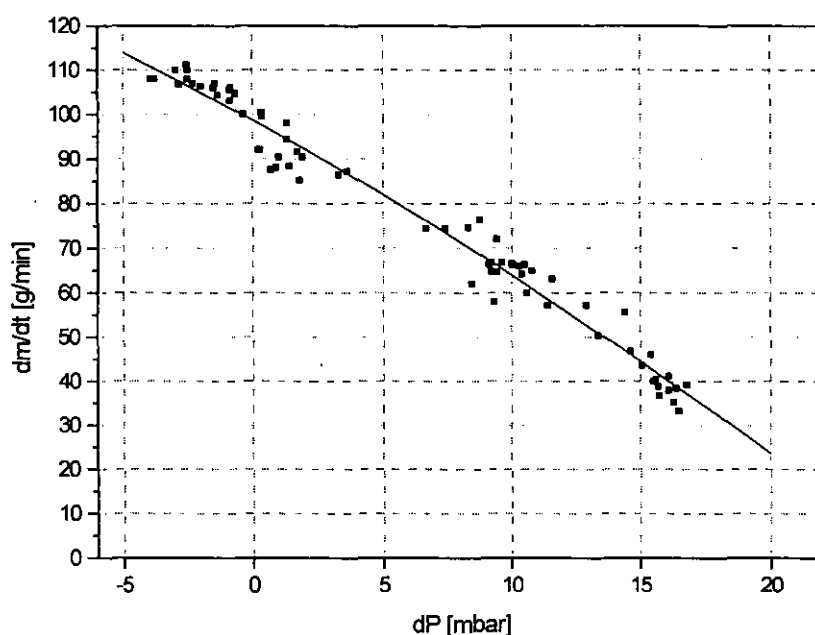


Figure 3.10: Calibration curve for the setting 4.0

The flow is zero at a differential pressure of 25.4 mbar. The relationship between differential pressure and flow rate can be described by the following equation 4.5:

$$dV/dt [\text{g/min}] = 98.707 - 3.193 \times dp [\text{mbar}] - 0.0279 \times (dp[\text{mbar}])^2 \quad 3.5$$

3.2.3. Bench Scale Mashing

Mashing was carried out in the BRFI Mashing Bath, a purpose built water bath with accurate temperature control (IOB, 1977). 500 ml of mash can be prepared in stainless steel beakers (see Figure 3.12). These beakers are inserted into the bath and held in position by rubber seals. The mash samples can be stirred by magnetic flea at two speeds or, more accurately

by an external stirrer described later. Stirring of the mash is not essential in this setup, because of the indirect heating no over-heating can occur.

The experimental conditions in the mashing bath were similar to the pilot scale trials. The mashing programme used a constant temperature of 65°C for 45 min and "mashing-off" of 75°C. The temperature rise from 65 to 75°C was achieved in 10 minutes. Mash samples were chilled to 20°C after 70 min total mashing time. Samples were stored in an ice bath and analysed immediately afterwards. The mash volume was 420 ml with a liquor to grist ratio of 3.5 : 1, in three trials higher concentrated mash was used (270 ml \equiv 2.5 : 1; 350 ml \equiv 2.8 : 1; 390 ml \equiv 3.2 : 1) to investigate higher power input. The higher concentrated samples were re-diluted after the mashing process to a liquor to grist ratio of 3.5 to 1. This made the results of the filterability tests comparable. Agitation was controlled using a Haake Rotovisco measuring head M1500 with a RV100 drive unit. This equipment allows accurate control of angular velocity ω and measurement of the torque τ created by the stirrer. The stirrer used for the trials was a two bladed paddle design (see Figure 3.12). Specific power input into mash was calculated from equation 3.6 and 3.7.

$$P = \omega \times \tau \quad 3.6$$

$$P_{\text{spec.}} = \frac{P}{V} \quad 3.7$$

where

$P_{\text{spec.}}$: specific mechanical power input per litre of mash

P : total power input

V : mash sample volume

Maximum tip speed achieved with the (paddle diameter: 40 mm) stirrer was 1.05 m/s. To adapt the velocity gradient between wall and blade to industrial scale, a smaller clearance, of 10 mm, from the bottom of the beaker was used. This increases the velocity gradient as calculated in Section 3.2.3.4. Direct monitoring of the velocity profiles, however, was not possible.

3.2.3.1. Torque Measurement in Laboratory Scale Mashing Trials

To enable a quantitative determination of the mechanical energy put into mash by a stirrer, it was necessary to measure the torque at the shaft of the stirrer and its angular velocity.

Measurement of torque at the shaft of a stirrer was facilitated using a Haake, Rotovisco RV100 (Haake, Karlsruhe, Germany) with an M 1500 measuring-drive unit. The RV100 provides the possibility to create a constant angular velocity in a range from 0 to 50.6 s^{-1} (which can be selected at the RV100 in a linear range from $D=0$ to $D=100\%$) at the M1500 drive unit.

Angular velocity ω and the velocity setting D at the instrument are related by:

$$\omega = 0.50508 \times D \quad 3.8$$

To create agitation in a beaker, a two-paddle impeller was used (see Figure 3.11). The torque created at the stirrer shaft was measured, over the mashing time, at the M1500 measuring unit and recorded at the RV100 as τ -t plot. Figure 3.11 shows an example of a typical plot. A factor at the ordinate τ enabled to adjust for a suitable sensitivity of the recording.

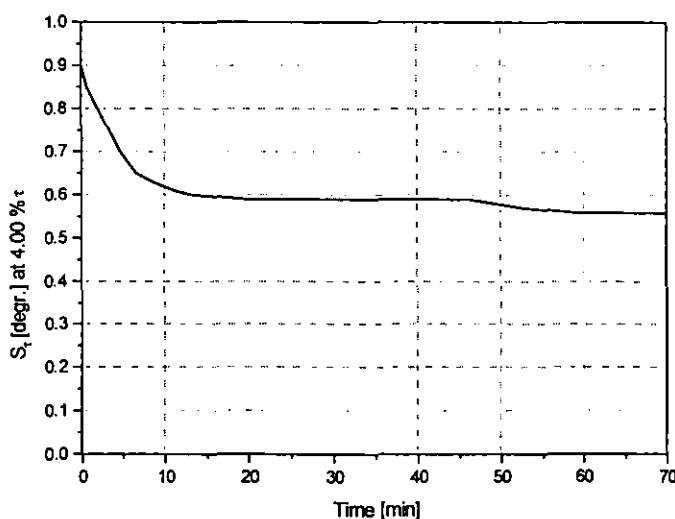


Figure 3.11: Example for a torque vs. time plot

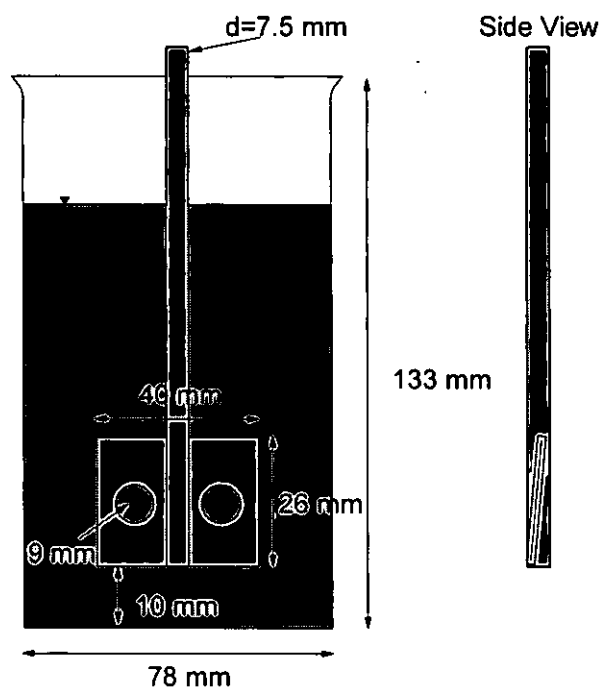


Figure 3.12: Bench scale experimental setup: Mash beaker and stirrer

3.2.3.2. Data Processing

To calculate a mean torque over the mashing time, the area under the curve (Figure 3.11) was integrated using Microcal Origin. In the example shown in Figure 3.11 an area of 42.0809 degr.min was calculated. The mean torque can then be calculated to:

$$\frac{42.1 \text{ degr.min}}{70 \text{ min}} = 0.60 \text{ degr.} \quad 3.9$$

The scale units (degr.) of the ordinate have been adjusted by a sensitivity factor of 4% which leads to:

$$0.60 \text{ degr.} \times 4\% = 2.4 \text{ degr.} \quad 3.10$$

The measuring-drive unit has been supplied with a constant which relates the scale graduations measured and recorded to the torque at the shaft.

The M1500 has a constant of $0.147 \text{ Nm degr}^{-1}$. With this constant the mean torque τ acting at the stirrer can be calculated:

$$2.4 \text{ degr.} \times 1.47 \times 10^{-3} \text{ Nm. degr.}^{-1} = 3.53 \times 10^{-3} \text{ Nm} \quad 3.11$$

In the given example, an angular velocity ω of the stirrer of 40.4 s^{-1} has been set. It is now possible to calculate the average power input P in the mash:

$$P = \omega \times \tau = 40.4 \text{ s}^{-1} \times 3.53 \times 10^{-3} \text{ Nm} = 0.14 \text{ W} \quad 3.12$$

The specific power input is the average power input related to the mash volume. Standard trials have been undertaken with a total volume V of 420 ml.

$$P_{\text{spec.}} = \frac{P}{V} = \frac{0.14 \text{ W}}{0.42 \text{ l}} = 0.33 \text{ W l}^{-1} \quad 3.13$$

3.2.3.3. Calculation of Shear Rates

Direct measurement of velocity profiles in the mash has not been possible, but the maximum shear rate can be calculated with one assumption.

If we assume a linear velocity gradient in the liquid, the velocity gradient will be maximum at the gap where the stirrer tip is closest to the wall. This condition applies at the gap between stirrer and bottom. The gap is 10 mm. Shear rates can then be calculated using equation 3.14:

$$G = \frac{(v_{\text{tip}} - v_{\text{min}})}{(d_{\text{gap}})} \quad 3.14$$

If the liquid velocity at the wall v_{min} is zero the equation can be simplified to:

$$G = \frac{v_{\text{tip}}}{d_{\text{gap}}} \quad 3.15$$

The shear rates determined using this equation have been plotted over the velocity of the tip (see Figure 3.13) for all trials. It can be seen that shear levels are in a range from 0 to 120 s⁻¹.

For large scale mash vessels, the following shear rate can be calculated using modern design requirements ($v_{\text{tip}} < 3 \text{ m s}^{-1}$; distance between stirrer-tip and bottom of the vessel, 0.05 m) described in Chapter 2.

$$G = \frac{v_{\text{tip}}}{d_{\text{gap}}} = \frac{3 \text{ m s}^{-1}}{0.05 \text{ m}} = 60 \text{ s}^{-1} \quad 3.16$$

This shows that small scale trials cover the same shear range as large scale applications.

3.2.4. Bench Scale Mash Filterability Test

A mash filterability test, designed as a quick comparability test for assessing the filterability of mash, has been developed. The sample volume is kept small to facilitate bench scale mashing experiments to be assessed. The test is carried out in a Millipore pressure filter cartridge with Whatman GF/D filter disks as filter medium; it requires a total operation time of about 20 min per sample.

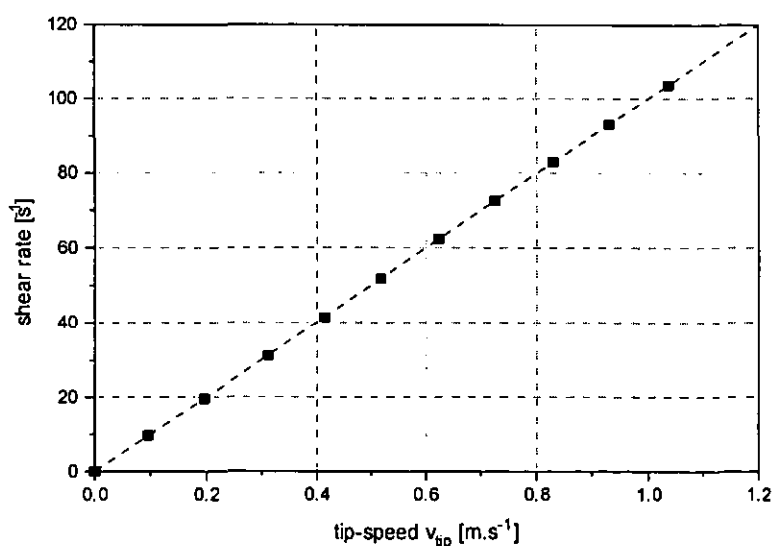


Figure 3.13: Shear rates in bench scale experiments calculated using the assumption of linear velocity gradient

3.2.4.1. Background

In order to analyse mash filterability in a reasonable time scale with a small sample volume it was necessary to develop a new analysis procedure. This test is designed to assess mainly the filterability of fines.

Previous trials, carried out in a pilot scale lauter tun confirm that fines (accumulating in the lauter tun in the upper layer of the cake) have predominant effects on lautering/filterability performance. Therefore results from a test focusing on the filterability of fines can be scaled-up for both mash filters and lauter tuns.

In the Millipore system, a spent grains cake similar to the lauter tun can not develop, as settling regimes, cake height and wall effects are totally different. Also, cake washing (sparging) and other procedures employed in large scale are not applicable.

3.2.4.2. Information Content

The Millipore Filter system in combination with a digital balance and printer can be used to determine filterability of mash in normal mash concentrations (Figure 3.14). From the slope of dt/dV vs. V plots the specific resistance of filter cakes and other filtration characteristics (such as the tendency for blockage) can be determined.

It is not appropriate to determine other cake properties (such as porosity) from the trials, as the size and structure of the cake is very different from large scale filters. Perhaps such information about the cake would be applicable for mash filter presses, if hammer milled malt is used.

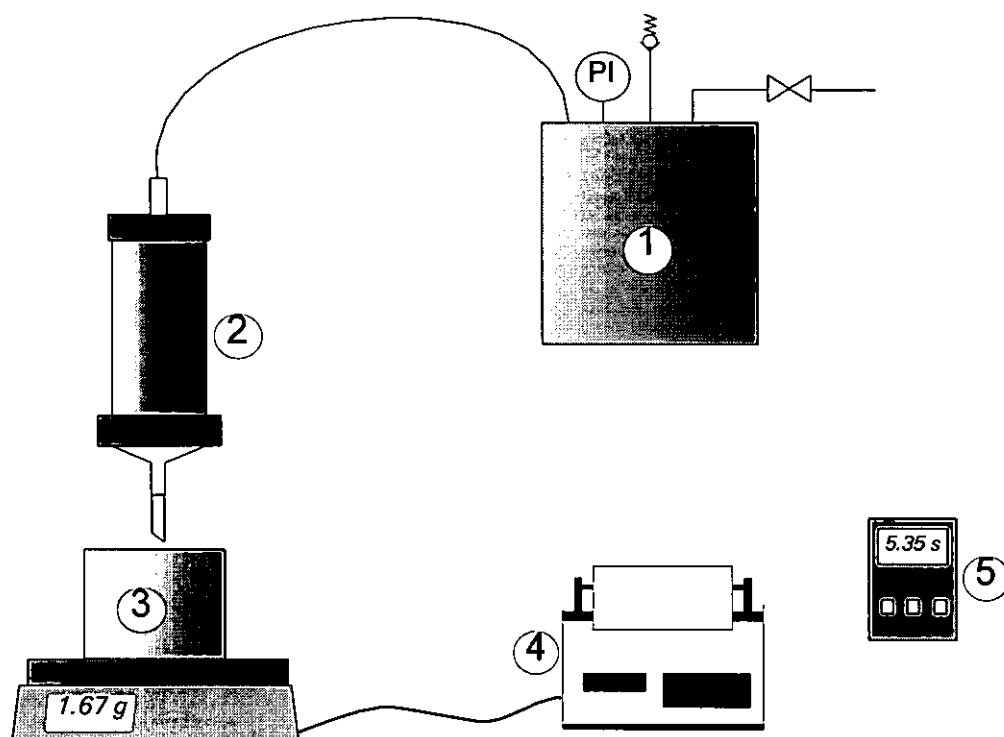


Figure 3.14: Bench scale mash filterability test

- 1 Pressure Vessel supplying constant pressure of 100 mbar
- 2 Millipore Filter
- 3 Digital Balance
- 4 Printer
- 5 Digital Stop Watch

3.2.4.3. Apparatus/Material

- Stainless steel pressure holder (Millipore, Watford, UK): diameter d_i = 3.5 cm, active filter area $A_{\text{filter}} = 9.62 \text{ cm}^2$
- Digital balance including printer: Mettler, High Wycombe, UK
- Digital stopwatch, accuracy $\pm 100 \text{ ms}$
- Low pressure device, supplying a constant pressure of $100 \text{ mbar} = 1 \times 10^4 \text{ Pa}$, measured at a pressure gauge, (Wika, Coulsdon, UK, range: 1 bar, accuracy: $\pm 1\%$)

- Water bath at 65°C

3.2.4.4. Operation

- Assemble the filter stand including balance, printer and low pressure vessel (see Fig. 3.14).
- Pre-heat filter including filter disk in the water bath (65°C).
- Shake sample well (50 - 60 ml in a centrifuge plastic tube) and pour into filter tube, keeping the outlet closed.
- Close lid and connect pressure tubing
- Open outlet
- Start filtration by opening valve to the low pressure device
- Print balance reading in constant intervals (0 - 1 min: every 5 sec; 1 - 5 min: every minute; then after 5, 7 and 10 minutes)

3.2.4.5. Processing of Results

Constant pressure filtration can be described using the following basic equation for cake filtration:

$$\frac{1}{A} \frac{dV}{dt} = \frac{A \Delta p}{\eta(\alpha c V + A R_m)} \quad 3.17$$

If R_m is zero, or the term allowing for the resistance of the filter medium is negligible, the equation reduces to

$$\frac{dV}{dt} = \frac{A^2 \Delta p}{\eta \alpha c V} \quad 3.18$$

or:

$$\frac{dV}{dt} = \frac{1}{KV} \quad 3.19$$

K can be determined by inverting the equation to:

$$\frac{dt}{dV} = K \times V$$

3.20

where K is the slope of the linear fit to the data sets in a dt/dV versus V plot.

Figure 3.15 shows an example of such a plot with linear functions fitted to the three sets of data.

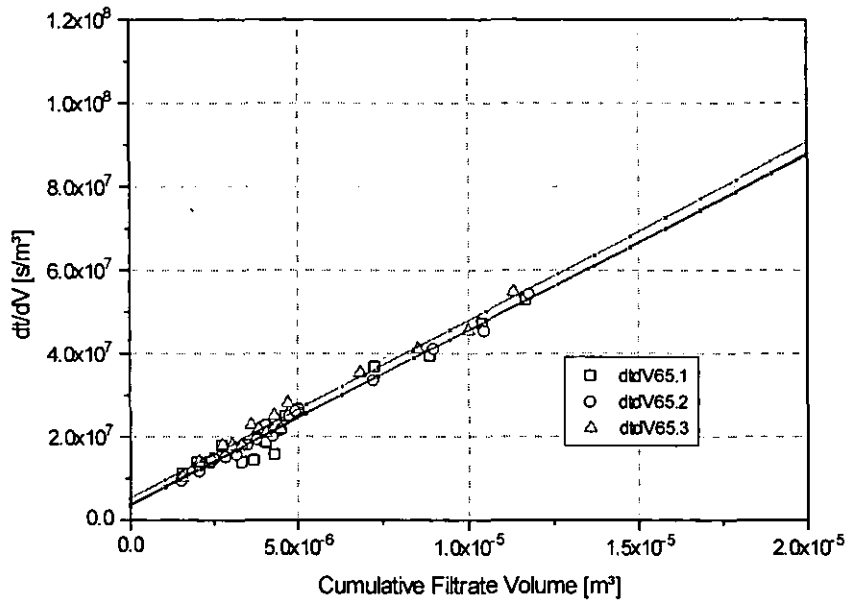


Figure 3.15: dt/dV versus V plot of reproducibility trials.

Slope K : (65.1): 4.216×10^{12}
 (65.2): 4.191×10^{12}
 (65.3): 4.276×10^{12}

3.2.4.6. Accuracy of Analysis

The repeatability of the filtration analysis was tested by analysing 3 samples, taken from the same mash (Trial 65). The slopes K of linear fits for the three trials have a variation coefficient of 1.027%.

3.3. Brewing Procedures

3.3.1. Milling

Milling of malt was carried out on a pilot scale two roller mill (Robert Boby, Bury St Edmunds, UK). On this mill the batch size for one brew (5 kg of malt) could be milled in about 25 minutes. The two rollers of the mill have the following dimensions:

- diameter of the rollers: 3"=7.62 cm
- width of the rollers: 2½"=6.35 cm
- revolution rate: 64 rpm

Figure 4.17 shows the mill. The gap between the two rollers is adjustable by a gear which moves the right roller. In addition the dosage of malt ahead of the gap can be controlled by an adjustable flap. The gap was set to 0.75 mm for all trials using the Blenheim malt batch. The gap is measured using a feeler gauge. In trials with undermodified malt quality the gap was set to 0.55 mm. These settings were found suitable to achieve a sieve distribution close to the recommended values given in literature for lauter tun processes. Details about the relevant experiments are given in Section 4.1.

The crushed malt grist was stored and transferred to the mashing in unit in a bucket with a lid. The milling procedure was usually done directly before mashing.

3.3.2. Mashing

The mashing in the pilot rig was carried out using 5 kg of grist and 17.5 kg of water (liquor to grist ratio 3.5 : 1).

After mixing water and grist, the mono pump was started and kept going for the entire mashing time.

The mashing procedure was adapted to the malt quality. For all trials an infusion mashing procedure with an initial mash temperature of 65°C was used. After 45 minutes the mash was heated to 75°C. The total mashing

time was fixed to 70 minutes. The heating rate was $0.6^{\circ}\text{C min}^{-1}$ at a mash volume of 21 litres (see Figure 3.17).

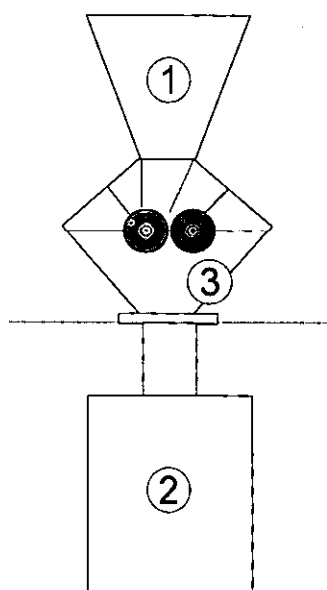
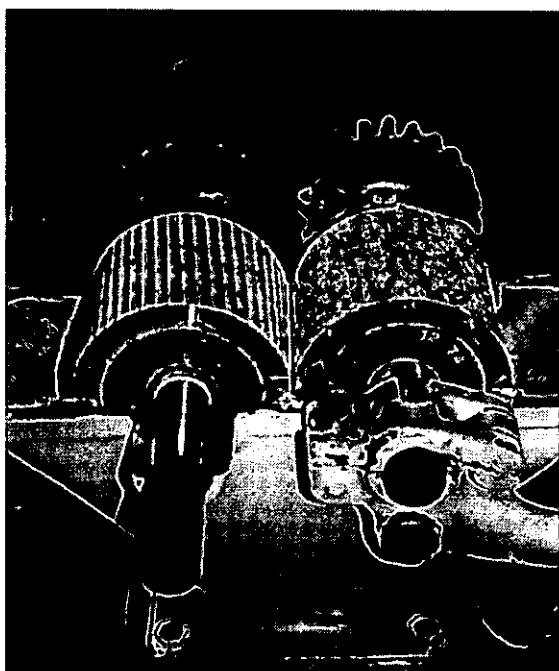


Figure 3.16: Schematic of the laboratory roller mill with
1. Hopper
2. 5 litre beaker
3. Milling chamber (adjustable parts in red)



Picture 3.3: Rollers of the mill

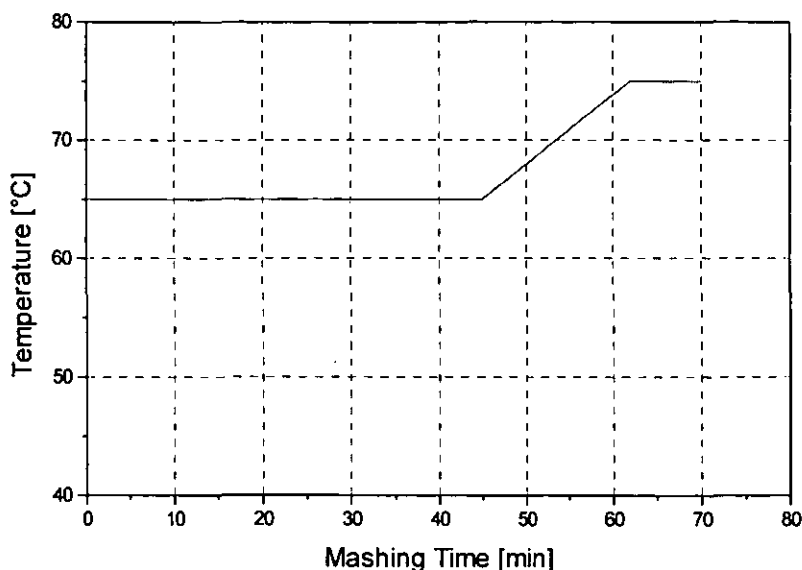


Figure 3.17: Temperature programme for mashing

3.3.2.1. Process Routine

In order to establish reproducible trial conditions all manual work had to be standardised. The following routine was set up:

1. Preparation, set the evening before the trial:

- Mash vessel - Temperature setting: 75°C, filled with water up to the edge of the cone.
- Liquor tank - Temperature setting: 72°C, filled with 120ℓ of reverse osmosis water.

2. Main Procedure:

- switch on temperature recorder
- circulate water in the MV until temperature is stable (about 65°C)
- switch off MV-heater and reset set-point of the temperature controller to 65°C
- pump the hot water into the lauter column
- add water from liquor tank (preheat pipework) about 15 seconds
- put mash grist into hopper

- start mashing in procedure - for 5 kg malt at 3.5 : 1 liquor to grist, leave pneumatic valve open for 82 seconds - after this the mashing timer is started
- start mash pump and switch on heater of the mash vessel
- Stir the mash gently for about 1 min to improve mixing
- adjust temperature controller to 75°C after 45 minutes

3. Mash transfer to the lauter tun

- stir the mash before the transfer
- open valve to the transfer pipe
- drain water/mash mixture into bucket
- switch the three way valve on the lauter tun mash inlet from draining to mash in position (mash starts to fill the lauter column)
- close the adjustable 90°-valve on the mashing plant to stop the mash to flow in the loop
- fill the column with mash to the 52.7 cm level
- switch the three way inlet valve immediately to drain position
- collect about 5 litres of mash sample in a beaker
- after the mash sample is collected, switch the mono pump off
- remove the sample from the drain pipe
- switch mash vessel heater off.

4. Shut down procedure

- remove the remaining mash from vessel and pipework, rinse and clean the plant

3.3.3. Lautering

The lautering procedure was used to analyse the filtration performance in terms of cake permeability, extraction/washing efficiency and the wort clarity. The following routine was used to get consistent information about the lautering performance.

3.3.3.1. Process Routine

1. Preparation, set the evening before the trial:

- fill the water tank of the lautering rig with reverse osmosis water
- heat the water up to 75°C

2. Main Procedure:

- fill the space between the lauter tun floor and the wire gauze with water from the bottom wort outlet to avoid air pockets to develop
- preheat the lauter column with hot water from the mash vessel
- start recirculation in the hot water loop of the lauter column jacket (set to 75°C)
- drain the water in the column just before pumping the mash in
- fill the mash into the column up to 9.5ℓ level (for details see mashing procedure)
- start the stop watch
- monitor sedimentation by measuring the height of the two interfaces (spent grains to fine particles phase and fine particles to clear headspace) every minute
- start filtration after 10 minutes by switching on the peristaltic pump
- monitor the following parameters during filtration every 5 minutes:
 - differential pressure
 - height of the fine particles and spent grains layer
 - total filtrate volume
 - extract in the filtrate (hand held refractometer)
 - haze reading at the turbidity meter
- switch off the pump when 11 litres of filtrate are collected

3. Shut down procedure

- release the silicone tubing from the peristaltic pump and drain the remaining water off
- discharge the spent grains by removing the bottom plate

- rinse and clean all parts of plant

During the lautering procedure mash samples were analysed to determine viscosity of the liquid phase of the mash at 75°C, density of the liquid phase of mash at 75°C, wet sieve analysis using a 1000 μm and a 150 μm sieve, extract concentration in the cold liquid mash phase (20°C) and particle size distribution of the fine fraction (that has passed a 106 μm sieve) in the mash.

The 11 ℓ wort sample was mixed and analysed immediately after the lautering for extract content, dry solids in the wort and particle size distribution. If required, samples were analysed for chemical composition.

The data collected during a trial were processed using QuattroPro (Borland, Twyford, UK) spreadsheets and Origin (MicroCal Software, Northampton, MA, USA) data analysis software. Examples of the standard lautering graphs are given in Figure 3.18.

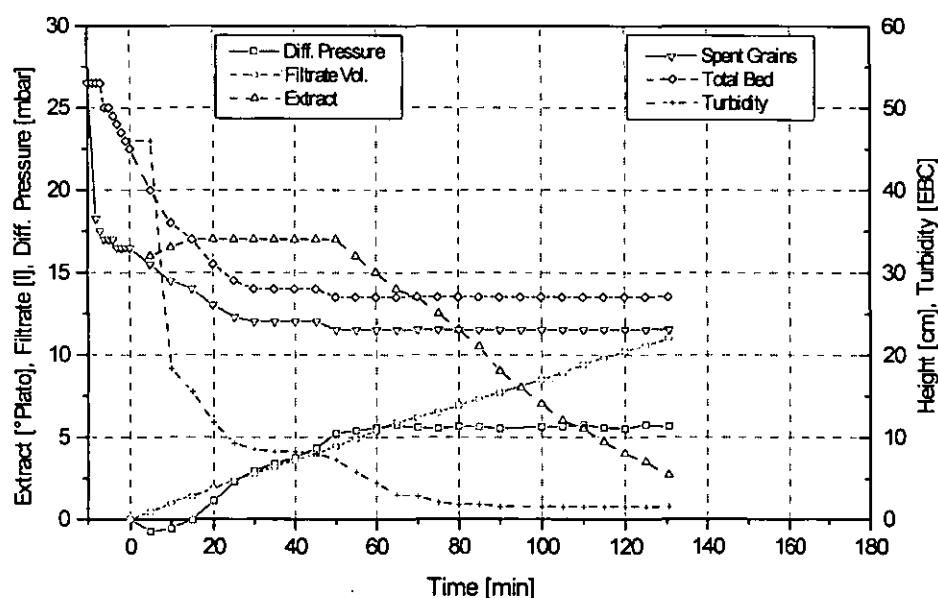


Figure 3.18: Lautering graph for a standard run

3.4. Analyses

3.4.1. Viscosity Analysis

The viscosity of wort and the liquid phase of the mash were determined at a run off temperature of 75°C directly after mashing/lautering. These analyses were determined in a falling ball viscometer ('Höppler' Viscometer, Zeiss, Jena Germany). The apparatus is displayed in Figure 3.19.

3.4.1.1. Measuring Principle

This instrument measures the time it takes for a ball to pass two ring marks in a cylindrical glass tube. This glass tube is inclined by an angle of 10° with respect to the vertical axis. This viscometer is designed to measure low to medium viscous and clear liquids which show Newtonian behaviour.

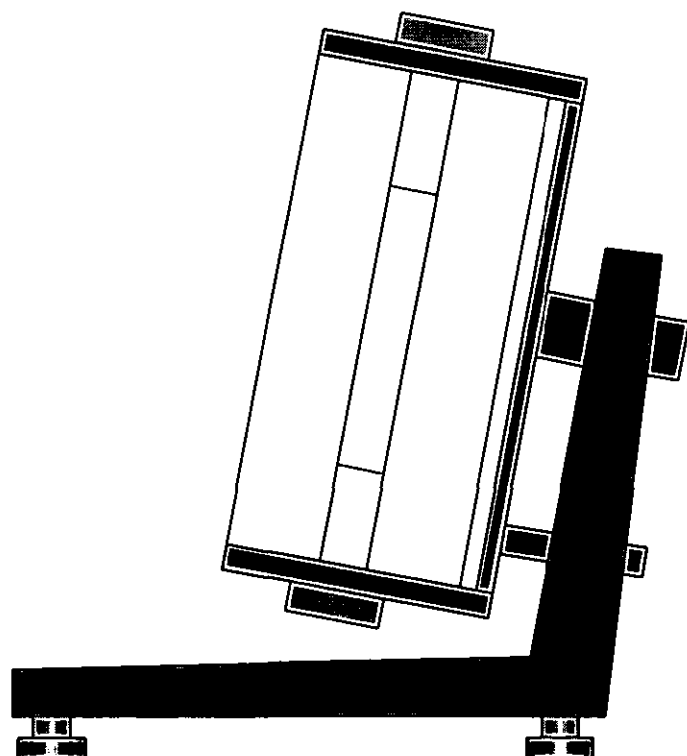


Figure 3.19: Falling ball viscometer

The system temperature is controlled by a water bath with circulation of water through the jacket of the viscometer. To move the ball to the top of

the tube the entire jacketed glass vessel is turned round by about 180°. To obtain a sufficient accuracy from the analysis, the fall of the ball was measured 4 times.

The dimensions of the glass ball had to be determined before the trials.

Glass ball dimensions:

Diameter: $d = 0.622 \text{ inch} = 1.580 \text{ cm}$

Volume: $V = \frac{1}{6} \pi d^3 = \frac{1}{6} \pi (1.580 \text{ cm})^3 = 2.065 \text{ cm}^3$

Mass: $M = 4.9579 \text{ g}$

Density: $\rho = \frac{m}{V} = \frac{4.9579 \text{ g}}{2.065 \text{ cm}^3} = 2.401 \frac{\text{g}}{\text{cm}^3}$

3.4.1.2. Calibration Constant of the Glass Ball:

The calibration trials were carried out with de-ionised water at 20 °C.

Properties of water: (at 20°C)

- dynamic viscosity $\eta_w = 1.002 \text{ mPas}$
- density $\rho = 0.9982 \text{ g/cm}^3$

time for the ball to fall between the two lines:

$\bar{t} = 67.87 \text{ s}$ (mean value: 67.87; standard deviation: 0.1388 s; variation coefficient: 0.2%)

Calculation of constant K_{b1} :

$$K_{b1} = \frac{\eta_w}{t(\rho_{b1} - \rho_w)} = \frac{1.002 \times 10^{-3} \text{ Pa s}}{67.87 \text{ s} (2.401 - 0.9982) \frac{\text{g}}{\text{cm}^3}} = 0.01054 \times 10^{-3} \frac{\text{Pa cm}^3 \text{ s}}{\text{g}}$$

3.18

The dynamic viscosity of a sample is calculated from the following formula:

$$\eta = t(\rho_1 - \rho_2) K_{b1} \quad 3.19$$

where:

η	dynamic viscosity	[mPas]
t	fall time of the ball	[s]
ρ_1	density of the ball	[g cm ⁻³]
ρ_2	density of the liquid	[g cm ⁻³]
K_{b1}	ball constant	[mPas cm ³ g ⁻¹ s ⁻¹].

3.4.1.3. Analysis Procedure

A sample of hot mash is filtered through pleated filter paper. The first 200 ml of the filtrate were transferred to the viscometer and the density bottle. Hot filtration together with use of the first 200 ml ensured that blinding of the filter and changes of the cut off size were minimal. Both analyses were measured directly after the sampling. This ensured that no gas bubbles occurred in the analyses.

The time interval for the fall of the ball was recorded four times, in order to reduce inaccuracies in temperature or stopping time.

The density bottle's temperature was adjusted in the water bath until equilibrium was reached (about 10 min). After that the bottle was chilled with cold water, in order to avoid evaporation, and measured immediately.

3.4.2. Filtrate Turbidity Analysis

The turbidity of the filtered wort is measured in an in-line turbidity meter (Ratio 2000 Turbidimeter, Hach, Namur, Belgium). The Ratio 2000 turbidimeter is equipped with three light detectors. One detects light at 90° angle, the second detects light transmitted through the sample, after being reduced in intensity by a 'black' mirror, and the third detects light scattered in a forward direction. This arrangement makes it possible to measure the nephelometric signal ratioed against a weighted sum of the transmitted and forward scatter signal. This ratioing improves the stability of the signal over long term and compensates for dust on optics. The turbidimeter was operated in a range from 0 to 200 NTU (Nephelometer Turbidity Units) which is equivalent to 0 to 800 EBC Units. Calibration was carried out with formazin standard solutions according to the operating handbook.

3.4.3. Coulter Counter, LS130

Sieved mash and wort samples were analysed on the laser sizer for all trials. In addition some samples of different sections of the spent grains cake were analysed.

Two different particle sizing methods are combined in the LS 130, (Coulter Electronics, Luton, UK) which enables the sizer to measure particles in a total size range from 0.1 to 900 μm .

3.4.3.1. Diffraction Sizing

The LS series uses laser light at 750 nm to size particles from 0.4 to 900 μm by light diffraction. The laser radiation passes through a spatial filter and projection lens to form a beam of collimated light. The sample cell of the fluid module shapes the suspension fluid into a thin sheet (3 mm) that flows at right angles to the laser beam's light path. This measurement geometry minimises the number of particles that re-scatter light, scattered from other particles in the cell.

A Fourier lens collects the diffracted light up to about 15° and focuses it onto two sets of detectors: one for the low-angle scattering and the other for mid-angle scattering. A second Fourier lens system collects the diffracted light from about 10° to 35° and focuses it into a third set of detectors.

3.4.3.2. Measurement

The fluid module's sampling system pumps the suspension fluid with sample particles through the diffraction sample cell where laser light is directed onto the particles for particle measurement. As the particles move through the cell, the collimated laser light is scattered, or diffracted, from each particle. A diffraction pattern is the pattern of scattered light intensity as a function of scattering angle, or simply by the amount of light scattered by the particle in different directions. The diffraction pattern of each particle is characteristic of its size.

The LS130 measures particle size by measuring the combined particle size-dependent diffraction patterns by means of a Fourier lens.

A Fourier lens is an ordinary lens that is used in a special way which gives it special properties. A Fourier lens is focusing any light striking the lens at a given angle onto a single annular area on its plane of focus, the Fourier plane. The Fourier lens is sensitive only to the angle of the light rays incident on it and not to the position of the source of light.

The Fourier lenses used in the LS 130 are used to focus light scattered at a given angle from any particle anywhere in the diffraction sample cell, independent of the particle speed, onto a single annulus on the detector plane. The result is that the Fourier lens forms an image of the entire diffraction pattern of each particle, the image being centred at a fixed spot on the Fourier plane. This image is centred at the same fixed spot regardless of the position or velocity of the sample of the particle in the diffraction sample cell. The individual diffraction patterns from the moving particles in the sample cell are superimposed, creating a single composite diffraction pattern that reflects the contributions of each particle. This composite diffraction pattern can be accurately sensed by the detectors judiciously placed on the Fourier plane.

3.4.3.3. Determining the Size Distribution

The diffraction detector system consists of 126 photo diode detectors in three sets. These are the low-angle (mainly for large particles), mid-angle (mainly for average particles) and high-angle (mainly for small particles) sections. Each detector is placed at a known angle from the optical axis. Since a particular sample always contains particles of different sizes, each with a corresponding set of diffraction patterns, the detectors produce an integrated flux pattern that contains composite size information for all the particles in the sample. This integrated flux pattern is decomposed into a number of diffraction patterns one for each size classification. The relative amplitude of each classification is used to measure the relative number, surface area or volume of particles of that size range.

3.4.3.4. PIDS Sizing

The LS130 provides the primary size information for the particles in the 0.1 to 0.4 μm range and enhances the resolution of the size distributions up to 1 μm . This additional measurement is needed because it is very

difficult to distinguish particle sizes by diffraction patterns alone when the particles are smaller than 0.5 μm in diameter.

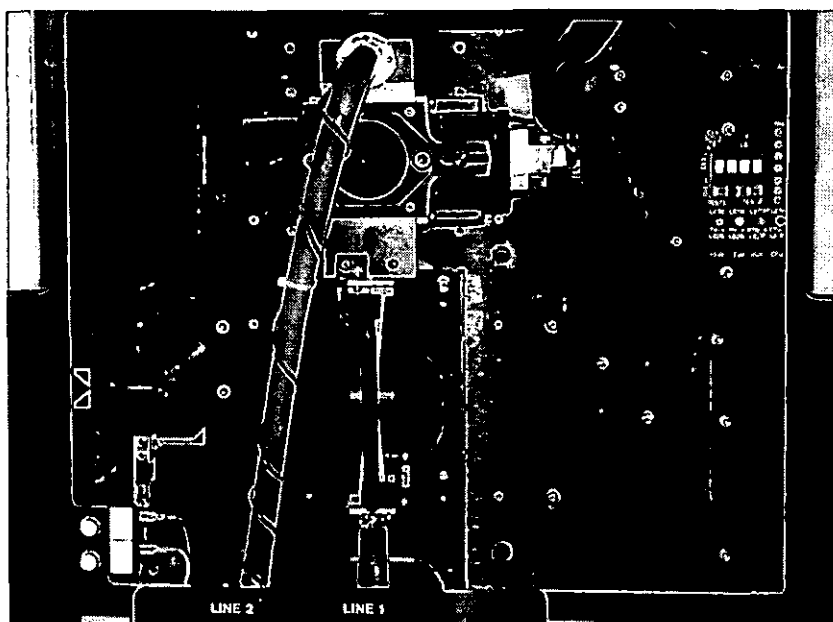
Polarisation Intensity Differential Scattering (PIDS) is based on a polarised light source. For particles in the range of sizes close to the wavelength of light, the difference in scattering of vertically or horizontally polarised light, when the scattering is observed at roughly right angles to the direction of propagation of the light, depends on the ratio of particle size to the wavelength of the light wave.

To get as much information as possible about the small particles measured by the PIDS assembly, it illuminates polarised light of three different wavelengths (colours). The three wavelengths of light permit three different ratios of particle sizes to light wavelength.

The PIDS assembly uses an incandescent tungsten halogen lamp and three sets of vertically and horizontally polarised filters to provide polarised monochromatic light at three different wavelengths: 450nm (blue), 600nm (orange) and 900nm (near-infrared). The light is focused through a slit that acts as a spatial filter and is formed into a narrow, slightly diverging beam that is projected through the PIDS sample cell.

The intensity of the light scattered in the plane perpendicular to the flow is measured at five different angles by photo detectors in the PIDS detector assembly. A sixth detector behind the cell measures the intensity of the un-scattered light to determine the amount of obscuration.

For three wavelengths, the different scattering pattern is detected at the five detectors. In total, the PIDS assembly makes 30 measurements of the light scattered from the sample: scattered light of two polarisations at three wavelengths and five scattering angles. These 30 measurements are then reduced to 15: the difference in scattering between the two polarisations measured at each of the three wavelength and five scattering angles. The 15 measurements form a pattern that varies sensitively with particle size.



Picture 3.4: Laser Sizer sample cell with laser diodes and PIDS assembly

3.4.3.5. Data Processing

The Laser Sizer LS130 acquires particle size information in 100 channels. Channels are logarithmic, progressively wider in span. For statistical data processing the median size at the centre of each channel is employed. The logarithmic median diameter d_{LC} (in μm) is calculated as follows:

$$d_{LC} = \text{antilog} \left[\frac{\log_{\text{lower boundary}} - \log_{\text{upper boundary}}}{2} \right] \quad 3.20$$

where d_{LC} is the logarithmic diameter.

To calculate the weightings, the median size is converted into the appropriate units. For example the formula for the weighting for volume in [μm^3] is:

$$\mu\text{m}^3 = \frac{(d_{LC})^3 \pi}{6} \quad 3.21$$

All experimental results refer to the geometric mean particle size (MPS) of a size distribution which can be calculated from the distribution:

$$MPS = \text{antilog} \left[\frac{\sum (n_c \times \log \bar{X}_c)}{\sum n_c} \right] \quad 3.22$$

\bar{X}_c = median size of the channel in μm for diameter, μm^2 for area and μm^3 for volume.

3.4.3.6. Sample Preparation for the Laser Sizer

60 ml of mash were diluted in 340 ml of cold tap water. This suspension was mixed and sieved through a 106 μm sieve. It is important that the sieve is pre-wetted to obtain a good sieving effect. Larger aperture sieves (710 μm and 250 μm) were tried first but larger particles passed through these sieves and masked any change in volume size distributions in the regions of interest. The sieved suspension was then added into the sampler (hazardous fluids module) of the Laser Sizer. The analysis of mash should be done directly after the mashing procedure.

3.4.4. Coulter Multisizer II

The Coulter Multisizer II has been employed as an alternative particle sizing apparatus to determine size distributions of fine particles (<106 μm class) in the mash.

The Multisizer II determines the number and size of particles suspended in a conductive liquid by monitoring the electrical current between the electrodes immersed in the conductive liquid on either side of the aperture, through which a suspension of the particles is forced to flow. As each particle passes through the aperture, it changes the impedance between the electrodes and produces an electrical pulse of short duration having a magnitude essentially proportional to the particle volume. The series of pulses is electronically scaled, counted and accumulated in a number of size related channels which, when their contents is displayed on the integral Visual Display, produces a size distribution curve.

The analyses were carried out using a 140 μm orifice tube which gives an analysis range from 2.504 to 77.96 μm . The size range is split logarithmically into 64 channels. The volume of suspension analysed was 500 μl .

50µl of the sample suspensions from the laser sizing (dilution 60 ml mash in 340 ml of water) analysis were diluted in 10 ml isotone. This is equal to a dilution rate of the mash of 1 to 1133.

3.4.5. Statistical Evaluation of Data

Particle size analysis and all other data were processed using either the built in computer facilities of the LS130 or by Origin, (MicroCal Software Inc., Northampton, MA, USA).

Where applicable standard deviation, coefficient of variation and confidence limits at 95% confidence were calculated.

In the LS 130 program the standard deviation of a distribution is calculated as:

$$SD = \sqrt{\frac{\sum [n_c (\log \bar{X}_c - \log \bar{X}_g)^2]}{\sum n_c}} \quad 3.23$$

where SD is the standard deviation, and n_c is the percentage of particles in each channel.

In more general statistical evaluations of analytical results, the standard deviation of the sample is calculated using:

$$SD = \sqrt{\frac{\sum_{i=1}^n (x_i - \bar{x})^2}{n-1}} \quad 3.24$$

The coefficient of variation, CV , is the standard deviation divided by the mean. It relates the measure of distribution to the average about which it is measured, as a percentage. Thus it measures the relative variation as opposed to the absolute variation, which is useful for comparing the distribution in different sets of data.

$$CV = \frac{SD \times 100\%}{\bar{x}} \quad 3.25$$

95% confidence limits were used to describe the size range ($\pm 2 \times SD$) about the mean value within which 95% of the values should fall.

3.4.6. Wet Sieving of Mash

This analysis was found suitable to detect the change in particle size during the mash conversion under different agitation regimes.

An evenly distributed mash sample volume was taken from the outlet of the mashing vessel, after filling the lauter column. 146.5 ml of mash were then added on top of a 1000 μm sieve. The mash is then washed through the 1000 μm and through a 150 μm sieve below it by spraying with tap water. The sieved suspension was collected in a bottom tray. Both sieves were then placed into a drying cabinet for 24 hours at 120°C. The liquid volume of the bottom tray was determined and 10 ml of this suspension were filtered through a Whatman No. 541 filter paper, to determine the dry solids of the fines. It proved impossible to filter the entire suspension as it showed a very bad filterability. Hence only a small quantity was analysed. The dry weight was re-calculated for the weight in the total sample. The relative concentrations in the three fractions of the mash samples were expressed as percent of the total weight of particles.

3.4.7. Scanning Electron Micrographs

Mash particles from different sections of a filter cake were analysed after lautering on the BRFI electron microscope (Phillips, Holland).

Different sections of filter cakes from two trials and the fines layers of two additional samples were analysed with this technique. Before analysis they were stored at -20°C. For the scanning samples were frozen in liquid nitrogen at -196°C then observed at -185°C. The results are shown in Appendix 7.2.

3.4.8. Other Physical and Chemical Analyses

The liquid fraction of mash and wort samples after lautering were analysed for their chemical composition. The following analyses were carried out by following standardised analysis procedures specified by the European Brewery Convention (Analytica EBC, 1988):

- Free Amino Nitrogen (FAN)
- Total Soluble Nitrogen (TSN)
- Polyphenols
- pH
- Colour
- Apparent Fermentability, F_A :

$$F_A = \frac{(G_{\text{bef.}} - G_{\text{after}})}{G_{\text{bef.}}} \times 100 \quad 3.26$$

where $G_{\text{bef.}}$ is the specific gravity before fermentation (°Plato) and $G_{\text{after.}}$ is the specific gravity after fermentation (°Plato).

Samples were analysed after storage in refrigerators 24 to 48 hours after lautering at the BRFI Quality Services Department, a NAMAS accredited laboratory.

Extract content in the mash and wort samples was measured off-line during mashing and lautering. Extract in the filtrate from the lauter tun was measured every five minutes during the trials on a laboratory hand-held refractometer (Fisons, Crawley, UK). The analysis has an accuracy of the reading of $\pm 0.25\%$ (w/w) extract. Samples of the filtered mash were measured with a hydrometer (Saccharometer, Glasbläserei der VLB Berlin, Germany) to determine the original extract content in the mash. The accuracy of the reading is $\pm 0.05\%$ (w/w) extract. The wort sample after lautering was also analysed with a hydrometer to obtain information about the dilution effect during cake washing.

3.5. Conclusion

This chapter describes the raw materials and the brewing procedures used in all trials. Some effort was put into developing standardised conditions for the trials, in order to achieve suitable reproducibility of the results. It can be seen that major emphasis was laid on the development of suitable analyses for filterability and lautering performance at either the laboratory or pilot scale.

The second part of this chapter describes the procedures used to analyse changes in mash composition. The second main emphasis of this work was put on the particle size analysis, especially of the fines fraction. The literature review showed that the relationship between particle size distribution of the fines in the mash and the influence on lautering performance is still unclear.

Particle sizing was verified by comparison of different analysis methods on the basis of laser diffraction sizing, electrozone measurement and electron microscopy. This was necessary mainly because the laser sizing, which is the most suitable analysis for most trials, is based on a model which relates the diffraction to the size.

Analyses of other physical conditions in the mash and the wort such as viscosity and extract concentration were also found very important. They can have direct influence on filterability of the mash.

Chemical analyses were employed to a lesser extent, not because of the availability of suitable methods, but more because the literature search indicated that even very sophisticated analyses could not show a clear relationship between mash/wort composition and lautering performance.

4. Results and Discussion

In this chapter the results of all trials are presented and discussed. Conclusions are drawn which guided subsequent trials and an overall conclusion is presented at the end.

4.1. Initial Trials

Chapter 4.1 reports the trials which were necessary to develop standard brewing conditions and verify the suitability of analysis procedures. In this chapter, the properties of different parts of the spent grains cake and the fines are also described.

4.1.1. Adjusting the Gap Setting of the Laboratory Mill

The milling of malt for all trials was carried out on a laboratory 2 roller mill (see Chapter 3.3.1). The gap was set to a distance suitable for grinding 'lauter tun grist'. This type of grist is defined by its sieve distribution. An 'optimum' sieve distribution for lautertun filtration performance was found empirically (e.g. Narziß, 1985). The gap setting between the two rollers had to be adjusted to achieve this optimum distribution of the grist. The following results were obtained for the three gap-settings tested (Figure 4.1). The sieve set used for the analysis (0.65 to 0.85 mm gap setting) was slightly different from the standard, recommended by MEBAK (Mittel-Europäische Brautechnische Analysen Kommission, 1987) (see Table 4.1). Table 4.1 shows the sieves used at BRFI in comparison to the standard Pfunststädter sieve set.

Figure 4.1 compares the sieve distributions obtained from three different settings of the laboratory mill with the optimum distribution recommended by Narziß (1985) for the use of two roller mills. This shows that the 0.75 mm setting is close to the recommended standard distribution. This gap setting was used for this batch of malt, for all trials.

Table 4.1: Sieve set and grit fractions

Fractions \ Sieve Set	Standard [μm]	BRFI [μm]
Husks	1270	1400
Coarse grits	1010	1000
Fine grits 1	540	500
Fine grits 2	250	250
Powder flour	150	150
Bottom	0	0

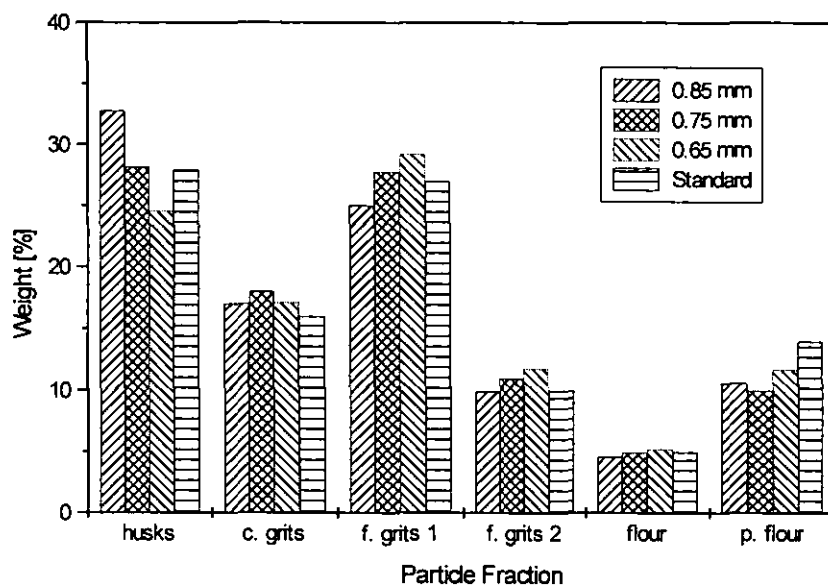


Figure 4.1: Sieve analysis for well modified malt

A more detailed sieve analysis has been carried out for the 0.75 mm gap setting. Figure 4.2 shows the sieve distribution.

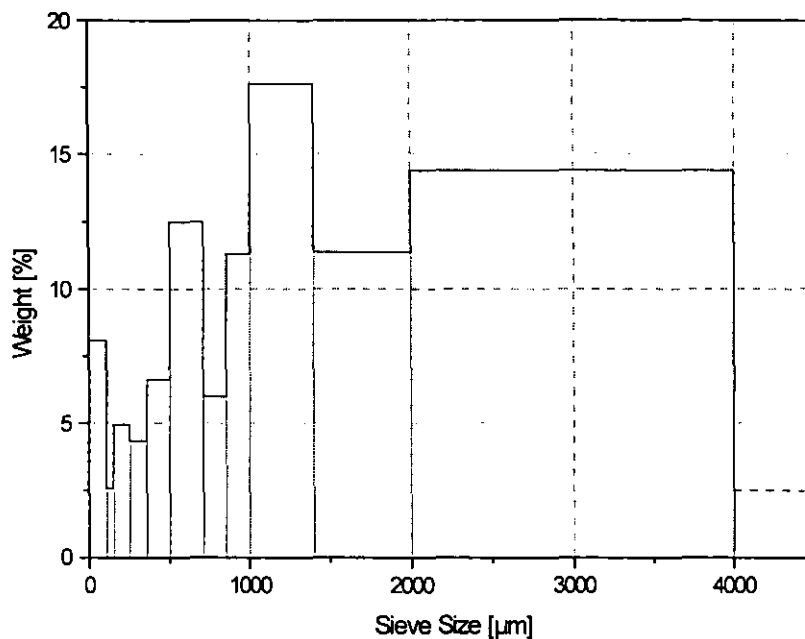


Figure 4.2: Sieve analysis for malt grist milled with 0.75 mm gap setting

The small particle range from 0.1 to 700 μm was easier to analyse by laser light scattering (LS 130). Figure 4.3 shows the differential volume distribution and the differential surface area distribution. The volume distribution has two characteristic peaks at 5 and 20 μm . These peaks represent small and big starch granules respectively. The fraction up to 40 μm accounts for 40% of the volume of particles below 710 μm . In terms of surface area the two peaks in the range from 1.3 to 35 μm account for 95% of the particles in this analysis. After mashing the fraction below 40 μm is smaller, however, there are still large amounts of such small particles present in the mash.

For the investigations of temperature effects a different malt batch with a lower modification was used. Malt modification influences the friability of the kernels. There are more cell wall components left in the malt and therefore the kernels are crushed into larger bits. This effect can be counteracted by a smaller setting of the roller gaps.

Figure 4.4 shows three sieve distributions for this malt batch. The gap setting 0.55 mm produces the sieve distribution closest to the standard. This setting was used to mill this malt batch.

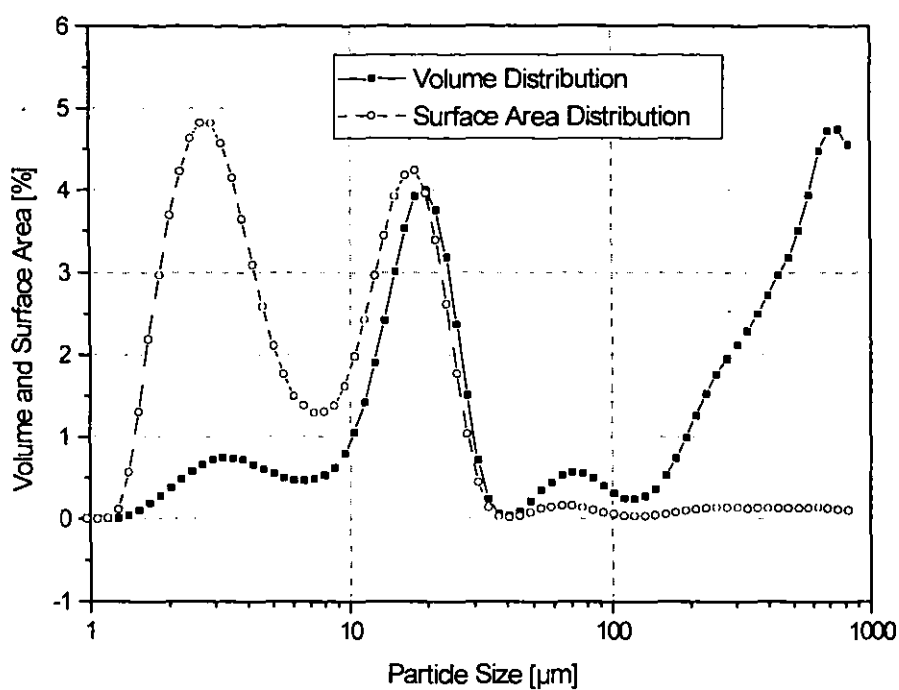


Figure 4.3: Particle size distribution, grist in water sieved at 710μm

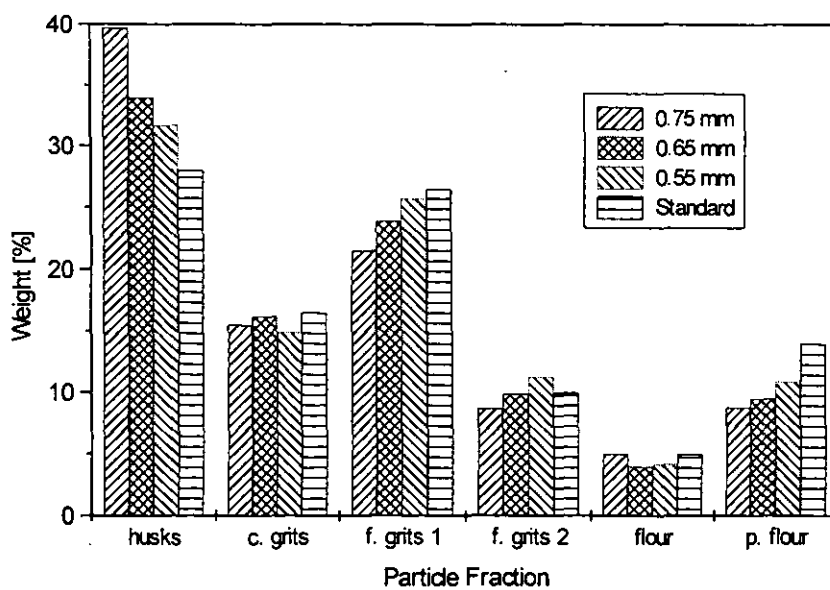


Figure 4.4: Sieve analysis for undermodified malt

4.1.2. Effect of Different Grinding Systems on Fine Malt Particles

Four different milling systems (Laboratory roller mill (see Chapter 3), a laboratory hammer mill, a household coffee grinder, and a laboratory disk mill) have been tested to investigate the influence of different milling systems on the break-up of fine particles such as starch. Figure 4.5 shows the volume distribution of the fine malt grist fraction, which was dry sieved using a 150 μm sieve.

It can be seen that all four milling systems were unable to break up starch granules. Bimodal distributions, showing large (size: approx. 20 μm) and small starch granules (size: 2 - 4 μm), were the same irrespective of the method of milling. The laboratory roller mill produced a larger amount of coarser particles which were in a shape suitable to pass the 150 μm sieve. Visual examination of this fraction of the grist revealed spike shaped particles often more than 10 times longer than the diameter.

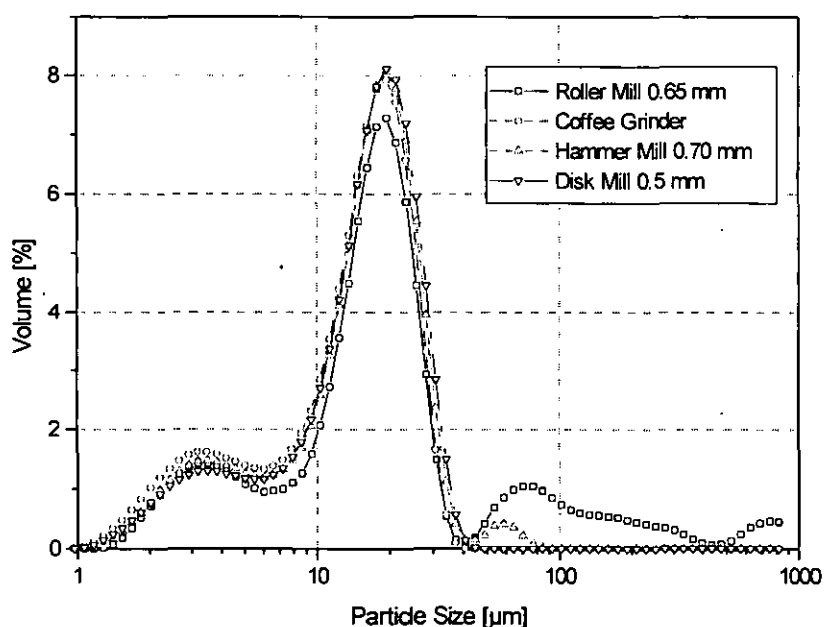


Figure 4.5: Particle size distribution of fine malt particles after a dry sieve step at 150 μm .
The legend gives the gap sizes of the different mills

4.1.3. Comparability of Different Particle Sizing Methods

Four different methods of particle sizing were used for the analysis of particle distributions in the mash.

Wet sieving of mash was used to detect particle attrition after mash conversion with different agitation regimes.

An evenly distributed mash sample volume was taken from the outlet of the mashing vessel, after filling the lauter column. 146.5 ml of mash were then placed on a 1000 μm sieve. The mash was then washed through the 1000 μm and through a 150 μm sieve below it with cold water. The sieved mash suspension was collected in a bottom tray. Normal tap water was used. The sieves were then placed into a drying cabinet for 24 hours at 120°C. The liquid volume of the bottom tray was determined and 10 ml of this suspension were filtered through a Whatman No. 541 filter paper, to determine the dry solids of the fine fraction.

The particle residues on each sieve and on the coarse paper filter were washed and dried. The dry weight of solids in three size classes was analysed for 12 trials (see Figure 4.6).

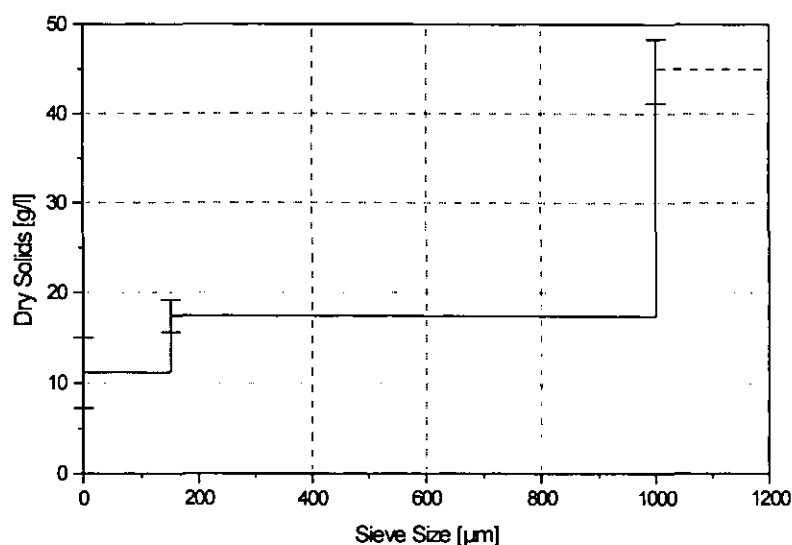


Figure 4.6: Dry solids after mashing (average of 12 trials with error bars ± 1 SD) in three size classes

It was found that this method is relatively inaccurate for the following reasons:

- Sampling of mash is difficult due to large amounts of large particles bigger than 1000 μm . These particles sediment quickly, hence it is difficult to create even mixtures. This reflects in the wide standard deviation of the $>1000\mu\text{m}$ fraction.
- Extract, mainly sugar, needs to be washed out of all fractions because it affects the dry weight of the solids. As the fine fraction does not filter well, washing is very time consuming and inaccurate. This affects mainly the fine fraction below 150 μm , which was filtered and washed to remove the sugars.

Despite the inaccuracy, the analysis can significantly indicate high attrition levels created in the 'valve' trials. This analysis was used for those experiments to quantify attrition.

The distribution of fine particles below 106 μm has never been analysed quantitatively. However, several references point out that fine particles have strong impact on lautering performance. Therefore fine particles in the sieve fraction below 106 μm were analysed in great detail using the Coulter Counter Multisizer and the LS 130 Laser Sizer. Laser sizing was used as a standard procedure, because of easier sample preparation and data handling.

The two different methods were used in parallel in a set of trials (Figure 4.7 and 4.8) to assess the relevance of the information and to verify the results of the Laser Sizer.

Both examples show in general similar distributions, however, the distribution of the Multisizer is narrower and the particle size is shifted towards smaller size. One explanation for the difference is the nature of the material analysed. The mash particles contain high amounts of protein. In aqueous solutions with high salt concentration these substances can dehydrate, which causes the particles to shrink. In addition, such proteinaceous material can be highly porous and, hence, the liquid volume replaced (Multisizer principle) by one particle is smaller than the volume which could be calculated from its surface area (Laser Sizer principle).

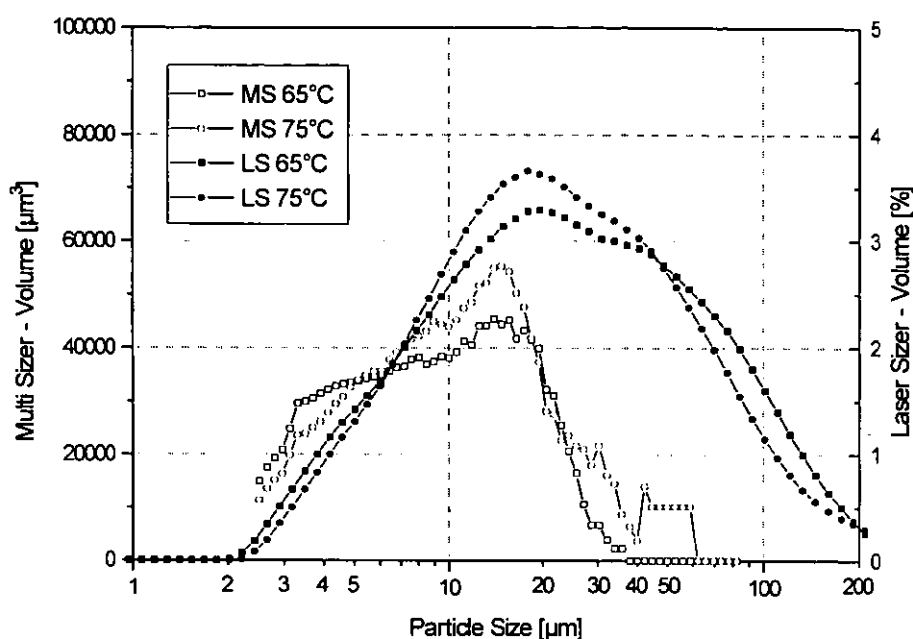


Figure 4.7: Trial 66 PSD of the fine fraction (below 106 μm sieve) analysed with both Multisizer and Laser Sizer.

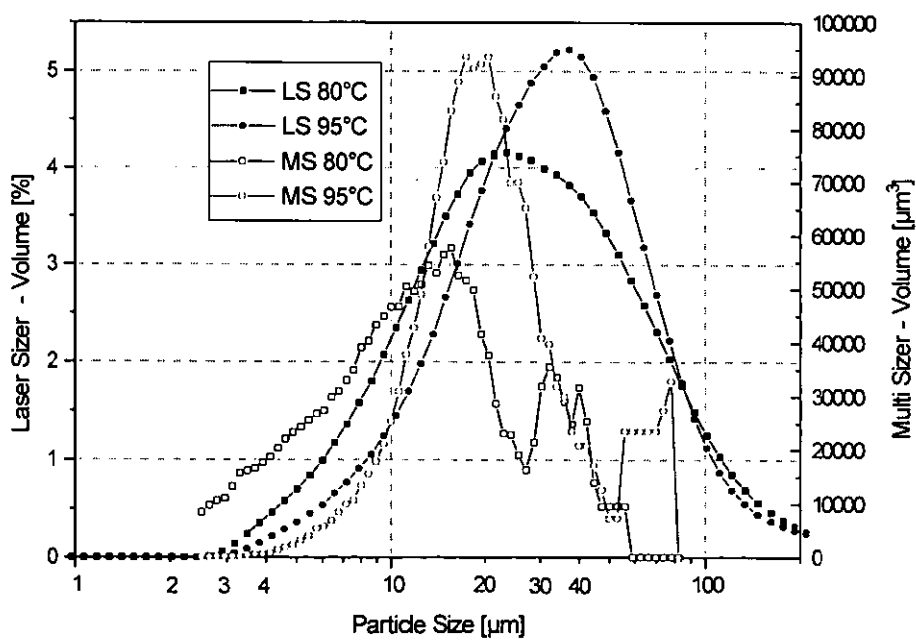


Figure 4.8: Trial 66 at 80 and 95°C on both Multisizer and Laser Sizer

The Multisizer was equipped with a 140 μm aperture tube; this gave an analysis range from 2.5 to 78 μm . In three distributions (at 65, 75 and 80°C) fine particles with particle diameter below 2.5 μm could be found and it can be assumed that even smaller particles were present, but could not be detected because of the analysis range.

The Laser Sizer detects mash particles down to 2 μm . As only relative concentrations are calculated with the diffraction model, smaller particles are not shown, because of the large concentration of bigger particles in the range of 20 to 40 μm present in the 106 μm sieved mash.

In addition to the particle analyses described before, image analysis of mash particles was undertaken using scanning electron microscopy (SEM). With this method it was possible to get more information about the shape of the fine particles in the mash.

The pictures attached in Appendix 7.5 show the amorphous, gelatinous structure of these particles. For this analysis fine particles from the samples prepared for the Multisizer were attached to a membrane disk (Millipore 0.45 μm) by filtration. It can be seen that the shape of most particles changes as they are drawn into the filter surface matrix. The size of these layers varies from sub micron to the 100 μm range. The three dimensional structure is very difficult to identify in this status, but it seems to vary with temperature. At temperatures from 65 and 75°C the 'sheets' of particles on the membrane are very flat, whereas particles incubated at higher temperatures (95°C) seemed to have a firmer three dimensional structure. In general the structure of these particles can be described as amorphous, which gives them a relatively high surface area.

4.1.4. Properties of Spent Grains Cake Layers

Two discrete layers can be identified in a spent grains cake. A relatively thin top layer which contains mainly fine material and a thick layer which contains a mixture of all other, bigger particles. A photograph of a vertical section of the entire cake is shown in Picture 4.1.

After filter cake washing the fines layer has a height of approximately 1 to 2 cm. The second layer of the cake is much thicker, approximately 25 cm in height. These two layers are characterised for their particles, particle size distributions and for their filtration properties.



Thin top layer
of fine particles

Picture 4.1: Vertical cut of a spent grains filter cake

4.1.4.1. Particles and Size Distributions in the Spent Grains Cake

The filtration properties of individual layers are largely dependent on the particle size, particle shape and the packing density in each layer. The permeability of a cake increases with the square of the particle diameter.

Particle distributions such as mash particles, with their wide dispersity will cause a reduction in porosity due to smaller particles occupying larger voids of the cake.

Figure 4.9 shows the change in distributions from top to bottom of the cake. All Layers were sieved at 700 μm to reduce the amount of coarse particles and enhance the resolution in the smaller range. The Figure shows that the fines layer at the top of the cake is depleted of big particles. This can also be seen in Figure 14 of Appendix 7.5, which shows the top layer of the spent grains cake.

Despite the sieve step at 700 μm a large quantity of bigger particles was present in the analysed suspension. This effect can be explained with the shape of the particles. Most large particles can be derived from the barley husk. The shell (husk) of the kernel is very hard and flexible. If it breaks, it will crack in the axial direction rather than across the length axis. This effect can be seen on the electron micrograph picture, Figure 7, in Appendix 7.5. The large husk in the centre of the picture is split in the axial direction. In addition this picture shows that the inner (concave) side of the shells are empty because this material has been degraded during the mashing process. Large mash particles are elongated, with a bent shape.

The layer close to the bottom of the cake has also been analysed by wet sieving (see Figure 4.10). The biggest fraction of particles is the fraction above 1000 μm . It contains the husks and makes up 65% of the weight of all sieve residues. The second largest group with 16% of the total dry weight consists of particles bigger than 710 μm . The remaining residue on the dried sieves makes up only approximately 20% of the total dry weight. The fines smaller than 106 μm were not analysed in this trial.

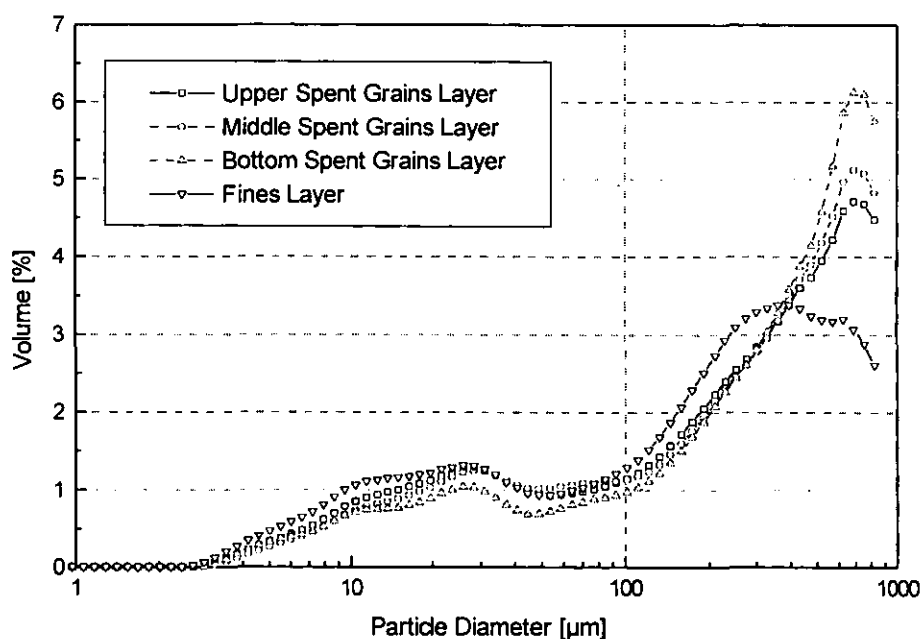


Figure 4.9: Particle size distributions in four different layers of the spent grains cake

4.1.4.2. Permeability of the Spent Grains Cake Layers

From two lautering trials (Trial 58 and 59) samples of the two spent grains layers were analysed separately in a laboratory scale filtration stand (EBC Filtration Stand). To achieve a satisfactory filtration effect, a needle felt type AMN (P+S Filtration, Rossendale, Lancs. UK) was used as a filter medium. The differential pressure across the cake was set constant at 100 mbar.

Table 4.2 shows that the permeability of the fines layer is approx. 40 times lower than the permeability of the spent grains layer. The difference in particle size distributions already indicated the different permeability. The fine particles cause much higher packing density and hence cause higher resistance to flow through the bed.

During subsequent experiments and in modelling of the lautering procedure, it was assumed that the fines layer is dominant in determining the permeability of the cake.

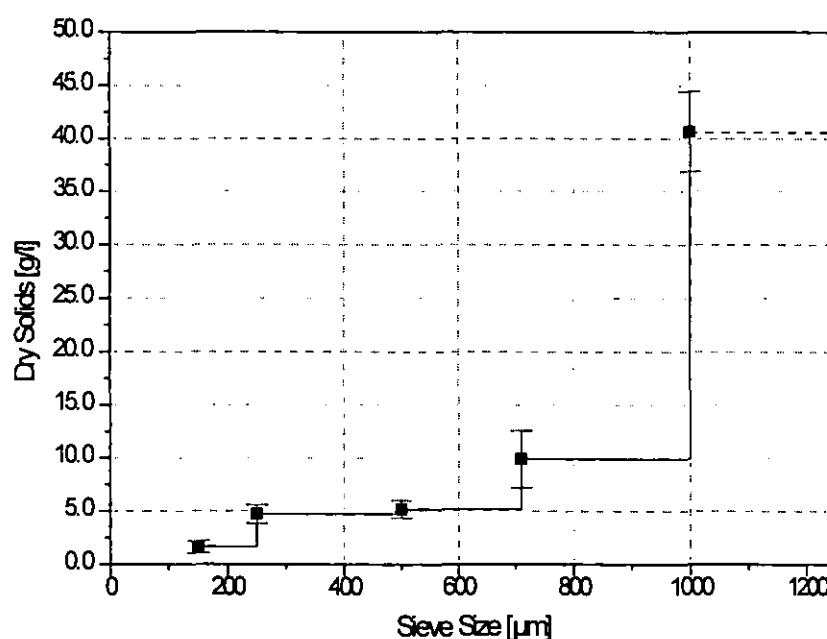


Figure 4.10: Wet sieve analysis of spent grains cake bottom layer. (5 analyses with error bars ± 1 SD)

Using the data in Table 4.2 it can be shown that this assumption is valid. Typically the height of the spent grains section of the cake is 0.2 m, the height of the fines section is approximately 0.02 m. Disregarding compaction of the cake with height, the calculated average resistance of the fines layer would then be $4 \times 10^{11} \text{ m}^{-1}$ and the resistance of the spent grains section would be $1 \times 10^{11} \text{ m}^{-1}$. This results in a total resistance of $R_{\text{total}} = R_{\text{SG}} + R_{\text{F}} = 1 \times 10^{11} \text{ m}^{-1} + 4 \times 10^{11} \text{ m}^{-1} = 5 \times 10^{11} \text{ m}^{-1}$.

Table 4.2: Filtration trials to determine the permeability of different spent grains layers

Sample	$\Delta V/\Delta t$ [ml/s]	L [mm]	Permeability [m^2]
Spent grains 58	3.64	30	2.048×10^{-12}
Fines 58	0.85	3	4.781×10^{-14}
Spent Grains 59	3.1	33	1.918×10^{-12}
Fines 59	0.95	3	5.344×10^{-14}

Another approach to determine the permeability of individual cake layers was undertaken in the pilot scale lauter column (Trial 12). Known quantities of cake sections were suspended in hot water (75°C) and pumped into the lauter column. After an initial sedimentation phase the clear supernatant was filtered through the cake. The flow rate of filtrate was set constant and the corresponding differential pressure was measured. The concentration of dry solids was determined. The fines had a dry weight of $1.90 \text{ g } \ell^{-1}$, the spent grains had a dry concentration of $2.16 \text{ g } \ell^{-1}$. The permeabilities of the individual layers are presented in Table 4.3. As the flow rate of the peristaltic pump was used as a parameter it was not possible to obtain two sets of data at identical differential pressure levels.

Table 4.3: Permeability of the two sections of filter cake

Sample	$\Delta V/\Delta t$ [ml/s]	L [mm]	Δp [mbar]	Permeability [m^2]
Spent Grains 12	4.036	65	10	7.342×10^{-10}
Fines 12	1.163	12	60	6.509×10^{-12}

The combined total resistance of these two layers (again ignoring the compressibility of the cake) would be (at a spent grains height of 0.2 m and a fines height 0.02 m):

$$R_{\text{total}} = R_{\text{SG}} + R_{\text{F}} = 2.724 \times 10^8 \text{ m}^{-1} + 3.073 \times 10^9 \text{ m}^{-1} = 3.345 \times 10^9 \text{ m}^{-1}.$$

The average resistance of a typical lauter tun cake (determined for example in the trials described in Chapter 5.2) with a height of 0.25 m would be $1.25 \times 10^{10} \text{ m}^{-1}$. The variations in overall resistance between these two trials and the lauter tun cake resistance could be assumed to be an effect of the different differential pressures across the cake.

More important than this calculated overall resistance is the fact that both trials showed a much lower permeability of the fines layer than of the remaining spent grains cake. This data supports the supposition further that the fines layer determines the filterability in lautering. It seems therefore valid to focus in more detail on effects of the mashing stage on the filterability of the fines layer to derive fundamental information about influences on lautering performance.

4.1.5. Change of Particle Size Distribution of the Fines during Mashing

In this study the particle size distribution of the fine fraction of mash was of major interest. The PSD of this fraction has been monitored during the standard mashing process (un-agitated sample in laboratory trial, see

Figure 4.11). A change in the distribution was found: the breakdown of starch particles during mashing decreases the size of the peaks at 4 and 20 μm . An additional peak occurs at 80 μm . This peak consists of proteinaceous material. A chemical analysis of the composition indicated a protein content of over 40% (w/w). Particles in this peak can be broken down enzymatically. Figure 4.12 shows the breakdown of these particles (from an agitated trial (Trial 29) by different groups of enzymes. This trial indicates that proteins and carbohydrate material is present in this group. Enzymes which are breaking down carbohydrate chains seem very effective in degrading these particles. However, the commercial enzymes applied in this trial very often contain small amounts of proteolytic activity, which makes it impossible to determine the nature of these particles with high accuracy. The particles in this fraction consist of carbohydrates and proteins.

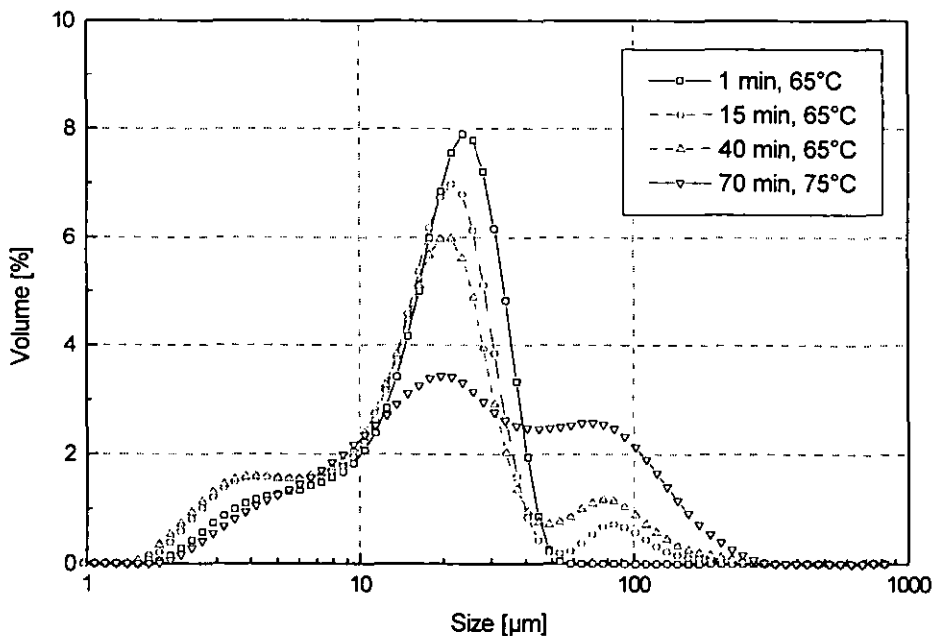


Figure 4.11: Change of particle size distribution of the sub 106 μm sieved fraction of mash during mashing

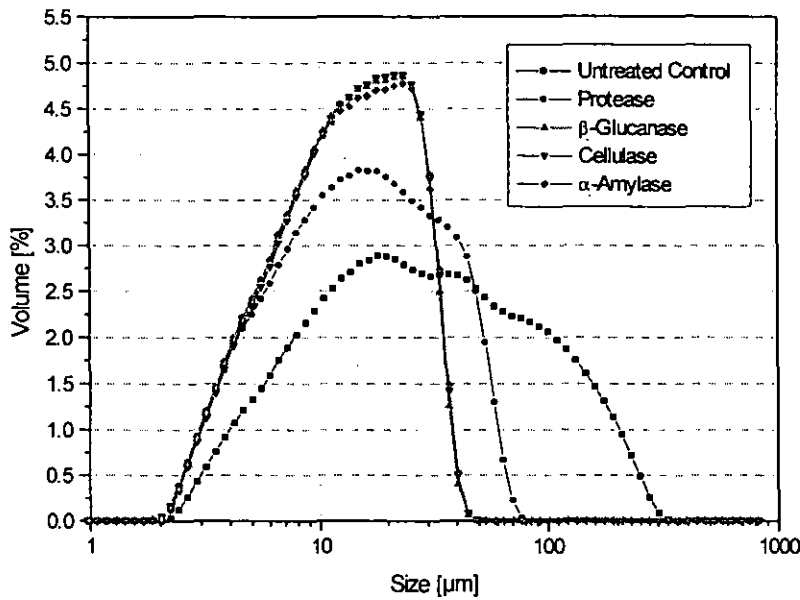


Figure 4.12: Particle breakdown in the 100µm range with enzymes

4.1.6. Density of Fine Mash Particles

This analysis is important for the modelling of sedimentation in the lauter tun. If particle shape and size and density are known it will be possible to predict the settling behaviour and relate it back to the performance in the lauter tun. Density of clear wort ρ_w and wort with particles ρ_{wp} have been measured using a density bottle.

The density of the clear liquid is determined by mass of liquid m_1 and volume of the density bottle V_0 :

$$\rho_1 = \frac{m_1}{V_0} \quad 4.1$$

The density of the suspension is composed of the mass of particulates and the mass (m_p and m_{w2}) of the liquid in the density bottle:

$$\rho_2 = \frac{m_2}{V_0} = \frac{m_p + m_{w2}}{V_p + V_{w2}} \quad 4.2$$

and the volumes of the solid and the liquid fraction:

$$V_0 = V_p + V_{w2} \quad 4.3$$

known variables: $\rho_1, m_1, V_0, \rho_2, m_2$,

The volume of the particles V_p has been analysed by centrifugation in a laboratory centrifuge. It is then possible to determine the liquid volume in the sample:

$$V_{w2} = V_0 - V_p \quad 4.4$$

The mass of the particles can now be calculated by combining equations 4.1, 4.2 and 4.4:

$$m_p = \frac{\rho_2 V_0}{m_p + (V_{w2} \times \rho_1)} \quad 4.5$$

The particle density can then be calculated:

$$\rho_p = \frac{m_p}{V_p} \quad 4.6$$

The densities of the fines fraction from three independent trials were analysed. The particle density covered a range of 1.090 to 1.150 g/ml.

4.1.7. Viscosity of Mash

4.1.7.1. Viscosity Change During Mashing

It was not possible to acquire information from the literature about the change of viscosity of mash during the conversion. Therefore trials had to be carried out, defining viscosity levels after different conversion intervals with different mash concentrations. Mash was incubated at 65°C for defined time intervals. As mash contains high amounts of big particles disturbing the viscosity analysis, the mash had to be filtered using a

pleated high capacity filter. The viscosity of the solid-free filtrate was then determined in a falling ball viscometer, described in Chapter 3. The following results were obtained (Figure 4.13 and Table 4.4):

Table 4.4: Viscosity in relation to conversion time and concentration

Liquor to grist ratio (mash concentration)	Viscosity after 10 min conversion time	Viscosity after 40 min conversion time	Viscosity after 70 min conversion time
3:1	1.033 mPas	1.056 mPas	1.067 mPas
3.5:1	1.023 mPas	1.049 mPas	1.055 mPas
4:1	0.704 mPas	0.834 mPas	0.811 mPas

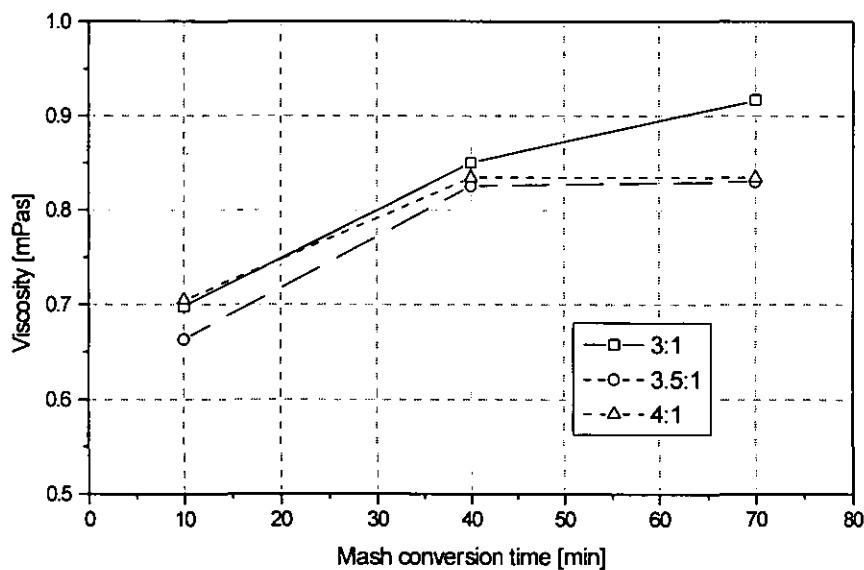


Figure 4.13: Viscosity in wort

This result shows that viscosity increases with conversion time. It is mainly the concentration of sugars and other soluble substances which increase viscosity. It can be concluded, that with concentrations below 3.5:1, a final maximum viscosity is reached after about 40 min of conversion. This

information is relevant for the determination of velocity gradients and shear rates, which are directly dependent on viscosity.

4.1.7.2. Effect of Temperature on Viscosity

Viscosity of wort (liquor to grist: 3.5:1) at 20°C is normally in the range of 2.5 to 3.0 mPas (Asselmeyer et al., 1973, Eyben and Hupe, 1980). The change of viscosity with temperature has influence on permeability of the spent grains cake in the lauter tun. It is therefore important to know the relationship between temperature and viscosity. In addition to data from the literature one trial was carried out using the falling ball viscometer and density bottle to get specific data for the malt and mash concentration used in all trials. Figure 4.14 shows that the data lie between the two worts analysed by Asselmeyer et al. (1973). The fitting curves which were fitted to the data are presented in Table 4.5. The viscosity at a given temperature is mainly dependent on extract, but the chemical structure of extract compounds has also a strong influence. This effect is shown in Chapter 4.3, where two different malt qualities were examined.

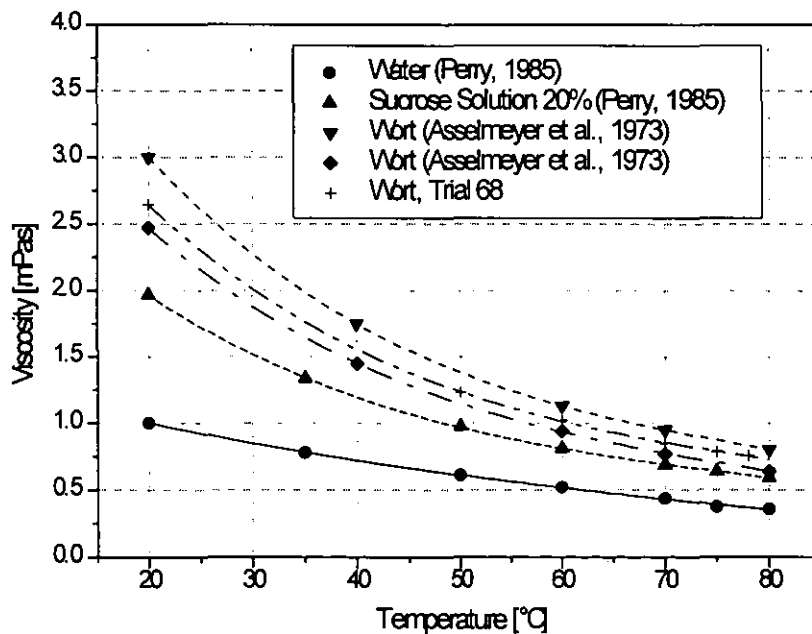


Figure 4.14: Viscosity related to temperature in water, sugar solution and wort samples

Table 4.5: Third order polynomial regression on viscosity vs. temperature data

Medium	Fitting Function	Regression Coefficient
Water (Perry, 1985)	$y = 1.408 - 0.02419 x + 2.117 \times 10^{-4} x^2 - 9.341 \times 10^{-7} x^3$	R =0.999
Sucrose 20% (w/w) (Perry, 1985)	$y = 3.349 - 0.08823 x + 0.0010 x^2 - 4.683E-6 x^3$	R =0.999
Wort 1, (Asselmeyer et al. 1973)	$y = 5.220 - 0.1409 x + 0.0016 x^2 - 7.083 x^3$	R =1
Wort 2, (Asselmeyer et al. 1973)	$y = 4.266 - 0.1139 x + 0.001322 x^2 - 5.811 \times 10^{-6} x^3$	R =0.999
Wort (Trial 68)	$y = 4.564 - 0.121 x + 0.00141 x^2 - 6.073 x^3$	R =0.999

4.1.8. Industrial Scale Power Input

In a questionnaire, 5 BRFI member breweries were asked to provide information on practical energy input into the mash during mashing. The following results were obtained from 5 different brewhouses (see Figure 4.15). Brewhouse A applied a decoction mashing procedure with two parts of the mash being boiled. All other brewhouse procedures were based on infusion mashing.

Figure 4.16 shows that mashing time and maximum power input levels vary in a wide range, even for infusion mashing procedures. This can be due to different stirring intensities. However, different stirrer design and different mash solids concentrations could have additional impact.

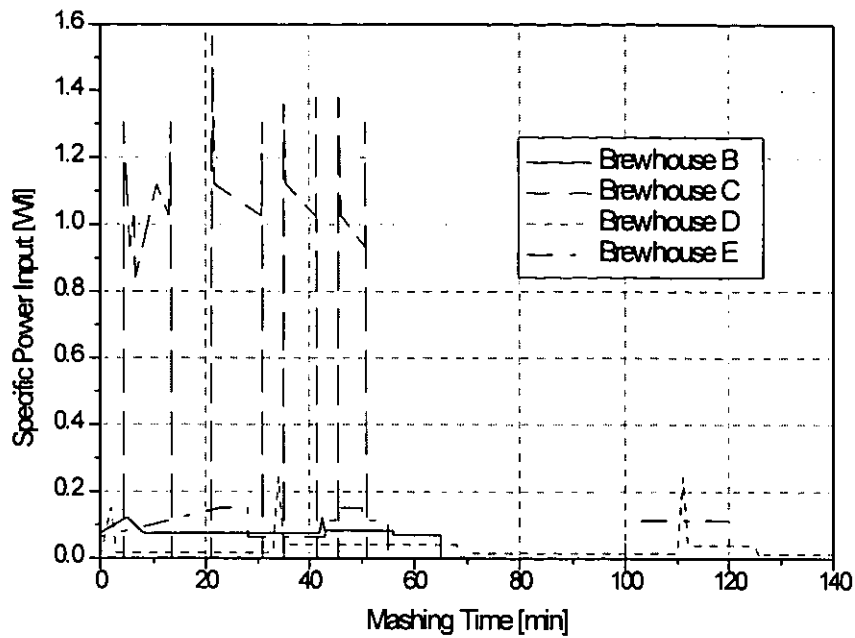


Figure 4.15: Variation of specific power input for different breweries (Brewhouse A could not be displayed because of the use of a decoction mashing procedure)

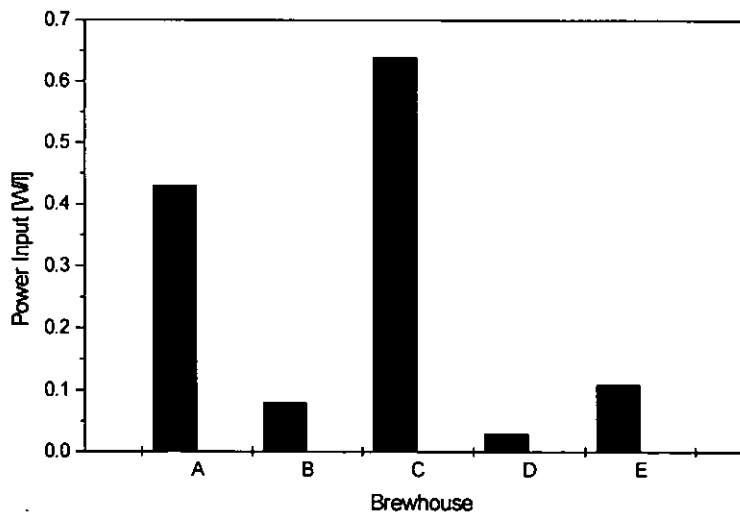


Figure 4.16: Average specific power input in different breweries

It can be seen that power levels for industrial mashing equipment vary over a wide range, between 0.11 and 0.64 W/l.

The total work input depends on the stirring time. Figure 4.16 shows that, due to the long mashing time in brewhouse A, the work input is the highest.

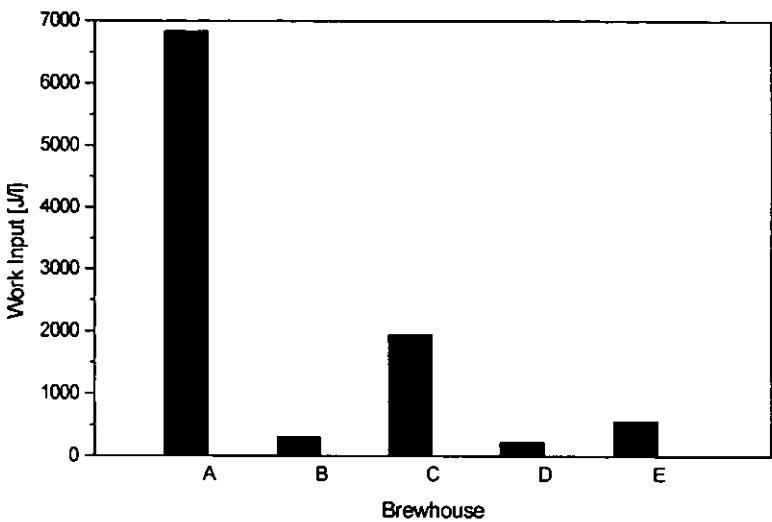


Figure 4.17: Specific work input over the entire mashing time.

4.2. Agitation Pilot Scale Trials

Pilot scale trials were carried out to get information about the effects of mash agitation on lautering performance. Different agitation levels were created in a flow loop, as shown in Chapter 3 by means of a single seat valve or with orifice plates. Trials of agitation effects on lautering performance were started at the pilot scale because this size would enable scale-up to large industrial scale much easier than bench scale tests. Results about parameters such as washing efficiency and clarity of the filtrate are also much easier to obtain.

4.2.1. Valve Trials

4.2.1.1. Introduction - Aims

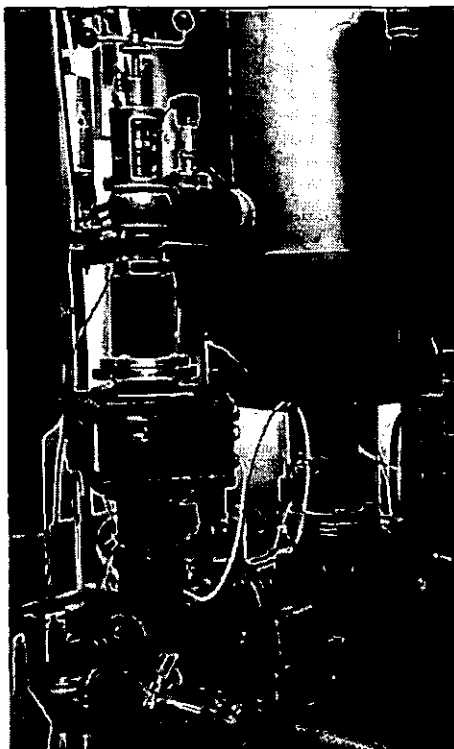
Different levels of energy loss were created in the flow loop of the pilot mashing rig using a single seat valve which creates constant pressure losses. The flow rate Q in the loop was kept constant at 25.3 l min^{-1} for all trials. The use of a positive displacement mono pump enabled constant flow even at different pressure losses. Sufficient mixing was achieved by constant recirculation of mash. The interface to air was constant, as the mash surface was kept quiescent. This was thought to be a clear advantage compared to stirring with an impeller. As oxygen was reported to have additional effects on lautering and wort composition, this was a suitable way of keeping this parameter constant.

The pressure loss at the valve was varied in a range from 0 to 1 bar. This range of pressure loss Δp can be related to the energy loss P as:

$$P = \Delta p \cdot Q \quad 4.7$$

The range of power loss can be related to the volume of mash in which this energy dissipates. It can be assumed that the energy dissipates in a small pipe section, along a length L , mainly before and after the valve. With this assumption, it is possible to calculate the specific power input into the mash across the valve to:

$$P_{spec.} = \frac{\Delta p \cdot Q}{V} = \frac{\Delta p \cdot Q}{\frac{d^2 \pi}{4} L} \quad 4.8$$



Picture 4.2: Flow loop at the mash vessel

Figure 4.18 shows the specific power input across the single seat valve, for a pipe length, L , of 17 cm ($V=295$ ml). This is the distance between the left corner of the vertical pipe and the centre of the pressure transducer.

4.2.1.2. Results

12 trials have been carried out, covering the pressure loss range from 0.0 to 1.0 bar. This relates to an energy input in the range 0 to 150 W/l (see Figure 4.18). This range covers even extremely high agitation conditions. Agitation effects, caused by the Mono pump were consistent for all trials, as the flow rate and the total pumping time were not varied. It has to be mentioned, that the power input of the Mono pump causes a background agitation level. Its magnitude could, however, not be quantified.

Different parameters relevant for lautering performance were analysed. These analyses are discussed below.

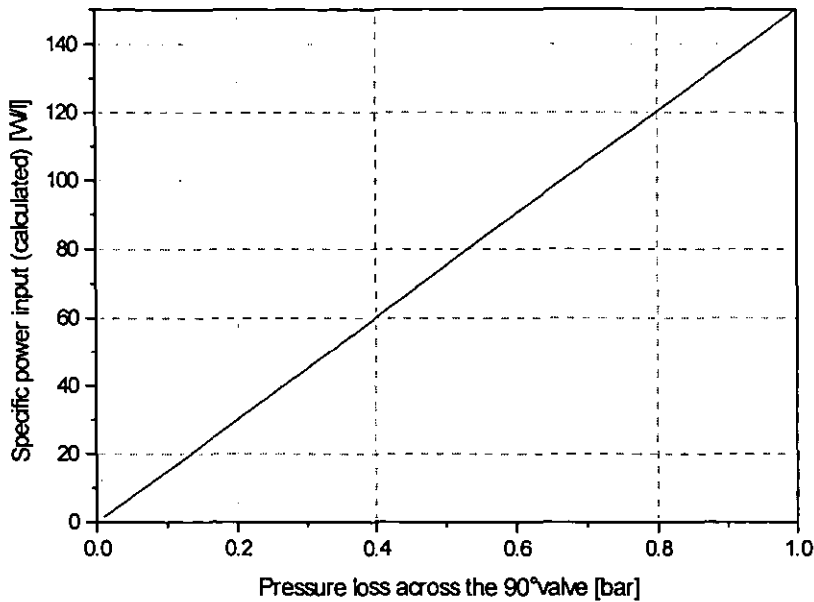


Figure 4.18: Specific power input at the single seat valve

Extract and viscosity of mash

Figure 4.19 shows extract and viscosity in relation to the power input. Both parameters show some variation, however, an influence from the parameter agitation couldn't be identified. Correlation coefficients from the linear fitting function are $R = 0.34$ for Extract and $R = 0.49$ for viscosity in the mash liquid phase. Different agitation levels seem to have very little effect on these parameters.

Wet sieving of mash

Mash samples were sieved through 1000 and 150 μm sieves, to investigate if particle break-up can be observed. Figure 4.20 shows the effect of particle attrition. With increasing amounts of power dissipated in the liquid, more fine particles are created ($R = -0.81$ for the fraction $>1000\mu\text{m}$ and $R = 0.82$ for the fraction $<150\mu\text{m}$).

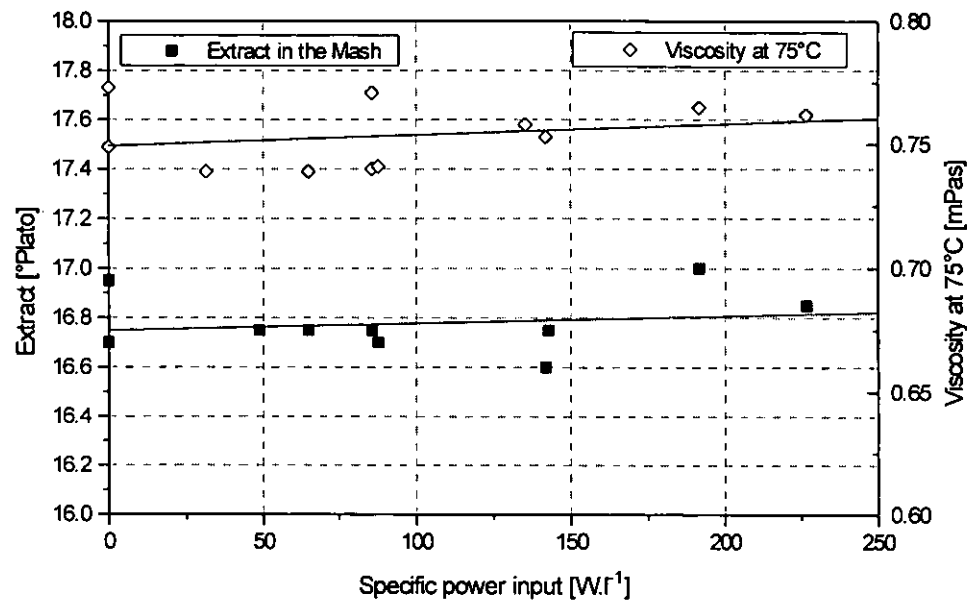


Figure 4.19: Extract and viscosity change with specific power input in the liquid phase of mash samples

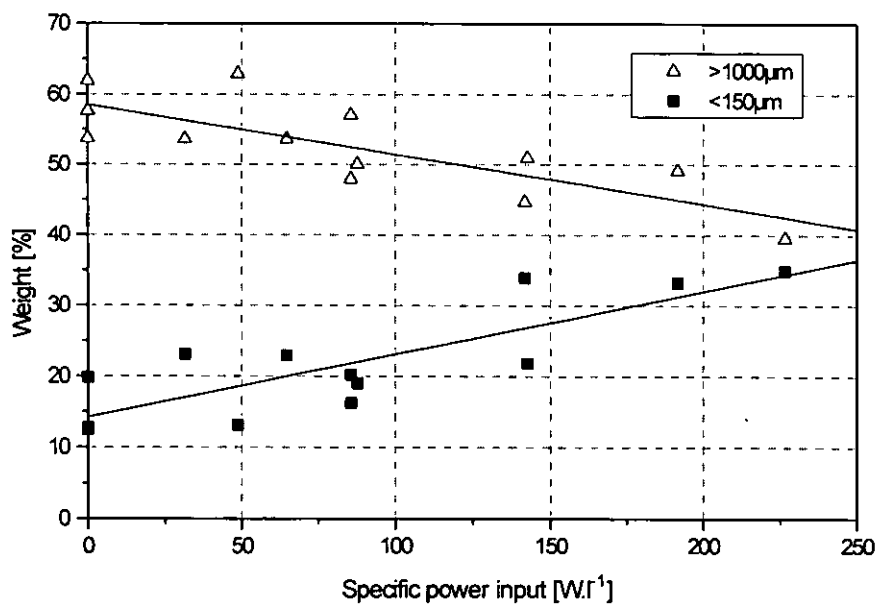


Figure 4.20: Dry weight of two sieve fractions of mash

Change of the particle size distribution in the fine particle fraction

Fine particles below 106 μm have been analysed in more detail using the LS130 Laser Sizer. Figure 4.21 shows a distinct change of the mean particle size (MPS) of the number distribution with power input. The biggest changes occur already at very low levels, which indicates that some fractions of mash particles are very sensitive to attrition. The smallest MPS found in the trials was at approximately 3.5 μm . This suggests that this is the lower end of the analysis range of the LS130.

Extract in Wort

Extract in the filtrate sample changes only slightly with agitation. The biggest changes were observed at minimal agitation levels (see Figure 4.22). At higher levels of agitation no significant changes are observable. This analysis is depending on the variations of water to grist ratio which could occur due to variations of the brewing procedures. This effect makes the data less accurate.

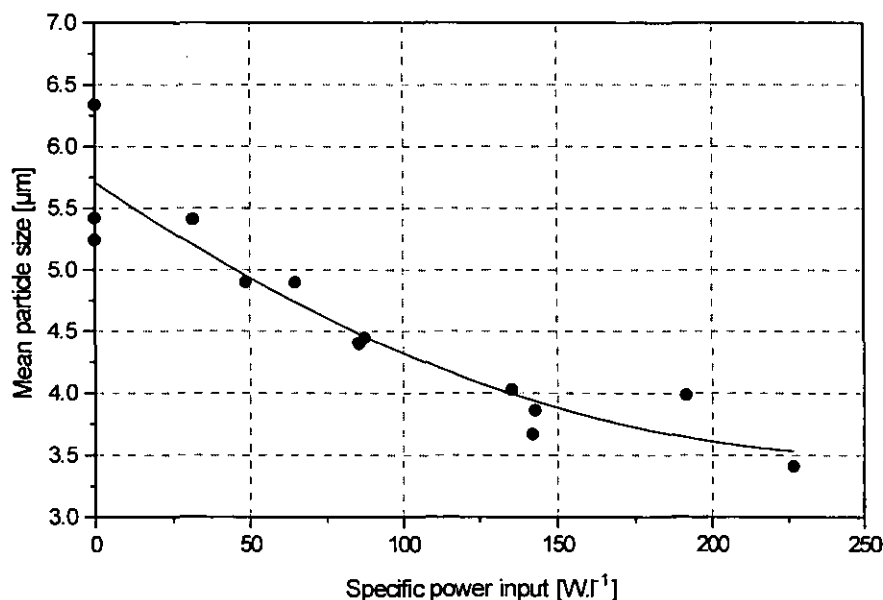


Figure 4.21: Change of MPS with increasing agitation

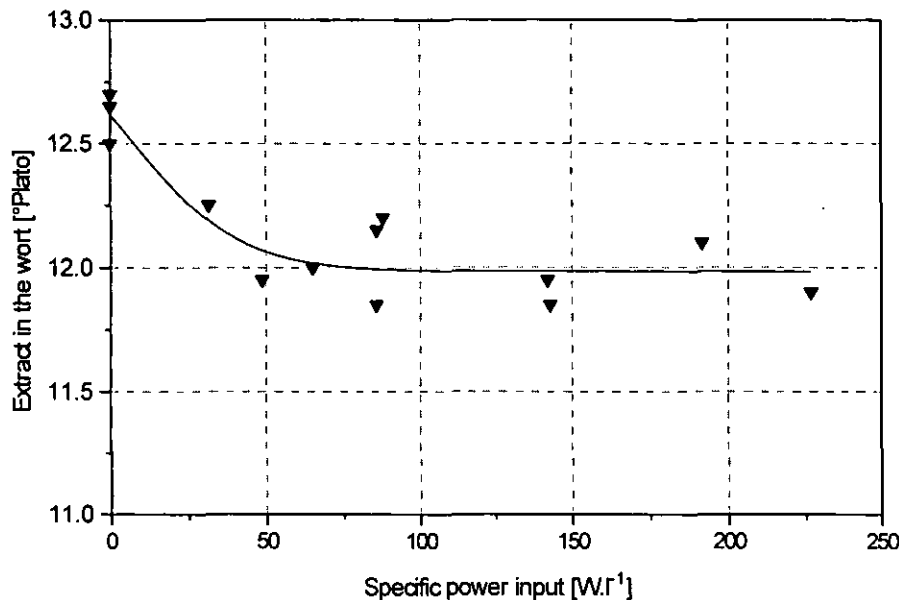


Figure 4.22: Change of extract content in wort with agitation

Mean turbidity of wort

Turbidity was measured in-line over the entire lautering time. The average value calculated after integration was related to the agitation input into the mash. It can be seen in Figure 4.23 that, with increasing agitation, the turbidity levels increase. This is in accordance to the findings in the dry solids analysis which showed an increase in the fines fraction and with the laser sizing analysis of the fines which showed a reduction in size of small particles. This analysis documents that smaller particles can not be restrained in the spent grains cake, they are carried over into the filtrate. The level of turbidity in the wort is relatively high compared to normal brewery conditions (Englmann and Wasmuth, 1993), which indicates that there were high amounts of fine particles in the mash. A direct comparison of this analysis with brewing practice is not possible as recirculation of the first cloudy wort back on top of the spent grains bed was not used.

Dry solids in wort

The dry solids loading increases with agitation ($R=0.67$) (see Figure 4.24). However, the analysis conditions show a high variation. This might be due

to difficulties in sub-sampling. Again normal brewhouses could achieve lower levels of solids of approx. 34-40 mg/l. 200 mg/l as obtained in these trials were described as hazy lautering (Englmann and Wasmuth, 1993).

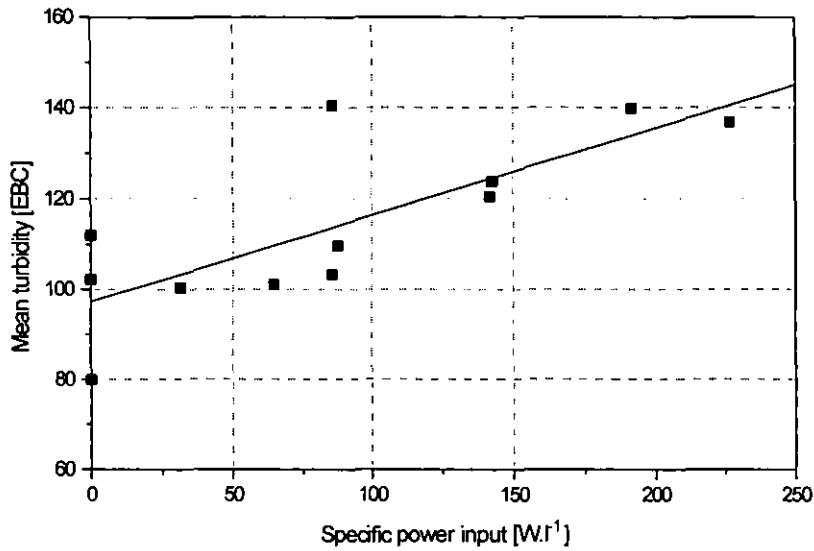


Figure 4.23: Turbidity increase with agitation

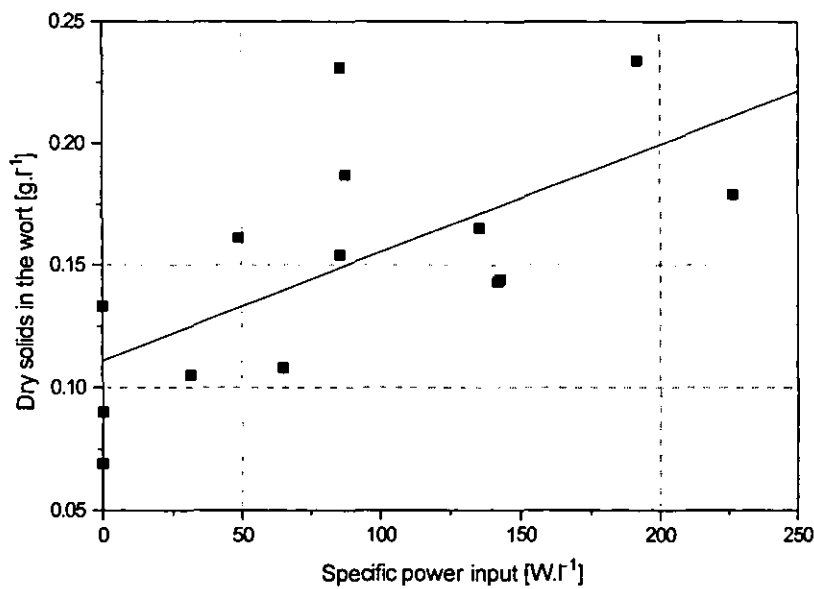


Figure 4.24: Dry solids in wort with regards to specific power input

Lautering

Lautering performance was determined as total lautering time, which was the time required to collect 11 litres of wort, and as extract ratio between mash extract and wort extract. Mash and wort volumes are constant, therefore the ratio between mash and wort extract can show differences in washing efficiency of the filter cake. In Figure 4.25 the total lautering time is plotted against the agitation regime. It is clearly visible that agitation affects wort run off, however, the variation between the trials was relatively high. The formation of the cake in the lauter tun can have additional effects on total lautering time. It was found in some trials, that an uneven distribution of the mash particles could cause great variations in run off rates, particularly if the amount of coarse particles was too low, when the run off rate was reduced. This effect was due to sedimentation of larger particles in the mash vessel. It was later found that this effect could be avoided, by application of manual stirring before the mash transfer.

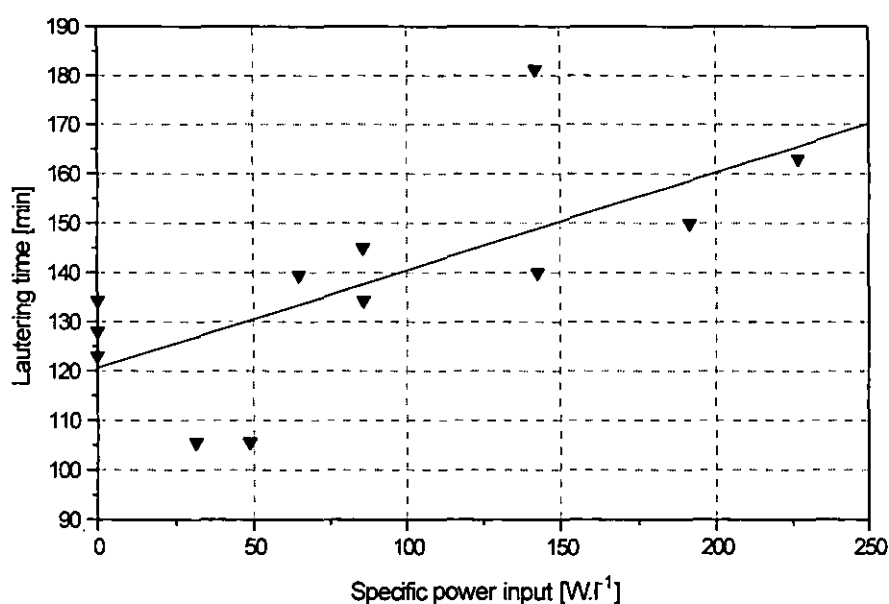


Figure 4.25: Effect of agitation on lautering time

Figure 4.26 shows the effect of agitation on washing efficiency in the pilot lauter tun. With increasing shear, the efficiency shows a trend to get lower. Biggest influences were again observed at the lower end of the agitation

range. The reduction in washing efficiency can be contributed to increased blockage of pores in the filter cake. Hence washing and leaching was less effective.

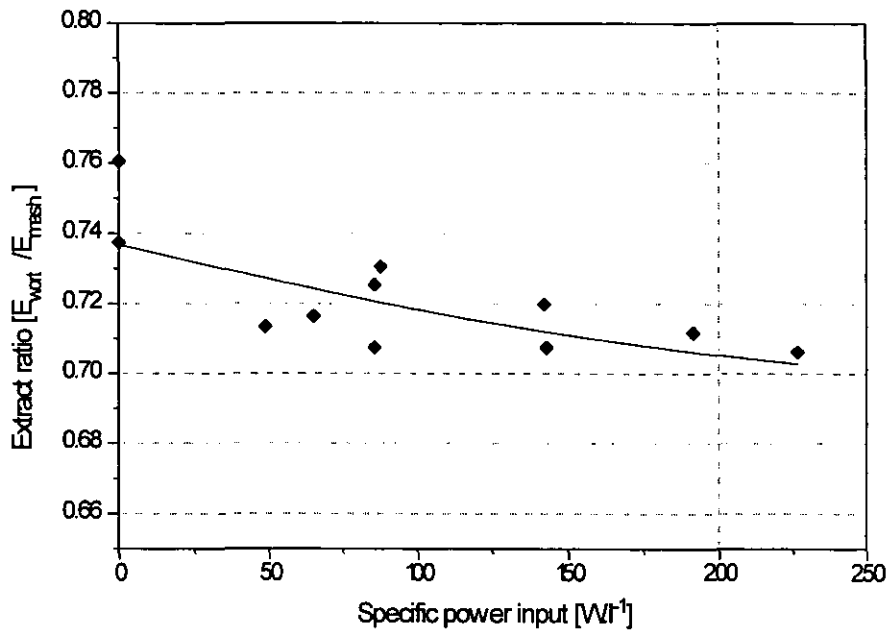


Figure 4.26: Extract ratio (Extract in the mash / Extract in the wort)

4.2.1.3. Conclusions

This set of trials showed that agitation measured as power input into the mash influences mashing and lautering parameters. Quality parameters (such as wort clarity) are affected as well as performance parameters (such as lautering time). However, these trials did not give an entirely conclusive picture of the effects. The low end of the power input showed the strongest influence in most of the parameters analysed.

Two effects may provide the reasons for this:

1. The biggest changes occur at very low power input. As brewers observed differences in lautering performance with agitators, it seems possible that significant changes happen only in the minimal power input range used in industry.

2. Due to mixing problems and sedimentation of solids in the mash vessel, local overheating could occur. This might have caused some changes in the composition of the mash particles. Initially, the temperature effect was not regarded very important for the mash composition and filtration properties.

Subsequent trials should investigate the effects in a power input range close to industrial scale conditions. This is a specific power input range from 0 to about $0.6 \text{ W } \ell^{-1}$ of mash (see Chapter 4.1). That is considerably lower than the power dissipated in this set of trials.

4.2.2. Orifice Trials

4.2.2.1. Aims

Previous trials showed that major changes in analysis parameters occurred at the lower range of power input. In addition, results from a questionnaire to the brewing industry showed that the small power input range is much closer related to practical conditions. This set of trials was designed to create power dissipation at an orifice in the mash flow loop in a similar range to industrial scale mash stirrers.

Trials were carried out using different orifice plates in a flow loop (see Chapter 3.2 for the design). The orifice diameters were designed to establish a specific power dissipation at the *vena contracta* of the orifice between 0 and $0.6 \text{ W } \ell^{-1}$. Figure 4.27 shows the power dissipation at the orifices, calculated from differential pressure loss measurement before and after the orifice. The flow rate in the loop was constant at $4.22 \times 10^{-4} \text{ m}^3 \text{ s}^{-1}$. The power dissipated in 0.12ℓ of mash.

This range of power input relates very closely to an industrially relevant power input of 0 to $0.8 \text{ W } \ell^{-1}$. It was assumed that the Mono pump in this flow loop caused a background power input small enough to observe changes in this range. All trials have been backed by chemical analyses of the mashes and worts. Specific power input was calculated using equation 4.9.

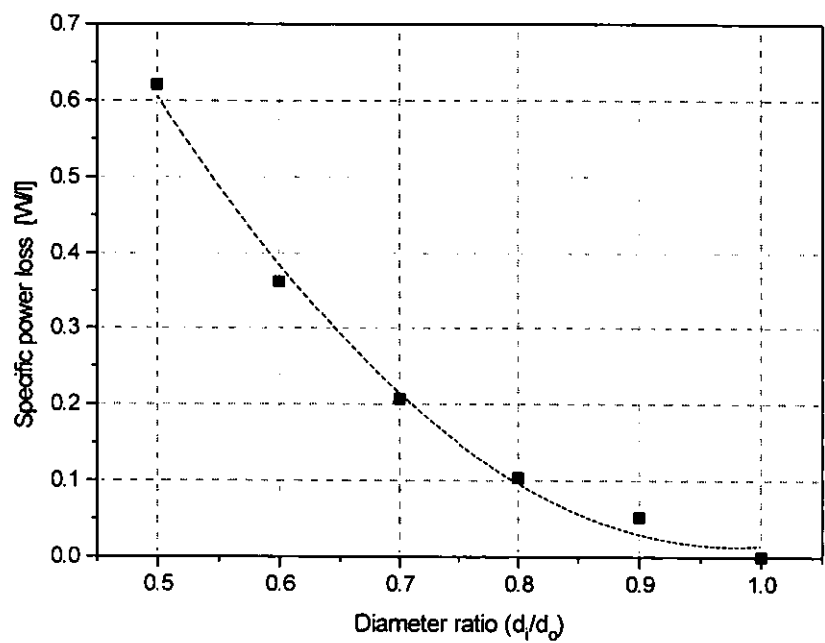


Figure 4.27: Specific power loss at the *vena contracta* of the orifices

The power dissipation at the orifice is:

$$P = \frac{Q \Delta p}{V}$$

4.9

where

- P : power loss in the fluid
- Q : flow rate
- Δp : pressure difference between the two measuring points and
- V : volume of mash between the two pressure tappings.

4.2.2.2. Results

Mash analyses

Extract content and viscosity measured in the liquid phase of the mash are not affected by increasing shear. Both parameters were constant over the agitation range.

The particle size distribution measured using two sieve steps (1000 μm and 150 μm) and laser light scattering analysis of the fine fraction (below 106 μm) showed no influence from increasing power input.

Wort analyses

Extract, in the filtered wort sample from the lauter tun, also showed no significant influence of shear. Wort clarity, analysed as mean haze reading over the filtration time in a turbidimeter, and as total dry solids in the filtered wort, was also not affected by the shear created at orifices.

Lautering Performance

The time to collect a known quantity of wort was not influenced by the agitation. It took an average 127 minutes to collect 11 ℓ of filtrate. Permeability of the spent grains bed is also constant over the range of power applied.

4.2.2.3. Conclusion

It could be shown that mechanical power induced at levels from 0 to 0.6 $\text{W } \ell^{-1}$ at an orifice had no significant effect on mash and wort properties. This behaviour may be caused by the use of a mono pump to move the mash in a loop. The mechanical power input of the pump may be high enough to cover any additional mechanical power dissipation at the orifices. Changes could be observed at very high power input levels, which are about 10 to 25 times higher than the maximum level created with the smallest orifice plate.

It can be concluded, that the arrangement of the mashing equipment with recirculation of the mash in a loop and the use of a mono pump was not suitable to investigate changes in low power input conditions. However, pumping was necessary to keep mash particles in suspension and to

avoid local overheating at the heating pads. Re-engineering of the pilot mashing equipment during the experimental phase of this thesis was not feasible. To obtain further data with small power input and to verify the observations in the pilot scale, trials in laboratory scale were therefore considered a suitable alternative.

Despite the difficulties with the available pilot scale mashing equipment, a sufficient range of data could be obtained which enabled the modelling of the lautering process to determine variations of the observed analysis parameters.

4.2.2.4. Reproducibility Test

Physical analysis of mash and wort/lautering

The reproducible behaviour of these trials irrespective of the power dissipated at the orifices made it possible to treat this set of trials as reproducibility tests for the pilot plant. Table 4.5 shows the statistical calculation of standard deviations for these analyses. The overall reproducibility seems acceptable as most analyses show little variation. Only the dry weight analyses of the fine particle fractions (sieve bottom-tray and dry solids in wort) and the wet sieving analysis shows a considerable variation. This may be due to the difficulties in "sub-sampling" heterogeneous mixtures.

Chemical analyses

Chemical analyses of filtered (laboratory filter) mash and wort samples (after lauter tun filtration) were obtained, which indicate that there are no changes occurring during mashing with different orifices. Table 4.6 gives the statistical evaluation of the results. The pilot plant allows the execution of highly reproducible trials. The standard deviations of all analyses are in the range of their analysis accuracy.

Table 4.5: Statistical evaluation of analysis data

Analysis	Mean	Sample standard deviation, <i>SD</i>	Variation Coefficient, <i>VC</i> [%]	Number of values
Extract mash	16.72 °Plato	0.13 °Plato	0.78	12
Viscosity	0.745 mPas	0.008 mPas	1.05	11
Mash residual dry weight 1000 µm sieve	61.1 %	5.0 %	8.02	12
Mash residual dry weight 150 µm sieve	23.7 %	2.4 %	10.20	12
Mash residual dry weight bottom-tray	15.2 %	5.3 %	35.16	12
MPS (mean particle size)	4.742 µm	0.255 µm	5.38	12
Extract wort	12.17 °Plato	0.16 °Plato	1.28	12
Dry solids in wort	0.175 g/l	0.035 g/l	20.09	10
Lautering time	127.15 min	7.56 min	5.95	10
Height of the spent grains cake	36.0 cm	2.2 cm	6.23	12
Permeability at 5 mbar	4.70E-9 m ²	6.73E-10 m ²	14.32	11

Table 4.6: Statistical results of chemical analyses.

Sample:	Mash			Wort		
Analysis	mean	standard deviation of sample	variation coefficient [%]	mean	standard deviation of sample	variation coefficient [%]
FAN (free amino nitrogen)	239 mg/l	3 mg/l	1.13	176 mg/l	3 mg/l	1.56
TSN (total soluble nitrogen)	1405 mg/l	19 mg/l	1.38	1013 mg/l	25 mg/l	2.45
Polyphenols	248 mg/l	16 mg/l	6.55	245	25	10.24
pH	5.59	0.13	2.38	5.63	0.12	2.11
Colour	8.30 EBC	0.00 EBC	0.00	7.20 EBC	0.10 EBC	1.39
Apparent fermentability	71.00 %	0.58 %	0.81	71.67%	0.47 %	0.66

4.2.3. Effect of Stirring on Mash Filtration Performance - Laboratory Scale Trials

4.2.3.1. Introduction

From the previous experiments, it could be concluded that the investigation of very low stirring regimes and conditions without agitation is only possible in small scale trials, where temperature control is achieved by a water bath. It was found in separate pilot scale experiments that temperature is an important parameter for the particle size distribution of fines and filterability of mash. Trials with varying mashing off temperatures were carried out separately from the main experimental programme to

investigate and quantify this effect. The results are presented later in this thesis, but were available to decide about the progress of the experimental programme. In conclusion, the results of the temperature trials made it clear that accurate control is required for the investigation of other mashing parameters such as agitation. Under industrial or pilot scale conditions, heating with steam or electrical heating pads would cause local overheating and charring on the heat exchange surfaces, because of insufficient heat transport under such conditions. Hence, it was decided to investigate these low levels of power input in a laboratory scale setup. Zero agitation does not occur in modern brewhouses, but to get information about the total range of power input would be useful to draw conclusions and to model the process.

4.2.3.2. Aims

The aim of this set of trials was to investigate agitation effects with small power input down to no agitation. Effects of agitation have been investigated previously in pilot scale facilities, however, very low agitation levels were not achievable, because of the constant power input required for recirculation.

In this set of trials the following analyses were carried out:

1. particle size distribution of fine particles in mash (fines) below 106 μm sieve size
2. viscosity in mash
3. concentration of fine particles (dry solids)
4. extract content determined as density
5. filterability of mash.

4.2.3.3. Results

The range of specific power applied was in the range from 0 - 0.5 $\text{W } \ell^{-1}$, (see Figure 4.28; using normal mash concentration and different impeller velocities). The more concentrated mashes had power inputs between 0.6 - 1.4 $\text{W } \ell^{-1}$. This higher range was carried out to link this set of trials to the pilot scale trials.

Specific power input

The specific power input relevant for large scale industrial mashing plants is in the range from 0.05 to 0.65 $\text{W } \ell^{-1}$ (see Chapter 4.1, with a maximum agitator tip speed of 3 m/s, at a distance of the agitator tip to the wall of 50 mm. The Haake stirring device is putting similar power levels into the mash (see Figure 4.28).

Effect of agitation on mean particle size (MPS) - LS130 analysis

Particle size distributions were analysed on diluted, sieved (106 μm) samples. This procedure enhances the analysis accuracy in the small particle range, most relevant for filterability performance. To enable comparisons to be made between unimodal particle size distributions, the MPS of the differential number distribution was used. It can be seen from Figure 4.29 that agitation causes attrition of particles - MPS decreases. For specific power inputs up to 0.1 $\text{W } \ell^{-1}$ the MPS is nearly constant. With higher levels of agitation, a significant decrease occurs, which reaches a minimum MPS of 3.3 μm at 0.3 $\text{W } \ell^{-1}$ and stays constant thereafter.

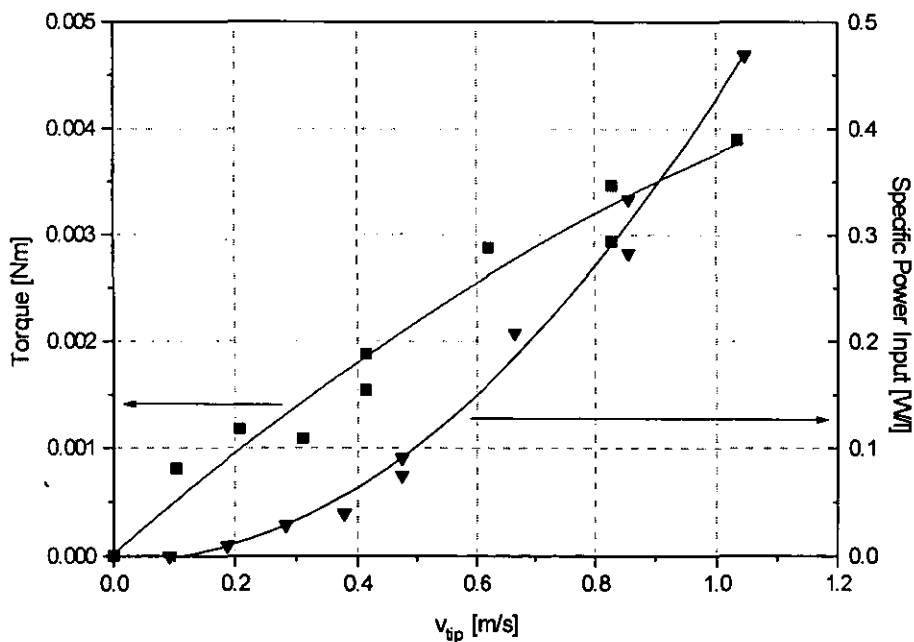


Figure 4.28: Effect of different stirrer velocities (as tip speed, v_{tip}) on torque and power input in mash (420 ml, mash, concentration: 3.5 : 1)

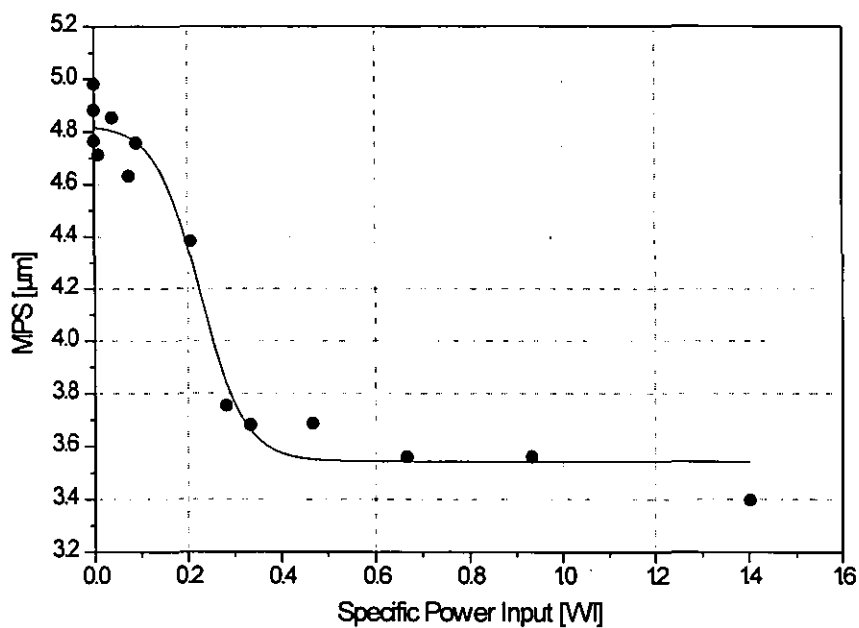


Figure 4.29: Effect of agitation on MPS

Concentration of fine particles

The dry weight of fine particles (particles below 106 μm sieve size) has been analysed. Figure 4.30 shows that with attrition more fine particles are created. From 0.2 - 0.3 $\text{W } \ell^{-1}$, the solids concentration of the fines does not increase further, which means no additional particles below 106 μm diameter are produced. It can be assumed that a specific material, which is sensitive to shear, is broken down into smaller particles. It can be assumed that only a limited quantity of such shear sensitive material is present in the mash, as a plateau of the fine particles concentration is reached.

Density of mash

The density of the liquid phase of mash was measured at 20°C. Figure 4.31 shows the influence of agitation on the release of soluble material into the liquid phase. Minimal agitation levels are already sufficient, to improve diffusion and thus enhance mass transport. Zero agitation shows wide variation, as convection during heating (from 65°C to 75°C) and

manual mixing of the cold sample (to ensure even sample distribution) after mashing might have had an effect on mash-density. The density remains constant, as soon as a minimal amount of mixing in the range of $0.05 \text{ W } \ell^{-1}$ has been applied. This means that more powerful stirring regimes will not enhance malt extraction, minimal levels are sufficient.

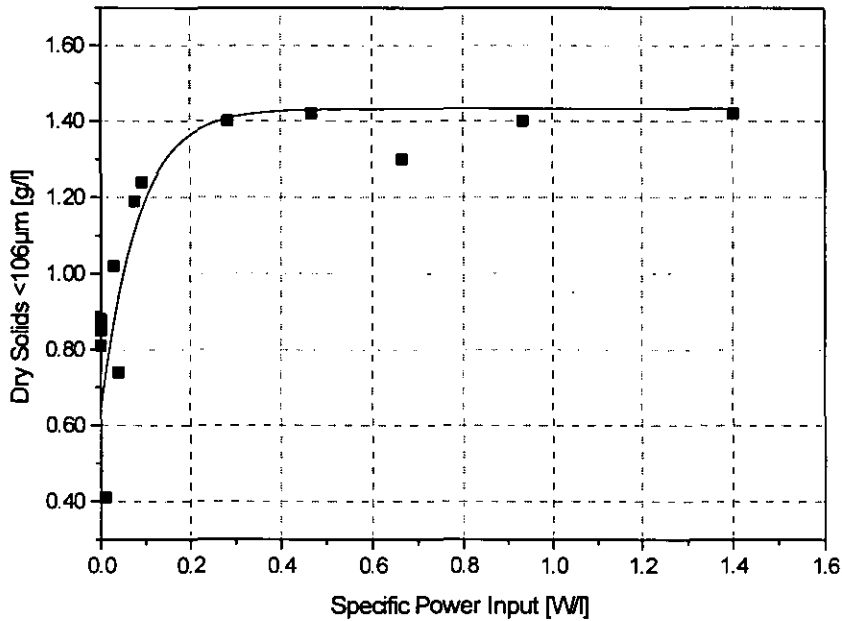


Figure 4.30: Effect of agitation on particle concentrations below $106\mu\text{m}$

Viscosity of mash

It can be shown that viscosity and density for this malt correlate well (see Figure 4.32). Therefore it is not surprising, that viscosity shows the same behaviour with agitation as density (see Figure 4.33). Even very high agitation levels ($>1 \text{ W } \ell^{-1}$) do not affect viscosity.

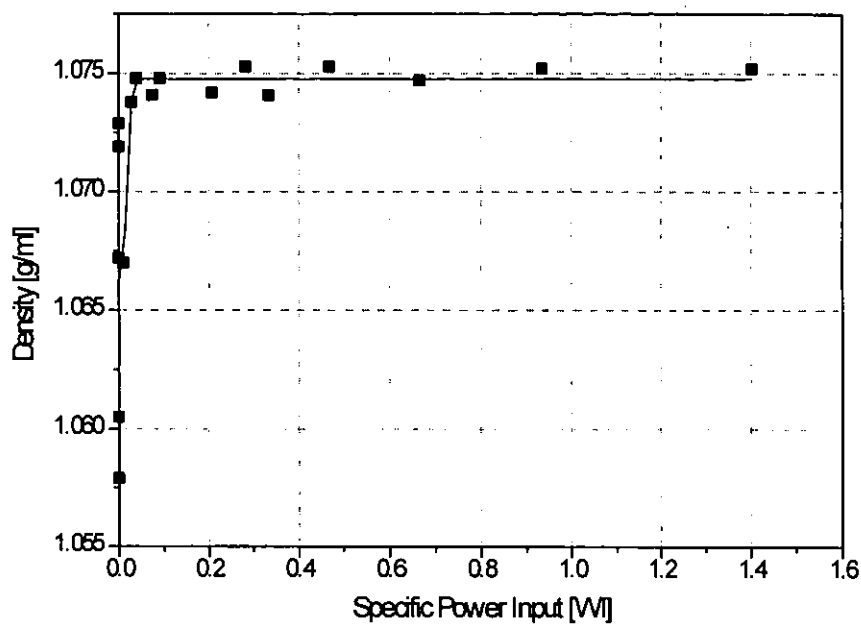


Figure 4.31: Effect of agitation on density in mash

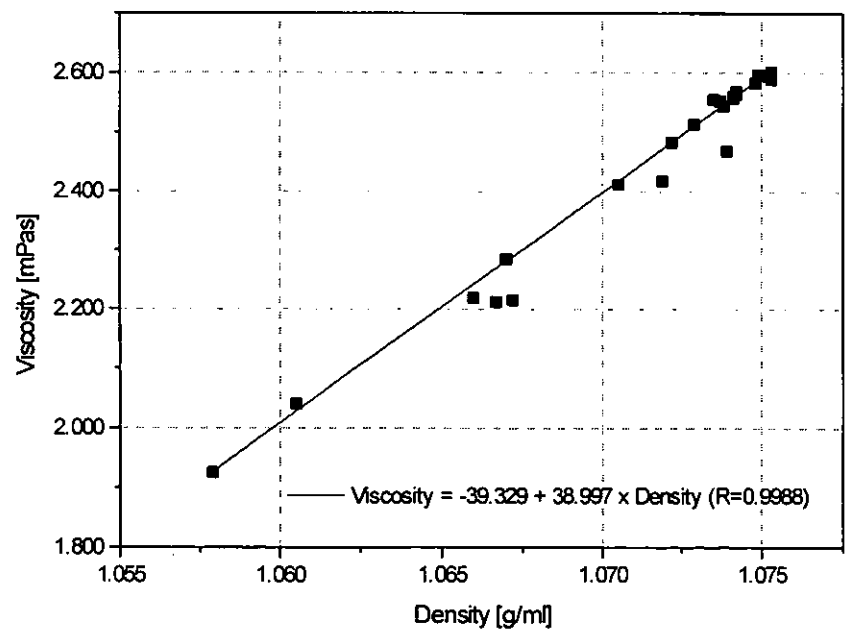


Figure 4.32: Density - viscosity correlation for small scale agitation trials

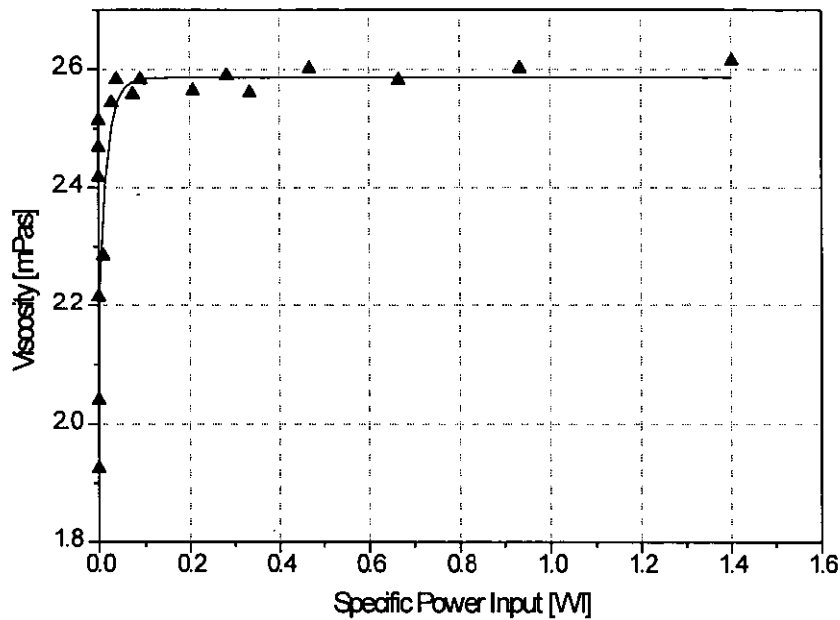


Figure 4.33: Effects of agitation on viscosity

Filterability of mash

Filterability $1/K$ was determined from the slope K of a dt/dV vs. V plot. This slope describes effects of viscosity, particle concentration and cake resistance, normalised to the filter area and the differential pressure applied (see equation 4.10).

$$\frac{dV}{dt} = \frac{A^2 \Delta p}{\eta \alpha c} \frac{1}{V} = \frac{1}{K} \frac{1}{V} \quad 4.10$$

Highest filterability levels were achieved at zero or at minimal agitation rates up to $0.1 \text{ W } \ell^{-1}$ (see Figure 4.34). Stirring with a power input higher than $0.1 \text{ W } \ell^{-1}$ caused a reduction in filterability. Again, the biggest changes were observed in the range from $0 - 0.4 \text{ W } \ell^{-1}$ specific power input. This indicates already the strong link to particle size effects where the biggest changes are also in this range. Filterability also approaches a plateau for specific power inputs above $0.5 \text{ W } \ell^{-1}$.

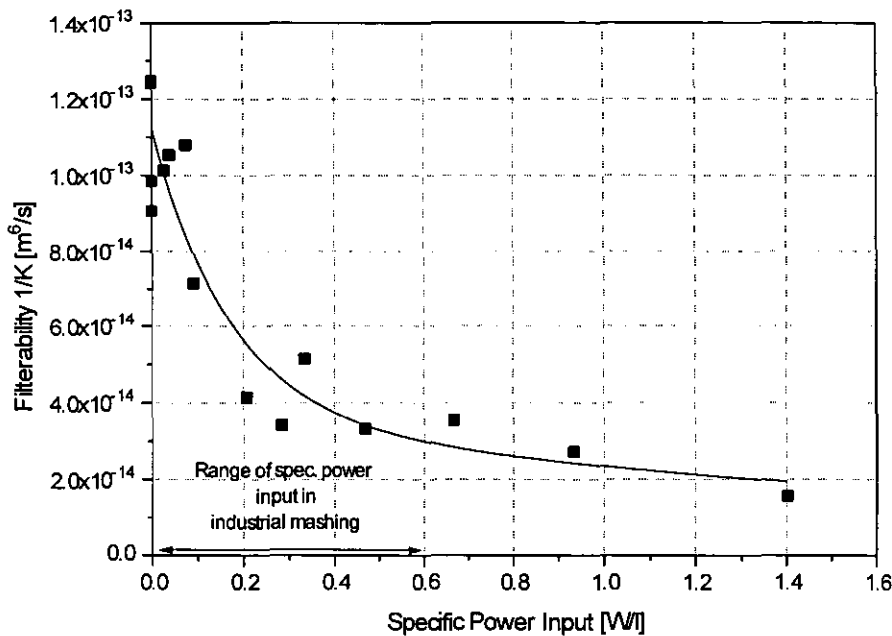


Figure 4.34: Filterability of mash in relation to agitation

Resistance

The specific resistance, α , of a mash cake, determined in the Millipore filter is shown in Figure 4.35. The specific resistance describes the structure of the cake, its voidage and the liquid-flow paths; parameters which are largely affected by particle surface and particle size distribution. It can be seen that the resistance of the bed increases linearly with the power input. The strong decrease in filterability at low power input ranges can therefore be explained mainly by the viscosity increase. The low power range (up to $0.1 \text{ W } \ell^{-1}$) again shows little change from the zero agitation trials.

Correlation between MPS and Filterability

As described above, filterability is directly affected by particle size distribution. Increases in particle diameter can increase filterability. Figure 4.36 shows this relationship. Better control of analysis conditions (mainly temperature during the viscosity and filtration analyses) would help to increase the accuracy of the filterability determination.

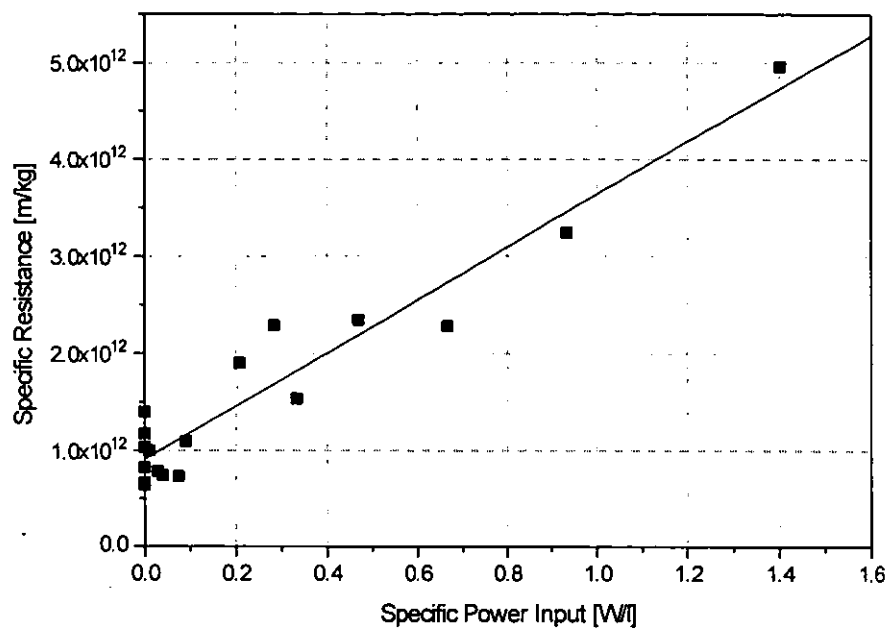


Figure 4.35: Effect of agitation on specific cake resistance

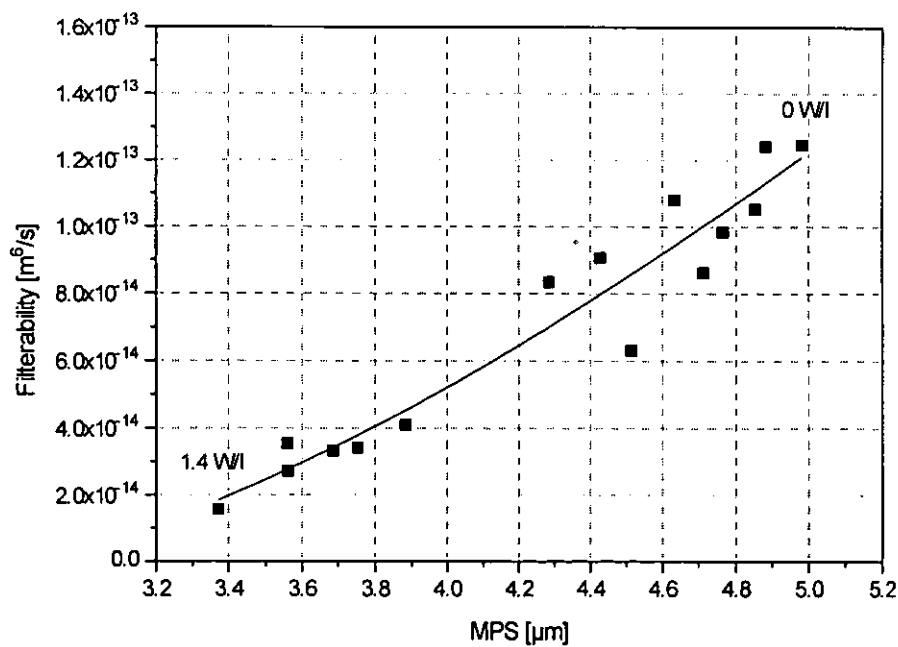


Figure 4.36: Correlation between MPS and filterability

4.2.3.4. Conclusion

This set of experiments made it possible to investigate lower levels of power input, without additional effects of temperature.

It was shown that all parameters are affected by agitation, however significant changes were mostly observed in a minimal power input range from 0 - 0.4 W ℓ^{-1} . Extract and viscosity, were affected in an even narrower band from 0 to 0.1 W ℓ^{-1} . The range of power applied in these trials was similar to industrial scales, which makes it possible to transfer the findings. It can be concluded that power input could be reduced down to 0.1 W ℓ^{-1} to reach optimum filterability, without extract loss.

Power input levels higher than 0.1 W ℓ^{-1} immediately exhibited negative effects on filterability: MPS in the fines decreases and total solids levels below 106 μm increase.

For all analyses a plateau is reached at 0.5 W ℓ^{-1} , for this well modified malt. Above this level analyses did not vary significantly. Pilot trials used a flow loop with valves and orifices, the mash was pumped by a mono pump. The mechanical energy input of this pump could not be quantified, but it is now possible to conclude that, as no significant changes in extract (density) or viscosity could be seen in pilot scale trials, its energy input must be in excess of 0.5 W ℓ^{-1} . Effects on filterability above 0.1 W ℓ^{-1} (where viscosity is constant) can be explained at a high significance level ($R=0.96$) by a change of the MPS.

4.3. Effects of Final Mashing Temperatures on Lautering Performance

4.3.1. Introduction

Effects of different final mashing temperatures on lautering performance have been previously reported in the literature. Increasing the temperature from 65 to 75°C was found to reduce filtration time (time to collect a given volume of filtrate) in lautering by over 40% (Kano and Karakawa, 1979). This was explained by the residual amount of starch in the spent grains, which is higher at lower temperatures.

In practice, the temperature of 78°C was found most suitable¹, because run off rates are higher than at lower temperatures. The only explanation for this increase of filterability with temperature was attributed to the reduction of viscosity with higher temperatures (Lüers, 1950; Hough et al. 1986; Narziß, 1985).

Particle size analyses of mash from previous trials indicated that significant changes can be observed with different mashing regimes. Strong agitation of mash, for example, created a higher proportion of fine particles. The mean particle size (MPS) of a 106 µm sieved mash sample was reduced. A good correlation between MPS (number distribution) and lautering performance (see Figure 4.37) was found.

These experiments were designed to investigate the effect of final temperatures on the particle size distribution of fines.

¹In large scale brewing, generally a final temperature in the mash of 78°C is used. At this temperature, a small α -Amylase activity remains in the mash for a limited period. Higher final mashing temperatures are not employed, because an extraction at higher temperatures would result in a solubilization of higher dextrins and other branched carbohydrates. These substances would not be degraded by the remaining enzyme activity. Higher viscosity and turbidity in wort and beer, together with microbiologically unstable products would be the consequence.

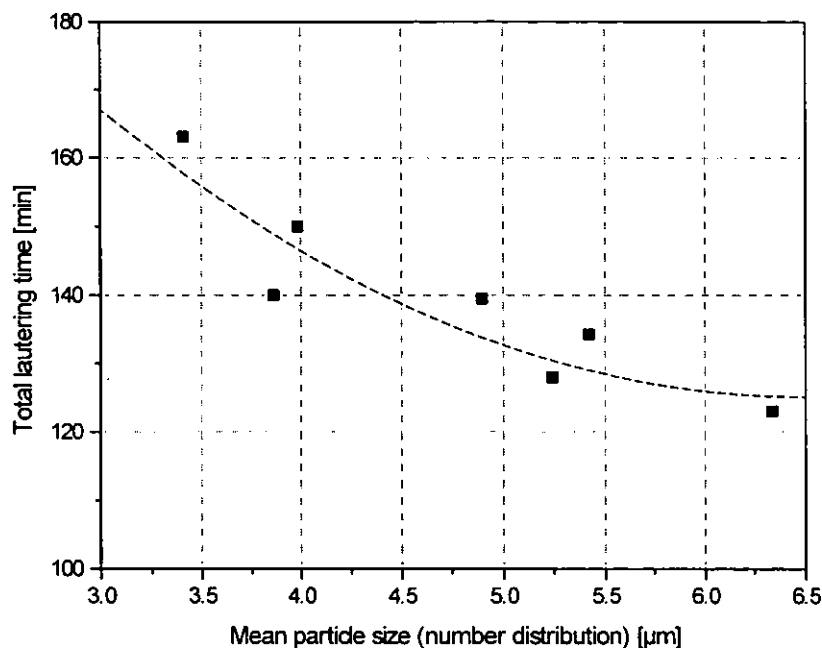


Figure 4.37: Effects from MPS on total lautering time

4.3.1.1. Aims

It was the aim of this set of trials firstly:

- to quantify the influence of mash temperature on PSD and viscosity, and, secondly
- to identify, whether changes in particle size distribution (due to temperature effects in mash) play a role in mash filterability. Consequently, the extent of PSD and viscosity effects on filterability should be quantified.

In this set of trials, specifically, the effects of final mashing temperatures between 65 and 100°C were quantified with the following analyses:

1. the particle size distribution of mash (PSD)
2. viscosity,
3. extract content and
4. filterability of mash.

4.3.1.2. Experimental

Infusion mashing was carried out at a constant temperature of 65°C for a time of 40 minutes. After the temperature rest, the mash was heated to 100°C. At 5°C-intervals, samples were taken from the mash.

In total, three trials were carried out. Two of these used the same well-modified malt and milling conditions but different brewhouses. One trial was done with an undermodified malt.

Trial 66 was carried out on the pilot plant set up for agitation work, under identical conditions to previous trials. The heating rate was set to an initial rate of 0.5°C.min⁻¹. During the entire mashing process the mash was recirculated in the Mono pump loop. Malt was from the batch used for all previous trials (Blenheim, 1992 harvest). The total heating interval from 65 to 100°C required 110 min.

Trial 67 was carried out using the same procedure as above; the only difference was the use of undermodified malt, prepared in the BRFI maltings, in combination with a finer gap setting (0.55 mm) of the roller mill. The setting was adjusted to obtain a similar grist sieve distribution to the well-modified malt. The total heating interval from 65 to 100°C required 105 min.

In trial 68, again well modified malt was used (same batch as trial 66) but in the BRFI pilot brewhouse. The water quality in the brewhouse is different from pilot trials, as 200 ppm CaSO₄ is added to the de-ionised water. However, the main difference between agitation pilot plant and brewhouse operation is the different mixing of the mash and the heating rate. This trial was carried out to see how mixing conditions and very short temperature incubation times influence the mash properties. Therefore the heating rate was set at 1°C.min⁻¹, up to 100°C. The heating interval from 65 to 100°C was 35 min in comparison to over 100 minutes in both other trials.

4.3.1.3. Results

Change of mean particle size - LS130 Analysis

Particle size distributions were analysed in a diluted, 106 µm sieved mash sample. This processing enhances the resolution of particle size changes

in a small size range, i.e. the sensitivity of the analysis is increased. Monitoring of fine particles is of great importance, as filterability in the lauter tun is directly dependent on amounts and properties of fine particles (Muts and Pesman, 1986).

The mean particle size (MPS) determined from the differential number distribution on the Laser Sizer (LS130) shows, for all trials, a significant change of the size with increasing temperature (see Figure 4.38).

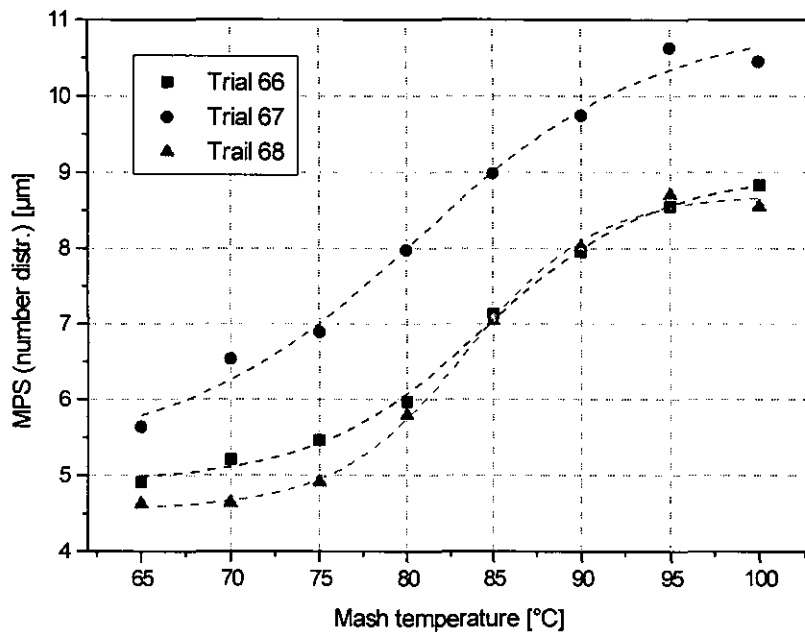


Figure 4.38: Effect of mash temperature on MPS (number distribution).

The well-modified malt (Trial 66, 68) is slightly less sensitive to temperature than the undermodified malt. It can be assumed that the higher level of the values obtained from undermodified malt (Trial 67) is due to a proportion of smaller particles (such as small starch granules) present in the mash. Trial 66 shows a slightly higher level at the start of heating, which could be caused by a mechanically induced precipitation reaction, due to elevated agitation levels (shear) or by chemical effects such as different redox values. Changes in the redox state could be explained by different oxygen uptake in the two brewing plants or by effects from the different water qualities (buffer capacity).

In general, change of the PSD in mash, which occur mainly in the size range between 2 and 40 μm can be described by the precipitation of proteins above 60°C. This effect was described by Lewis et al. (1984, 1985). They observed changes in protein content and protein molecular weight distribution due to denaturation of proteins and precipitation with polyphenolic substances.

Change of particle size distribution (PSD) - Multisizer Analysis

The Laser Sizer can describe PSD changes with mashing temperature. However, it is not possible to quantify particle concentrations. Therefore additional particle size analyses were carried out with the Multisizer to determine particle concentrations in the 106 μm sieved mash samples. The Laser Sizer and the Multisizer operate different particle detection systems, thus corroborating the Laser Sizer analysis and proving that differences in the particle size distribution can be observed with mashing temperature.

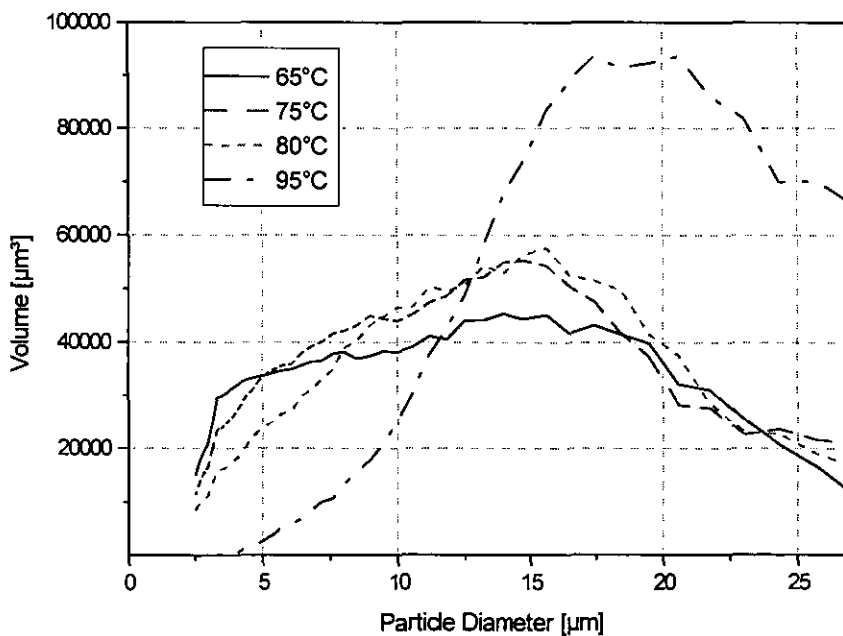


Figure 4.39: PSD of mash (Volume distribution), Trial 66, analysed on the Multisizer.

Figure 4.39 shows the change of the PSD (differential volume distribution) for Trial 66. It is clearly visible that smaller particles disappear with higher temperatures. The sharp inflexion at 2 μm in the curves for 65 and 75°C show the lower end of the analysis range of the 140 μm orifice on the Multisizer. Even smaller particles can be expected, below this level, from the shape of the curves. Results for both other trials are similar.

Concentration of fine particles

The volumetric particle concentration of a diluted suspension, sieved with a 106 μm sieve was determined in the Multisizer. Increasing fine particle concentrations generally have a negative effect on the filterability of a suspension. It can be shown, that particle concentration changes during the heating period are not significant: no additional fine particles are created in either of the two brewhouses and even different malts have no significant effect (see Figure 4.40).

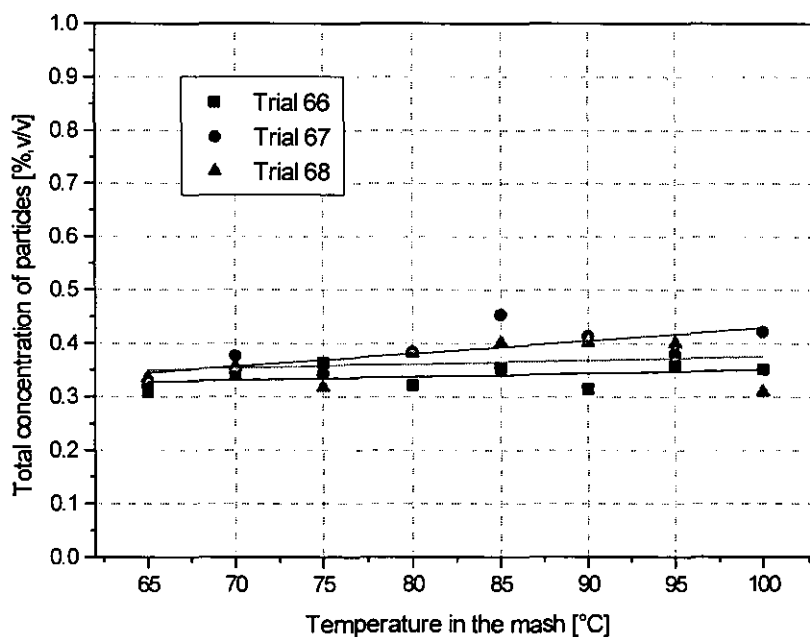


Figure 4.40: Volumetric particle concentration of fines in the analysis suspension

A similar result has been obtained from the dry solids analysis: the standard deviation of this analysis was found to be high in relation to the small solids content in the 106µm sieved, diluted sample. Changes in dry solids could not be observed. It can be concluded that no additional fines are forced into solution by agitation during the heating period (see Figure 4.41).

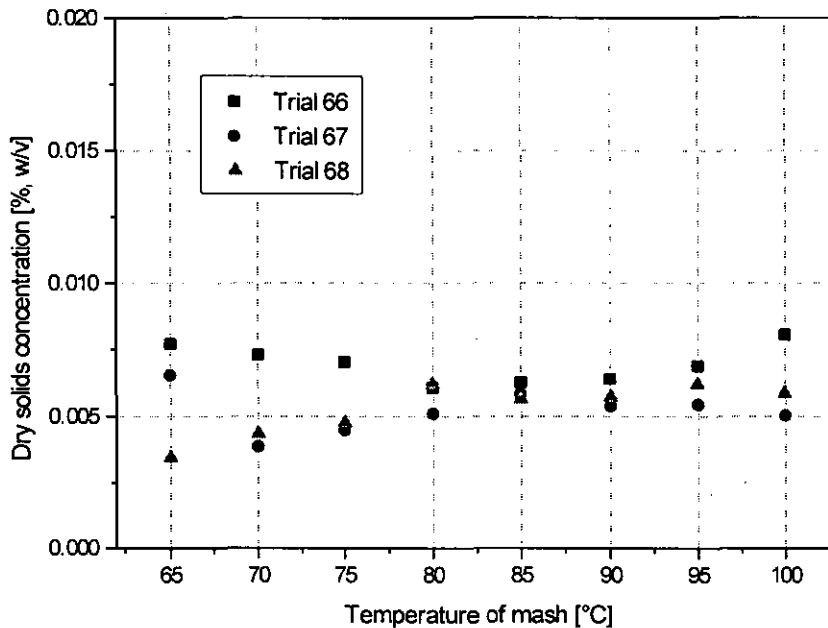


Figure 4.41: Dry solids concentration of fines (<106µm sieve step) in mash

Viscosity of mash

The viscosity of samples, taken every 5°C, typically, from 65 to 100°C, was determined at 20°C. As filterability trials were carried out at 65°C, it was necessary to recalculate the viscosity to this temperature level. This was done by a viscosity vs. temperature calibration curve established for one mash sample (Trial 68). Figure 4.42 shows the effect of temperature on viscosities of wort, water and sucrose solution.

The following equation was employed to relate viscosities obtained at 20°C to those at 65°C:

$$\eta_{65} = 0.188 + 0.272 \eta_{20}.$$

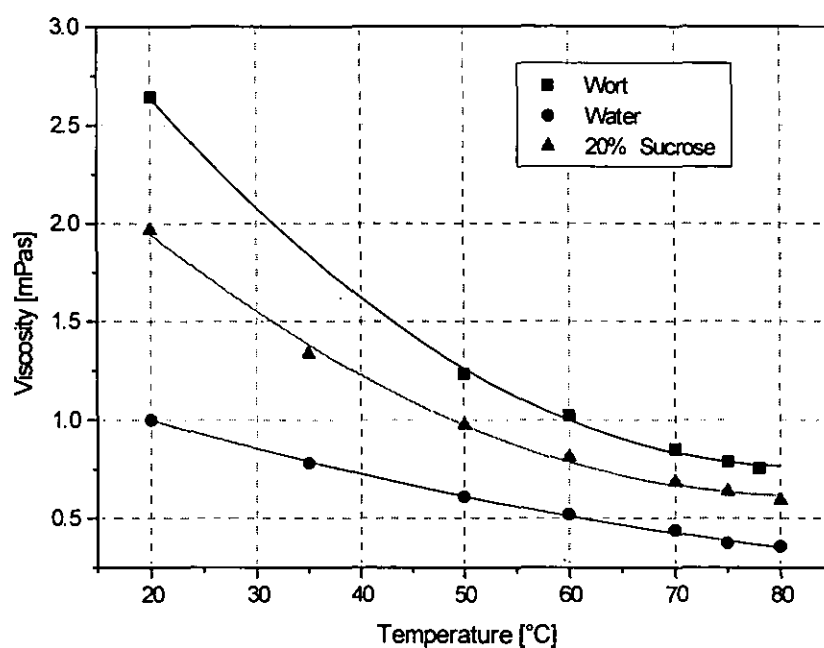


Figure 4.42: Change of viscosity with temperature

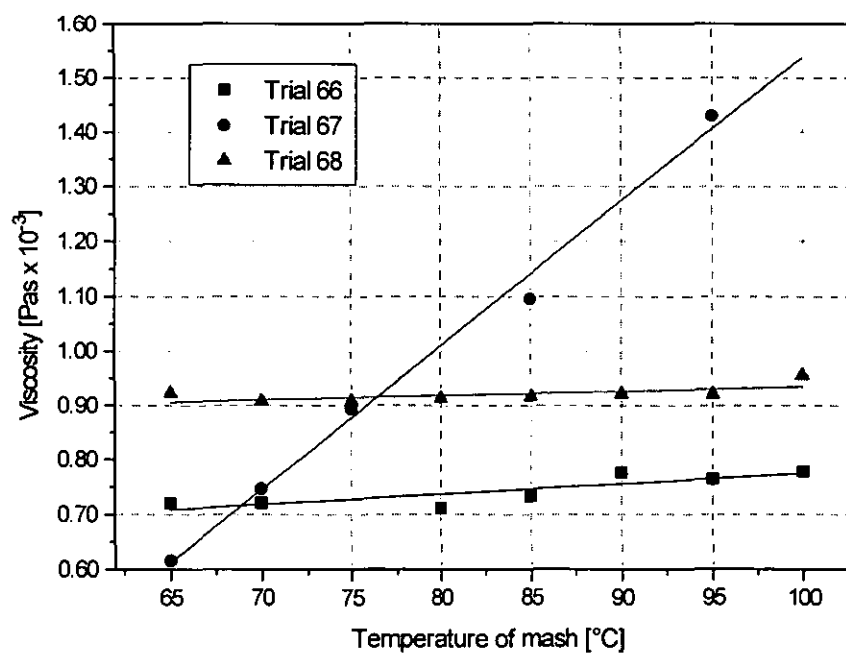


Figure 4.43: Viscosity at 65°C in the liquid phase of mash; (samples taken at different mash temperatures)

It can be seen in Figure 4.43 that viscosities for both well-modified malt mashes (Trial 66 and 68) do not change to a great extent. The different levels between Trial 66 and 68 are caused by different amounts of extract in solution. Viscosity of Trial 67, using undermodified malt, however, shows a strong increase of the viscosity with mashing temperature. As the extract level is only slightly increasing (see Figure 4.44), it can be concluded that this drastic viscosity increase is due to release of high molecular weight material (such as dextrins and β -glucan and gums) into soluble form. The three dimensional structure of these substances is capable of increasing viscosity. Release of these materials could be due to temperature effects or, additionally, due to agitation regimes present in the pilot plant.

It is important to mention again, that viscosity increase for the well modified malt is minimal. As subsequent filterability trials were carried out at 65°C, it can be said that the effect from viscosity on a change of filterability is very small.

Density of mash

Density of the liquid phase of mash was measured at 20°C. Figure 4.44 shows the results for the trials. It is clear that the liquor-to-grist ratio for the two experimental set-ups were different (Trial 66 and 68). Trial 68 was mashed at a higher concentration.

Interestingly, the slopes of extract formation with mashing temperature are different (see Table 4.7) between the two brewhouses (Trial 66 and 68).

Table 4.7: Slopes for linear fits of density and extract vs. mash temperature

	Density slopes (fit for 65 - 95°C) g/ml/°C	Extract slope (fit for 65 - 95°C) °Plato/°C
Trial 66	7×10^{-5}	0.07
Trial 67	5×10^{-5}	0.05
Trial 68	5×10^{-5}	0.05

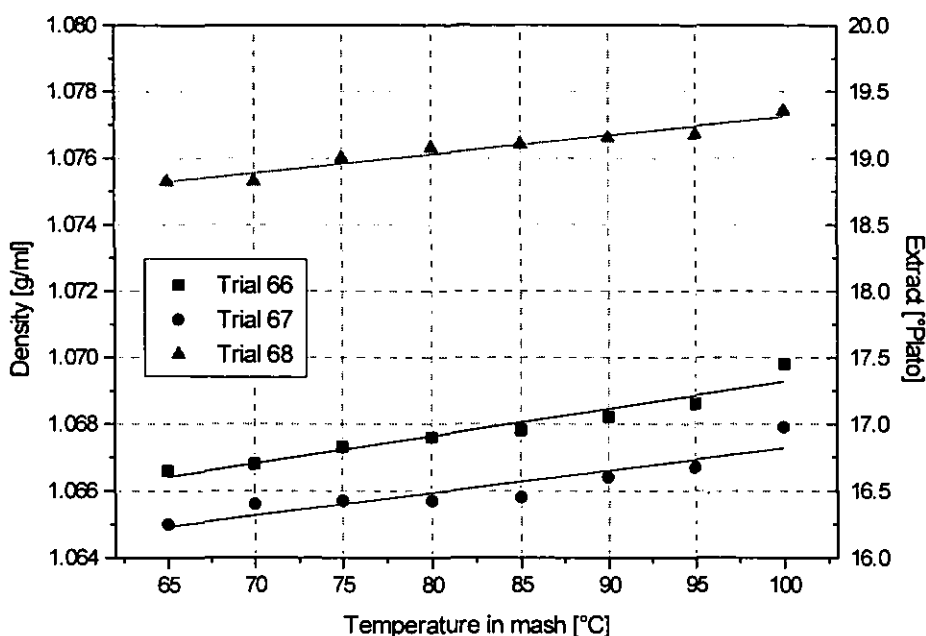


Figure 4.44: Density (Extract) in the liquid phase of mash

This indicates that the stronger mixing conditions enhanced extract formation (density increase) at higher temperatures.

Filterability of Mash

Filterability was tested using a Millipore filter cell. The filtration of all mash samples was carried out at 65°C. This temperature was chosen to avoid cold trub formation (below 65°C) and to avoid additional effects on mash, described above, beyond 65°C. Filtration curves were plotted as dt/dV over V diagrams. In these diagrams the resistance of the filter medium (Whatman GF/D filter paper) could be determined as zero (section of the fitted line at the ordinate is negative or zero).

An example of a plot is given in Figure 4.45 for Trial 67. It can be seen that filtration experiments (for individual temperatures) can deviate from standard cake filtration when a certain volume has been filtered, because of pore blockage. Linear fitting functions have been drawn for data points only, which are in accordance with cake filtration laws. This fact will reduce filtration performance further, as only a very limited volume can be filtered before blockage of the filter occurs.

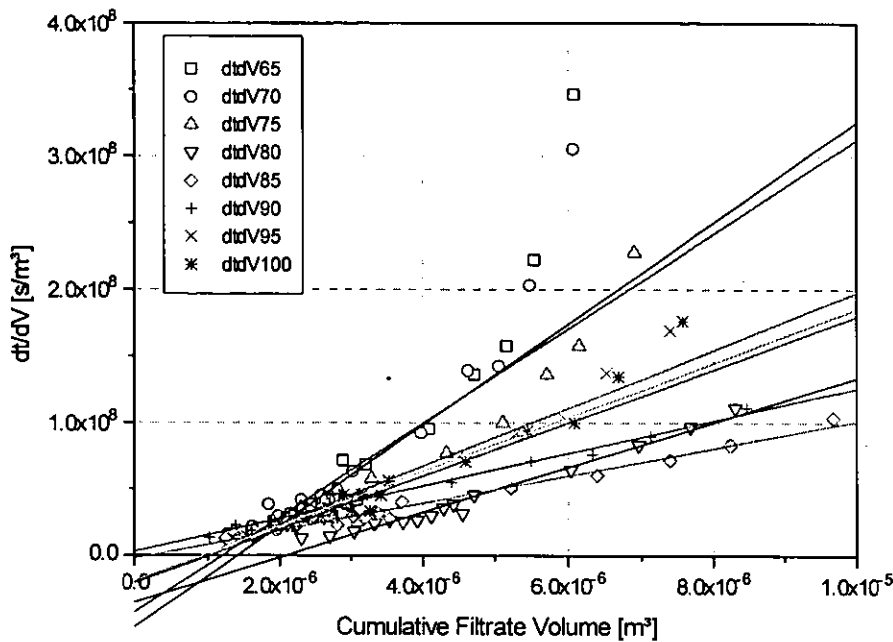


Figure 4.45: Trial 67, dt/dV vs. V plot with linear fits for data points in accordance with cake filtration law

Filterability $1/K$ of the slurry can be determined directly from the slope K of the linear fit in dt/dV vs. V plots as:

$$\frac{dV}{dt} = \frac{1}{K} V \quad 4.12$$

It is also possible to calculate the average specific resistance α of the filter cake from the slope K of the filtration curve, as viscosity η , concentration of the slurry c , A and Δp are known.

$$\frac{dt}{dV} = \frac{\eta \alpha c}{A^2 \Delta p} V = K V \quad 4.13$$

The effects of mashing temperatures on filterability $1/K$ are displayed in Figure 4.46. If a limited filtrate volume in accordance with cake filtration laws was observed this was marked at the data point.

It can be seen, that filterability increases dramatically with the temperature in the mash samples. The differences of the malt quality are also visible: Trial 67 shows the lowest filterability and the maximum filterability is

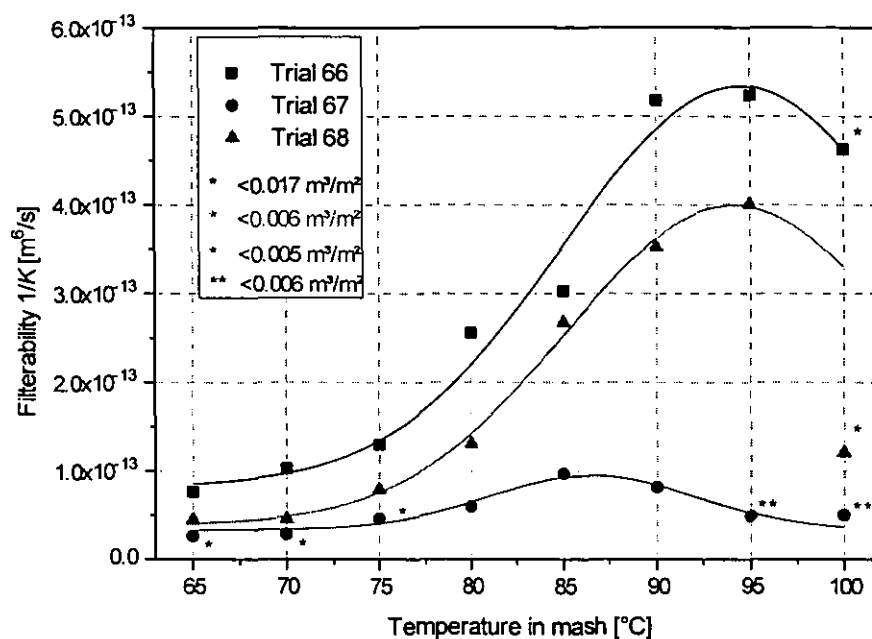


Figure 4.46: Filterability measured in a Millipore filter cell for different mashing temperatures (* and ** maximum volume filtered per filter area before blockage occurred)

already reached at a lower temperature. This can be explained by the strong increase of viscosity in Trial 67 with mashing temperature, which counteracts any improvement of filterability with higher temperatures. Trials 66 and 67 show a very similar shape of the filterability curve, only the initial value is elevated, an improvement in filterability between mashing temperatures of 65°C and 78°C could be clearly seen.

Table 4.8: Filterability increase between 65 and 78°C

Trial No.	Filterability (1/K) at 65°C [m ⁶ .s ⁻¹]	Filterability (1/K) at 78°C [m ⁶ .s ⁻¹]	Increase in filterability [%]
66	0.82 x 10 ⁻¹³	1.89 x 10 ⁻¹³	230
67	0.17 x 10 ⁻¹³	0.47 x 10 ⁻¹³	276
68	0.41 x 10 ⁻¹³	1.18 x 10 ⁻¹³	288

The change of filterability could be due to a change of the viscosity η , the resistance of the filter cake α or the concentration of the solids in the mash c (see Equation 4.14).

$$\alpha = \frac{K A^2 \Delta p}{\eta c} \quad 4.14$$

c and η are known as well as the differential pressure over the cake Δp and the filter area A , which makes it possible to calculate the resistance of the cake. As already described earlier, the total amount of solids in the mash c does not change significantly during heating. The viscosity η is also near constant for the well-modified malt (Trials 66 and 68). These facts leave only the average specific resistance α to explain the changes in filterability (see Figure 4.47).

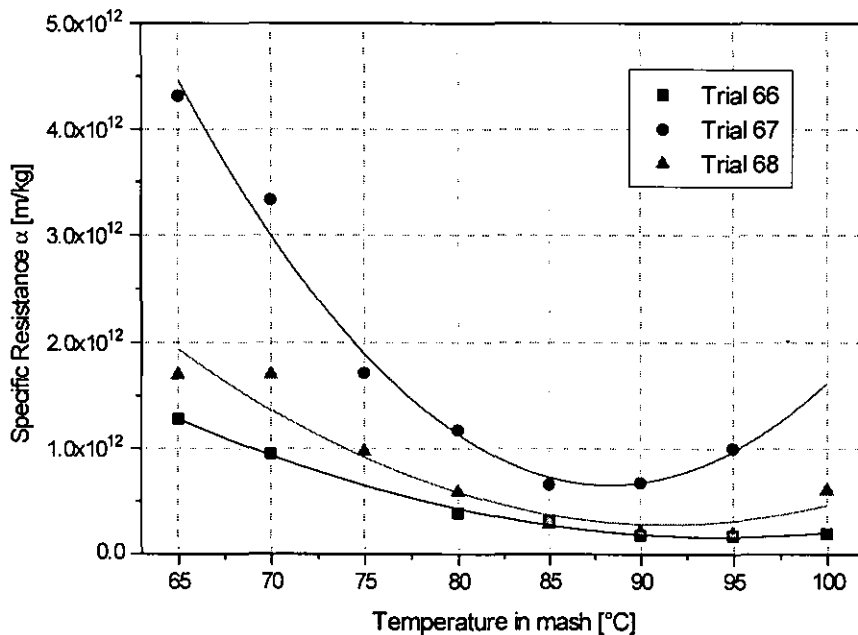


Figure 4.47: Specific resistance of filter cakes with mashing temperature

The specific resistance of the filter cakes reduces with mashing temperature. Curve fitting gives similar equations to the filterability plot (see Figures 4.46 and 4.47). It can be concluded that resistance is the predominant effect for filterability.

Trials 66 and 68 show no major difference in specific resistance, which means that differences observed in the levels of filterability are due to different viscosities. Trial 67 shows a higher level than both other trials, an observation which could be explained by the different malt modification.

In general, it was found, under all test conditions, that the improvement of filterability is caused by a change of the specific cake resistance and is not caused by viscosity changes. (As filtration was carried out at 65°C for all mash samples, no viscosity differences occurred due to filtration temperature.)

This effect of reduced specific cake resistance with higher temperatures can only be explained by a change of the mash composition with higher mash temperatures. As enzymatic effects could only cause changes up to about 75°C, there must be other reasons for the big increase of filterability with temperature.

If the specific resistance α is plotted against mean particle size (MPS) (see Figure 4.48) it can be seen that the decrease in resistance can be described with high correlation ($R=0.96 - 0.98$) with the MPS-increase, in a range from 65 up to about 85°C. The change of the cake resistance with temperature in the practical temperature environment can be explained solely by MPS changes. However, it is not possible from this plot to predict the resistance of the filter cake from MPS. Therefore, additional information about the nature of the material will be required.

The mash produced in the agitation pilot plant showed the lowest level of resistance. Reasons for this behaviour have to be investigated further.

4.3.1.4. Conclusion

These results show that previous assumptions, about the improvement of lautering/filterability with mash temperature have not taken the importance of the change of particle size distributions into account. In the literature, viscosity change due to a temperature increase is given as the only explanation. Viscosity has a linear influence on filterability; however, an increase due to higher filtration temperature (78°C instead of 65°C) will affect filterability in lautering by about 20 to 25%.

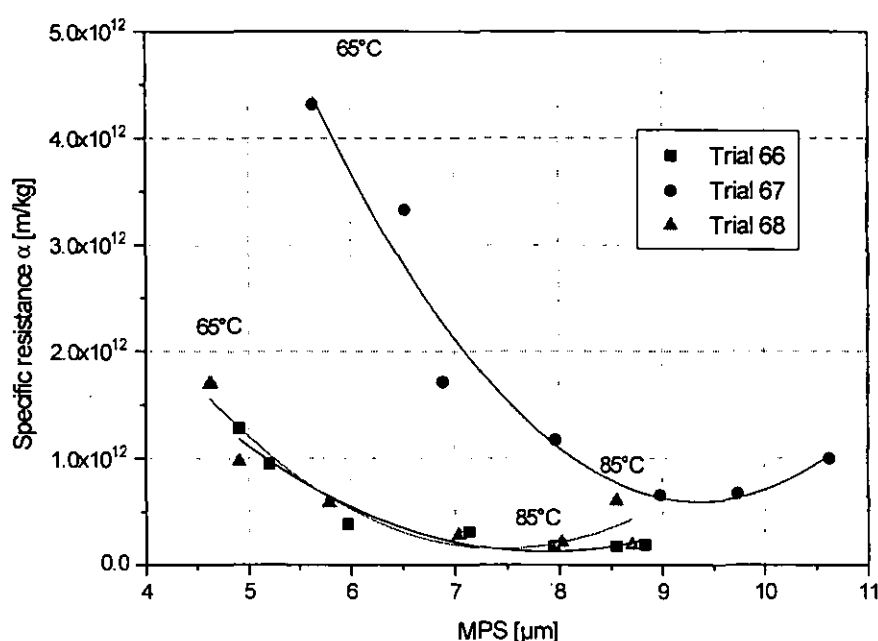


Figure 4.48: Specific cake resistance vs. MPS

Filterability actually changes by over 200% from 65 to 78°C in small scale (Millipore) trials, without the beneficial influence of lower viscosity. This big increase can only be explained by a fundamental change of the specific resistance of filter cakes with mashing temperatures.

The importance of particle size effects in mashing are demonstrated here. The reduction of fines in the mash, described using the MPS is able to explain the drastic changes in cake resistance with temperature.

The change of the particle size and the reduction of fine matter below 2 - 4 μm could be due to precipitation and aggregation effects of proteinaceous material with polyphenols (Lewis and Wahnnon, 1984; Lewis and Oh, 1985; Lewis et al., 1992) and other components capable of reacting with proteins.

4.3.1.5. Applicability to Lautering and Practical Mashing

In pilot scale lauter tun operation, a change in lautering run-off rate could be observed with changing mean particle size similar to these trials. This indicates, that the particle size change affects lautering performance as

well as filtration rates in the Millipore cell. It has been shown, that the conditions in the pilot scale lauter tun are similar to large scale operation, which makes the results and observations of these trials valid for the industrial scale of brewing.

In relation to agitation effects (see Chapter 4.2.3), the maximum reduction in specific resistance observed with temperature increase was less pronounced (see Table 4.9). This means that the application of higher final mashing temperatures can not "cure" problems caused by agitation.

Table 4.9: Maximum change of specific resistance due to agitation and temperature effects

Effect:	max. specific resistance at:	min. specific resistance at:	Reduction in specific resistance
Temperature (Trial 68)	65°C	95°C	$1.50 \times 10^{12} \text{ m kg}^{-1}$
Agitation	1.4 W/l	0 W/l	$4.46 \times 10^{12} \text{ m kg}^{-1}$

Additional trials investigated the effects of higher lautering temperatures downstream in fermentation and conditioning. It was found that higher temperature lautering causes the formation of additional haze during conditioning. Fermentation rates were similar to normal lautering temperatures. The haze observed in the conditioned beer consisted of neutral polysaccharide material, mainly starch and β -glucan. The application of external heat stable enzymes during lautering or of malt inherent enzyme extracts during the fermentation and conditioning stage could reduce such haze formation.

4.4. Particle Size Changes in the Fine Fraction of Mash and the Effects on Lautering Performance

4.4.1. Aim

It could be concluded from the results presented above that MPS of fine particles in mash varies with mashing off temperature and agitation conditions in the mash. To expand the MPS range in pilot scale trials, additional trials were carried out at MPS levels not covered by previous investigations. To obtain such extremes higher mashing off temperatures (above 75°C), as described in Chapter 4.3, were used. The aim of these trials was to obtain correlations between pilot scale lauter tun performance (spent grains bed permeability and extraction) and the particle size distribution of the fines. These correlations were required for the modelling work.

4.4.2. Results and Discussion

The following graph shows effects from MPS change on the permeability of a lauter tun cake. As permeability changes with height of the bed and viscosity, the permeability varies during lautering. The permeability of the spent grains bed approaches a constant value during cake washing. In this phase the height of the bed is constant and viscosity which is a function of extract content is also constant. This constant level was reached after collection of 8 litres of wort.

The graph in Figure 4.49 shows that MPS of the fines has a clear effect on permeability. Linearity was achieved by plotting the square of the MPS against permeability. This might suggest that the surface area of the particles contributes to this change, as the surface area is proportional to the square of the mean particle size.

Not only permeability of the cake is affected by MPS change but also the washing efficiency. The washing efficiency was determined as $E_{\text{wort}}/E_{\text{mash}}$; the higher the efficiency the better the washing. Best results were achieved when the fines were aggregated to larger particles. In practical circumstances this means that less water is needed to achieve the same washing effect. The maximum amount of washing liquor used is limited

firstly by the total volume of wort which can be boiled and secondly by the minimum extract level permitted before boiling. Lower extract levels would require a longer boiling and evaporation phase, and more energy would be required to achieve sufficient evaporation.

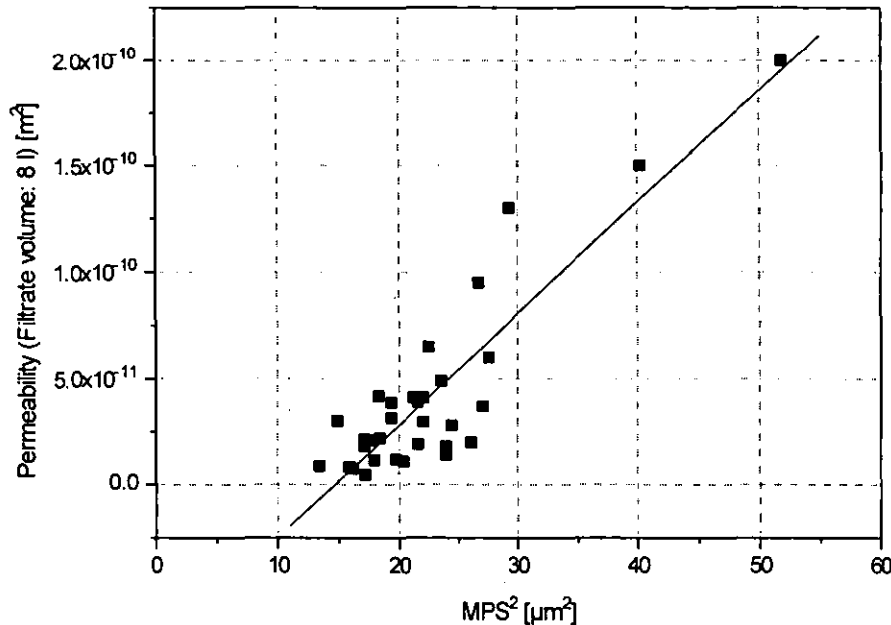


Figure 4.49: Effect of MPS on permeability of the spent grains cake ($R = 0.88$)

The third parameter analysed as a function of MPS is the turbidity of the wort. It could be observed already in the first trials in the lauter tun that wort with higher agitation was less clear. This effect relates also to the particle size distribution of the fines. Finer particles cannot be restrained in the filter cake and they cause increased turbidity.

Under industrial conditions turbidity levels could be reduced by recirculation, however this would extend the total lautering time, a fact which is not often tolerable.

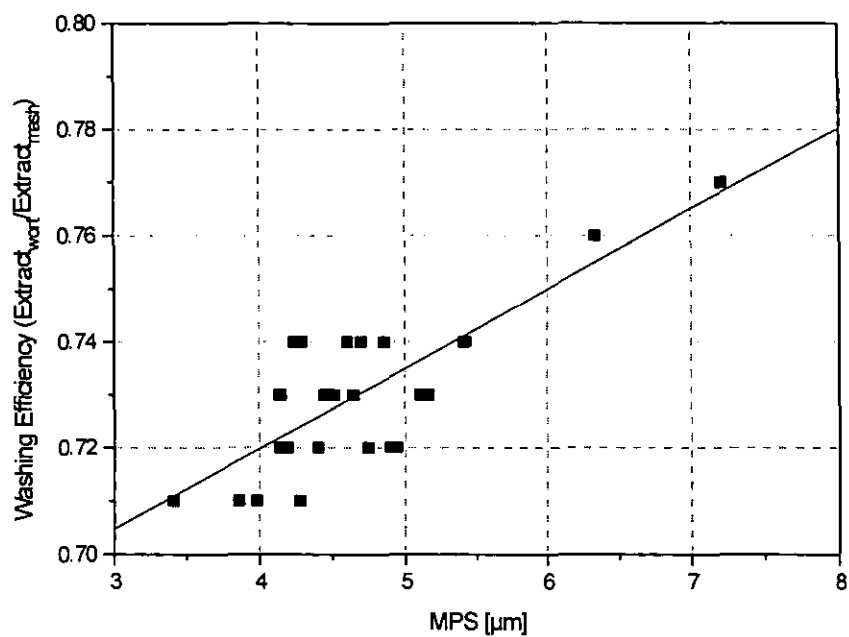


Figure 4.50: Effect of MPS on washing efficiency (R = 0.79)

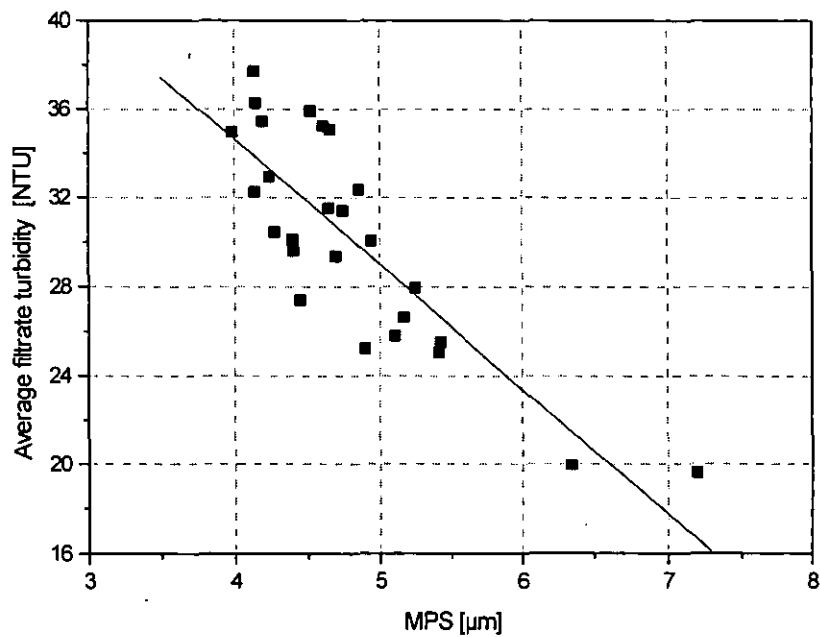


Figure 4.51: Effect of MPS on turbidity in the filtrate (R = 0.83)

4.5. Overall Conclusions

The experimental programme of this thesis focused on the investigation of the two parameters of the mashing process, maximum temperature and mechanical power input.

Mechanical power input is a function of the shear stress acting in the mash slurry. The effects of particle attrition causing a reduction in filtration performance and a reduced clarity of the wort were already known from the literature. (However, chemical analyses of mash and wort could not describe the effects of particle size change.) A detailed study of the attrition of fine particles with shear was done here for the first time.

It is now possible to look at industrial brewhouses and study effects of attrition on site. Effects on mash filterability can be computed from the combined effects of MPS and viscosity. The next step will be to develop a computer model which describes these effects on lautering performance. For different types of malt there might be additional parameters, which are related neither to viscosity nor to particle size change. Investigation of different malts or other raw materials might reveal these effects. However, for one combination of raw materials it will be possible to optimise the lautering performance in industrial size brewhouses.

It could be shown that the mean particle size correlates with the filterability of mash in bench scale and in pilot scale trials.

In the literature, the temperature of the mash before lautering was considered a balance between enzyme activity and reduction in viscosity with higher temperatures. Effects of temperature in the range from 65 to 78 °C on particle precipitation were mentioned in the literature (Kano and Karakawa, 1979, Lewis and Wahnnon, 1984; Lewis and Oh, 1985; Lewis et al., 1992.) The effects on particle aggregation, however, were never quantified. Additional effects from processing conditions or raw material quality might be existing.

5. Modelling of the Lautering Process

5.1. Description of the Process

In this chapter the lauter tun filtration procedure is modelled. The results obtained in previous experimental work were assembled to outline the process unit operations mathematically. The parameters identified previously as important in determining lautering performance were used to model the procedure.

The program used for the model is based on the findings in the pilot scale experiments. The model was designed to react to changes in particle size distribution of the fines and in viscosity. As already described earlier, particle size is affected by temperature and agitation. Viscosity is mainly affected by temperature and the soluble extract concentration for this malt quality.

Temperature is a parameter which is relatively easy to measure, it was therefore put directly into the model. Agitation, however, is difficult to quantify. The MPS change in the brewery due to shear or agitation in the mash needs to be measured directly. The analysis of fine particles with laser sizing is easy to carry out.

5.1.1. The Effect of Temperature on MPS

Mash temperatures above the minimum 'saccharification' temperature of 65°C causes particle aggregation in the fine fraction. Thus, the MPS increases with mash temperatures above 65°C. This behaviour, investigated in Chapter 4.3, could be incorporated into the lautering model.

The maximum temperature in the mash has a permanent effect on the MPS. In the mashing procedure for all agitation trials the maximum temperature was 75°C. The MPS figure at this temperature was used as an input variable to calculate the MPS at temperatures from 65°C up to 95°C.

The change of the MPS with the mash temperature t can be described with the following equation (graph shown in Figure 5.1):

$$MPS = MPS_{75^{\circ}\text{C}} - 0.144 \times (t - 75^{\circ}\text{C}) + 0.0052 \times (t - 75^{\circ}\text{C})^2 - 1.869\text{E-}4 \times (t - 75^{\circ}\text{C})^3 \quad 5.1$$

with an accuracy of $R = 0.97$.

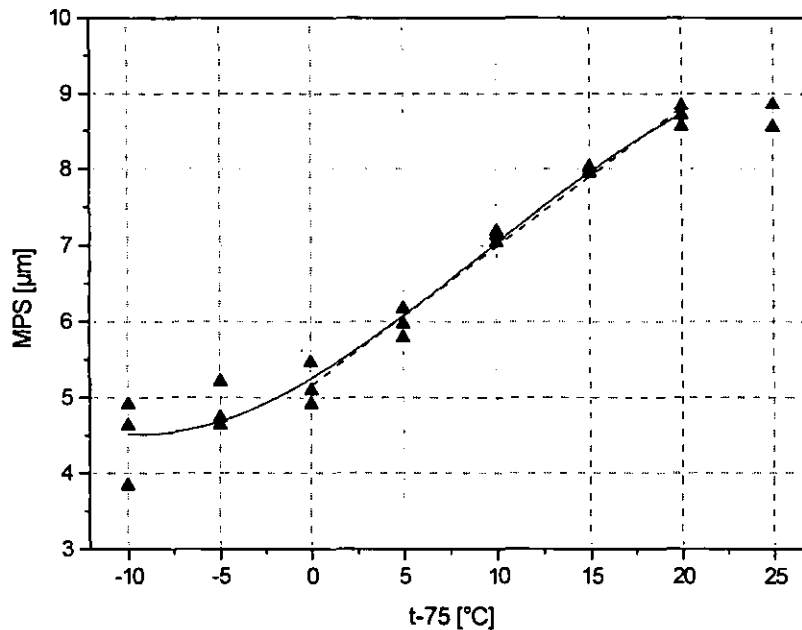


Figure 5.1: MPS-temperature relationship

MPS depends on temperature in a linear way ($R=0.99$) in the range from 75 to 95°C. The following equation (dotted line) was fitted in this range:

$$MPS = MPS_{75^{\circ}\text{C}} + 0.18 \times (t - 75^{\circ}\text{C}) \quad 5.2$$

5.1.2. Effect of Temperature on Viscosity of the Liquid Phase of Mash

Brewery laboratories determine viscosity at 20°C. To enable the use of routine analysis, it was necessary to correlate viscosity at 20°C to that at 70°C, therefore the viscosity-temperature trial (Trial 68a) was extended down to 20°C. In addition, Eyben and Hupe (1980) report the temperature correlation between 20 and 70°C for worts from over 20 different malt samples. This relationship is displayed in Figure 5.2.

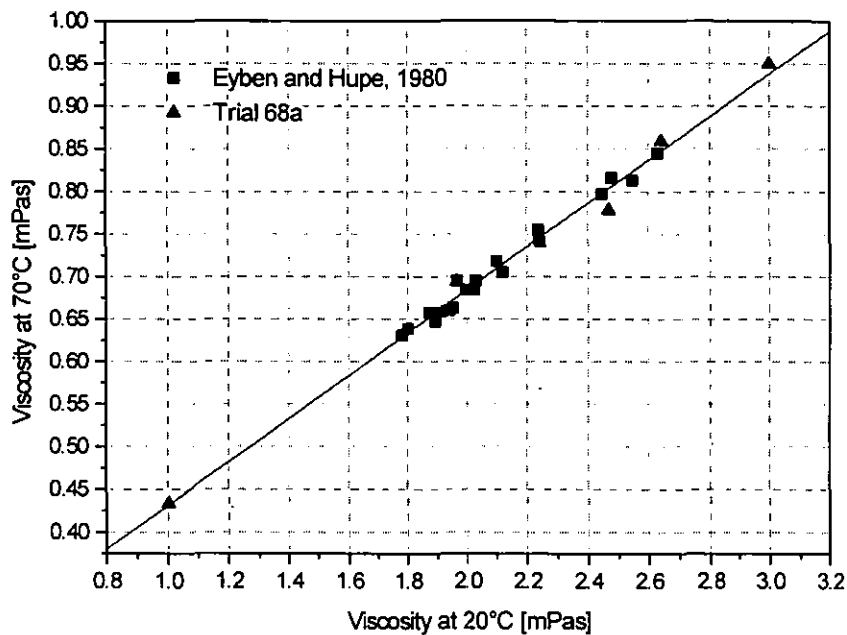


Figure 5.2: Relationship between viscosities at 20°C and 70°C

The linear fit has the following relationship ($R=0.99$):

$$\eta_{70} = 0.180 + 0.254 \times \eta_{20} \text{ [mPas]} \quad 5.3$$

This relationship was incorporated in the computer-model to avoid the need for a viscosity analysis at higher temperatures.

For all trials viscosity in the liquid phase of mash (wort) was measured at 75°C. This temperature was also used for lautering.

As temperature in the lautering stage may vary in industry, this would affect the viscosity of a wort. To obtain a relationship between temperature and viscosity, a trial was carried out applying temperatures up to 85°C (Trial 68a). In addition, data sets from the literature about temperature effects on water (Perry, 1985), sugar solution (Perry, 1985) and wort (Asselmeyer et al., 1973) were used.

It was shown in the previous experiment that viscosity at 70°C can be predicted from 20°C analysis. The fitting function shown in Figure 5.3 was now used to determine the viscosity (from the 70°C value) at any lautering

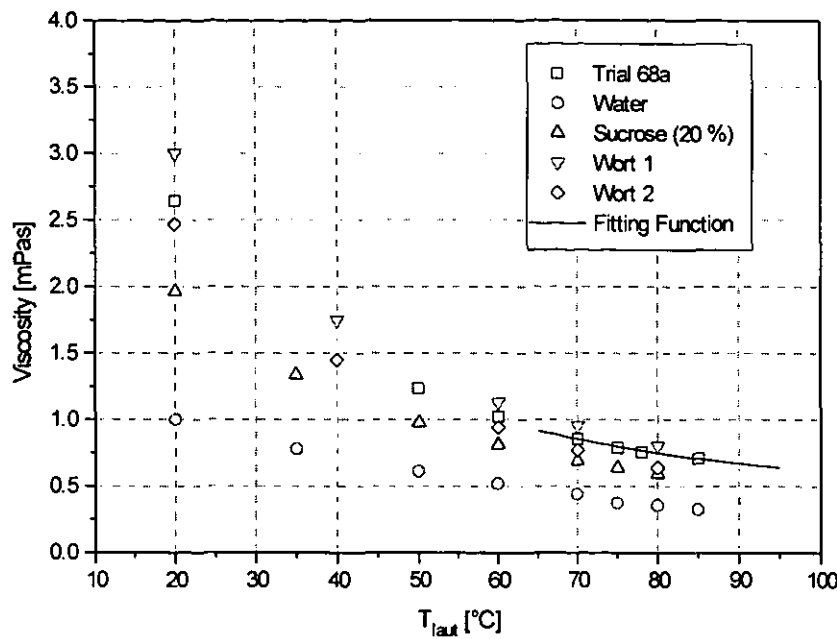


Figure 5.3: Viscosity-temperature relationship, with fitting function covering the range from 65 to 95°C

temperature in the range from 65 to 95°C:

$$\eta_{\text{laut}} = \eta_0 + 0.0298 \times T_{\text{laut}} + 1.30 \times 10^{-4} \times T_{\text{laut}}^2 \quad 5.4$$

The following procedure is used in the model:

1. viscosity at 20°C is the input value
2. viscosity at 70°C is calculated using equation 5.3
3. using equation 5.4 η_0 is calculated using the known data pair $\eta_{\text{laut}}-T_{\text{laut}}$ at 70°C.
4. the viscosity at the lautering temperature used in the brewhouse is calculated using equation 5.4 with η_0 .

In addition to temperature, soluble extract in the filtrate influences viscosity. Viscosity increases with soluble extract concentration. This

effect influences lautering at the washing stage. With increasing dilution of the extract the viscosity drops and, hence, filtration rates increase.

The change of viscosity with extract concentration was measured by Kolbach (1960). Kolbach's data can be fitted with the following equation with a correlation coefficient of $R=0.99998$.

$$\eta = \eta_0 + 5.856 \times 10^{-2} \times E - 1.4188 \times 10^{-4} \times E^2 + 1.4646 \times 10^{-4} \times E^3 \quad 5.5$$

This equation was used to describe the viscosity change during lautering as a function of extract concentration. The dilution of the extract concentration during washing causes the viscosity of the filtrate to decrease with filtrate volume. The differential pressure across the cake decreases with viscosity and, as filtrate flow rate and pressure drop are linked, the flow rate increases during cake washing.

5.1.3. Sedimentation - The Cake Height after Settling

Particles from the mash settle in the lauter tun. Due to the wide particle size distribution, a fine particle fraction settles in a separate layer on top of the spent grains. This sedimentation determines the total bed height at the start of the filtration.

The sedimentation of fine particles is influenced by two factors:

1. density difference between particles and the liquid and
2. particle size of the fines (MPS).

Solid-liquid density differences and viscosities in mash were kept constant in the trials. Hence it is possible to plot the settling rate against the square of the MPS. It can be reasoned that the surface area of the particles affects settling velocity; e.g. in Stokes' law, the settling rate is proportional to the square of the particle size.

$$-\frac{dh}{dt} = -\frac{g(\rho_p - \rho_l)MPS^2}{18 \eta} \quad 5.6$$

This relationship is shown in Figure 5.4. It can be seen that the assumption of the square influence of the MPS is right.

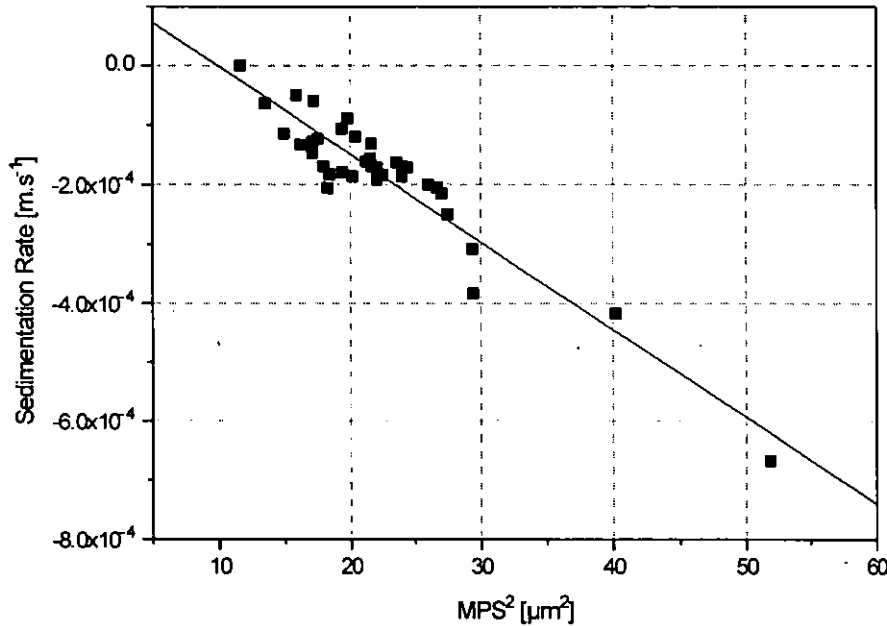


Figure 5.4: Sedimentation rate vs. MPS². Linear regression: with R = -0.93822

$$dh dt^{-1} = 1.474 \times 10^{-4} - 1.4802 \times 10^{-5} \times MPS^2 \quad [ms^{-1}] \quad 5.7$$

Variations in the behaviour might be due to inconsistency of temperature or viscosity during settling.

Analysis of the sedimentation rate and the above correlation may be a suitable way to replace the particle size analysis where a laser sizer is not available.

In the pilot scale lautering procedure, the settling was limited to 10 minutes. After this interval the filtration was started. The lowest possible level of the bed after sedimentation is 0.42 m. This level is dependent on the total concentration of solids, the load of mash in the vessel and the packing density of the spent grains. Due to the complexity of the input variables, it would be suitable to measure the final sedimentation height for each application. In the experiments used to establish this model, the total concentration of solids was kept constant at a level of 74 g ℓ⁻¹. This

value is directly related to the water to dry grist ratio of 3.5 to 1. The filling level of mash was constant at 0.53 m, hence the maximum sedimentation height at the start was 0.53 m. Figure 5.5 shows calculated and measured data for the total cake height after sedimentation.

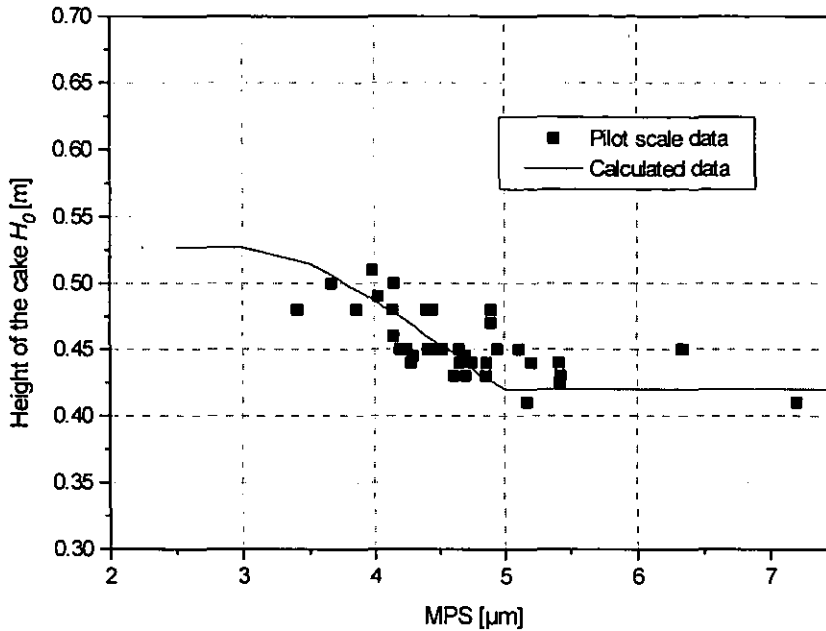


Figure 5.5: Measured data compared with calculated data using the following equation for $0.42 \text{ m} < H_0 < 0.53 \text{ m}$

$$H_0 = 0.53 + (1.474 \times 10^{-4} - 1.4802 \times 10^{-5} \times \text{MPS}^2 \times 540) [\text{m}] \quad 5.8$$

5.1.4. Final Permeability of the Cake

The permeability, K was calculated for all pilot scale trials from the following measurements using Darcy's equation (equation 5.9).

- Height of the bed, L
- filtration rate, dV/dt
- viscosity, η , and
- differential pressure across the cake, dp .

$$K = \frac{dV\eta L}{dt dp}$$

5.9

Constant permeabilities were achieved after 8 litres of wort were collected. Due to inaccuracies in the pilot scale analyses, especially at the beginning of the experimental programme, the calculated values for the permeability are spread at the lower end of the permeability range. However there is a clear relationship between MPS² and the permeability of the cake. The linear regression for the data had a coefficient of $R = 0.83$. The permeability analysis of the bench scale work could verify that the assumption of inaccuracies during the measurement is valid, as small scale work carried out on the Millipore filter cell (see Chapters 4.2.3 and 4.3) shows a much stronger correlation (see Figure 5.7). In this case the parameters were easier to control.

The fitted lines (Figures 5.6 and 5.7) show a distinct off-set on the x-axis from the origin. The reasons for this are the characteristics of the Laser Sizer LS130 for the analysis of fines and the model used to calculate the size distribution. Expressed as number distribution the limit of the MPS value was approximately 3 μm .

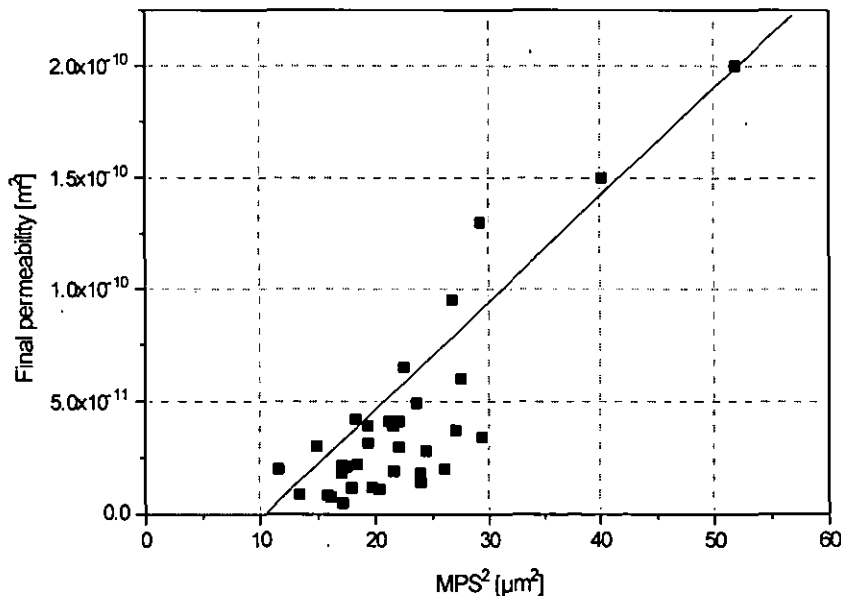


Figure 5.6: Final permeability vs. MPS²

These correlations verify that MPS^2 from the fines is the key parameter determining permeability of the filter cake. It was therefore decided to focus the computer model on this effect. Effects from the coarse particles layer seem negligible for the modelling of agitation and temperature aspects (see also Chapter 4.1.3.2).

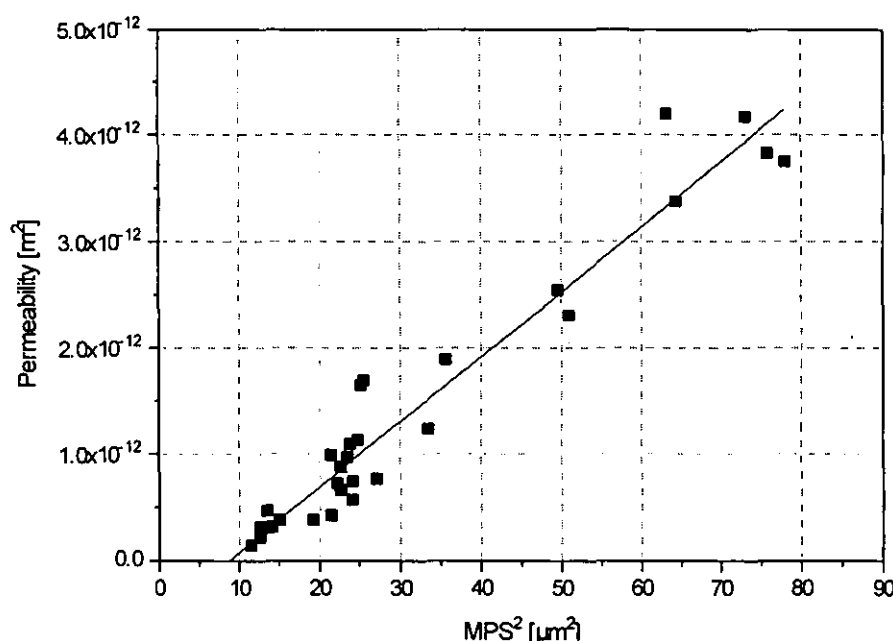


Figure 5.7: Bench scale permeability for trials with agitation and temperature variation. Pressure was constant at 100 mbar. Correlation coefficient $R = 0.97$

5.1.5. Effect of Pressure on the Final Cake Height

The final filter cake height in the lauter tun is affected by pressure. The relationship between pressure and cake height is important for the calculation of the final pressure. For the pilot scale trials another trend in the behaviour could be detected.

It has already been shown that the initial height of the cake after sedimentation is affected by particle sedimentation behaviour. This relates to the volume of the particles, and hence to the MPS. During the progress of the filtration, smaller particles compact to a greater extent than larger ones, and hence permeability of the filter bed is lower. This trend is shown in Figure 5.8 with a regression coefficient of $R = 0.80$.

A curve with the following equation was fitted:

$$L_{\min} = 4.2215177 - 15.733068 \times L_0 + 15.445633 \times L_0^2 \quad 5.10$$

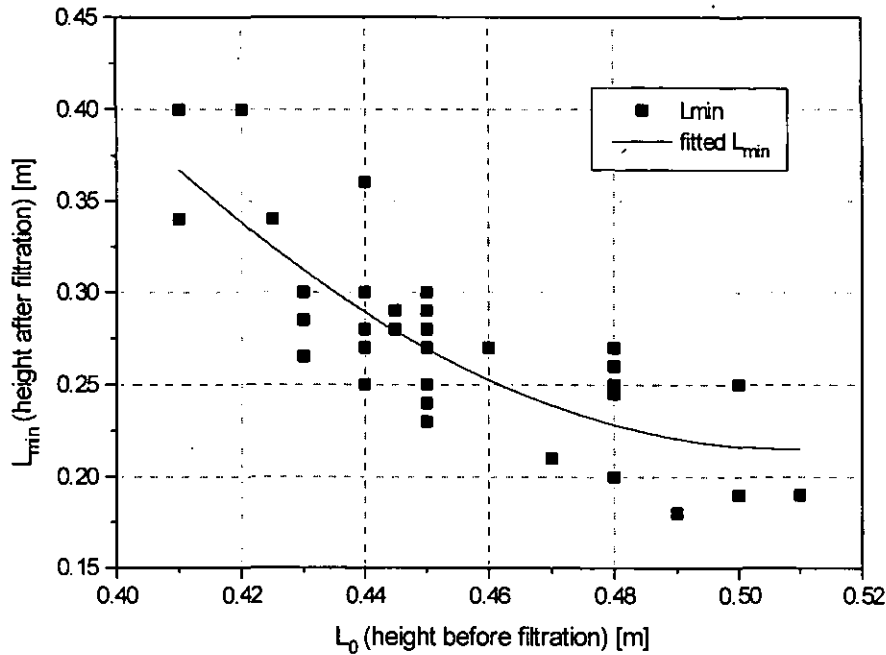


Figure 5.8: Height of the cake before and after filtration

The pressure across the bed was plotted for 11 trials against the cake height. In this plot (see Figure 5.9) the changing initial cake height has influence on the maximum pressure drop. The higher the initial cake height, the higher the span of the differential pressure. It is the purpose of this graph to build a relationship between the final pressure and the final height of the cake.

The following function (red line) was fitted ($R = 0.94$):

$$L = 0.35 - 1.17 \times 10^{-4} \times \Delta p + 2.18 \times 10^{-8} \times \Delta p^2 \quad 5.11$$

The pressure at the final height of the bed after compaction can now be calculated using the relationship between MPS and minimum Permeability, the Darcy equation and the final height-pressure correlation.

Maximum compression, where the cake height would be independent from the pressure across the cake, is not reached in this graph because the pressure used in the pilot scale trials was too small.

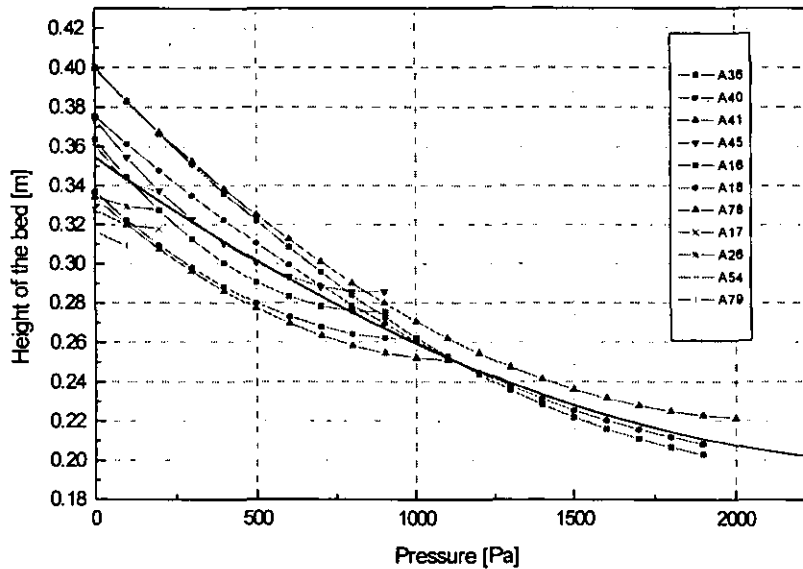


Figure 5.9: Effect of pressure on cake height

5.1.6. Compaction of the Cake over Filtrate Volume

The initial cake height L_0 (after the sedimentation step) and the final cake height L_{\min} at the end of filtration were already defined in previous steps. The progressing compaction of the bed with increasing filtrate volume is influenced by different effects:

- firstly, wort drains from the cake and voids in the cake decrease their size (compaction) and
- secondly, the cake exerts a resistance as liquid flows through the bed. As the top layer has the highest resistance, the bed is compressing with increasing differential pressure across the cake.

These effects occur simultaneously and are combined in the model. The height difference $L - L_{\min}$ per volume of filtrate for nine trials is plotted in Figure 5.10. The experimental data can be fitted with first order exponential decay functions.

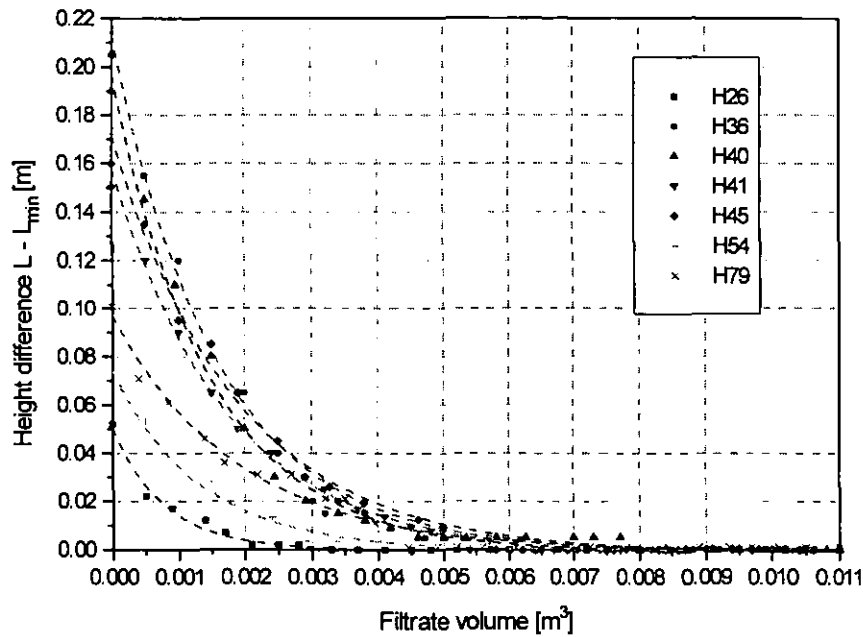


Figure 5.10: Height of the bed vs. filtrate volume, trial data with fitted exponential decay
Fits for all trials were obtained to establish correlations between the fitting parameters of the exponential decay function and the minimum cake height. Figure 5.11 shows the decay constant t plotted over L_{\min} : L_{\min} determines the decay constant.

The decrease of the height of the cake with filtrate volume from start of filtration to the point where cake height reaches its minimum, can be described using the parameters L_0 , L_{\min} and t in a first order exponential decay function. The following equation applies from $V = 0$ to $V = V_{\text{total}}$:

$$L = L_0 - \left\{ (L_0 - L_{\min}) \times e^{\frac{-V}{t_{\text{decay}}}} \right\} \quad 5.12$$

The fitting function shown in Figure 5.11 replaces t in equation 5.12

$$t_{\text{decay}} = 0.00247 - 0.00310 \times L_{\min} - 0.00246 \times L_{\min}^2 \quad 5.13$$

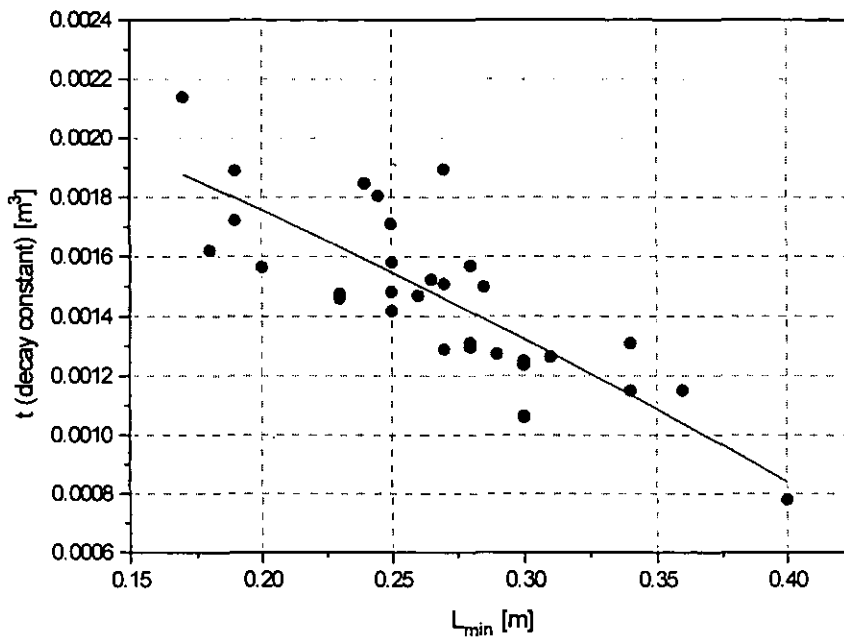


Figure 5.11: Decay constant, t vs. L_{\min} ($R = 0.80$)

5.1.7. Effects of Cake Height on Permeability

Permeability of the cake is affected by its packing density. The packing density is a function of cake height, because the total mass of solids is constant over the lauterer process. For the final bed height the corresponding permeabilities are shown in Figure 5.12. The equation for the fitting curve is:

$$B = 1.31 \times 10^{-8} \times L^{4.68} \quad 5.14$$

The effects of compaction and reduction in porosity on permeability can be described using the Kozeny equation

$$B = \frac{\varepsilon^3}{K_0 S_0^2 (1 - \varepsilon)^2} \quad 5.15$$

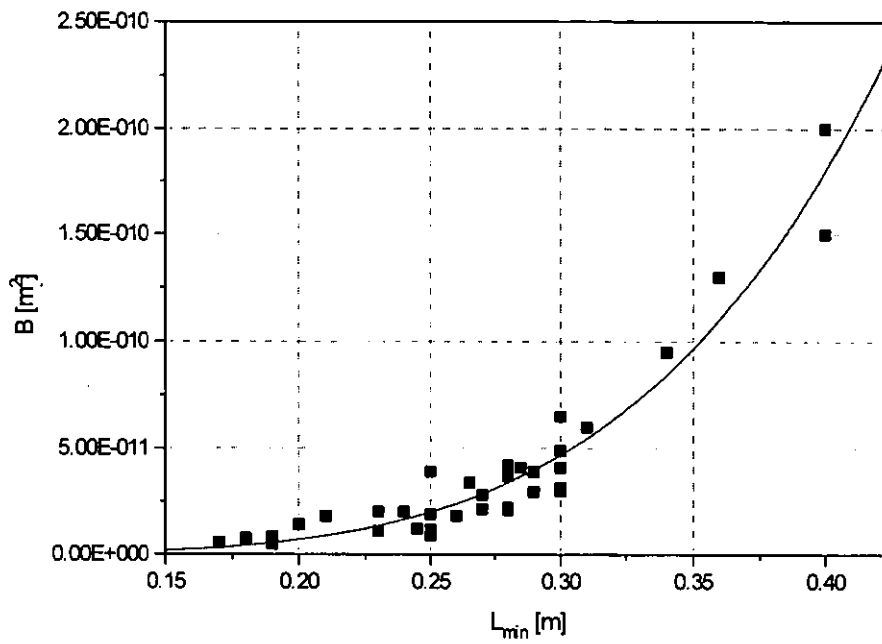


Figure 5.12: Permeability - height of the cake, after L_{\min} = constant

Since the total volume of solids, V_s , is constant, the porosity, ε , is a function of cake height, L_c , as a first approximation. As

$$\varepsilon = \frac{A L_c - V_s}{A L_c} = f(L_c) \quad 5.16$$

and

$$1 - \varepsilon = \frac{V_s}{A L_c} = f\left(\frac{1}{L_c}\right) \quad 5.17$$

hence,

$$B = f\left(\frac{\varepsilon^3}{(1 - \varepsilon)^2}\right) = f\left(L_c^3 \times L_c^2\right) = f(L_c^5) \quad 5.18$$

This correlation was used to describe the change of porosity with height of the bed.

The examples shown in Figure 5.13 indicate that this assumption is reasonable in a range of $\varepsilon = 0.25 - 0.55$ (related to $L_c = 20 - 35 \text{ cm}$)¹¹. Deviations from this model occur at the beginning of filtration, when the porosity of the bed is above $\varepsilon = 0.65$. At this stage, the wort is not filtered through the entire cake but filtrate is also flowing from the pores of the lower part of the cake. This effect agrees with the limitations of the Carman-Kozeny model described by Dullien (1975).

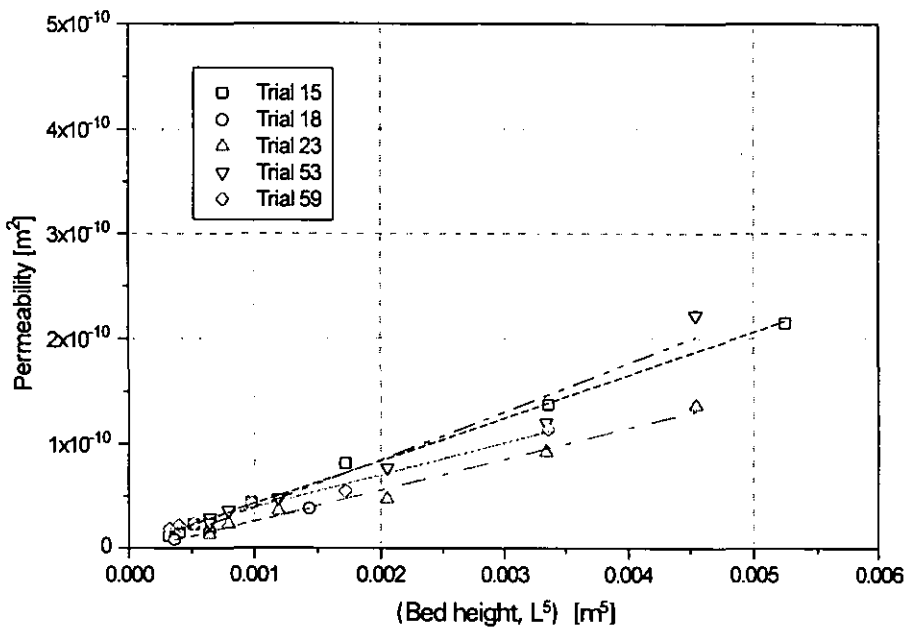


Figure 5.13: Permeability change as a function of cake height

The flow rate dV/dt is linked to Δp by the peristaltic pump control equipment. The relationship was adjusted in the calibration experiments (see Chapter 3.2.2) and can be described by the equation,

$$dV/dt = 1.65 \times 10^{-6} - 5.32 \times 10^{-10} \times \Delta p - 4.66 \times 10^{-14} \times \Delta p^2 \quad 5.19$$

¹¹For a further discussion on cake porosity see the conclusions of this chapter.

5.1.8. Change of Extract with Time - Cake Washing

Extract in the filtrate changes with filtrate volume. Initially the water below the slotted bottom and in the pipework dilutes the wort. As filtration proceeds the extract content rises to a maximum. This maximum depends on the concentration of the mash. With further progress of the filtration, the wash water added on top of the cake dilutes the filtrate and leaches soluble substances from the cake.

Cake washing in lautering was described by Hermia and Rahier (1990) with the so called dispersion model. For washing of spent grains with pure water, and because there are no sorption effects of the cake, the model can be simplified as follows.

$$\frac{c}{c_0} = \frac{1}{2} \left[1 + \operatorname{erf} \left(\frac{1-W}{2\sqrt{W}} \right) \sqrt{\frac{uL}{D_L}} \right] \quad 5.20$$

To verify that experimental extract data fits this model some examples of the trials have been tested. To compare the data with fittings of washing curves, the void volume of the cake was calculated.

The volume of the cake at maximum compression can be determined from equation 5.11. A minimum cake volume of $2.65 \times 10^{-3} \text{ m}^3$ was determined for these trials. It was assumed that at this compression the cake voidage is near zero, the volume of the cake would be the volume of the particles only. It can be anticipated that milling, concentration of the malt and the raw material source influence the volume of the solids and the packing density in the cake. The void volume can then be determined as.

$$V_{\text{void}} = V_{\text{cake}} - V_{\text{particles}} \quad 5.21$$

The void volume of the cakes can be calculated using the individual final height of the cake and the filtration area of the cake. With these Figures it is now possible to determine the volumes of wash liquor used per void volume of the cake.

Washing of the cake starts when all supernatant wort is drawn into the cake. The total volume of wort to be filtered before washing occurs is calculated using the following equation:

$$V_{\text{wort}} = V_{\text{total}} - \left[(H_0 - L_{\min}) \times A \right] \quad 5.22$$

The extract content per volume of filtrate was normalised by the maximum extract content in the filtrate.

Figure 5.14 shows the result of this fitting process. It can be seen that the axial dispersion model with the assumptions described before fit the washing of the spent grains cake quite well.

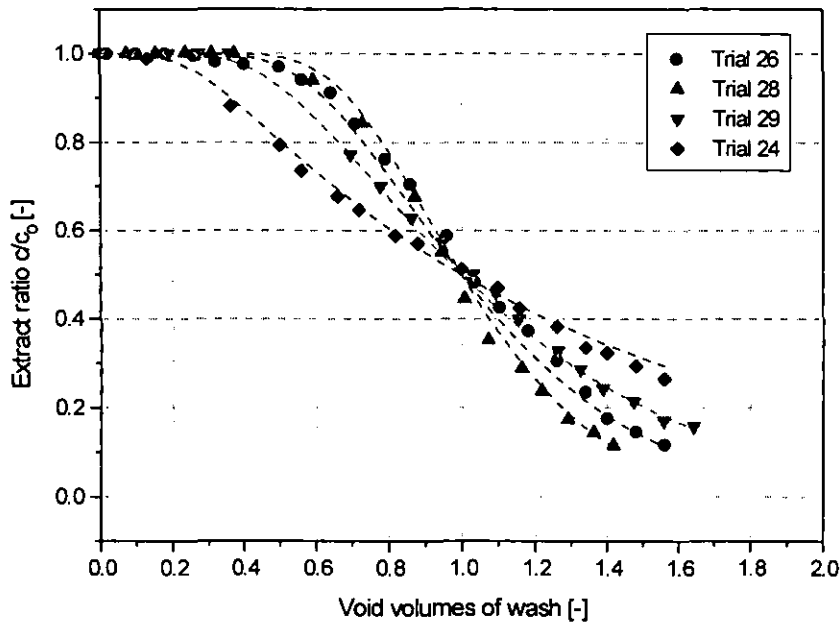


Figure 5.14: Washing curves of data and fitting functions (dashed curves with Trial 26:

$$\frac{uL}{D} = 3.7909; \text{ Trial 28: } \frac{uL}{D} = 4.8833; \text{ Trial 29: } \frac{uL}{D} = 2.8786; \text{ Trial 24: } \frac{uL}{D} = 1.7051.$$

In the model the extract curves were not fitted with the dispersion model but directly with a sigmoidal function. This made modelling much easier and reduced the number of necessary calculation steps. The sigmoidal fitting functions is described with the following equation.

$$E = \frac{E_{\max} - E_0}{1 + \exp \frac{(V - X_c)}{dX}} + E_0 \quad 5.23$$

where:

X_c : centre of the curve

dX : width of curve

E_{max} : initial extract

E_0 : final extract level

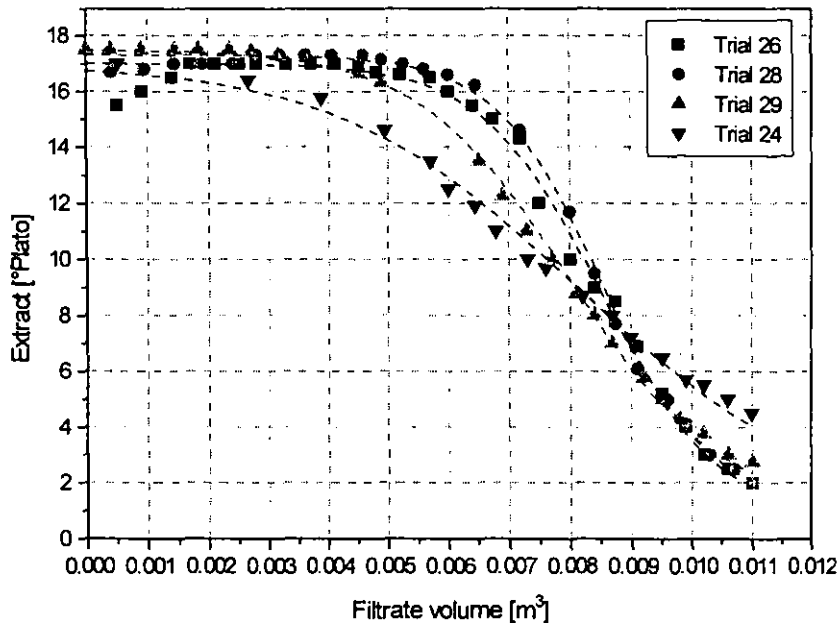


Figure 5.15: Sigmoidal fitting curves on trials data. In general, these sigmoidal curves described the trial data quite well, over nearly the entire range of the filtration. The four trials above were the same as for fitting the dispersion model; this shows that the sigmoidal fits are able to describe the extraction curves.

The only problem is that this function cannot describe the dilution effect at the beginning of the filtration procedure. Despite this deficit, the sigmoidal equation was used in the computer model, because the dilution effect is not consistent for all trials and will also depend on the geometry of the equipment used.

Table 5.1 shows that mainly dX varies between the trials. This parameter describes the change of extract over the filtrate volume. The smaller this parameter the better the washing effect.

Table 5.1: Parameters for the fitting curves of the above examples

	Trial 26	Trial 28	Trial 29	Trial 24
E_{\max}	17.0	17.3	17.5	17.0
E_0	1	1	1	1
X_c	0.0847163	0.0852383	0.0797507	0.0810564
dX	0.009572	0.0086533	0.0130718	0.0206695

It has been shown in Chapter 4.4 that the washing efficiency (defined as extract in the mash to extract in the wort) changes with MPS (see Figure 5.17). With high MPS in the fines better washing efficiency was achieved. This effect will be outlined now.

Bigger particle size in the fines could increase tortuosity in the cake as less pores would be blocked with layers of particles with low permeability. The tortuosity of channels in the bed would be increased. This effect results in a decrease of the axial dispersion coefficient and a better washing efficiency. Another important effect is the height of the cake during cake washing. It is affected by the compaction of the cake. This effect is described above: MPS affects permeability of the bed and permeability has been correlated to L_{\min} , hence MPS affects L_{\min} . Again lower MPS values in the fines cause lower final bed heights. Cake washing would be less efficient.

This correlation between small particles and the washing efficiency was investigated. For all trials sigmoidal functions were fitted and a dX - MPS relationship was established. The results showed no clear correlation between dX and the MPS ($R=0.38$). X_c was set constant to 0.0086m^3 .

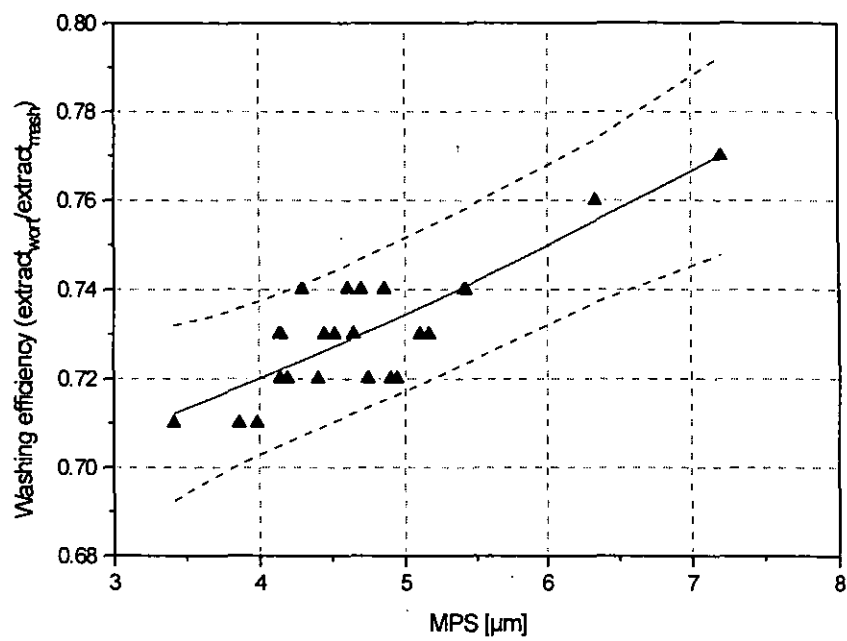


Figure 5.16: Washing efficiency as a function of MPS

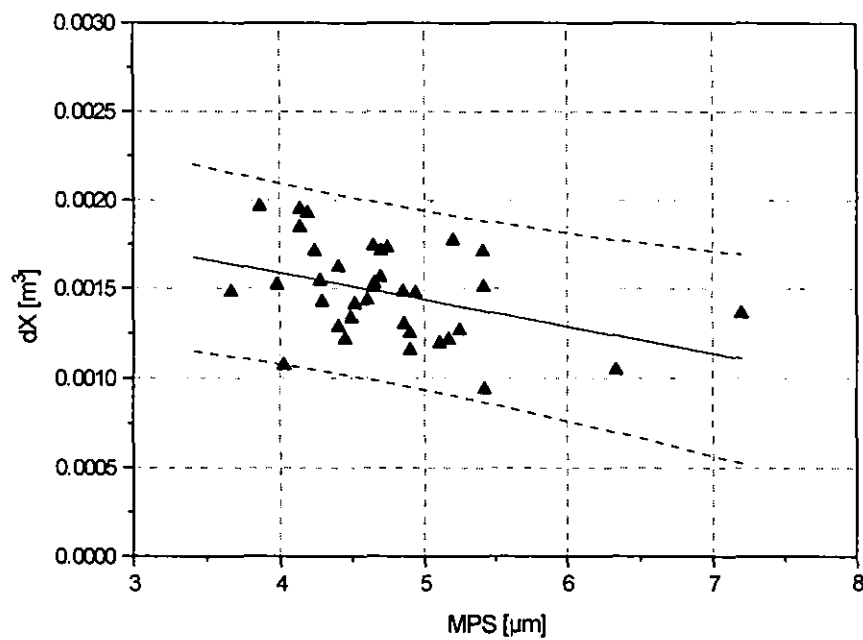


Figure 5.17: Width of the sigmoidal fitting curve versus MPS with linear correlation and upper and lower limits (2 \times SD)

The described influence of the MPS on the washing curve can therefore not be verified. The effect of the MPS on extraction, however, has been shown before with a much clearer correlation. One of the reasons for this unclear correlation with extract data over filtrate volume may be the inaccuracy of the analysis. Extraction data was determined after filtration with hydrometers, an analysis with relatively high accuracy ($E = \pm 0.05$ °Plato). The extract over volume curve (to which the sigmoidal curve was fitted) was determined directly during filtration with a refraction analysis and total volume of filtrate determination, which is less accurate ($E = \pm 0.5$ °Plato, $V = \pm 0.25$ l).

5.2. A Computer Model describing Lautering

5.2.1. Development of the Computer Model

The computer algorithm shown in this section was derived from the correlations explained above. It assembles the various relationships which originate from viscosity and MPS variations.

The initial calculations (see Figure 5.18) determine the MPS and the viscosity at filtration temperature from the input variables.

The next stage of the programme calculates the height of the filter cake after sedimentation, before filtration starts. The sedimentation rate is calculated using equation 5.7. The total time for sedimentation is 10 minutes. The initial height of the cake is influenced by the size of the fines. Higher initial levels are caused by slower settling rates. After the sedimentation stage, filtration starts.

In the following calculation the final height of the bed after washing was determined. It was found that this is a function of the permeability. The permeability of the cake is dominated by the permeability of the fines. As shown in Figures 5.6 and 5.7, mainly the MPS of the fines affects this parameter.

The main part the algorithm is shown in Figure 5.19. This part calculates the main parameters for the filtration run and the washing process. As neither differential pressure nor flow rate are constant over filtration time the total time required to collect a pre-set volume of wort and individual

values of cake height and extract concentration were calculated by iteration. The following flowcharts show the different parts of the computer program.

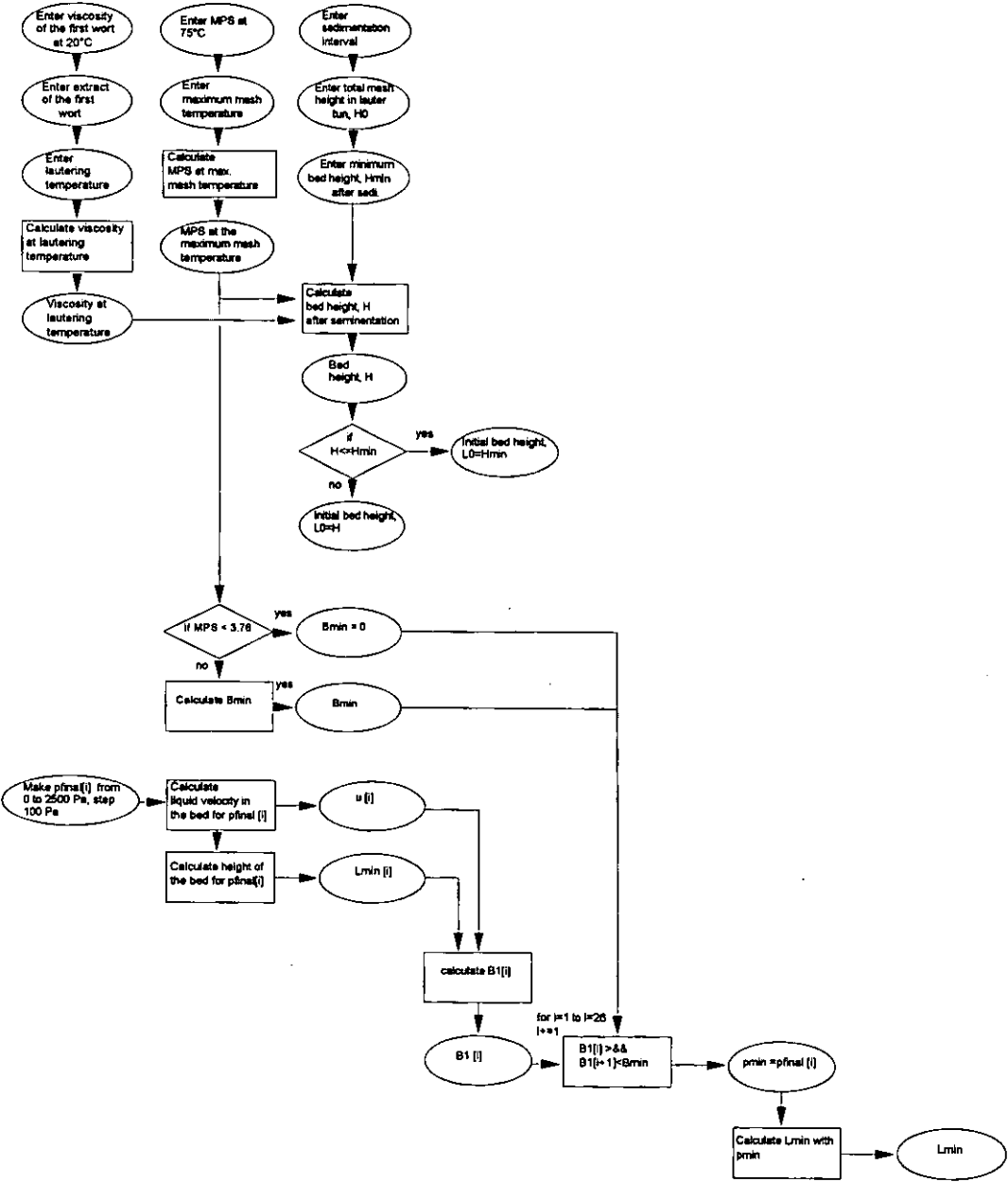


Figure 5.18: Initial calculations to determine MPS and viscosity at lautering temperature, initial and final cake height

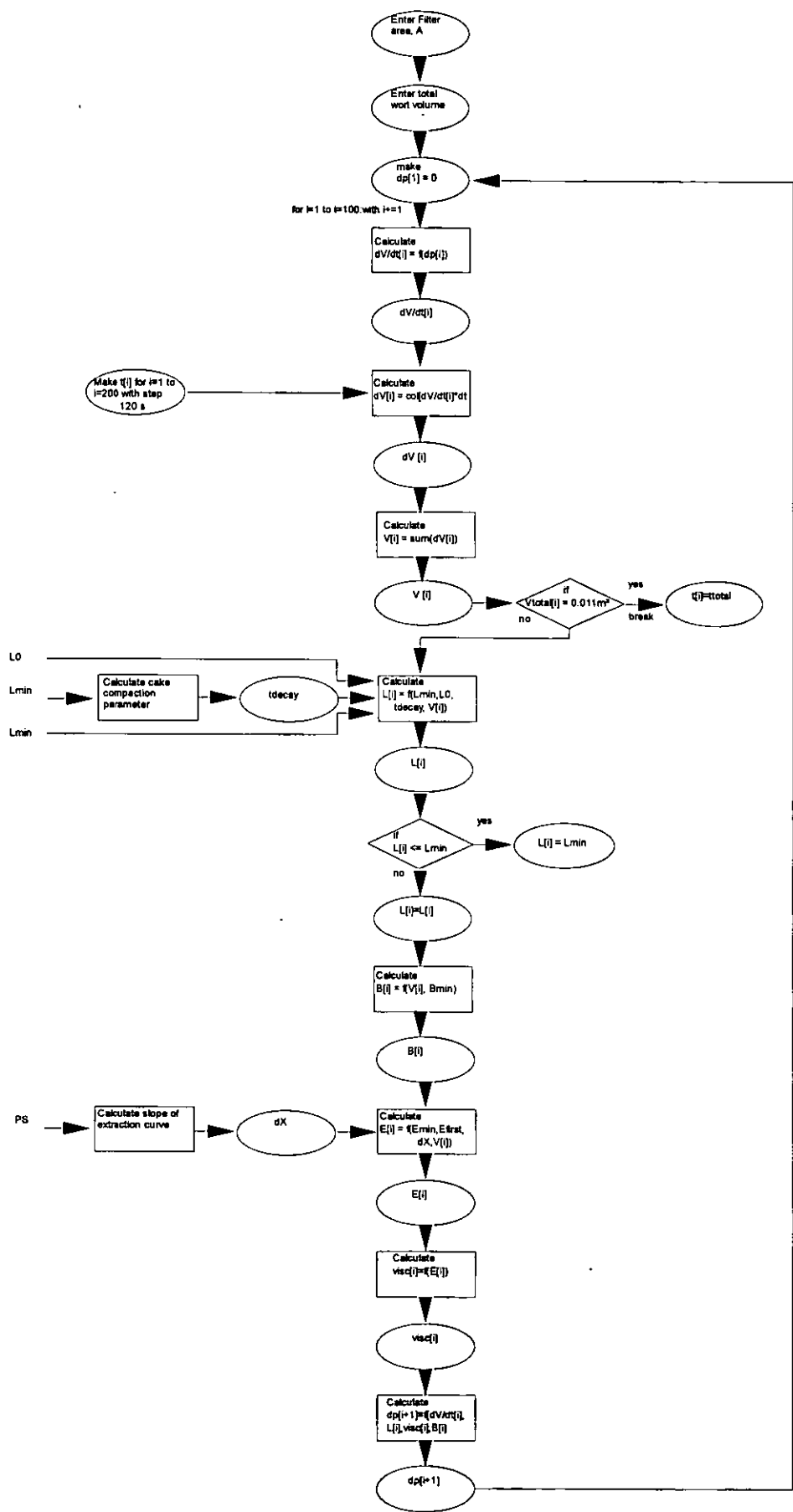


Figure 5.19: Main part of the lautering model

The following list shows the text of the program, written in MicroCal Origin's programming language, LabTalk™, which is based on the languages DOS and C++.

The program is started with the command in `lauterin.txt`. It runs the batch of commands in `prog_run.txt`.

`lauterin.txt`

```
run c:\origin\prog_run.txt;
```

The individual programs in the batch are carried out in a sequence. The modular structure made changes and de-bugging much easier.

`prog_run.txt`

```
run c:\origin\mps_temp.txt;
run c:\origin\vis_temp.txt;
run c:\origin\ltmod1.txt;
run c:\origin\ltmod2.txt;
run c:\origin\ltmod8.txt;
```

The individual algorithms of each program module are listed below.

`mps_temp.txt`

```
/*Subroutine to calculate the MPS at maximum mash temperature
 *mps_temp.txt*/

getn    (MPS (no shear) at 75°C) MPSgiven (Max. mash temperature ) TMax (Please
insert the malt specific MPS and your maximum mash temperature:);

MPSdt=75-65;                /*calculates the lab mash
                             *temperature difference to 65°C*/

MPS0=MPSgiven-0.045*MPSdt-0.0032*MPSdt^2;
                             /*calculates the MPS at 65°C*/

dtemp=Tmax-65;              /*calculates the brewhouse
                             *mash temperature
                             *difference to 65°C*/
```

```
MPS = MPS0 + 0.045*dtemp + 0.0032*dtemp^2; /*defines MPS change
                                     *with temperature*/
```

```
type -c ("MPS at the given temperature is $(MPS,.3)µm");
```

vis_temp.txt

```
/*Subroutine to calculate viscosity at lautering temperature and the Slope A1 of the
viscosity-extract relationship, vis_temp.txt*/
```

```
getnum (Viscosity of 'first wort') visc20 (Please insert the first wort viscosity at 20°C
[mPas]);
```

```
getnum (Extract of 'first wort') Efirst (Please insert the first wort extract at 20°C [°Plato]);
```

```
getnum (Temperature) Tlaut (Please insert Your lautering temperature [°C]);
```

```
A0 = 1.324 - 0.01776*Tlaut + 7.058E-5*Tlaut^2;
```

```
                                     /*Viscosity of water at lautering
                                     temperature*/
```

```
visc70 = 0.177 + 0.254*visc20;          /*calculates the viscosity
                                     *at 70°C*/
```

```
visczero = visc70 + 0.0298*70 - 1.3E-4*70^2;
                                     /*calculates the imaginative
                                     *viscosity at 0°C,
                                     *for a square relationship
                                     *between 65 and 98°C*/
```

```
visclaut = visczero - 0.0298*Tlaut + 1.3E-4*(Tlaut)^2;
                                     /*calculates the
                                     *viscosity at the given
                                     *lautering temperature*/
```

```
A1 = (visclaut - A0 + (3.604E-5*Efirst^2) - (3.720E-5*Efirst^3)) / Efirst;
```

```
type -c ("The viscosity at Your lautering temperature is $(visclaut,.3) mPas");
```

ltmod1.txt

```

/*Subroutine: Calculation of the final bed height in the pilot lauter tun:
*ltmod1.txt*/

Bmin=-6.92E-11+4.889E-12*MPS^2; /*Minimum Permeability
                                *at end of filtration
                                *in the pilot lauter tun*/

if (MPS < 3.76) {Bmin=0}; /*minimum value, Bmin should
                           *not get negative*/

pfinal=data(0,2500,100); /*make pressure data from 0 - 2500 Pa*/

col(1) = pfinal; /*Pressure range in [Pa] used
                  *in Pilot Lauter Tun*/

A=0.0134; /*Area Lauter Tun in [m^2]*/

eta=visclaut * 1E-3; /*viscosity in [Pa.s] at end
                     *of filtration assumes: end = beginning*/

u=(1.65E-6-5.32E-10*pfinal-4.66E-14*(pfinal^2));

/*velocity in [m^3/s],p in [Pa]
*related to dp*/

LP=(0.35-1.17E-4*pfinal+2.18E-8*(pfinal^2));

/*height of the bed in [m],p in [Pa]
*related to lauter tun
*final pressure*/

B1=(u*eta*LP)/(A*pfinal); /*Darcy Equation to obtain
                           *the final pressure by
                           *substitution*/

col(2)=B1; /*assign col(2) for B1 data*/

```

```

for(i=1;i<=26;i+=1) {

    if(col(2)[i] > Bmin && col(2)[i+1] < Bmin) {

        pmin=(col(1)[i]);

        Lmin=0.35-1.17E-4*pmin+2.18E-8*pmin^2;

                                /*calculate the final bed
                                *height in [m]*/;

    }

}

type -c "The final pressure across the bed is $(pmin,.0) Pa";

type -c ("Lmin=$(Lmin,.2)m");

```

ltmod2.txt

```

/*2.Calculation of the cake height after 10 minutes sedimentation:
*ltmod2.txt*/

t=600;                                /*total sedimentation interval [s]*/

H0=0.527;                             /*Liquid Level in the Lauter Tun
* [m]*/

Hmin = 0.42;                           /*minimal level of the bed [m]*/

dhdt = 1.5E-4 - 1.4E-5 * MPS^2; /*Sedimentation Rate (dh/dt)
* [m/s]*/

ts = 0.9 * t;                          /*Effective Sedimentation Time
* [m/s]*/

H=H0+dhdt*ts;                          /*Height of cake calculated after
*sedimentation rest*/

```

```

if (H <= Hmin) {L0=Hmin;};

if (H > Hmin) {L0 = H;};

if (H > H0) {L0 = H0;};

type -c "The final sedimentation level is $(L0,.2) m";

```

ltmod8.txt

```

/*Main Program to calculate the Lautering Time incl. extraction: ltmod8.txt*/

dt = 120;                      /*time-interval for steps: 2 minutes*/
A = 0.0123;                    /*filter area*/
Vtotal=0.011m³                /*total filtration volume*/
tdecay = 0.0027 - 0.00431 * Lmin; /*decay constant for the compaction of
                                *the cake*/
B0=1.31E-8 * Lmin^4.679;      /*permeability at minimum cake height*/
Emin = 0;                     /*minimum extract level at end of
                                *washing*/
EEff = 0.66 + 0.015 * MPS;    /*washing efficiency as afunction of
                                *MPS*/
X0=0.78xVtotal                /*centre of extraction curve*/
dX = 6.22E-3 - 6.49E-3 * EEff; /*width of sigmoidal extraction curve*/

for (i=1;i<=101;i+=1) {col(3)[i]=dt*(i-1)};

col(3)[i] = t[i];
col(4)[i] = dp[i];
col(5)[i] = dVdt[i];
col(6)[i] = dV[i];
col(7)[i] = Vtotal[i];
col(8)[i] = L[i];
col(9)[i] = B[i];
col(10)[i] = E[i];
col(11)[i] = visc[i];
for (i=1; i<=100; i+=1) {
    col(dp)[1] = 0;

```



```

col(dVdt)[i] = 1.65E-6 - 5.32E-10*col(dp)[i] - 4.66E-14*col(dp)[i]^2;
col(dV)[i] = col(dVdt)[i] * dt;
col(Vtotal)[i] = sum(col(dV))[i];
col(L)[i] = Lmin + (L0-Lmin) * e^(-col(Vtotal)[i]/tdecay);
if (col(L)[i]<=Lmin) {L[i]=Lmin};
col(B)[i] = 1/3E7 * (col(L)[i])^5;
col(E)[i] = (Efirst-Emin) / (1 + e^((col(Vtotal)[i] - X0)/dX));
col(visc)[i] = A0 + A1*col(E)[i] - 3.604E-5*col(E)[i]^2 + 3.720E-5*col(E)[i]^3;
col(dp)[i+1] = (col(dVdt)[i] * col(L)[i] * (col(visc)[i] * 1E-3) / (A*col(B)[i]));
if (col(Vtotal)[i]>= 0.011) {ttotal=col(t)[i]; break};
}
tminutes=ttotal/60;
type -c "The total lautering time is $(tminutes) minutes;

```

The model runs in MicroCal Origin, a Microsoft Windows™ based scientific graphics program. Due to use of the Windows user interface the program is user friendly. Display of graphs and use of the program is possible on any computer running the Windows Version 3.1 or higher.

5.2.2. Predicting Lautering Performance with the Model

The computer model shown above was developed from all data available from the experimental work. To check the accuracy and relevance of the model for different input parameters, results from individual trials were tested against the model. The following lautering diagrams (Figure 5.20 - 5. 23) show real data from experiments compared with the calculated data of the model.

It can be seen that lautering time can be predicted from the model with good accuracy, whereas extraction of the cake during washing is averaging the real data. The change of the cake height fits the real data with good accuracy. As explained in section 5.1, the cake height plays a crucial function in determining total lautering time.

The lautering time observed in the trials was compared with data calculated from the model by varying the input values for MPS. Viscosity was kept constant. Figure 5.24 shows that the lautering time predicted from the model lies in the same range as the measured data. The slope of

the fitted curves with MPS are very similar. The relatively large variation in lautering time is mainly due to variations in viscosity in the real data.

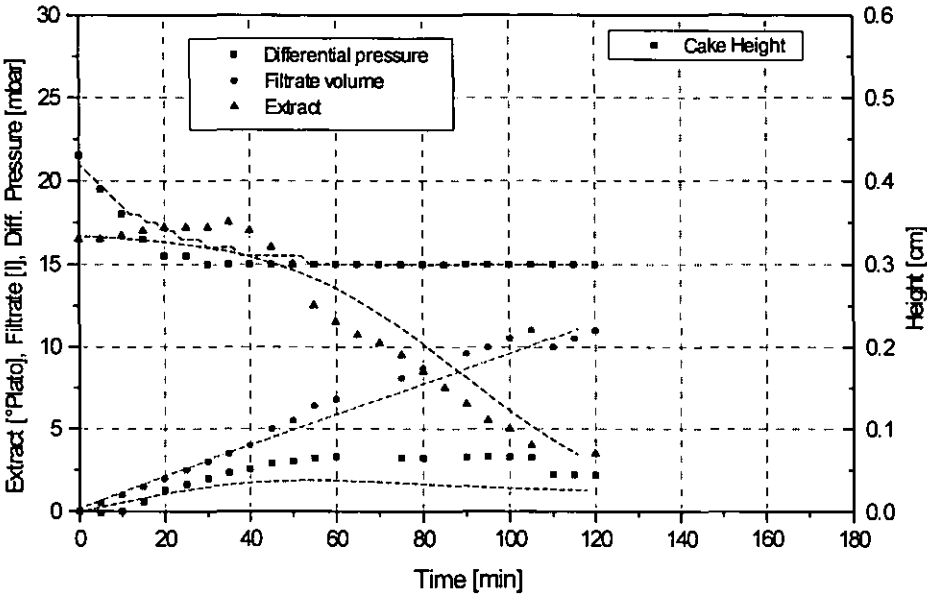


Figure 5.20: Trial 57 real (data points) and calculated data (lines)

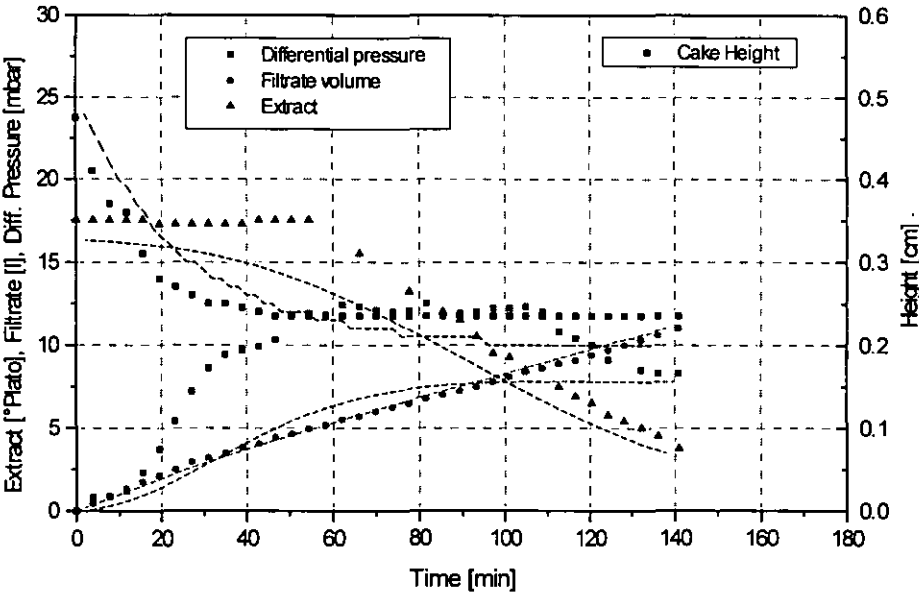


Figure 5.21: Trial 30 real (data points) and calculated data (lines)

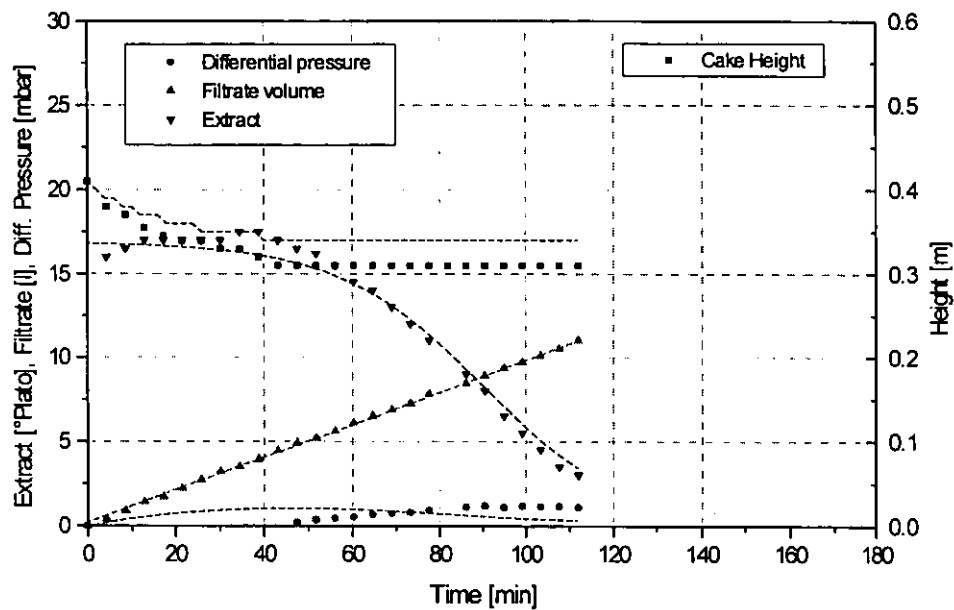


Figure 5.22: Trial 54 real (data points) and calculated data (lines)

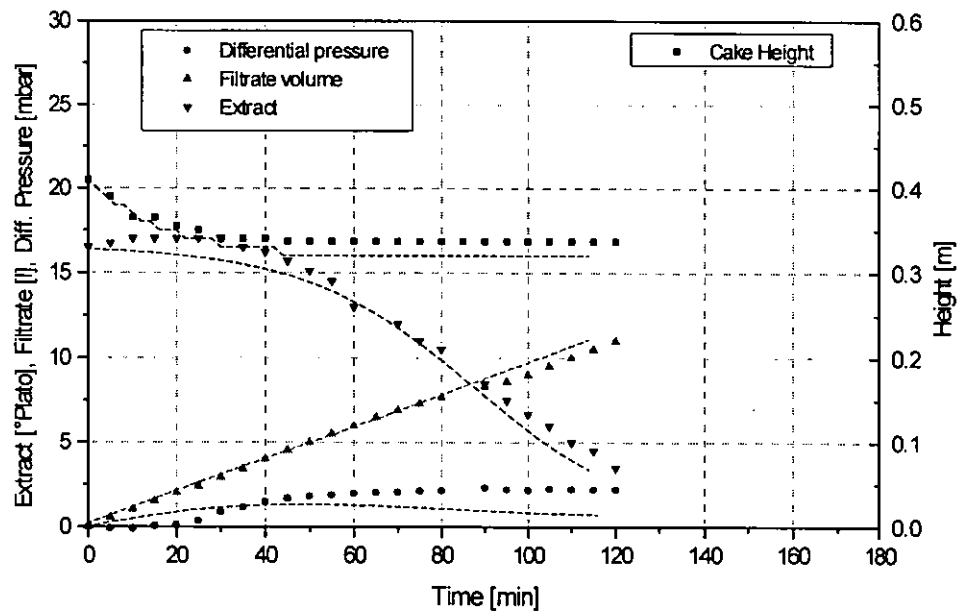


Figure 5.23: Trial 79 real (data points) and calculated data (lines)

It can be seen that the model can predict lautering performance for variations in viscosity and MPS, other parameters such as raw materials

and milling have to be constant. The temperature and MPS in the fines can be varied over the range found in industrial conditions.

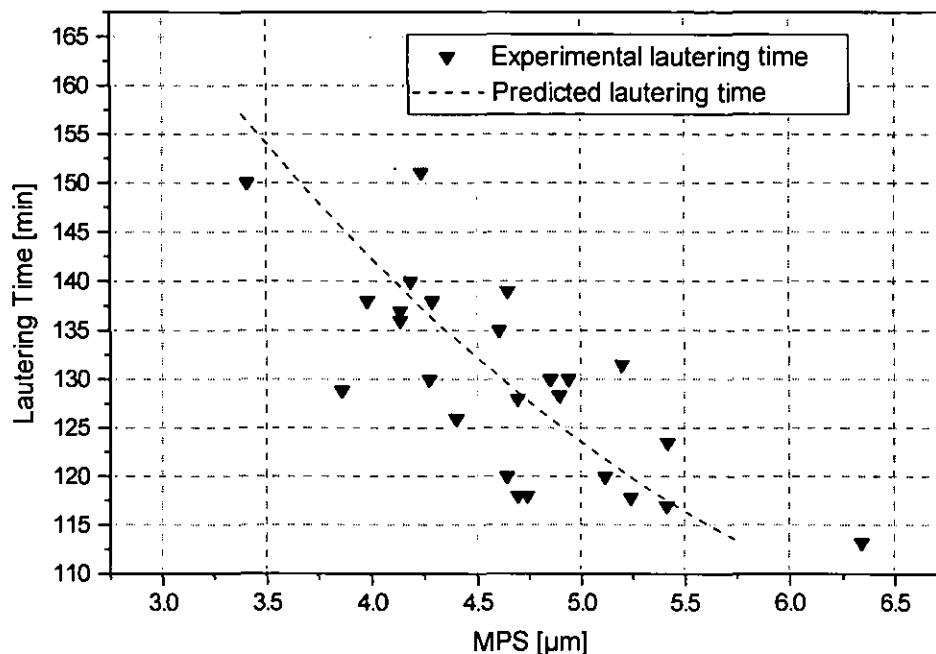


Figure 5.24: Predicted lauter time (dotted line) and measured data (triangles)

Only one set of data are available to test the predictive capability of the model in respect of lauter performance. In this case there are limitations. The trial has been carried out at constant pressure conditions (10 mbar) with a swan-neck run off. Hence, there was no differential pressure-flow rate correlation. The model was changed to accommodate for these different conditions. It can be seen that with these changes a good correlation to measured data was found (Figure 5.25).

Further tests were not possible, because, in addition to the above mentioned changes in operation conditions of the pilot lauter column, raw material parameters and milling were changed.

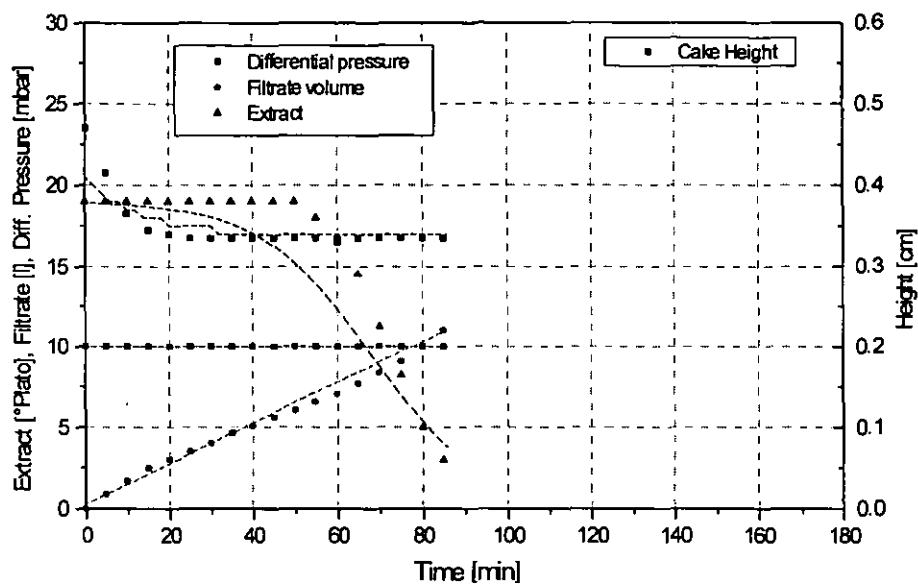


Figure 5.25: Comparison between measured (data points) and predicted data (lines) (Trial carried out by Robin Thorn)

5.3. Conclusions

A computer model has been developed which models the physical parameters in mashing and their influence on lautering performance.

The model has been based on the findings from the experimental programme of this thesis. Temperature effects on viscosity and MPS have been incorporated by correlation. Agitation is difficult to measure. The effects of agitation, however, on particle attrition can be determined quickly in the laboratory with high accuracy. Therefore MPS has been included as a parameter representing attrition.

Both viscosity and particle size effects have been combined to model lautering. Effects relevant to lautering performance such as sedimentation, compaction of the bed, permeability and washing efficiency were derived from the experimental data. The determination of total lautering time has been based on an iterative algorithm. Direct calculation was not possible due to the variable pressure, variable flow rate condition in the experiments. This condition complicated modelling; however, the model is much easier to apply to large scale industrial brewing.

A major weakness of the model is the assumption of cake porosity. It was assumed that cake porosity is zero when at maximum compression. This assumption was made because experimental data on wet and dry cake mass was not available. For further work it would be recommended to determine the porosity by measuring dry and wet cake mass and the average density of solids in the cake (see equation 2.45).

The computer model has been shown to be flexible enough to give realistic results with the input variables given. However, there are still areas where the model could be extended and improved. For such investigations a different malt quality, perhaps also different milling could be investigated and the findings incorporated into the model. As this thesis work focused on the variation of process parameters in mashing it does not include variation of such parameters.

6. Conclusion

6.1. General Comments and Overall Conclusions

This thesis describes effects of the mashing parameters temperature and agitation, on mash properties. In the main, two properties are influenced by these parameters, the viscosity and the particle size distribution in the fines.

For the first time particle size effects in mash were investigated systematically. The importance of fine particles for lautering performance could be confirmed and quantified. In the trials attrition effects were investigated using only one malt quality, thus enabling the work to focus on mashing parameters.

The precipitation and aggregation of fine particles with increasing temperatures in mashing could be monitored. It was shown that this parameter is not malt dependent. Mashings from different malts react in the same way.

Viscosity effects on lautering performance have been reported in the literature as the main influencing factor. It could be shown using constant filtration temperatures and the variation of MPS that this parameter is more important than viscosity in determining mash filterability.

Experiments were carried out either at a pilot scale or at a laboratory scale. It was found that a stirrer with torque meter was ideal to determine power input and to relate large scale trials to laboratory scale.

Filter cake washing was described with the dispersion model for mash filter applications. The suitability of this model was confirmed.

In pilot scale trials it was tried to mimic different agitation conditions using a circulation loop with a mono pump. It could be shown that the effect of the pump masked any additional variation of the power input in the loop by single seat valves or orifices. However, it was still possible to get sufficient data in a wide MPS range to enable modelling of the particle size parameter with pilot scale data.

Small scale trials using a stirrer with torque meter revealed that minimal power input up to 0.1 W/l was sufficient to achieve optimum extraction of the malt. Additional power input had negative influence on filterability of the samples. It was confirmed that this is due to attrition effects mainly in the particle fraction below 106 μm . Due to a careful selection of the malt quality, viscosity changes could be excluded and it was therefore possible to establish a very close correlation between filterability and MPS change.

The comparison of attrition effects with temperature-induced aggregation shows that higher temperature lautering cannot cure high attrition rates. However, aggregation of particles by heat can improve lautering performance.

In this thesis, the lautering process has been modelled for the first time. Previous attempts of modelling mash filtration have focused on the application of filter presses, which is the second, most used method in the brewing industry. The sedimentation behaviour of mash will only be observed in lauter tuns. It has not been described and modelled before. Bockstal et al. (1985) described the sedimentation for hammer milled malt, which appears to settle in one band only.

The model described here has been based on the findings from the experimental programme of the pilot trials of this thesis. At present the model is limited to one malt quality, and only mashing parameters are included. Data predicted from the model showed good correlation with real data.

6.2. Implications for Industrial Brewing Practice

The findings presented in this thesis will have significant influence on practical brewing. Mashing conditions beneficial for lautering have been developed and optimised empirically. It is now possible to optimise these conditions by monitoring the key parameters for lautering in the mashing process.

There are two areas where optimisation is possible, temperature and agitation regimes. The brewhouse manufacturers agree that agitation in mashing should be minimal. This is particularly so where mixing is not essential for enzymatic conversion or for a good heat transfer. This is at

temperatures above 72°C and at stages where temperature is constant, i.e. at mash transfer into the lauter tun.

Higher mashing off temperatures have been proposed by several authors as a measure to increase lauter tun filtration rates. The main reason why run off rates are much higher at higher temperatures has not been identified. Effects of higher temperature have been contributed to viscosity only.

Higher mashing temperatures above 78°C have found widespread application in practical brewing in decoction mashing, where parts of the mash are boiled in separate vessels. This procedure has been proven suitable for the preparation of mashes with lower modified malt. Dependence on raw material quality can be reduced and consistent lautering rates can be achieved. Boiling affects extraction of malt grist in a positive way and improves the particle size distribution in the fines by aggregation of the protein fraction. Boiling time has been optimised empirically for optimum extraction. It might now be possible to optimise also the particle aggregation and hence increase lautering rates.

Only particle aggregation due to heat has been described in this thesis. From the literature it could be assumed that other parameters such as polyphenol content of the mash, cation concentrations or acidity of the mash could also influence particle aggregation. Consequently, a careful optimisation of these parameters for enhanced mash filtration rates might be possible.

The computer model makes it possible to test effects of particle size distribution and viscosity on mash filtration performance. It could be used directly as a tool for optimisation of mashing conditions and in the development of new procedures.

7. Appendix

7.1. Nomenclature

A	activation energy	kcal mol ⁻¹
A	cross sectional area (face area)	m ²
a	exponent	-
a	constant: $a = \alpha\eta c$	-
A_L	area taken by liquid	m ²
A_p	area taken by particles	m ²
A_p	projectional area normal to the direction of motion	m ²
B	permeability of the cake	m ²
b	constant: $b = \eta R_m$	-
c	coefficient relating to a reference temperature T_2 or reaction rate k_2	-
c	concentration	kg m ⁻³
C_d	drag force coefficient	-
c_g	gravimetric concentration (w/w)	-
c_p	specific heat at constant pressure	kJ kg ⁻¹ K ⁻¹
c_v	(solids) concentration by volume (w/v)	-
c_w	concentration in the wash liquid	kg m ⁻³
c_0	initial concentration	kg m ⁻³
CV	coefficient of variation	%
D	velocity setting on the Haake Rotovisco	-

D	molecular diffusivity	$\text{m}^2 \text{s}^{-1}$
D	dispersion coefficient	$\text{m}^2 \text{s}^{-1}$
d	diameter	m
D_a	diameter of impeller	m
d_{gap}	gap between stirrer blade (tip) and wall	m
d_i	internal (pipe) diameter	m
D_L	axial diffusion coefficient	$\text{m}^2 \text{s}^{-1}$
d_{LC}	logarithmic median diameter	μm
d_o	orifice diameter	m
d_p	diameter of particles	m
D_R	diameter of the stirrer	m
D_t	diameter of agitated vessel	m
degr.	degree of a scale from 0 to 1	-
dh	differential height	m
dt	differential time	s
dX	width of the extract fitting function	m^3
E	extract level	°Plato
E	extract content in the wort	°Plato
E	turbulent mass transfer coefficient	$\text{m}^2 \text{s}^{-1}$
e	exponent	-
E_{max}	maximum extract content	°Plato
E_0	extract content in the wort at V_{total}	°Plato
E_{∞}	extract level after infinite time of conversion	%(w/v)

F	filterability	$\text{m}^6 \text{s}^{-1}$
f	constant	-
F_A	apparent fermentability	%
F_A	buoyancy force	N
F_d	drag force	N
F_G	force due to the mass of the particle	N
F_W	drag at the wall of a particle	N
Fr	Froude number	-
G	shear rate	s^{-1}
g	gravitational acceleration	m s^{-2}
G_{after}	specific gravity after fermentation	°Plato
G_{bef}	specific gravity before fermentation	°Plato
G_m	shear rate	s^{-1}
h	head of fluid	m
h_j	individual heat transfer coefficient	$\text{W m}^{-2} \text{K}^{-1}$
H_0	height of the cake after sedimentation	m
K	permeability	m^2
K	constant	-
k	thermal conductivity	$\text{W m}^{-1} \text{K}^{-1}$
K_{b1}	ball constant	$\text{Pa cm}^3 \text{g}^{-1} \text{s}$
K_0	Kozeny constant	-
K_1	constant	-
K_2	constant	-

L	length or thickness	m
L_c	height of the filter cake	m
L_{\min}	minimum height of the cake	m
L_0	initial height of the cake before start of filtration	m
M	absolute mass deposited	kg
m	exponent	-
m	moisture content	-
m	mass	kg
m	mass of cake deposited per unit area	kg m ⁻²
m	diffusion mass-flow density	kg m ⁻² s ⁻¹
m_F	mass of the filter	kg
m_p	mass of particles in the density bottle	kg
m_{w2}	mass of the liquid fraction in the density bottle	kg
m_1	mass of cake deposited with volume of filtrate	kg m ⁻³
m_1	mass of clear liquid in the density bottle	kg
M_2	mass of particles sedimenting	kg
m_2	mass of suspension in the density bottle	kg
MPS	mean particle size of a number distribution	μm
n	impeller (stirrer) speed	min ⁻¹
n	exponent (compressibility index)	-
n	number of data points	-
n_c	percentage of particles in a channel	%
P	power input	W

p_s	solids pressure	N m^{-2}
P_{spec}	specific power input	W l^{-1}
Pe	Peclet number	-
Q	volumetric flowrate	$\text{m}^3 \text{s}^{-1}$
R	universal gas constant	$1.98 \text{ cal mol}^{-1} \text{ K}^{-1}$
R	cake resistance	m^{-1}
R_c	resistance of the filter cake	m^{-1}
R_F	resistance of the fines layer	m^{-1}
R_m	resistance of a filter medium	m^{-1}
R_{SG}	resistance of the spent grains layer	m^{-1}
R_{total}	total resistance	m^{-1}
RA	remaining alkalinity (degrees of hardness)	$^{\circ}\text{d}$
Re	Reynolds number	-
s	solids concentration in a slurry (mass fraction)	-
S_0	specific surface of the particles in the cake	$\text{m}^2 \text{m}^{-3}$
Sc	Schmidt number	-
T	absolute temperature	K
t	mashing time, time interval	min
t_{decay}	decay constant	m^3
T_{laut}	lautering temperature	$^{\circ}\text{C}$
u	average liquid velocity through a filter cake	ms^{-1}
V	volume of liquid	m^3

v	velocity of the tips of an impeller ($v = \frac{n}{60} D_a$)	m s^{-1}
v	mean velocity over cross section in a tube	m s^{-1}
v_0	sedimentation velocity	m s^{-1}
V_a	cake volume before contraction	m^3
V_b	cake volume after contraction	m^3
V_{cake}	cake volume	m^3
V_L	volume of liquid replaced by particles	m^3
\dot{V}_L	flow rate of liquid	$\text{m}^3 \text{ s}^{-1}$
V_p	Volume of the particle fraction in a density bottle	m^3
V_p	volume of particles settling	m^3
$V_{\text{particles}}$	particle volume	m^3
\dot{V}_p	flow rate of particles	$\text{m}^3 \text{ s}^{-1}$
v_r	velocity of the tip of a stirrer relative to the liquid	m s^{-1}
V_s	volume of solids	m^3
v_s	settling velocity of particles	m s^{-1}
V_t	collected filtrate volume at time t	m^3
V_{total}	total wort collected	m^3
V_{void}	void volume	m^3
V_{w2}	volume of the liquid fraction in a density bottle	m^3
V_{wort}	wort volume	m^3
V_0	volume of a density bottle	m^3
W	wash ratio	-

W	total mass of cake deposited	kg
w	mass of solids deposited per filter area	kg m ⁻²
w_L	liquid velocity	m s ⁻¹
W_m	mean work	Nm
w_p	free settling velocity of particles	m s ⁻¹
w_{PR}	reduced settling velocity	m s ⁻¹
W_2	mass deposited by sedimentation	kg
x	distance variable in vertical direction	m
\bar{x}	average of a group of data points	-
X_c	centre of the extract fitting function	m ³
\bar{X}_c	median size of a channel	μm
\bar{X}_g	geometric mean of all channels	μm
x_i	individual value	-
α	specific cake resistance	m kg ⁻¹
$\bar{\alpha}$	average specific resistance	m kg ⁻¹
α_{AV}	average specific filter resistance	m kg ⁻¹
α_0	specific resistance at unit applied pressure drop	m kg ⁻¹
Δc	concentration difference	kg m ⁻³
ΔL	distance	m
Δp	pressure difference	N m ⁻²
Δp_c	pressure loss across the filter cake	N m ⁻²
Δx	distance	m
$\Delta \rho$	density difference between solid and liquid	kg m ⁻³

ε	porosity	-
ε_{av}	average porosity	-
η	dynamic viscosity	$\text{N m}^{-2} \text{ s}$
η	dynamic viscosity at lautering temperature	$\text{N m}^{-2} \text{ s}$
η_w	dynamic viscosity	$\text{N m}^{-2} \text{ s}$
η_0	dynamic viscosity at 0°C	$\text{N m}^{-2} \text{ s}$
η_{20}	dynamic viscosity at 20°C	$\text{N m}^{-2} \text{ s}$
η_{65}	dynamic viscosity at 65°C	$\text{N m}^{-2} \text{ s}$
η_{70}	dynamic viscosity at 70°C	$\text{N m}^{-2} \text{ s}$
ν	kinematic viscosity of a fluid ($\nu=\eta/\rho$)	$\text{m}^2 \text{ s}^{-1}$
λ	exponent (compressibility index)	-
λ	defined by equation 3.64	
π	universal constant	-
ρ	density	kg m^{-3}
ρ_{FL}	density of a fluid	kg m^{-3}
ρ_L	density of liquid	kg m^{-3}
ρ_p	density of particles	kg m^{-3}
ρ_s	density of solids in the cake	kg m^{-3}
ρ_1	density (ball)	kg m^{-3}
ρ_2	density (liquid)	kg m^{-3}
τ	torque	Nm
ω	angular velocity	s^{-1}

7.2. References

- Aastrup, S., Erdal, K., A mass balance study of β -glucan in malt, spent grains and wort using the Calcofluor method, EBC Proceedings of the 21. Congress, Madrid, 1987, 353 - 360.
- Ahvenainen, J., Vilpola, A., Mäkinen, V., Einfluß der Läuterarbeit auf Brauprozess und Bierqualität, Monatsschrift für Brauwissenschaft, 36, (1983), 2, 69 - 73.
- Arndt, G., Linke, L., Labortechnische Untersuchungen zum Maischprozeß bei der Bierherstellung, Lebensmittelindustrie 26, (1979), 10, 461 - 465.
- Asselmeyer, F., Höhn, K., Issing, E., Die Temperaturabhängigkeit von Viskosität und Dichte bei Bieren, Ausschlag- und Vorderwürzen, Monatsschrift für Brauwissenschaft 26, (1973), 4, 93 - 101.
- Baluais, G., Leclerc, D., Moll, M., Lenoel, M., Washing and compression dewatering of brewing mash, EBC Monogr. XI, Wort Production, Mafflier, (1986), 52 - 71.
- Bamforth, C.W., Barley β -glucans, their role in malting and brewing, Brewers Digest (1982), 6, 22 - 35.
- Barrett, J., Clapperton, J.F., Divers, D.M., Rennie, H., Factors affecting wort separation, J. Inst. Brew. 79, (1973), 407 - 413.
- Barrett, J., Bathgate, G.N., Clapperton, J.F., The composition of fine particles which affect mash filtration, J. Inst. Brew., 81, (1975), 1/2, 31 - 36.
- Baxter, E.D., Wainwright, T., The importance in malting and mashing of hordein proteins with a relatively high sulphur content. EBC Proceedings of the 17. Congress, Berlin (West), (1979), 131 - 143.
- Bockstal, F., Fourage, L., Hermia J., Rahier, G., Constant pressure cake filtration with simultaneous sedimentation, Filtration & Separation, 22, (1985), 4, 255 - 257.
- Briggs of Burton, Exhibition Catalogue, Interbrau 1993, Munich

Bühler GmbH, Braunschweig, Exhibition Catalogue, Interbrau 1993, Munich

Camp, Th. R., Stein, P.C., Velocity gradients and internal work in fluid motion, Journal of the Boston Society of Civil Engineers, XXX, (1943), 4, 219 - 237.

Carman, P.C., Fluid Flow Through Granular Beds, Transactions of the Institute of Chemical Engineers, 14, (1937), 15, 150 - 166.

Coulson, J.M., Richardson, J.F., Backhurst, J.R., Harker, J.H., Chemical Engineering, Volume 2: Unit operations, 3rd Edition, Pergamon Press Ltd., Oxford, 1985.

Chladek, L., Mathematisches Modell des Läuterprozesses bei der Bierherstellung, Die Lebensmittel-Industrie 24 (1977), 9, 416 - 420.

Curtis, N.S., The impact of R&D on brewery design, MBAA Technical Quarterly, 16, (1979), 4, 198 - 203.

De Clerck, J., A textbook of brewing, Vol. 1, English translation, Chapman and Hall, London, 1957, 286 - 295.

Dick R.I., and Ewing, B.B., Evaluation of activated sludge thickening theories, Journ. of the Sanitary Eng. Division, 9, (1967), 9 - 29.

Dufour, J.P., Alvarez, P., Devreux, A., Gerardi, W., Influence of the filtration procedure on the relationship between wort turbidity and its lipids content, Monatsschrift für Brauwissenschaft, 39, (1986), 3, 115 - 121.

Dullien, F.A.L., Chem. Eng. J. 10, 1, (1975)

Einenkel, W.-D., Mersmann, A., Erforderliche Drehzahl zum Suspendieren in Rührwerken, Verfahrenstechnik, 11, (1977), 2, 90 - 94.

Englmann, J., Wasmuht, K., Influence of lautering on fermentation and beer properties, Brauwelt International, 9, (1993), III, 206 - 210.

European Brewery Convention, Analytica EBC, 4. Edition, Brauerei und Getränke-Rundschau, Zürich, 1987

Eyben, D., Hupe, J., Filterability of wort and beer and its relationship with viscosity, EBC Symposium on the relationship between malt and beer, Helsinki, 1980, 201 - 212.

Ferenczy, L., Bendek, G., Untersuchung der Veränderung der Würzeproteinzusammensetzung während des Maischprozesses mit der SDS-PAGE-Gelelektrophorese und deren Einfluß auf das Abläutern, Monatsschrift für Brauwissenschaft, 44, (1991), 5, 191 - 200.

Fitch, B., Sedimentation process fundamentals, Am. Inst. Min. Met. & Petrol Engr. (Society of mining engineers), 223, (1962), 6, 129 - 137.

Graveland, A., Bongers, P., Bosveld, P., Extraction and fractionation of wheat flour proteins, Journal of the science of food and agriculture, 30, (1979), 71 - 84.

Greffin, W., Krauß, G., Schrotten und Läutern, II., Monatsschrift für Brauerei, 31 (1978), 192 - 212.

Hermia, J., Eyben, D., Considerations sur les procede de filtration en brasserie, EBC Proceedings of the 19. Congress, London, 1983, 209 - 224.

Hermia, J., Rahier, G., Designing a new wort filter, Filtration & Separation, 22, (1990), 11/12, 421, 422, 424.

Herrmann, H., The state of technology in the brewhouse, Brauerei Journal, (1991), 27 - 30.

Herrmann, H., Kantelberg, B., Lenz, B., New lauter tuns, Engineering practice - technology - field experience, Brauwelt International, 6 (1990), I, 22 - 28.

Heyse, U., Aktuelle Situation im Bereich des Sudhauses, Brauwelt, 133, (1993), 13, 573 - 574.

Home, S., Pietilä, K., Sjöholm, K., Control of glucanolytic in mashing, Journal of the ASBC, 51, (1993), 3, 108 - 113.

Horn, E.-M., Eindickung und Abscheidung von Feststoffen aus Suspensionen im vertikal durchströmten Sedimentationsapparat, Fortschr.-Ber. VDI Reihe 15, No. 62, Düsseldorf, 1988,

Hough, J.S., Briggs, D.E., Stevens, R., Young, T.W., *Malting and Brewing Science, Vol.1 Malt and Sweet Wort*, Chapman & Hall, London, 1986.

Hug, H., Anderegg, P., Mändli, H., Pfenninger, H., Zum Einfluß des Sauerstoffs bei der Würzebereitung-Halbstechnische Brauversuche unter Extrembedingungen, *Brauerei-Rundschau*, 97, (1986), 6, 113 - 140.

Huige, N.J., Westermann, D.H., Effect of malt particle size distribution on mashing and lautering performance, *MBAA Technical Quarterly*, 12, (1975), 1, 31 - 40.

IOB, *Recommended Methods of the Institute of Brewing*, 1977

Jäger, P., Damköhler, G., Winzig, K., Püspök, J., Die Viskosität als Maßstab für die Läutergeschwindigkeit, *Mitteilungen der Versuchsstation für das Gärungsgewerbe in Wien*, (1977), 5/6, 52 - 59.

Johnstone, J., Liquid solid separation in the brewhouse, *MBAA Technical Quarterly*, 29, (1992), 1 - 5.

Kano, Y., Karakawa, T., Importance of residual starch in the spent grains for wort run-off, *Bulletin of Brewing Science*, 25, (1979), 1 - 7.

Klotz, K., Dallmann, W., Die Mikroprozesse der Kuchenfiltration und ihre gegenwärtige theoretische Beschreibung, *Chem. Techn.* 36, (1984), 4, 152 - 156.

Koglin, B., Einfluß der Agglomeration auf die Filtrierbarkeit von Suspensionen, *Chemie Ingenieur Technik*, 56, (1984), 2, 111 - 117.

Kolbach, P., Die Umrechnung von Würze und Bier auf einen bestimmten Extraktgehalt, *Monatsschrift für Brauerei* 13, (1960) 21.

Krauß, G., Schroten und Läutern, I., *Monatsschrift für Brauerei*, 26, (1973), 214 - 219.

Kynch, G.J., A theory of sedimentation, *Transactions of the Faraday Society*, 48, (1952), 161 - 176.

Laing, H., Taylor, D.G., Factors affecting mash bed permeability, *IOB Austr. and N.Z.*, Adelaide, 1984, 109 - 114.

Leberle, H., Schuster, K., Die Bierbrauerei, Volume 2: Die Technologie des Sudhauses, Ferdinand Enke, Stuttgart, 1956.

Leedham, P.A., Savage, D.J., Crabb, D., Morgan, G.T., Materials and methods of wort production that influence beer filtration, EBC Proceedings of the 15. Congress, Nice, 1975, 201 - 216.

Lewis, M.J., Wahnou, N.N., Precipitation of protein during mashing: Evaluation of the role of calcium, phosphate, and mash pH, Journal of the ASBC, 42, (1984), 159 - 163.

Lewis, M.J., Oh, S.S., Influence of precipitation of malt proteins in lautering, MBAA Technical Quarterly, 22, (1985), 108 - 111.

Lewis, M.J., Robertson, I.C., Dankers, S.U., Proteolysis in the Protein Rest of Mashing - An Appraisal, MBAA Technical Quarterly, 29, (1992), 4, 117 - 121.

Lewis, M.J., Serbia, J.W., Aggregation of protein and precipitation by polyphenol in mashing, Journal of the ASBC, 42 (1984), 40 - 43.

Lie, S., Grindem, T., Jacobsen, T., Oxygen absorbtion in the brewhouse, a quantitative study, EBC Proceedings of the 16. Congress, Amsterdam, 1977, 235 - 243.

Lüers, H., Die wissenschaftlichen Grundlagen von Mälzerei und Brauerei Hans Carl, Nürnberg, 1950.

Marc, A., Engasser, J.-M., Moll, M., Flayeux, R., Kinetics and modelling of starch hydrolysis during mashing, Util. Enzymes Technol. Aliment. Symp.Int. (1982), 115 - 119.

McCabe, W.L., Smith, J.C., Harriott, P., Unit operations of chemical engineering, McGraw - Hill Book Company, London, 1985.

McFarlane, I.K., Mash conversion and preparation, Ferment, 6, (1993), 3, 177 - 183.

MEBAK, Mitteleuropäische Brautechnische Analysenkommission Brautechnische Analysenmethoden, Volume II, Freising, 1987, 15 - 17.

Meddings, P.J., Potter, O.E., Physical and chemical processes in mashing. Effect of particle size, J. Inst. Brew. 77, (1977), 246 - 252.

Michaels, A.S., Bolger, J.C., Settling rates and sediment volumes of flocculated Kaolin suspensions, Ind. Eng. Chem. Fundam. 1 (1962), 24 - 33.

Moll, M., Baluais, G., Dodds, J. Leclerc, D., A process engineering and technological approach to mash separation, MBAA Technical Quarterly, 28, (1991), 12 - 17.

Muts, G.C.J., Krakebeeke, M.G., Pesman, L., van den Berg R., Malt characteristics and filtration, Proc. of the IOB, Austral. and N.Z. Section, Adelaide, (1984), 115 - 120.

Muts, G.C.J., Pesman, L., The influence of raw materials and brewing process on lautertun filtration, EBC Monograph XI, Mafflier, 1986, 25 - 35.

Narziß, L., Die Bierbrauerei, Volume 2: Die Technologie der Würzebereitung, 6. Edition, Ferdinand Enke, Stuttgart, 1985.

Narziß, L., Der Einfluß der Sudhauseinrichtung auf die Qualität von Würze und Bier, Brauwelt, 127, (1987), 6, 207 - 213.

Narziß, L., Personal Information, 1990.

Narziß, L., Das moderne Sudhaus mit besonderer Berücksichtigung der Abläuterung, Der Weihenstephaner, (1992), 1, 74 - 76.

Narziß, L., Qualitative und quantitative Aspekte beim Maischen, Brauwelt, 132, (1992), 23, 1072 - 1091.

Narziß, Reicheneder, E., Edney, M.J., The control of beta-glucan in the brewery, Monatsschrift für Brauwissenschaft, 43, (1990), 2, 66 - 76.

Narziß, L., Reicheneder, E., Färber, W., Freudenstein, L., Sauerstoffaufnahme beim Maischen, Brauwelt, 126, (1986), 1/2, 11 - 25.

Neumann, L., Zaake, S., Beta-Glucangehalt des Malzes, Viscosität der 80-Grad-Hartongmaische, Viscosität der Kongreßwürze und Filtrierbarkeit, Monatsschrift für Brauerei, 33, (1980), 6, 214 - 218.

Nielsen, H., The importance of running clear lauter wort, MBAA Technical Quarterly 10, (1973), 1, 11 - 15.

Perry, R.H., Green, D., Chemical Engineers Handbook, Singapore, McGraw-Hill Book, Inc., 1985.

Pierce, J.S., Influence of beta-glucan and beta-glucanase levels in barley and malt on extract yield and run-off, EBC Symposium Barley and Malt, Helsinki, 1980, 179 - 185.

Purchas, D.B., Wakeman, R.J., Proposals for unifying cake filtration tests, in: Purchas, D.B., Wakeman, R.J., (Editors) Solid Liquid Separation Scale-Up, Uplands Press Ltd, London, 1986.

Richter, K., Reaktionsgeschwindigkeiten beim Maischen und Abtrennung mit einem Dekanter, EBC Proceedings of the 24. Congress, Oslo, 1993, 173 - 182.

Robertson, J., Wort production, The Brewer, (1990), 3, 91 - 95.

Ruth, B.F., Correlating filtration theory with practice, Ind.Eng.Chem., 38, (1946), 564.

Salzgeber, B., Zur freien Durchgangsfläche des Senkbodens bei Läuterbottichen, Brauwelt, 116 (1976), 42, 1368 - 1371.

Schöffel, F., Rühren der Maische, ein spezieller verfahrenstechnischer Grundvorgang, Monatsschrift für Brauwissenschaft, 31, (1978), 1, 4 - 10.

Schur, F., Pfenninger, H.B., Anderegg, P., Nachteilige mechanische Effekte auf dem Bierproduktionsweg, Proceedings of the 18. EBC Congress, Copenhagen, 1981, 129 - 136.

Schur, F., Pfenninger, H., Narziß, L., Kinetische und energetische Untersuchungen über den Maischprozeß, Schweizer Brauerei Rundschau, 86, (1975), 10, 193 - 216.

Schuster, K., Narziß, L., Kumada, J., Über die Gummistoffe der Gerste und ihr Verhalten während der Malz- und Bierbereitung, I. Problemstellung und Analysenmethoden, Monatsschrift für Brauwissenschaft, 20, (1967), 4, 125 - 135.

Schuster, K., Narziß, L., Kumada, J., Über die Gummistoffe der Gerste und ihr Verhalten während der Malz- und Bierbereitung, II. Gummistoffe in der Gerste und ihre Veränderungen beim Mälzen und Maischen, Monatsschrift für Brauwissenschaft, 20, (1967), 5, 185 - 206.

Stippler, K., Advanced brewhouse technology taking oxygen under consideration, MBAA Technical Quarterly, 25, (1988), 54 - 61.

Talmage, W.P., Fitch, E.B., Determining thickener unit areas, Ind. Eng. Chem., 47, (1955), 1, 38 - 41.

Tiller, F.M., and Crump, J.R., Recent advances in compressible cake filtration theory, in: Rushton, A., (Editor) Mathematical Models and Design Methods in Solid-Liquid Separation, Martinus Nijhoff Publishers, Dordrecht, 1985.

Uhlig, K., Vasquez, S., Measuring of shear effect during mashing, Brauwelt International, 8, (1992), IV, 356 - 357.

Van den Berg, R., Muts, G.C.J., Drost, B.W., Graveland, A., Proteins from barley to wort, EBC Proceedings of the 18. Congress, Copenhagen, 1981, 461 - 469.

Van Waesberghe, J.W.M., Shearing forces and air uptake during mashing, Brauwelt International, 4, (1988), I, 50.

Vauck, W.R.A., Müller, H.A., Grundoperationen chemischer Verfahrenstechnik, 4th revised Edition, Theodor Steinkopff, Dresden, 1974, Mechanisches Rühren, 317 - 326.

Wackerbauer, K., Zufall, C., Hölscher, K., Der Einfluß von Hammermühlenschrot auf die Würze- und Bierqualität, Brauwelt, 132 (1992), 29, 1366 - 1374.

Wainwright, T., Update on β -Glucans, Brewers Guardian, 119, (1990), 1, 9 - 13.

Wakeman, R.J., Filtration Post-Treatment Processes, Elsevier, Amsterdam, 1975.

Wakeman, R.J., Filter Cake Washing, in: Svarovsky, L., (Editor) Solid Liquid Separation, 2nd Edition, Butterworths, London, 1981.

Webster, R.D.J., Prediction of the lautering performance of malt, J. Inst. Brew., 87, (1981), 52 - 56.

Webster, R.D.J., Raw materials-Effect on mash separation, Brewers Guardian, 116, (1978), 7, 51 - 53, 56.

Zangrando, T. Über den Einfluß der Klarheit der Läuterwürze auf die Bierqualität, Mitt. d. Versuchsstation f. d. Gärungsgewerbe in Wien, (1978), 9/10, 101 - 105.

Ziemann GmbH, Ludwigsburg, Exhibition Catalogue, Interbrau 1993, Munich.

Zürcher, Ch. Gruß, R., Oxygen uptake during mashing and lautering, Brauwelt International, 5, (1989), IV, 350 - 355.

7.3. Glossary of Brewing Terms

Adjunct

Any brewing material, other than malted barley used for brewing as a source of extract. (i.e. cereals, sugar, starch etc.)

Barley

A cereal used for food and when germinated in malting gives malt, for the production of fermented drinks such as beer.

Break

Precipitation of proteinaceous material and other components from wort, occurring after boiling (hot break) and with cooling of the wort (cold break) below temperatures of 60°C.

Brewhouse

The building, housing the wort production vessels and equipment including mills, mashing vessels (mash cookers), mash tuns, lauter tuns, coppers, wort coolers.

Cast wort

Wort after boiling.

Cleaning-In-Place (CIP)

An automatic system installed to clean large closed brewery vessels. Cleaning fluid from a storage tank and wash water are circulated through the vessel from spray heads, permanently fitted in it, or a portable rig. There is no need to open the vessel since no worker need enter. This system is now a normal feature in breweries which have installed large vessels.

Cold break

Precipitate formed when wort is cooled to room temperatures. Also known as the fine break since the material, which sediments is much finer and less in quantity than that of the hot break.

Collection vessel

A measured vessel used to collect wort for the assessment of Excise duty.

Copper

The vessel in which wort is boiled with hops. Previously the vessels were

of copper but now many are in stainless steel. Also known as the wort copper or wort kettle.

Decoction mashing method

Mashing procedure in which part of the mash is withdrawn, boiled, then returned to the main mash to raise its temperature in steps. There are several variations known as the one, two and three mash method. The decoction mashing method is traditionally used in continental Europe for lager brewing.

Degree Plato, (°Plato)

Expression of the wort extract as a percentage of sucrose in aqueous solution (weight/weight).

Extract

The material solubilized in the wort during mashing of malt. Measured in percent (w/w) expressed as °Plato.

First runnings

The first small volume of wort (first wort), often turbid in appearance, run from the lauter tun. It is sometimes returned to the lauter tun.

First wort

First filtrate (wort) drained off the lauter tun. The extract content of this wort is directly depending on the water to grist ratio and the mashing conditions.

Grist

Mixture of coarsely ground malt or raw cereals.

Grist case

Grist storage container originally situated above the mash vessel.

High gravity brewing

The practice of producing and fermenting wort at a higher original gravity than is required to package. Normally the original gravity is adjusted by dilution with water at the final filtration stage.

Holding time

Period of time at which a process such as the mashing process is maintained under certain fixed conditions.

Hot break

Coagulum (trub) which appears soon after boiling wort begins to cool. Sometimes called coarse break since the material settling is coarse in appearance compared with that of the cold or →fine break

Hot liquor tank

Vessel where water for mashing is heated and stored.

Infusion mashing

A mashing procedure in which hot water and malt grist are mixed to give a defined temperature (i.e. 65°C). In single infusion mashing this temperature is hold over a time of ½ to 1½ hours. In programmed mashing different temperature steps, between 40 and 78°C are held.

Iodine test

A quick analytical test to determine whether undegraded starch, which gives a blue colour with iodine solution, remains in the mash.

Last runnings

The last volume of low gravity (low extract) wort from the lauter tun.

Lauter tun

A filtration vessel used in modern mashing techniques, sometimes partitioned and fitted with rakes.

Lautering

A filtration procedure for the separation of wort from spent grains in a lauter tun. Lauter tuns are since long time the most widely used separation devices.

Malt

Barley or other cereal produced for brewing or distilling by steeping, germinating and kilning. In brewing, malt is assumed to be malted barley.

Malt mills

Traditionally malt mills are of the roll type with two, four or six revolving rolls, with pairs spaced a short distance apart, crushing and milling the malt fractions selectively. The aim is to preserve the husk in length wise fragments which assists drainage of wort during mash separation in the lauter tun, by forming a filter bed.

Malting

The process converting barley to malt

Mash

The mixture of crushed malt grist and hot liquor which yields wort.

Mash conversion

The action of malt enzymes in degrading and converting malt constituents such as starch and protein during mashing.

Mash filter

Originally a frame and plate filter with a filter cloth either of cotton or polypropylene, as an alternative for the lauter tun. The new type of mash filters (since 1989) are filter presses using membrane-plates to compress the cake and dewater it.

Mash (mixing) vessel

In this survey this container is a heatable vessel, containing the mash during the infusion mashing procedure.

Mash thickness

The ration of grist weight to water in the mash. For dark beers ratios from 2.5 to about 3.2 are used, for pale Pilsner or Export type beers (Lager) ratios of 3.0 to 4.0 are common.

Mashing

General expression for decoction or infusion mashing.

Mashing in

Mixing of grist and liquor in the mash vessel.

Modification

Describes the degree of conversion of malt kernels during malting. Malt modification can be correlated mainly with the following laboratory analyses: fine coarse extract difference, viscosity and friability

Original gravity (O.G.)

The specific gravity of the finished wort, at 20°C, before pitching with yeast, on which Excise duty is paid.

Pilsner or Pilsener

A pale lager beer having medium hoppy flavour. Originally brewed in Pilsen in Czech Republic but now brewed elsewhere.

°Plato

Extract in wort

Protein rest

A temperature step at 52 - 55°C in the programmed infusion mashing procedure. It enhances the action of proteolytic enzymes which degrade insoluble proteinaceous material to water soluble, small peptides and aminoacids.

Run-off rate

Rate of filtrate flux in the lauter tun

Saccharification

Enzymatic hydrolysis of starch by amylolytic enzymes producing low molecular sugars with one, two or three glucose molecules.

Second wort

Weak wort obtained by sparging

Sparge arm

Specially designed revolving tubing distributing sparge liquor over spent grains.

Sparge liquor

Hot brewing water used to wash wort from spent grains in a lauter tun.

Spent grains

Exhausted residue of malt grist remaining in the lauter tun after wort run off and sparging. Mainly used as cattle feed.

Sweet wort

Unboiled wort before the addition of hops; also called unhopped wort.

Tun

Used to describe many vessels in the brewery.

Wort

The sugary liquid produced by mashing an infusion of malt which on fermentation gives beer.

7.4. Table of Figures

Figure 2.1: Flow Diagram and Functions of Brewhouse Operations	4
Figure 2.2: Roller Mill	5
Figure 2.3: Vortex Pre-masher, (McFarlane, 1993)	8
Figure 2.4: Premasher System (Stippler, 1988).....	8
Figure 2.5: Flow sheet of a mashing vessel (Briggs, 1993)	10
Figure 2.6: Concentration of gel-proteins and effects on lautering performance	12
Figure 2.7: Typical lauter tun with additional equipment (Ziemann, 1993).....	18
Figure 2.8: Mash Stirrer (Briggs, 1993).....	22
Figure 2.9: Influence of stirring of mash on permeability	24
Figure 2.10: Heat transfer in a mashing vessel.....	29
Figure 2.11: Sedimentation curve (after Horn, 1988).....	34
Figure 2.12: Settling of particles in closed systems	35
Figure 2.13: Forces exerted on particles in compacted beds	38
Figure 2.14: Washing curve	48
Picture 3.1: Mashing and lautering pilot plant	58
Figure 3.1: Top view of the mashing rig	58
Figure 3.2: Flow rate and revolution rate vs. setting of the frequency controller	59
Figure 3.3: Pressure measurement at the mashing flow-loop	60

Figure 3.4: Orifice plate with pressure tappings at a distance of $0.5 \times d$ and $1 \times d$ from the plate. Discs with a diameter d_o of $0.5, 0.6, 0.7, 0.8, 0.9 \times d$ were available.	60
Figure 3.5: Mashing-in unit	61
Figure 3.6: Calibration curve for the premasher timed water dosage	62
Figure 3.7: Lauter Tun Setup	63
Figure 3.8: Bottom plate for the lauter tun	64
Picture 3.2: Pilot lauter column with peristaltic pump, control equipment and turbidimeter	65
Figure 3.9: Calibration procedure for the lauter tun pump control unit	66
Figure 3.10: Calibration curve for the setting 4.0	67
Figure 3.11: Example for a torque vs. time plot	69
Figure 3.12: Bench scale experimental setup: Mash beaker and stirrer.....	70
Figure 3.13: Shear rates in bench scale experiments calculated using the above assumptions	72
Figure 3.14: Bench scale mash filterability test 1 Pressure Vessel supplying constant pressure of 100 mbar2 Millipore Filter3 Digital Balance4 Printer5 Digital Stop Watch	74
Figure 3.15: dt/dV versus V plot of reproducibility trials.	76
Figure 3.16: Schematic of the laboratory roller mill.....	78
Picture 3.3: Rollers of the mill	78
Figure 3.17: Temperature programme for mashing	79
Figure 3.18: Lautering graph for a standard run	82
Figure 3.19: Falling ball viscometer	83

Picture 3.4: Laser Sizer sample cell with laser diodes and PIDS assembly	89
Figure 4.1: Sieve analysis for well modified malt	96
Figure 4.2: Sieve analysis for malt grist milled with 0.75 mm gap setting	97
Figure 4.3: Particle size distribution, grist in water sieved at 710µm.....	98
Figure 4.4: Sieve analysis for undermodified malt	98
Figure 4.5: Particle size distribution of fine malt particles after a dry sieve step at 150µm. The legend gives the gap sizes of the different mills.....	99
Figure 4.6: Dry solids after mashing (average of 12 trials with error bars ± 1 SD) in three size classes.....	100
Figure 4.7: Trial 66 PSD of the fine fraction (below 106 µm sieve) analysed with both Multisizer and Laser Sizer.	102
Figure 4.8: Trial 66 at 80 and 95°C on both Multisizer and Laser Sizer.....	102
Picture 4.1: Vertical cut of a spent grains filter cake	104
Figure 4.9: Particle size distributions in four different layers of the spent grains cake.....	105
Figure 4.10: Wet sieve analysis of spent grains cake bottom layer. (5 analyses with error bars ± 1 SD).....	106
Figure 4.11: Change of particle size distribution of the sub 106 µm sieved fraction of mash during mashing.....	109
Figure 4.12: Particle breakdown in the 100µm range with enzymes.....	110
Figure 4.13: Viscosity in wort.....	112

Figure 4.14: Viscosity related to temperature in water, sugar solution and wort samples	113
Figure 4.15: Variation of specific power input for different brewhouses (Brewhouse A could not be displayed because of the use of a decoction mashing procedure)	115
Figure 4.16: Average specific power input in different brewhouses.....	115
Figure 4.17: Specific work input over the entire mashing time.	116
Picture 4.2: Flow loop at the mash vessel.....	118
Figure 4.18: Specific power input at the single seat valve	119
Figure 4.19: Extract and viscosity change with specific power input in the liquid phase of mash samples	120
Figure 4.20: Sieve analysis of mash	120
Figure 4.21: Change of MPS with increasing agitation	121
Figure 4.22: Change of extract content in wort with agitation	122
Figure 4.23: Turbidity increase with agitation.....	123
Figure 4.24: Dry solids in wort with regards to specific power input	123
Figure 4.25: Effect of agitation on lautering time.....	124
Figure 4.26: Extract ratio (Extract in the mash / Extract in the wort)	125
Figure 4.27: Specific power loss at the vena contracta of the orifices.....	127
Figure 4.28: Effect of different stirrer velocities (as tip speed, v_{tip}) on torque and power input in mash (420 ml mash, concentration: 3.5 : 1)	133
Figure 4.29: Effect of agitation on MPS	134

Figure 4.30: Effect of agitation on particle concentrations below 106 μ m.....	135
Figure 4.31: Effect of agitation on density in mash	136
Figure 4.32: Density - viscosity correlation for small scale agitation trials.....	136
Figure 4.33: Effects from agitation on viscosity.....	137
Figure 4.34: Filterability of mash in relation to agitation	138
Figure 4.35: Effect of agitation on specific cake resistance	139
Figure 4.36: Correlation between MPS and filterability	139
Figure 4.37: Effects from MPS on total lautering time.....	142
Figure 4.38: Effect from mash temperature on MPS (number distribution).	144
Figure 4.39: PSD of mash (Volume distribution), Trial 66, analysed on the Multisizer.	145
Figure 4.40: Volumetric particle concentration of fines in the analysis suspension.....	146
Figure 4.41: Dry solids concentration of fines (<106 μ m sieve step) in mash	147
Figure 4.42: Change of viscosity with temperature	148
Figure 4.43: Viscosity at 65°C in the liquid phase of mash; (samples taken at different mash temperatures).....	148
Table 4.7: Slopes for linear fits of density and extract vs. mash temperature.....	149
Figure 4.44: Density (Extract) in the liquid phase of mash.....	150
Figure 4.45: Trial 67, dt/dV vs. V plot with linear fits for data points in accordance with cake filtration law	151

Figure 4.46: Filterability measured in a Millipore filter cell for different mashing temperatures (* and ** maximum volume filtered per filter area before blockage occurred).....	152
Table 4.8: Filterability increase between 65 and 78°C.....	152
Figure 4.47: Specific resistance of filter cakes with mashing temperature.....	153
Figure 4.48: Specific cake resistance vs. MPS.....	155
Figure 4.49: Effect of MPS on permeability of the spent grains cake ($R = 0.88$).....	158
Figure 4.50: Effect of MPS on washing efficiency ($R = 0.79$).....	159
Figure 4.51: Effect of MPS on turbidity in the filtrate ($R = 0.83$).....	159
Figure 5.1: MPS-temperature relationship	162
Figure 5.2: Relationship between viscosities at 20°C and 70°C.....	163
Figure 5.3: Viscosity-temperature relationship, with fitting function covering the range from 65 to 95°C	164
Figure 5.4: Sedimentation rate vs. MPS2. Linear regression: with $R = -0.93822$	166
Figure 5.5: Measured data compared with calculated data using the following equation for $0.42 \text{ m} < H_0 < 0.53 \text{ m}$	167
Figure 5.6: Final permeability vs. MPS2	168
Figure 5.7: Bench scale permeability for trials with agitation and temperature variation. Pressure was constant at 100 mbar. Correlation coefficient $R = 0.97$	169
Figure 5.8: Height of the cake before and after filtration.....	170
Figure 5.9: Effect of pressure on cake height	171

Figure 5.10: Height of the bed vs. filtrate volume, trial data with fitted exponential decay	172
Figure 5.11: Decay constant, t vs. L_{min} ($R = 0.80$).....	173
Figure 5.12: Permeability - height of the cake, after L_{min} =constant	174
Figure 5.13: Permeability change as a function of cake height	175
Figure 5.14: Washing curves of data and fitting functions with.....	177
Figure 5.15: Sigmoidal fitting curves on trials data	178
Table 5.1: Parameters for the fitting curves of the above examples.....	179
Figure 5.16: Washing efficiency as a function of MPS.....	180
Figure 5.17: Width of the sigmoidal fitting curve versus MPS with linear correlation and upper and lower limits ($2 \times SD$).....	181
Figure 5.18: Initial calculations to determine MPS and viscosity at lautering temperature, initial and final cake height	183
Figure 5.19: Main part of the lautering model	184
Figure 5.20: Trial 57 real (data points) and calculated data (lines)	191
Figure 5.21: Trial 30 real (data points) and calculated data (lines)	191
Figure 5.22: Trial 54 real (data points) and calculated data (lines)	192
Figure 5.23: Trial 79 real (data points) and calculated data (lines)	192

Figure 5.24: Predicted lautering time (dotted line) and
measured data (triangles) 193

Figure 5.25: Trial carried out by Robin Thorn real (data
points) and predicted data (lines)..... 194

7.5. Pictures and Electron Micrographs

Filter cakes from two different cakes were analysed using scanning electron microscopy. The samples were stored frozen at -20°C . The analysis was carried out after deep freezing at -185°C . Prior to this the samples were freeze etched at -60°C for a few seconds. Three different layers were observed. Figure 1 shows a vertical cut through the cake with different layers, Figure 2 is an enlarged part of the top section. The different particle structures are clearly visible

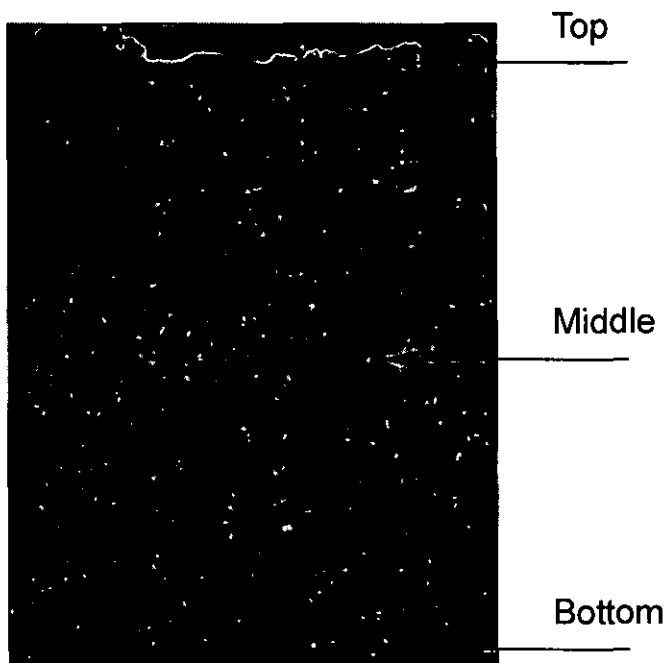


Fig. 1: Vertical cut through a cake



Fig. 2 Enlarged area of the top section

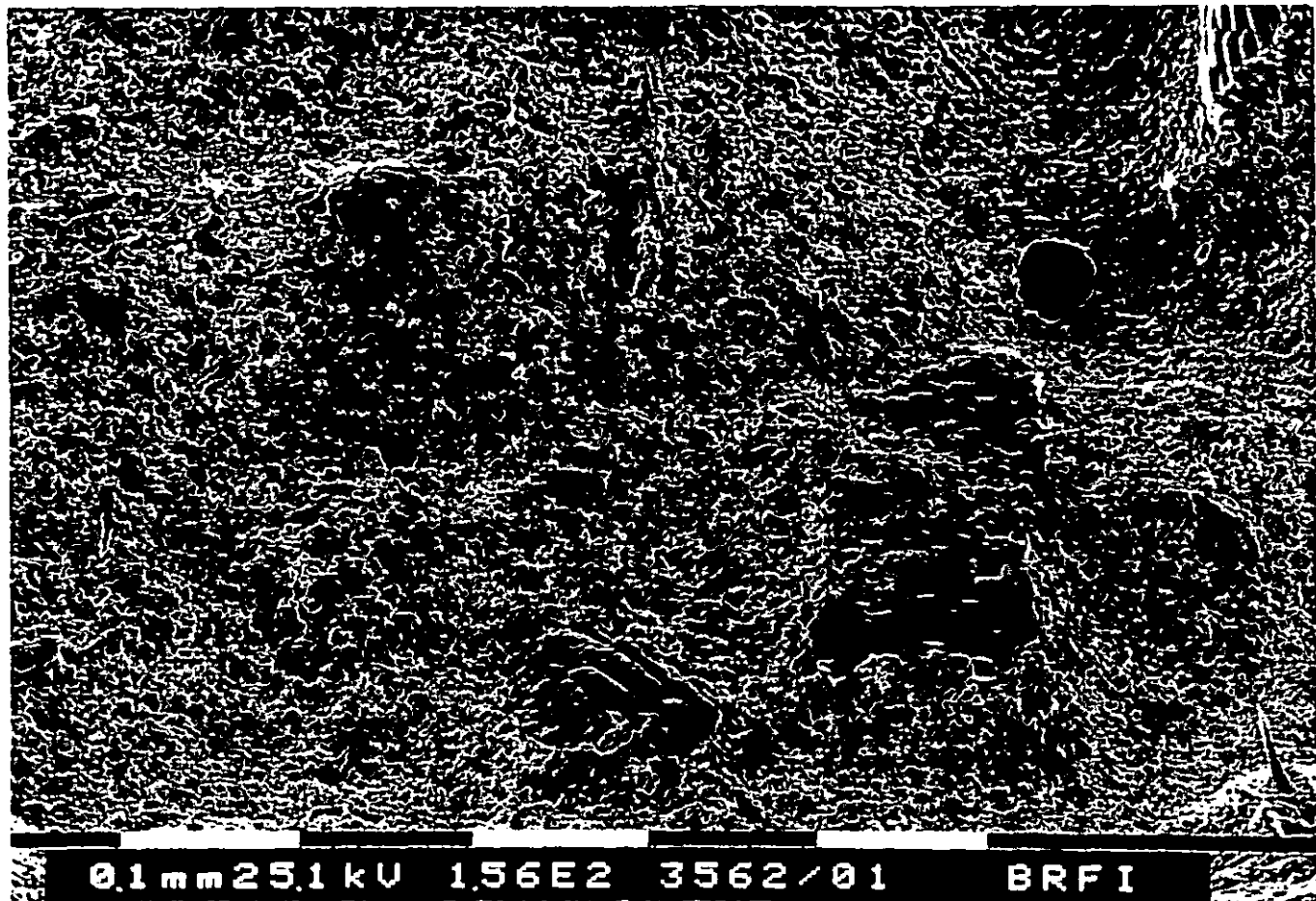


Fig 3: Micrograph from top section (Trial 9, $2210s^{-1}$): general view showing husk and starch granules. Starch granules were very abundant together with parts of the husk and endosperm.

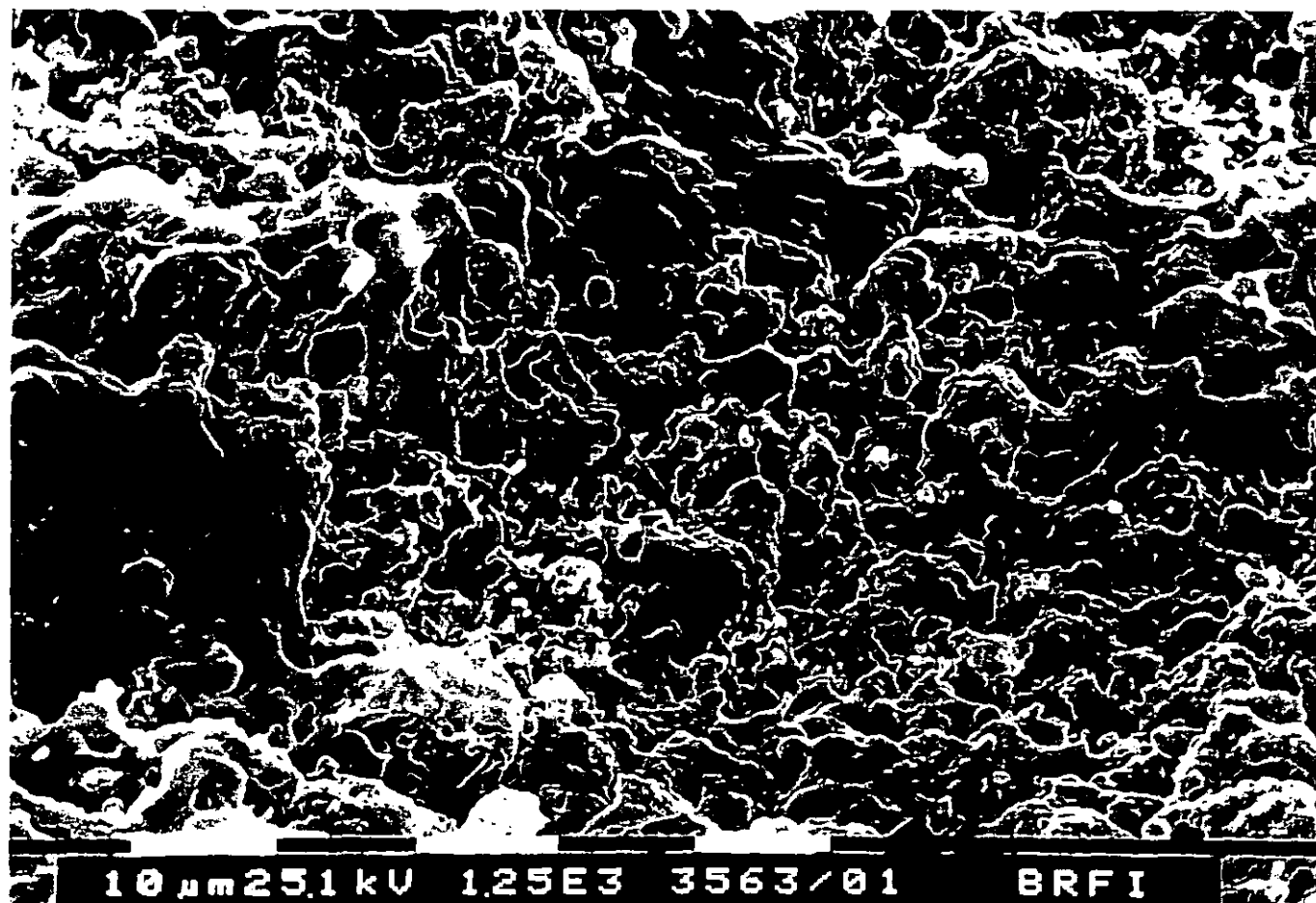


Fig 4: Starch granules in a glucan and starch matrix.

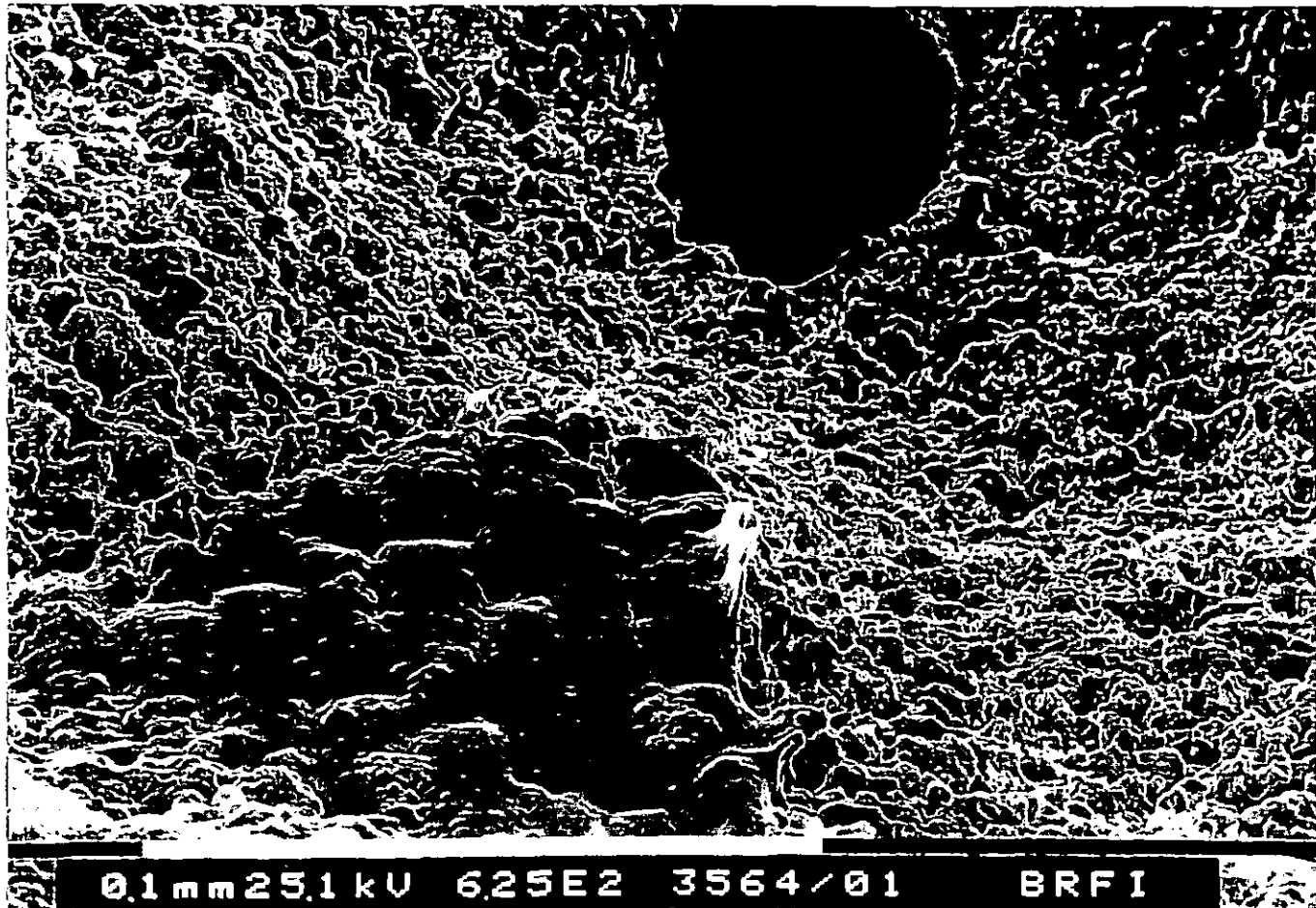


Fig. 5: Shows a holed structure in the glucan/starch matrix

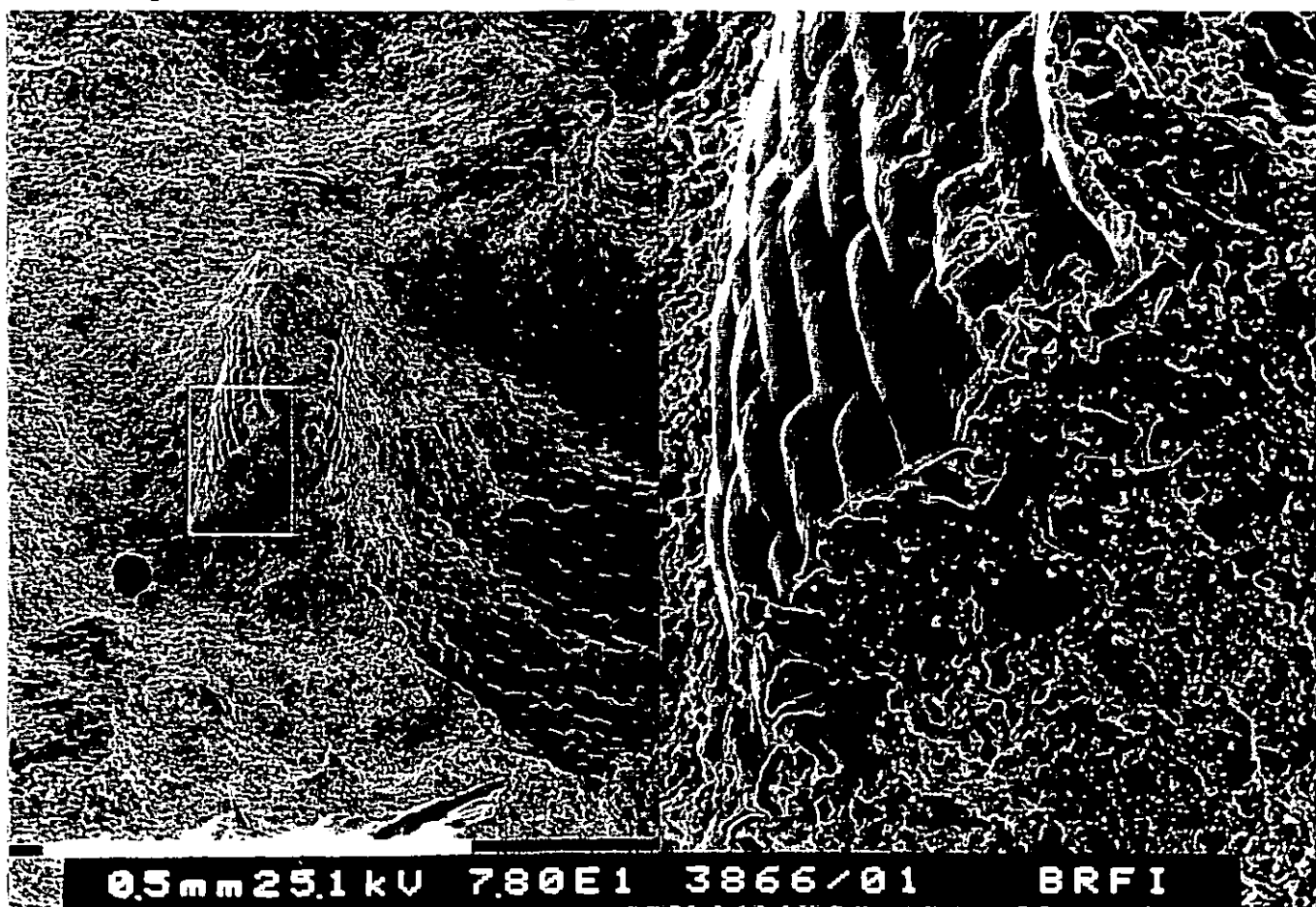


Fig. 6: Large areas of husk evident.

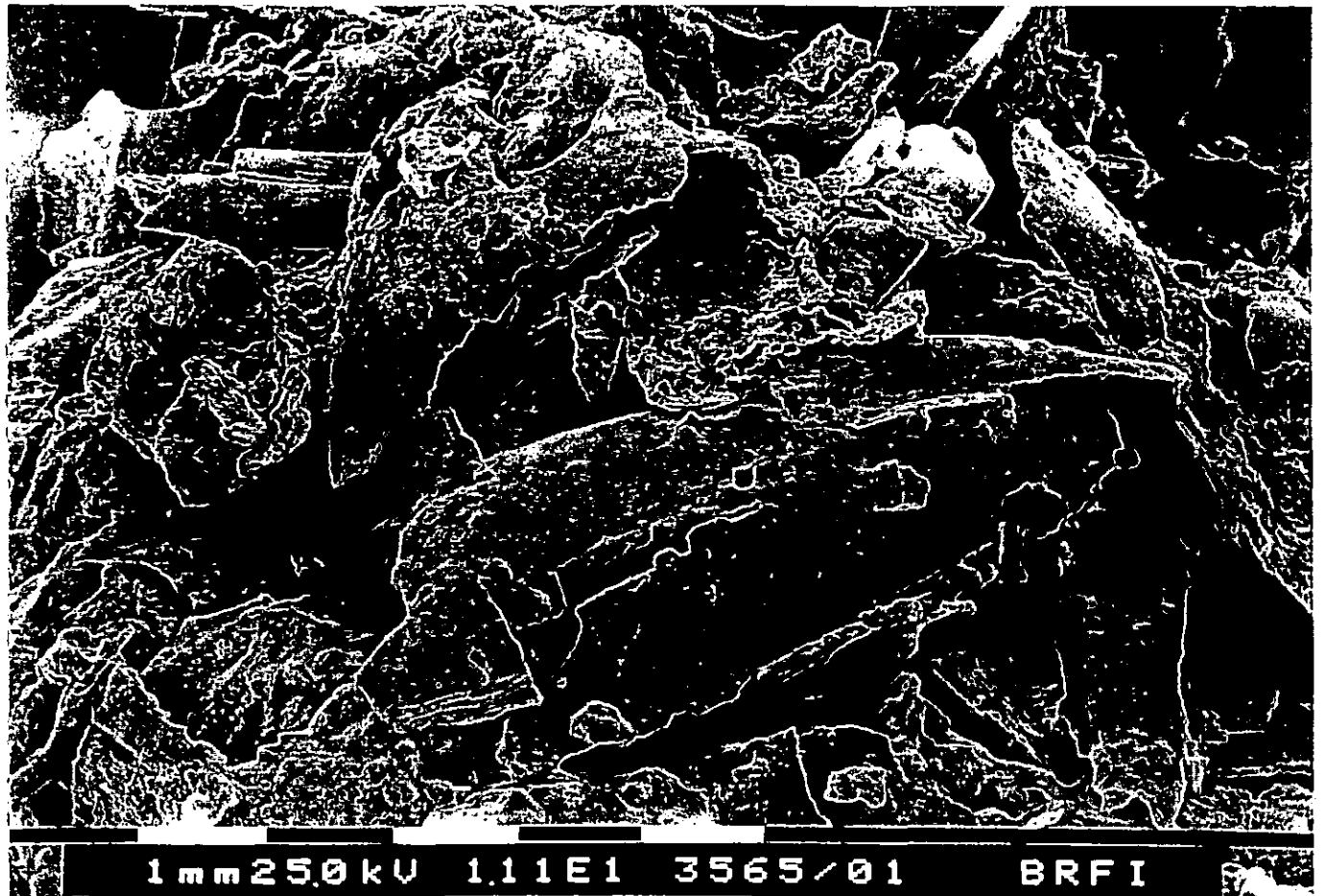


Fig. 7: Area beneath the top layer: general view showing intact or broken grains.

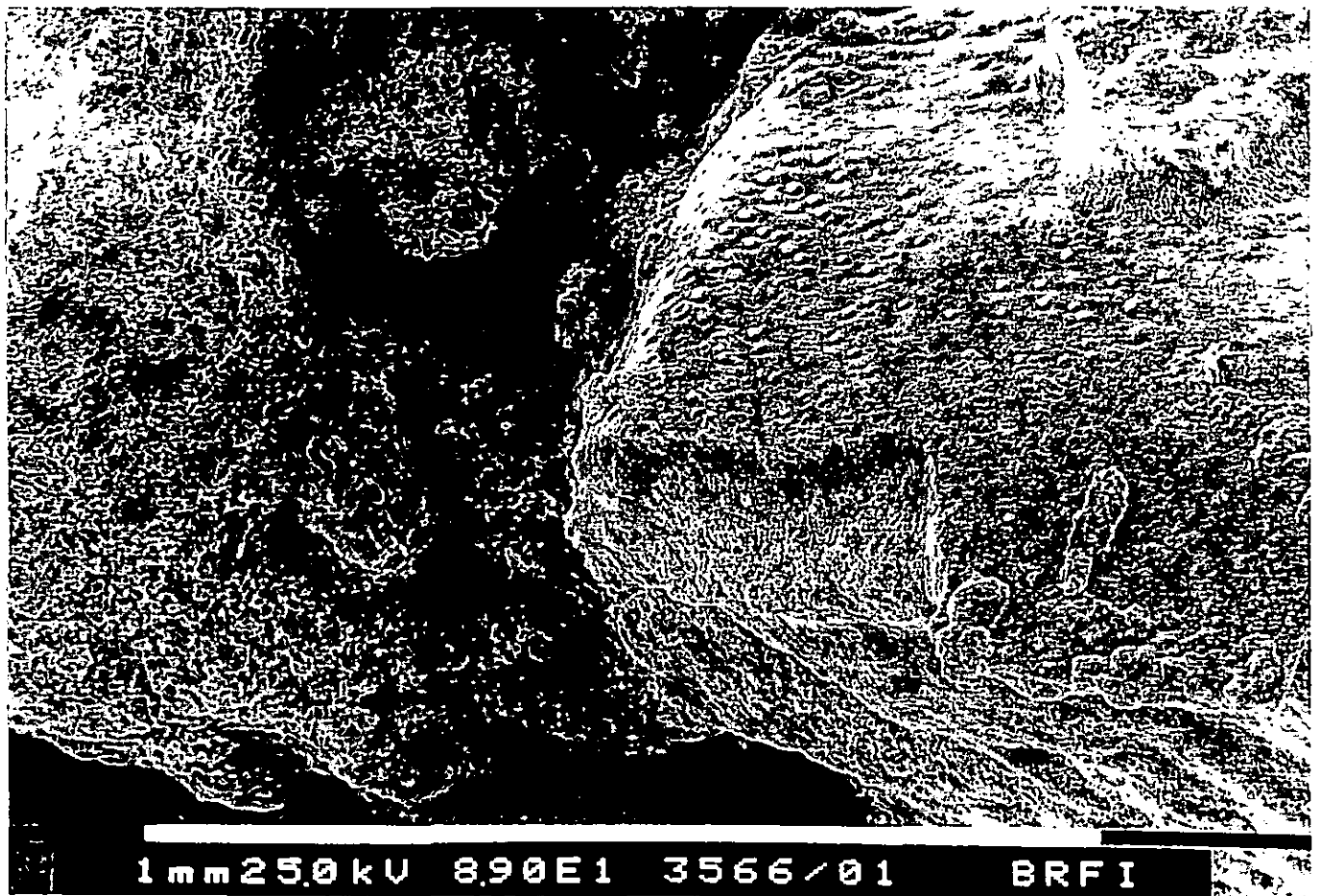


Fig. 8: Husk surface and protein/glucan/starch matrix.

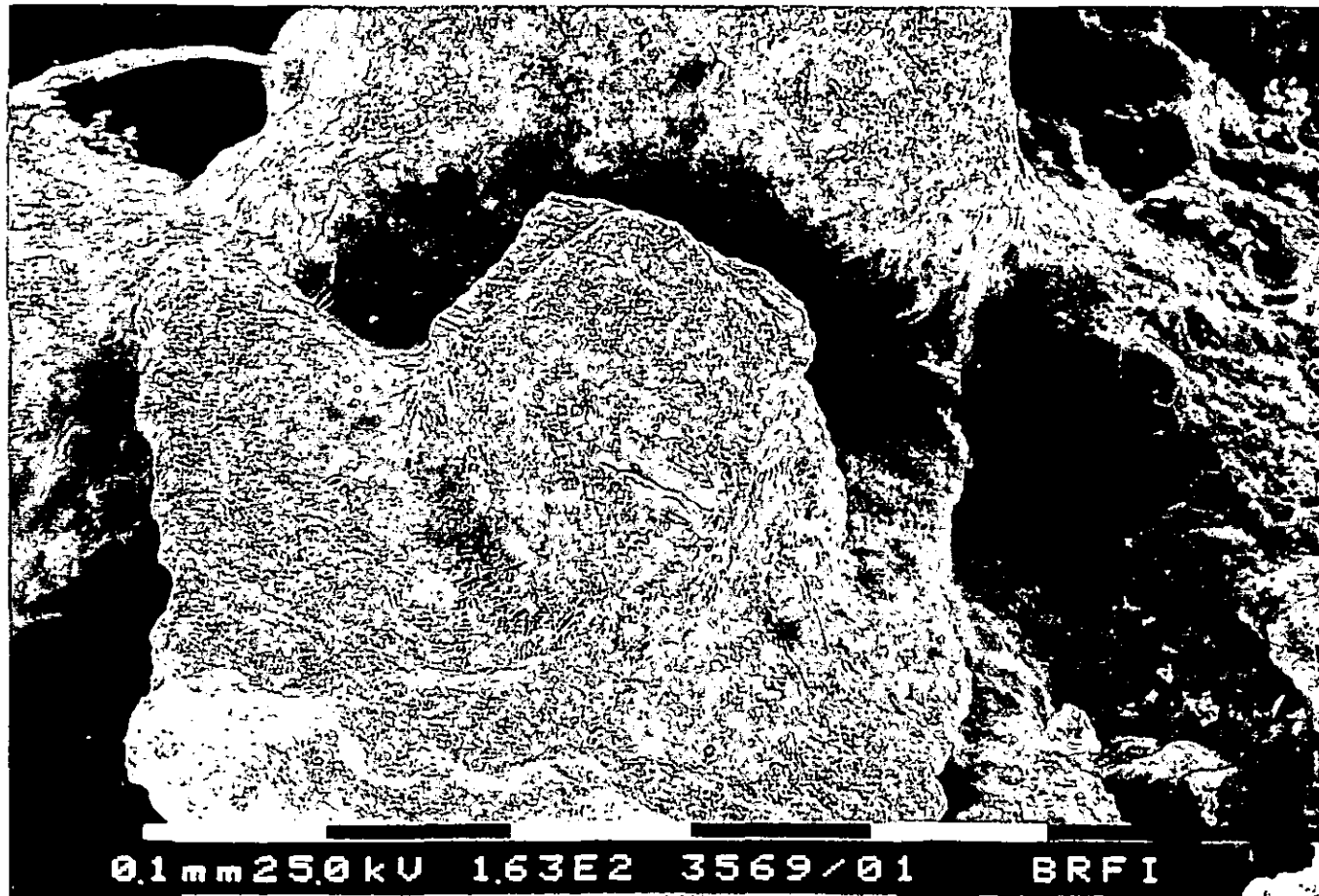


Fig 9: Large piece of fenestrated glucan/starch sheet



Fig 10: Starch and glucan matrix

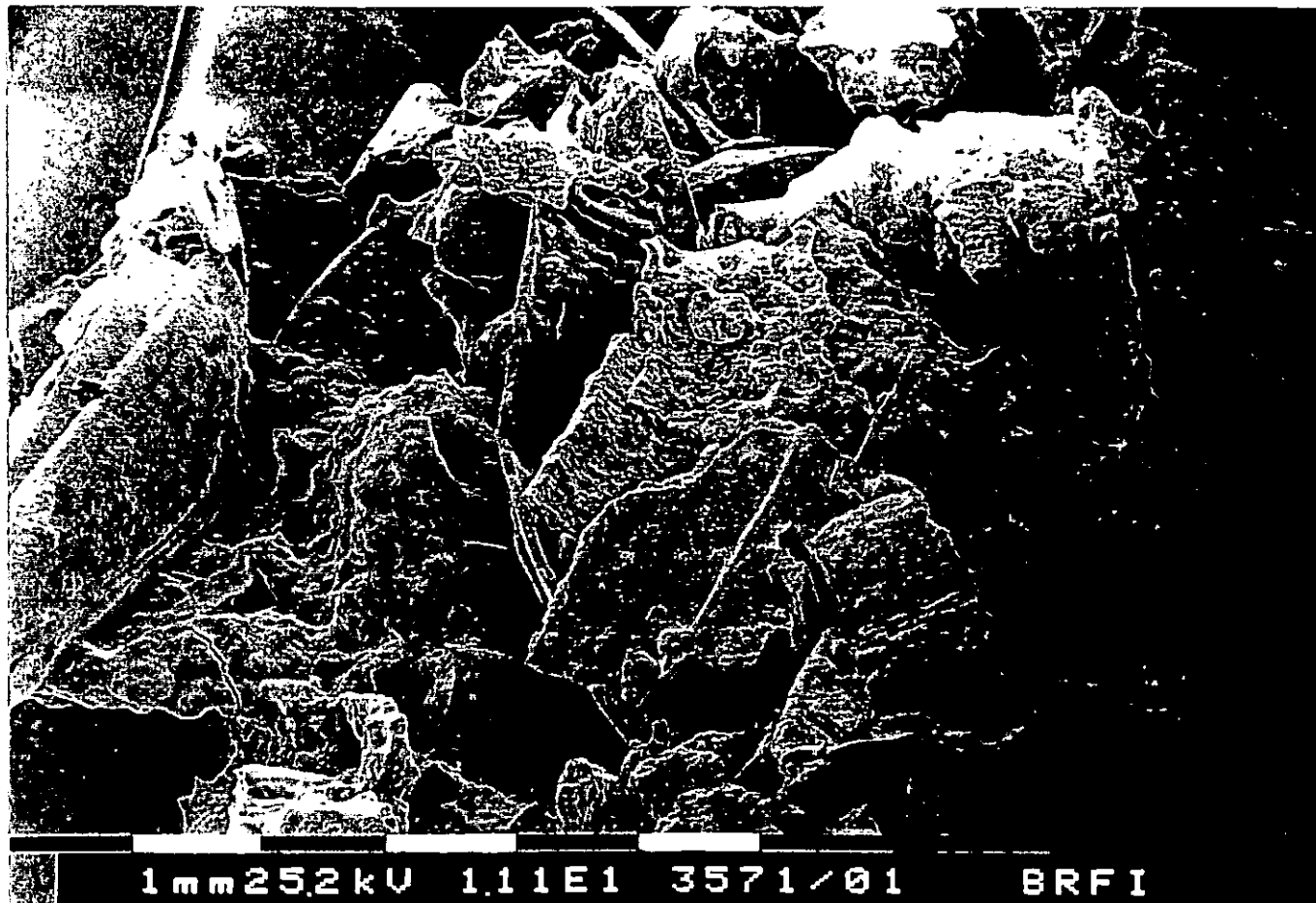


Fig 11: Middle section: general view

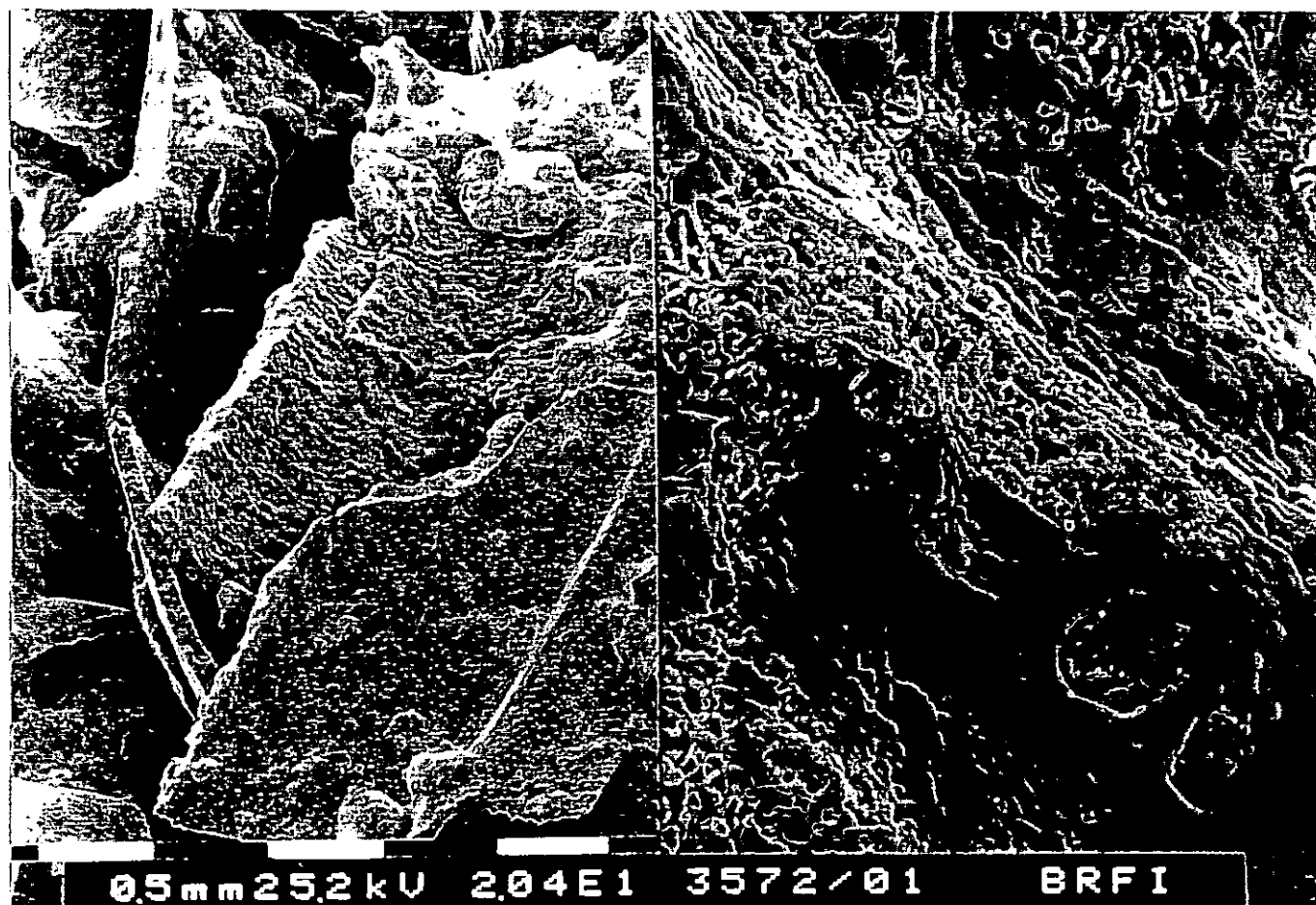


Fig 12: Part of a grain that had lost nearly all the starch but had retained a protein/glucan matrix



Fig 13: A starchy area

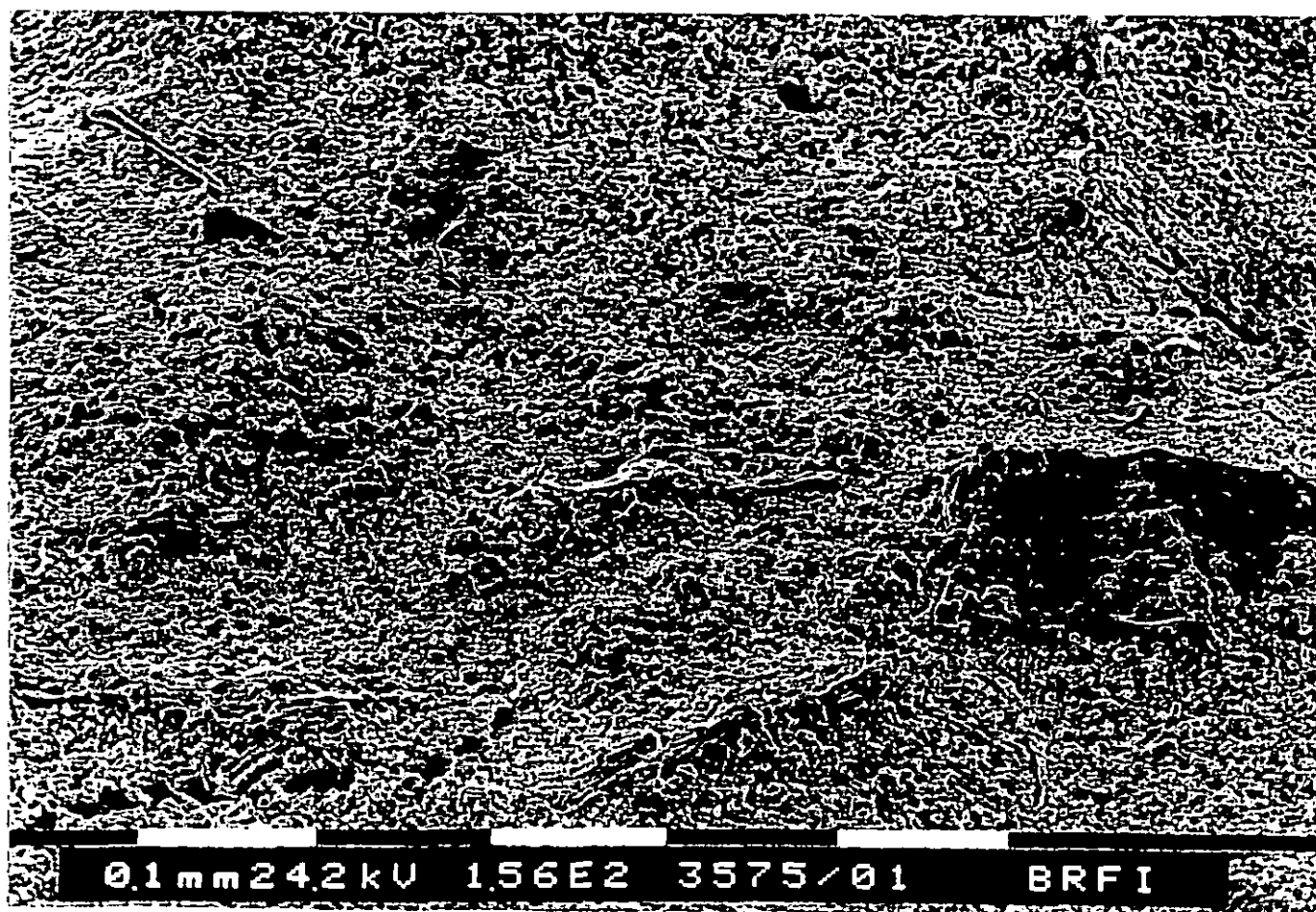


Fig 14: Trial 10, ($>5000 \text{ s}^{-1}$) top layer: general view

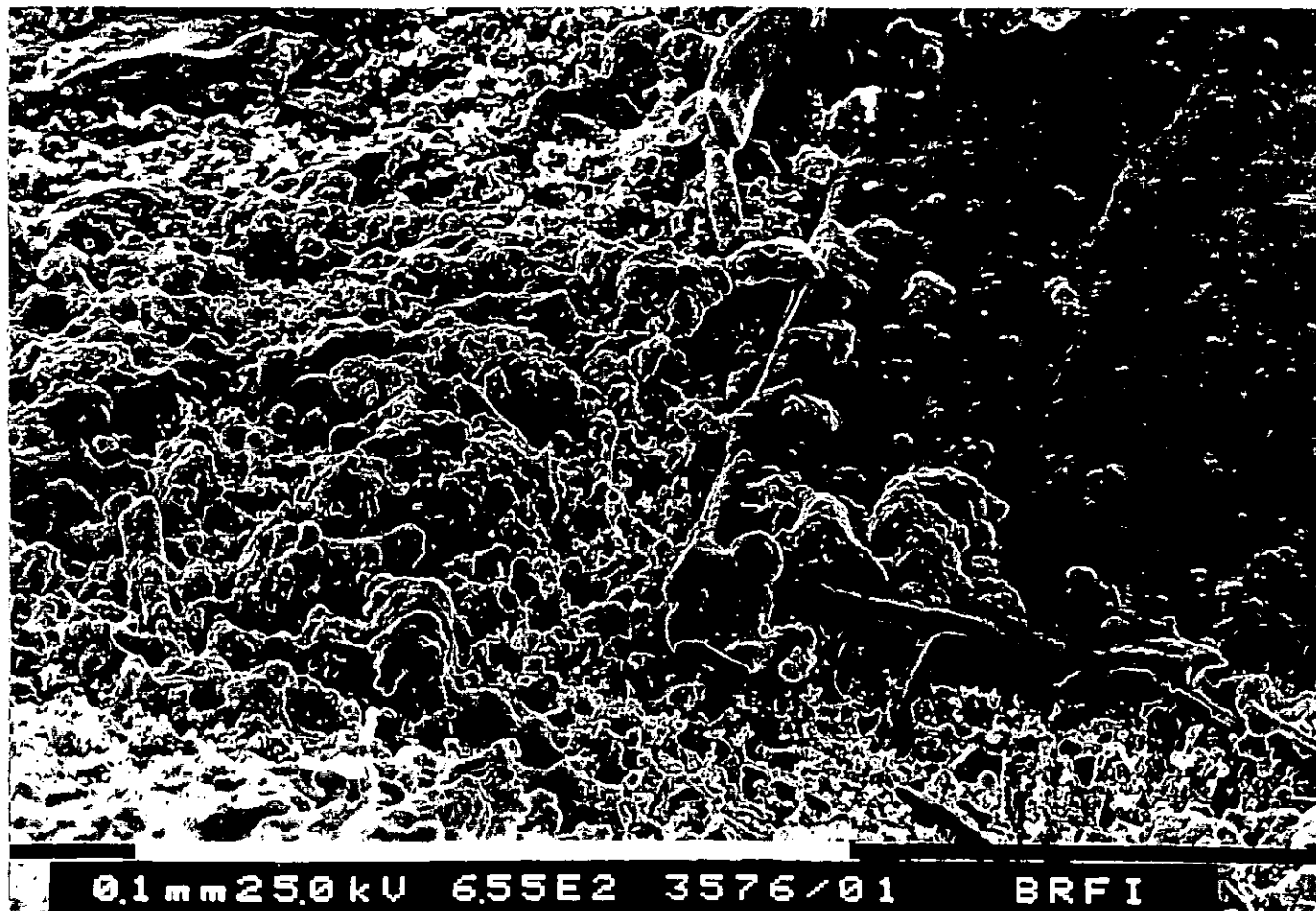


Fig 15: Husk with aleurone, starch and glucan (fenestrated).

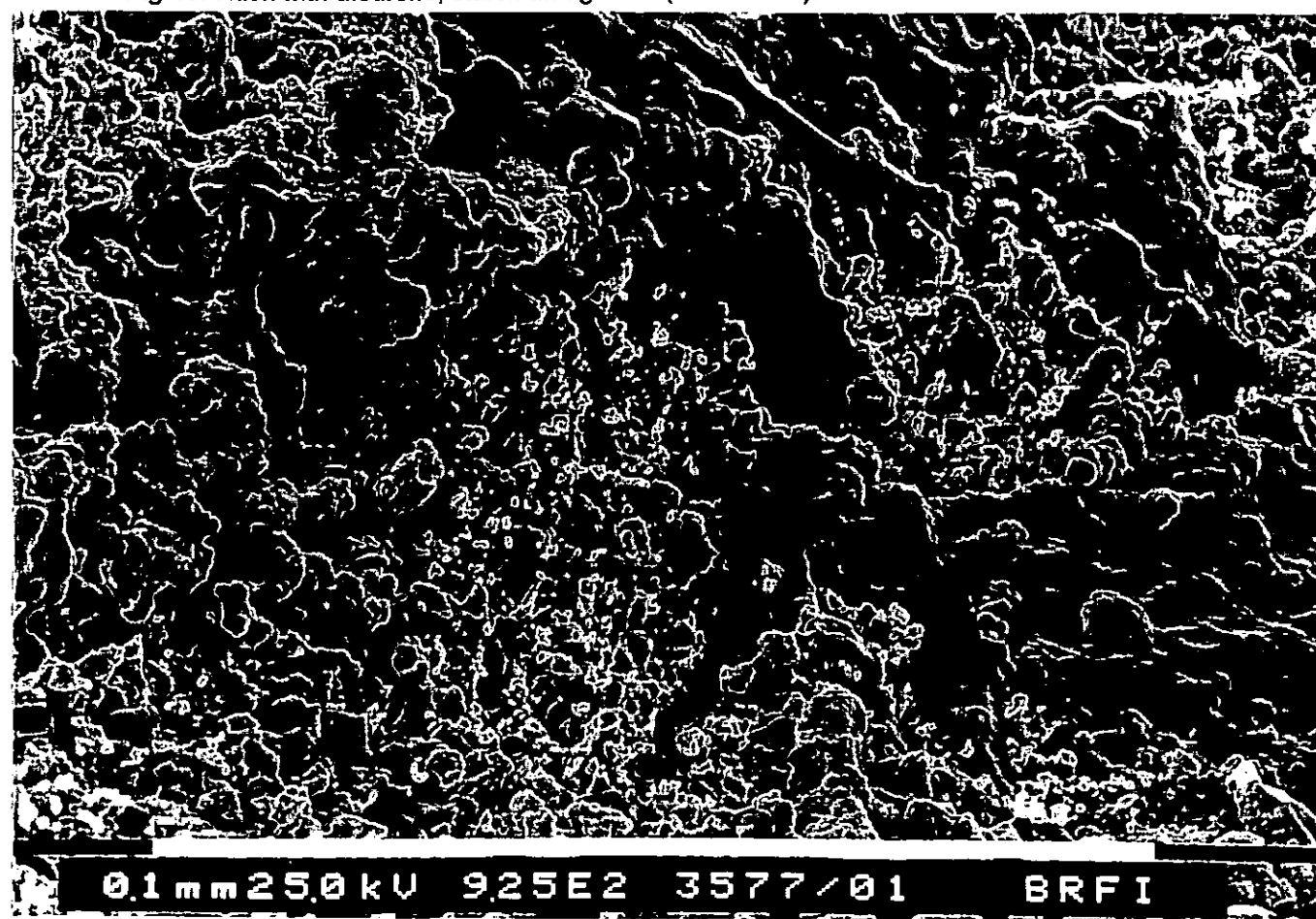


Fig 16: Large glucan sheets over starch

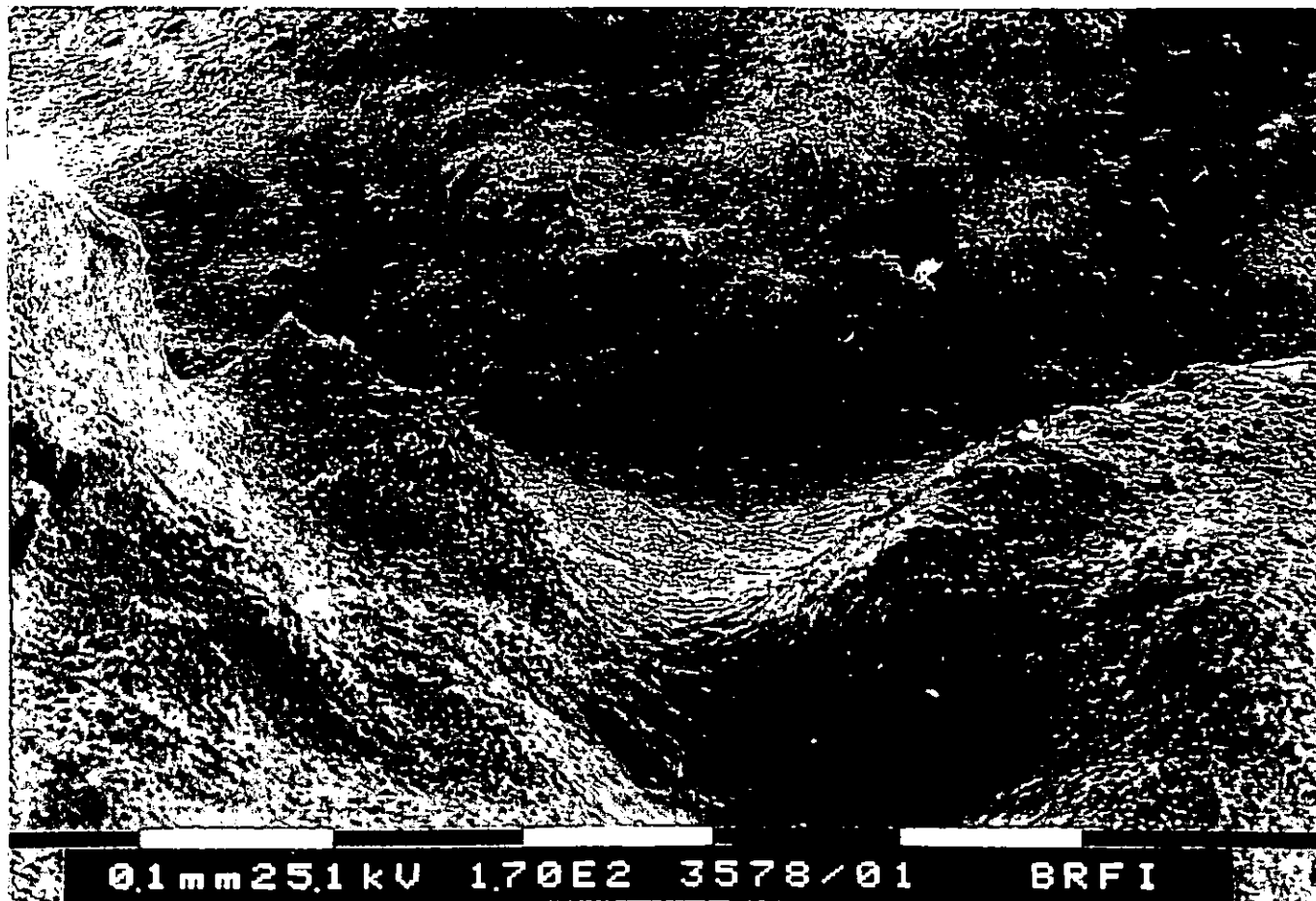


Fig 17: Middle layer: general view. This layer contained a lot of starch and glucan

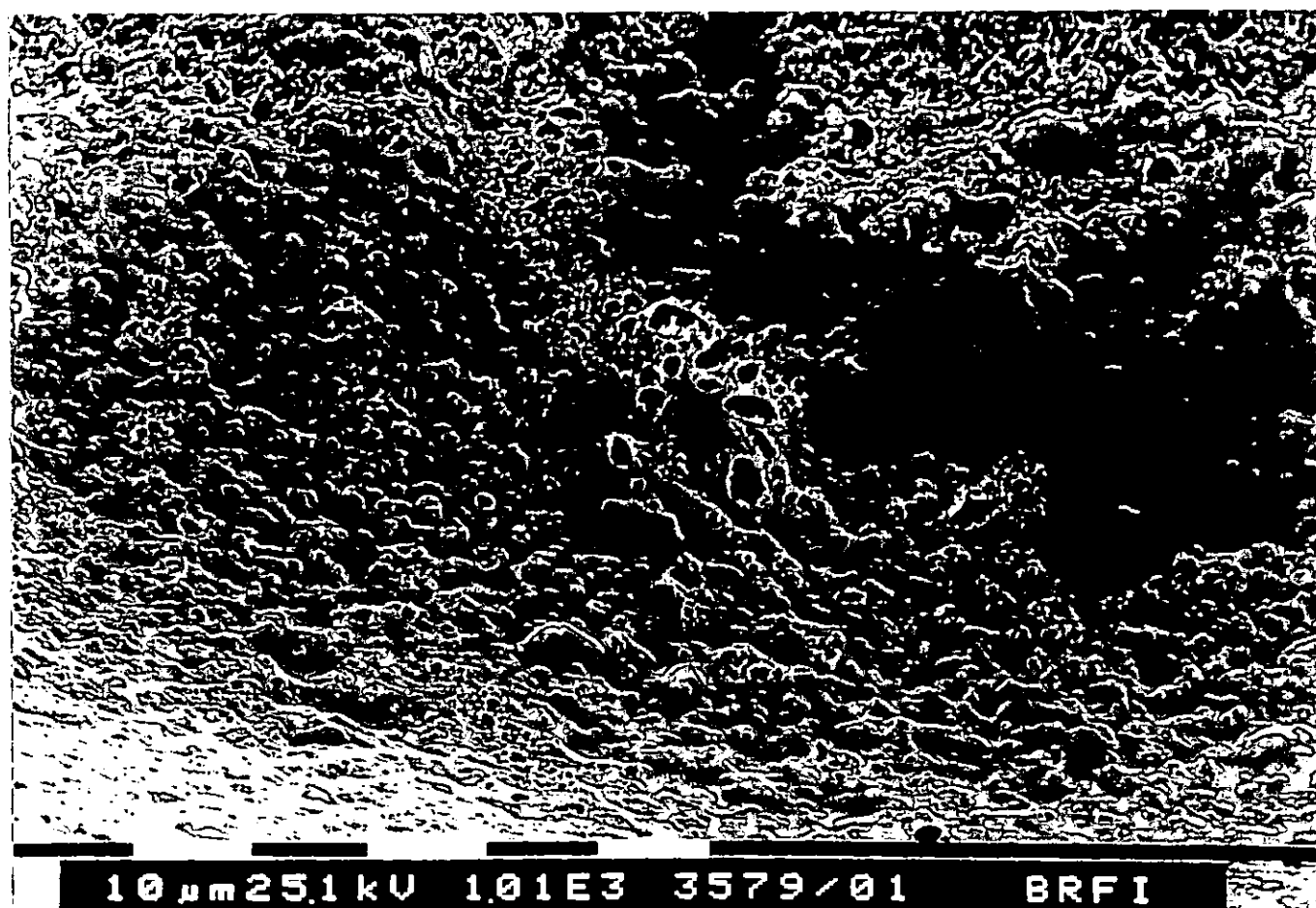


Fig 18: Large glucan sheet

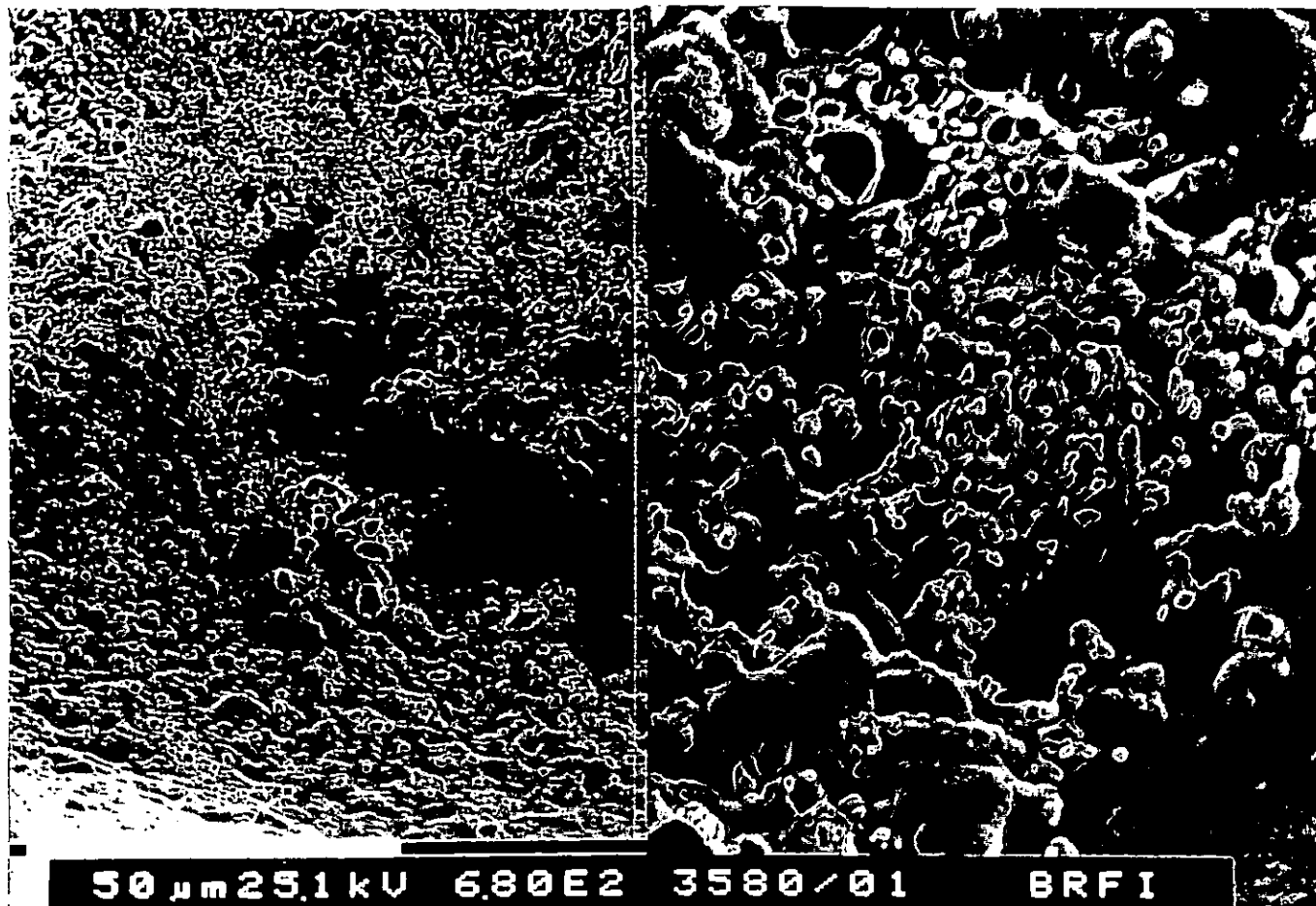


Fig 19: Detail of glucan matrix

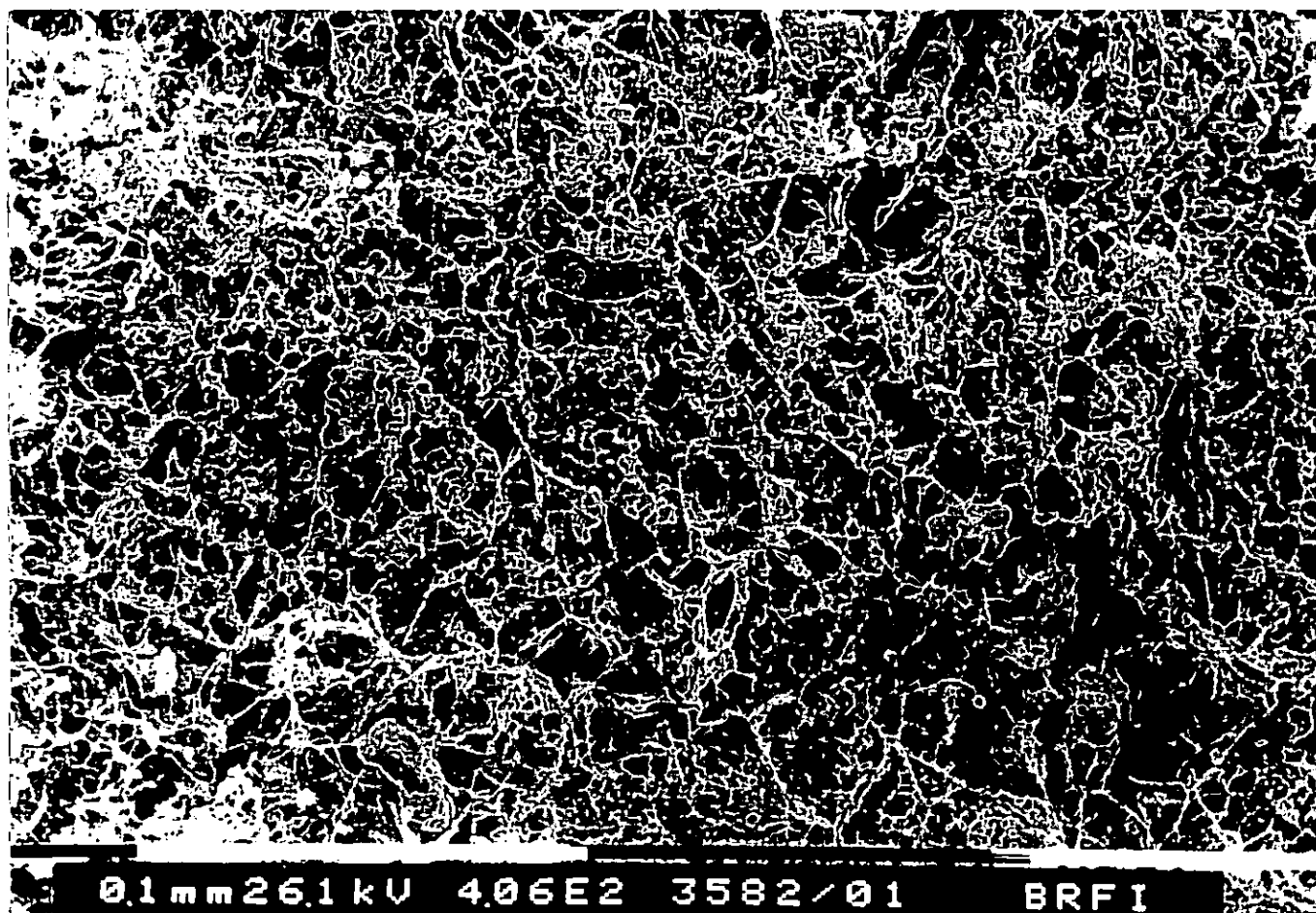


Fig 20: Bottom layer. This layer was the same as the middle layer. The preparations were, however, freeze etched longer to reveal the intricate cross-linking of the glucan/protein matrix.

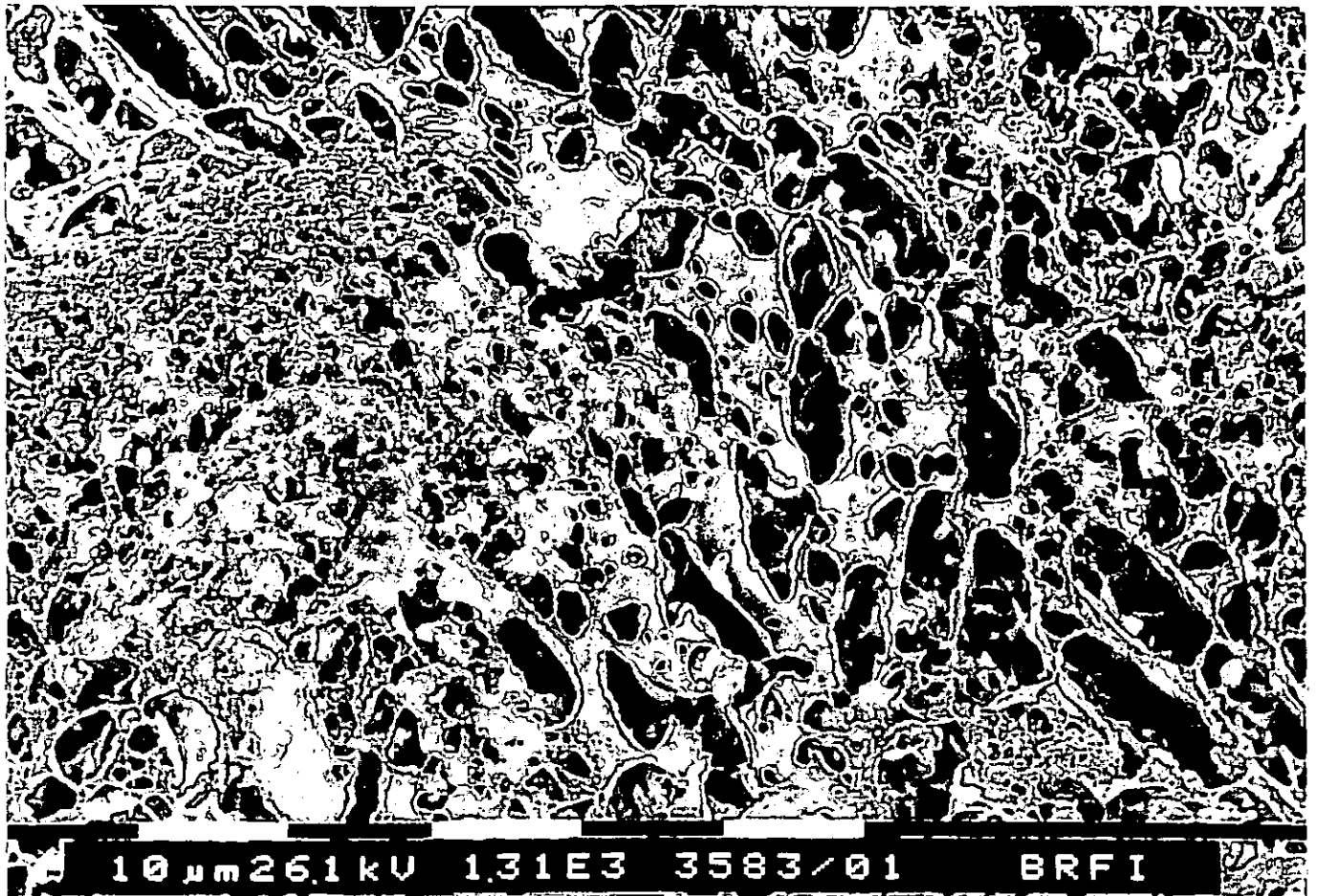


Fig 21: Freeze etched sample

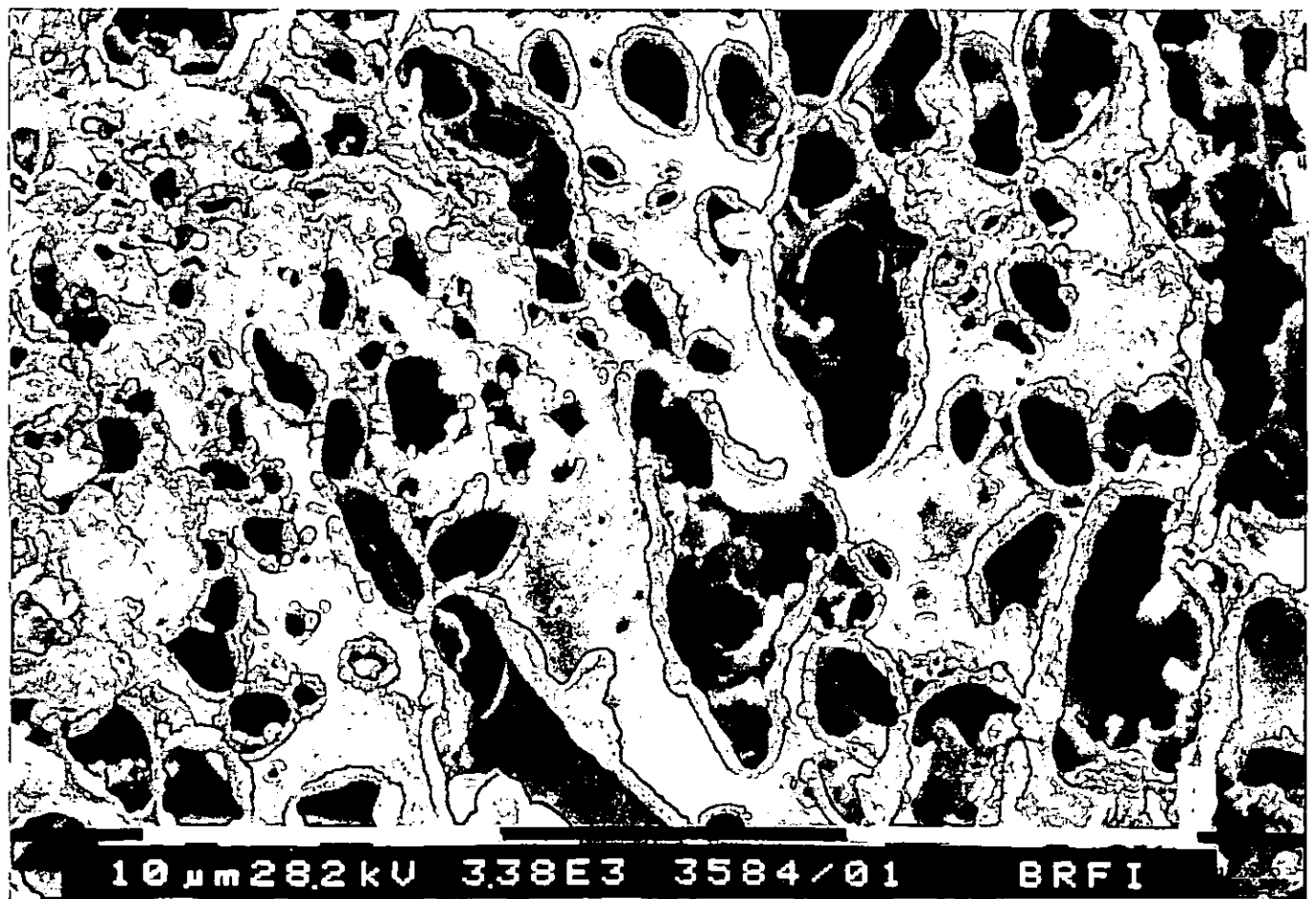


Fig 22: Freeze etched sample

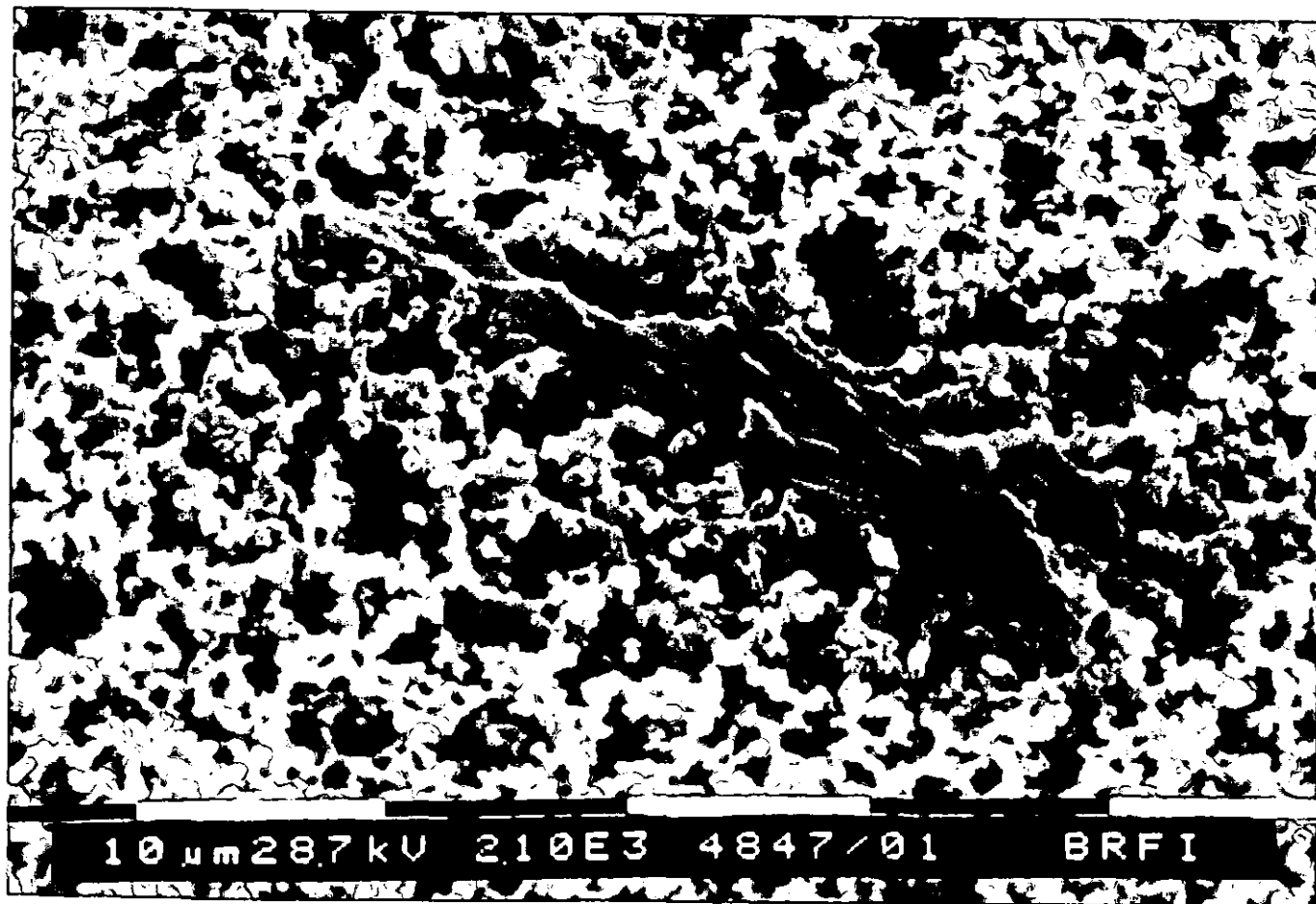


Fig. 23: Sample Trial 68 (Temperature Trials), 65°C - irregular shaped particle



Fig. 24: Sample Trial 68, 65°C - angular particle

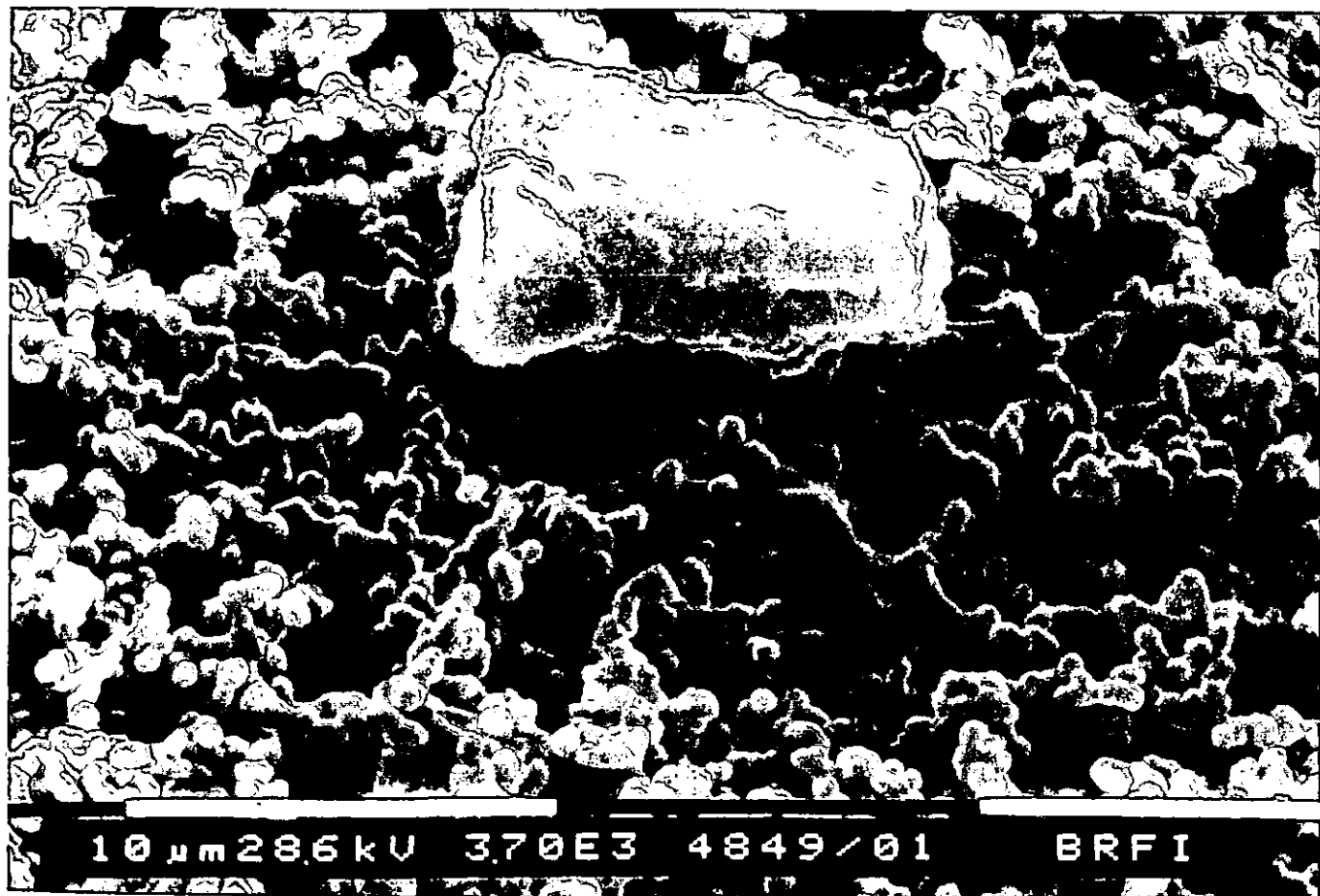


Fig. 25: Sample Trial 68, 65°C - angular particle

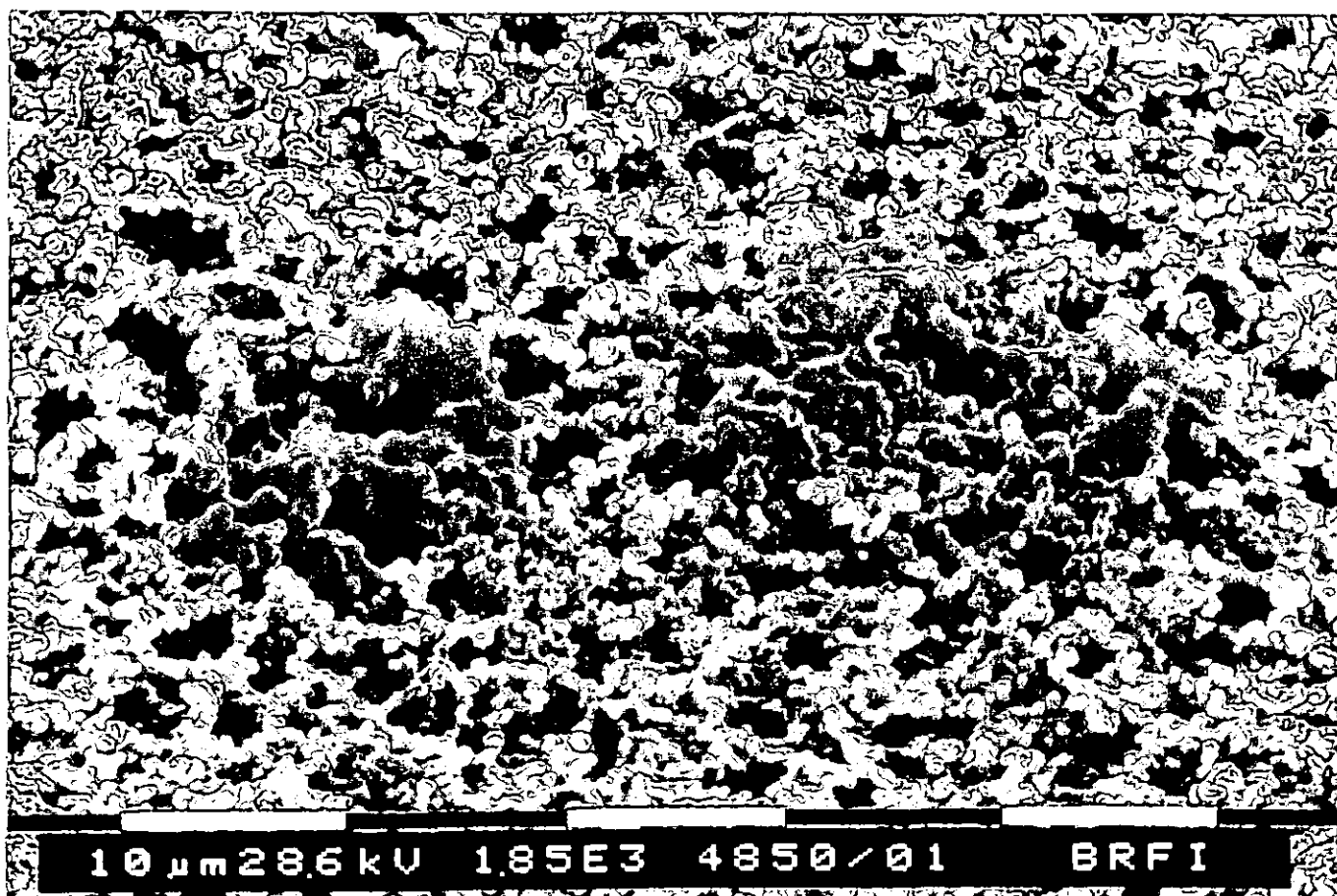


Fig. 26: Sample Trial 68, 65°C - smooth film

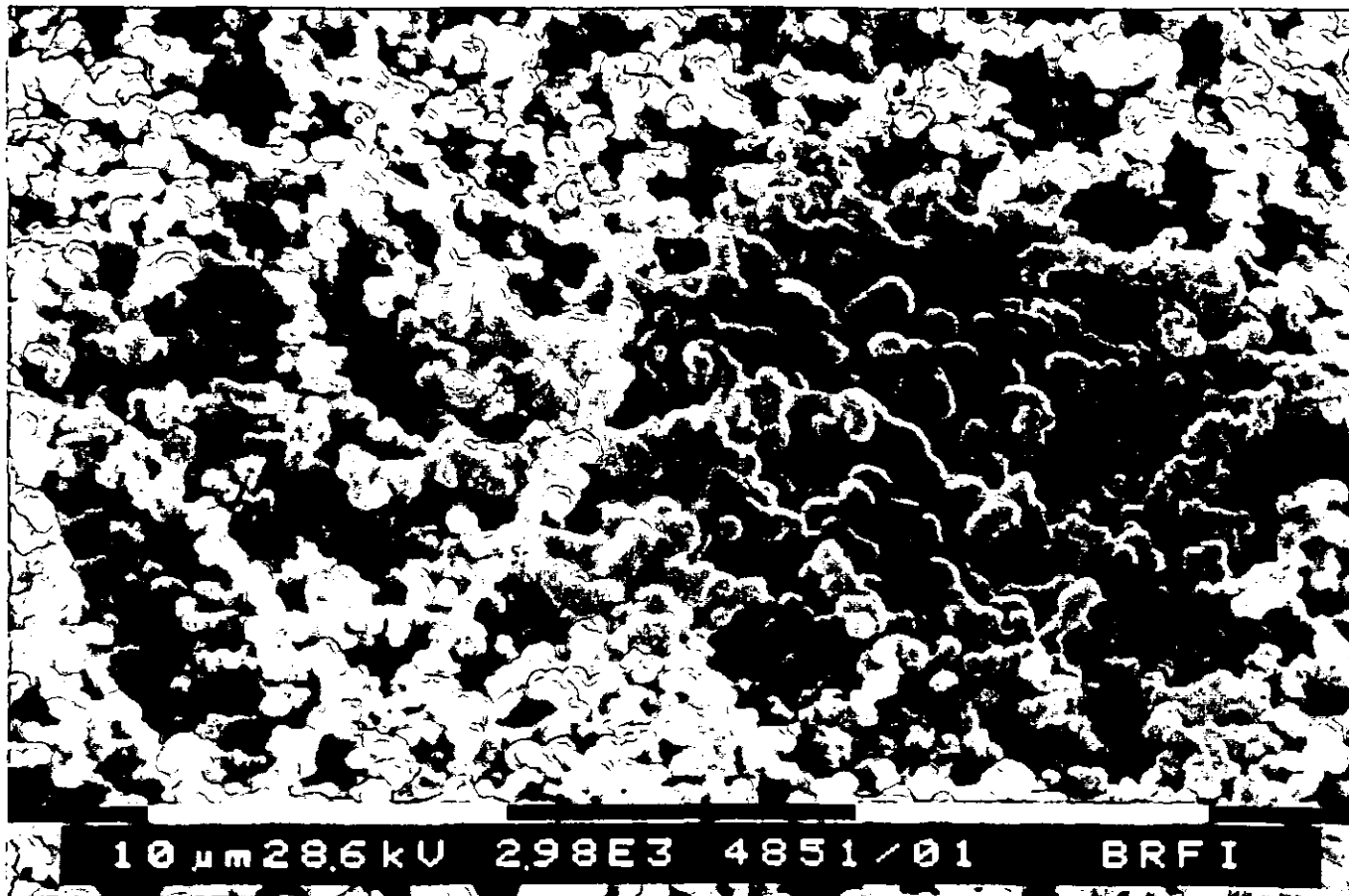


Fig. 27: Sample Trial 68, 75°C - smooth film

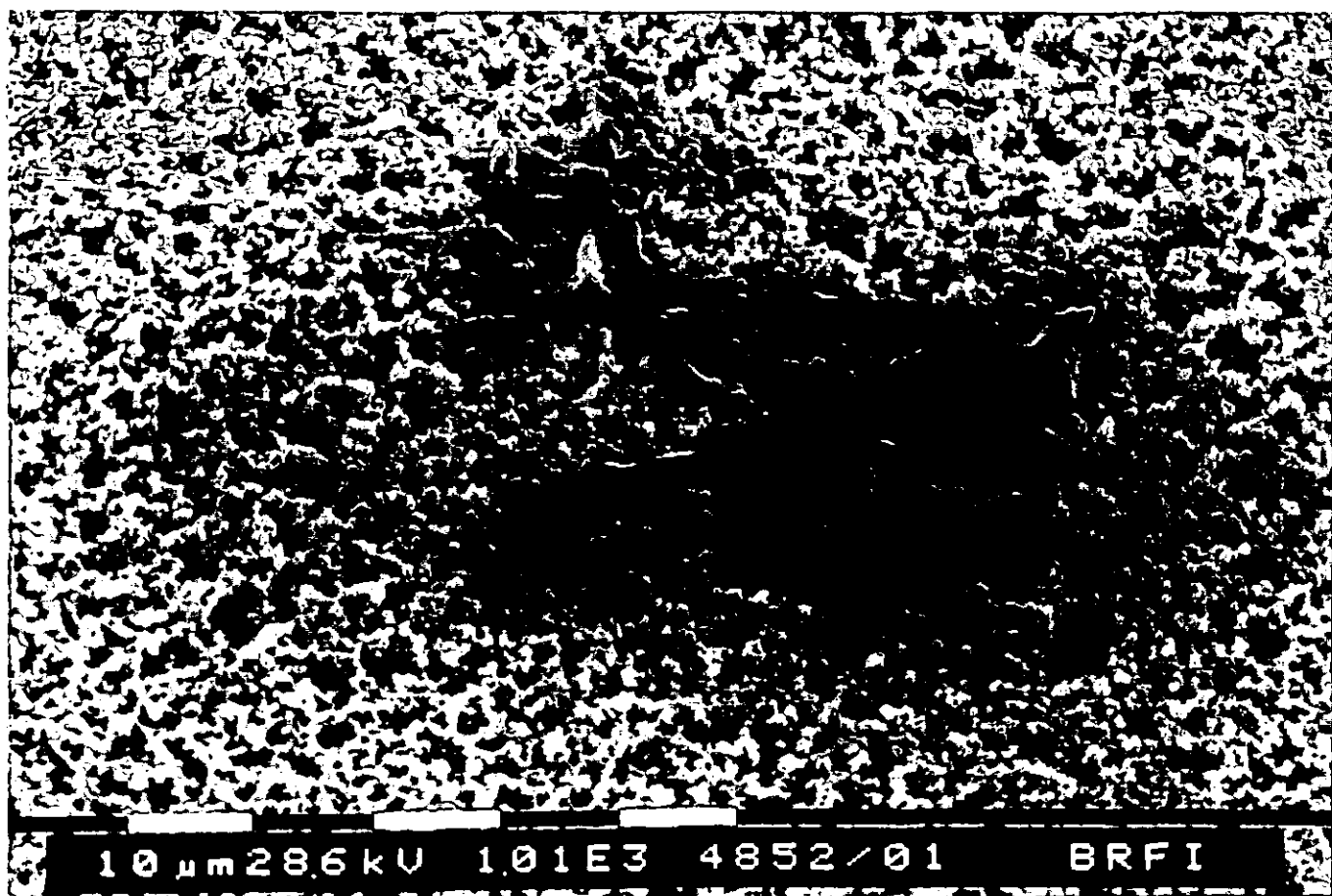


Fig. 28: Sample Trial 68, 75°C - larger smooth area

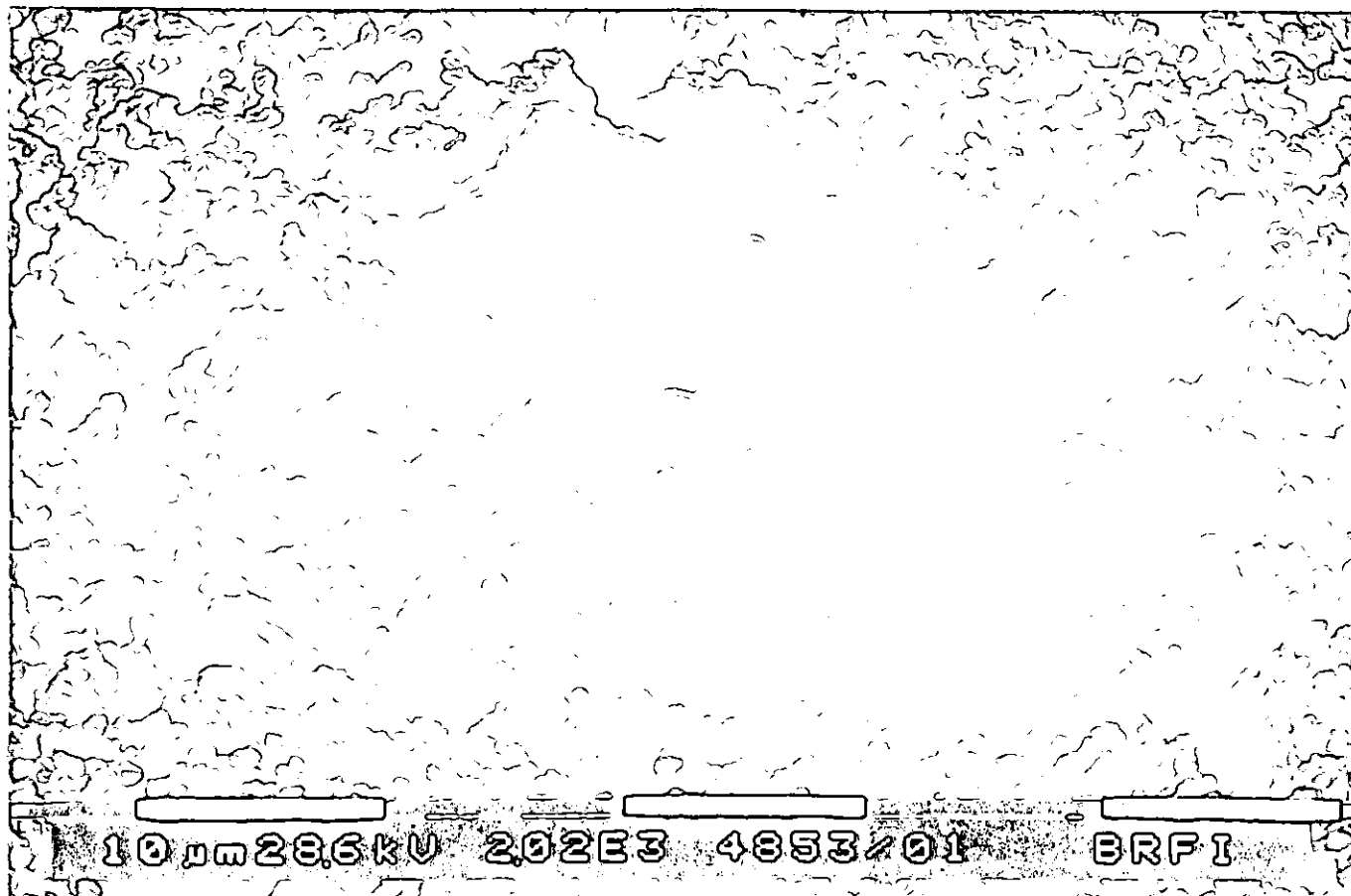


Fig. 29: Sample Trial 68, 80°C - smooth area

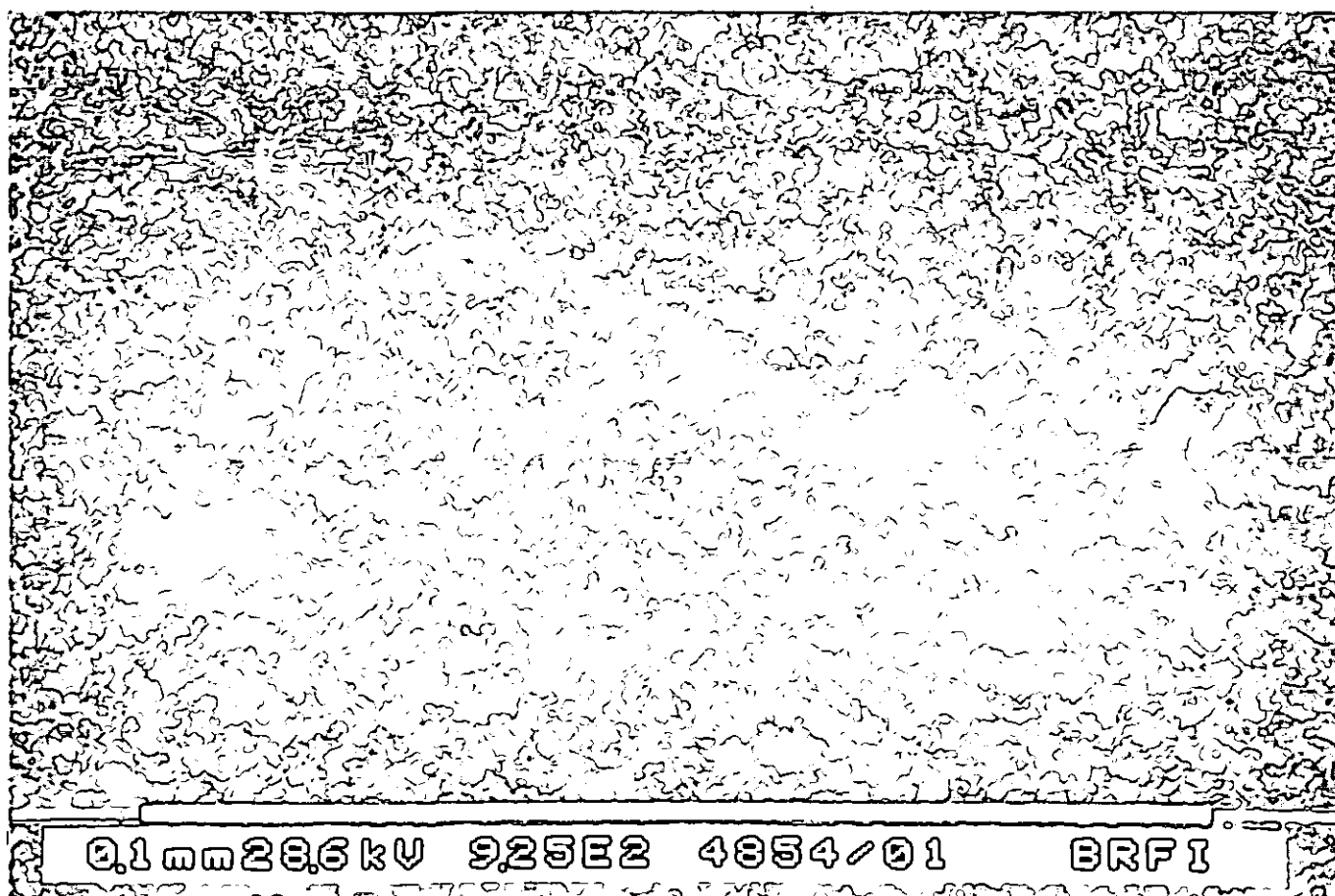


Fig. 30: Sample Trial 68, 80°C - a network of film-covered areas

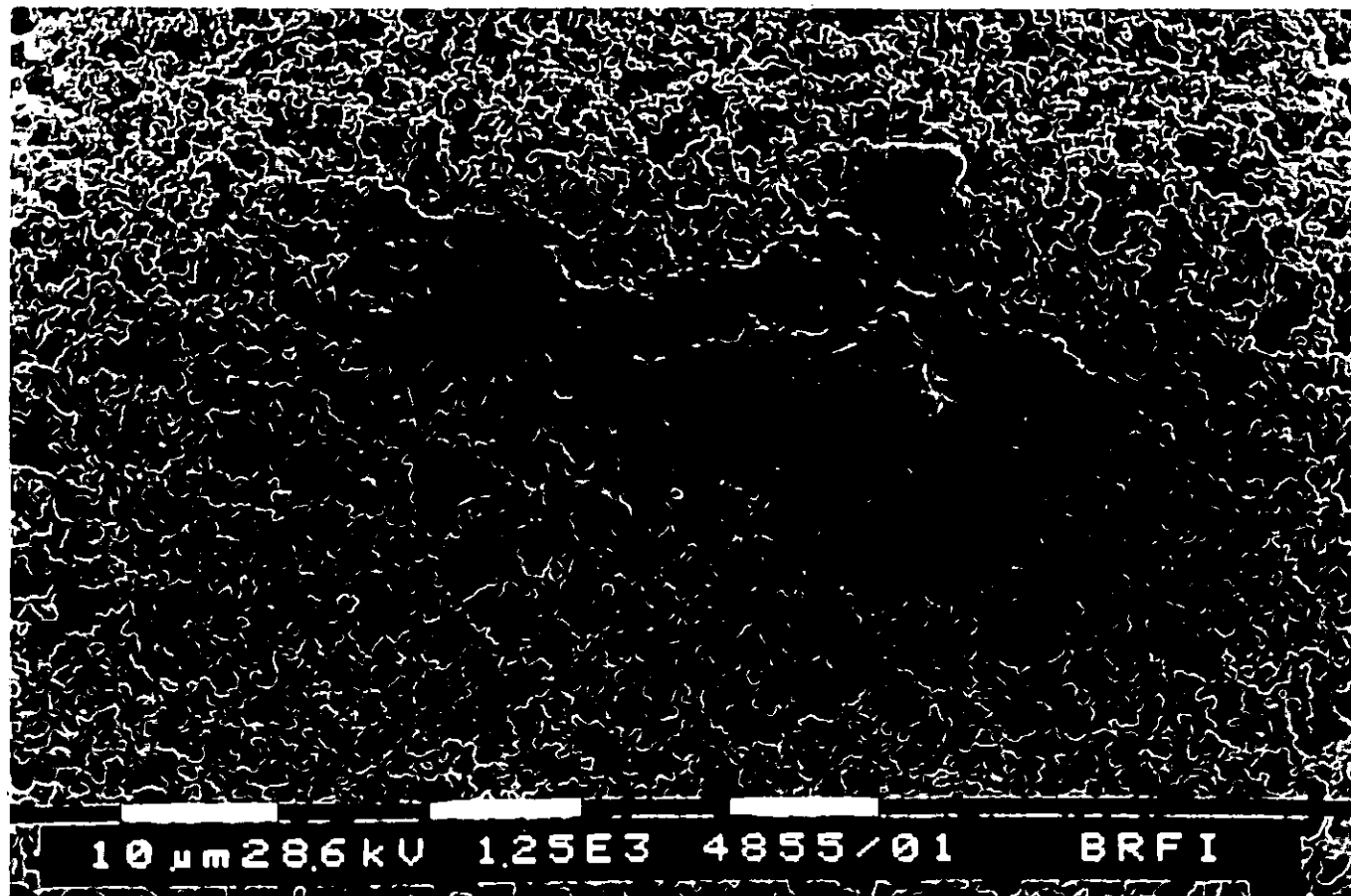


Fig. 31: Sample Trial 68, 95°C - film area with stronger three dimensional structure

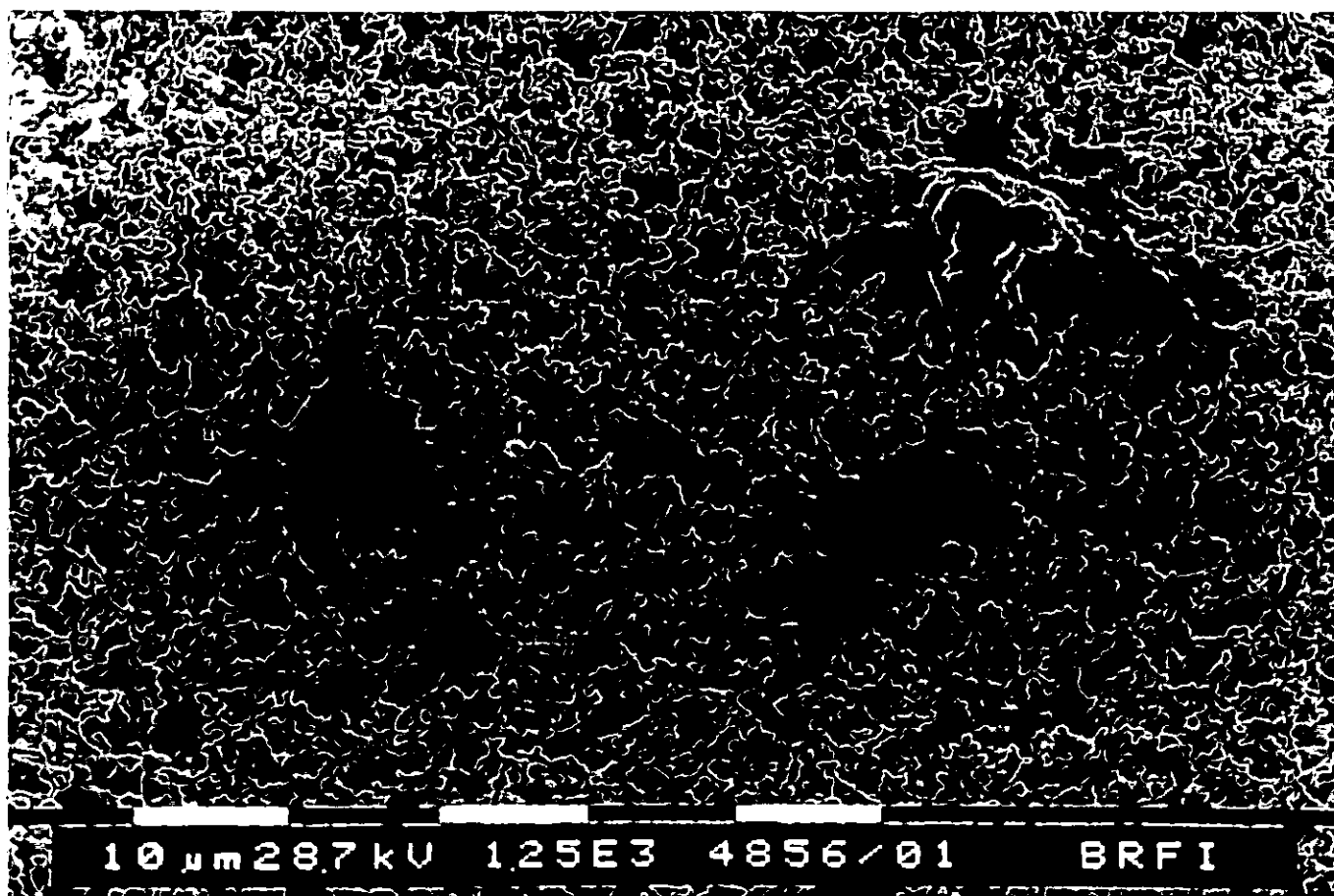


Fig. 32: Sample Trial 68, 95°C - 3-D structured film

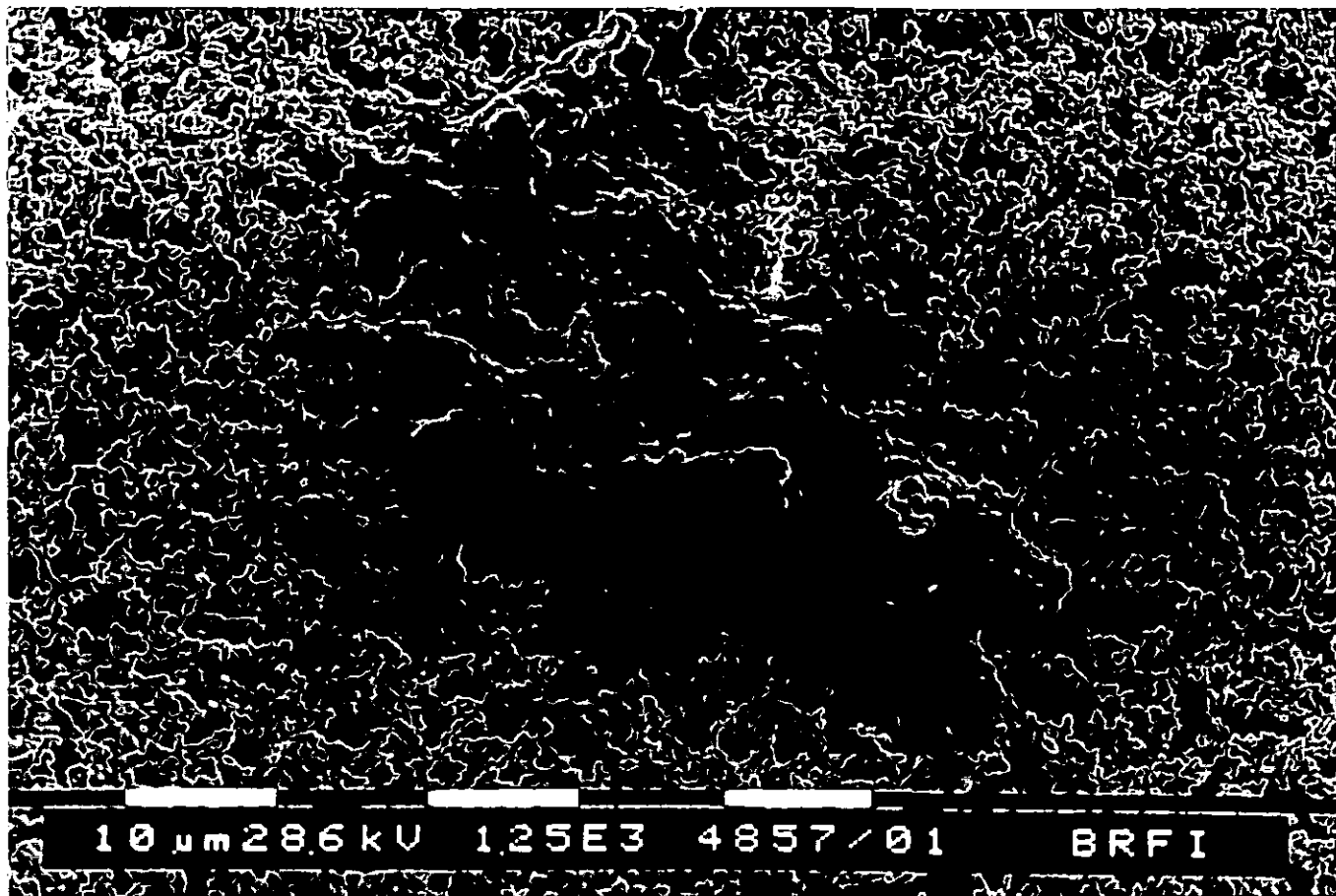


Fig. 33: Sample Trial 68, 95°C - a large three dimensional matrix

7.6. Publications

This section contains the following three publications:

1. Bühler, T.M., Matzner, G., Mckechnie, M.T., Agitation in mashing, EBC Proceedings of the 25th Congress, Brussels, Oxford University Press, 1995, 293 - 300.
2. Bühler, T.M., Mckechnie, M.T., Wakeman, R.J., A model describing the lautering process, Monatsschrift für Brauwissenschaft, 7/8, 1996, 226 - 233.
3. Bühler, T.M., Mckechnie, M.T., Wakeman, R.J., Temperature induced particle aggregation in mashing and its effects on filtration performance, Trans. Inst. Chem., Eng. 74, (1996) 12, 207 - 211.

Agitation in mashing

T.M. Bühler, G. Matzner & M.T. McKechnie

BRF International, Lyttel Hall, Coopers Hill Road, Nutfield, Redhill, Surrey RH1 4HY, United Kingdom

Descriptors

Lautering, mashing conditions, particle size distribution

SUMMARY

The effects of different mashing parameters (including mechanical energy input and "mashing-off" temperatures) on particle size distribution in mash and wort run-off have been investigated. The mean size of particles of mash, measured using novel laser particle sizing, is reduced with increasing shear levels. Raising of mashing off temperature markedly increases mean particle size. It was shown that this particle aggregation and not reduction in viscosity is the most important contributor to improved run off rates with higher mashing off temperatures. Highly significant correlations between the resistance of spent grains cakes and the mean particle size were found.

AGITATION AU BRASSAGE

Descripteurs

Conditions de brassage, distribution de dimension de particules, séparation de la maische en cuve filtre

RESUME

L'effet de différents paramètres de brassage (incluant l'énergie mécanique et la température d'empâtage) sur la distribution de la dimension des particules dans la maische et la vitesse de filtration a été étudié. La dimension moyenne des particules de la maische mesurée grâce à un nouvel appareil de mesure de la taille des particules par laser est réduite lorsque les forces de cisaillement augmentent. L'augmentation des températures d'empâtage augmente nettement la taille des particules. Il est démontré que ce sont ces agrégats et pas la réduction de viscosité qui contribuent le plus efficacement à l'amélioration de la vitesse de filtration lors d'empâtage à température élevée. On a démontré qu'il existait une corrélation hautement significative entre la résistance du gâteau de drêche et la dimension moyenne des particules.

Deskriptoren

Abläutern (Läuterbottich), Korngrösseverteilung, Maischeführung

ZUSAMMENFASSUNG

Die Auswirkungen unterschiedlicher Maischparameter (z.B. Eintrag mechanischer Energie, Abmaischtemperaturen) auf die Partikelgrößenverteilung in Maische und die Abläutergeschwindigkeit wurden untersucht. Die mittlere Partikelgröße von Maische, gemessen mit einem neuartigen Laserbeugungsspektrometer, verringert sich mit zunehmender Scherbelastung. Die Anhebung der Abmaischtemperatur hingegen erhöht die mittlere Partikelgröße. Es konnte gezeigt werden, daß diese Aggregation von Partikeln der wichtigste Einflußfaktor für eine verbesserte Abläutergeschwindigkeit mit höheren Abmaischtemperaturen ist und nicht eine etwaige Verringerung der Viskosität. Hochsignifikante Korrelationen zwischen dem spezifischen Widerstand der Treber und der mittleren Partikelgröße wurden aufgestellt.

Introduction

Fine particles in mashes can impair rates of wort separation and wort quality. Various mashing parameters influencing the concentration, shape and size of such fines have been investigated. The two key parameters are agitation and maximum temperature to which the mash is taken. Sufficient agitation of mash is crucial for heat and mass transfer, however stirring or pumping causes particle attrition: shear-sensitive material is broken up into smaller particles [1]. Temperatures above 65°C can aggregate fines. It will be demonstrated that the size distribution of particles within the fines correlates with mash filterability. This is the key parameter determining mash separation performance.

Materials and Methods

Mashing trials were carried out in a pilot scale brewhouse, using two different qualities of malt: a highly modified malt (Trial 1 and 3) and an undermodified malt (Trial 2). The mash was kept at 65°C for 45 minutes before the temperature was increased. The heating rate was 0.3°C/minute in Trials 1 and 2 and 1°C/minute in Trial 3. Samples of mash were taken at temperature intervals of 5°C.

In agitation trials the mash was heated to 75°C at 0.3°C/min and held at this temperature for 10 minutes before mashing off.

Filterability of mash was analysed in a Millipore filter cell (60 ml volume) using a constant pressure of 100 mbar at 65°C. Wort flow was recorded as volume of wort collected with respect to time. Lautering performance was assessed in an automated pilot scale lauter tun (see Figure 1). In addition, the following analyses were performed:

1. particle size distribution, using a Coulter Electronics Laser Sizer, LS 130, (the sample was wet sieved through a 106 µm pore sieve before analysis);
2. dry solids concentration of mash;
3. extract, determined as specific gravity measured with a Paar Densitometer;
4. viscosity, measured with an automatic capillary suction viscometer.

Filtration Theory

The run off rate of wort (filtration rate) can be described using Equation 1 [2]:

$$\frac{dV}{dt} = \frac{A^2 \Delta p}{\eta \alpha c V} = \frac{1}{K} \frac{1}{V} \quad (1)$$

where dV/dt is the run off rate per unit filter area, η is the viscosity, α the specific resistance of the spent grains cake, c is the concentration of solids in the mash, Δp is the differential pressure across the filter cake.

The specific resistance α accounts for the structure of the spent grains bed (i.e. size of channels in the cake, tortuosity of the flow path, voidage etc.). It is directly affected by the particle diameter and the distribution of particle sizes. $1/K$ is the filterability, which describes the run off performance combining all filtration parameters.

Alternatively the run off rate can be described by Darcy's Law [2]:

$$\frac{dV}{dt} = B \frac{A \Delta p}{\eta L} \quad (2)$$

where B is the permeability of the cake, L the height of the cake and A is the filter area.

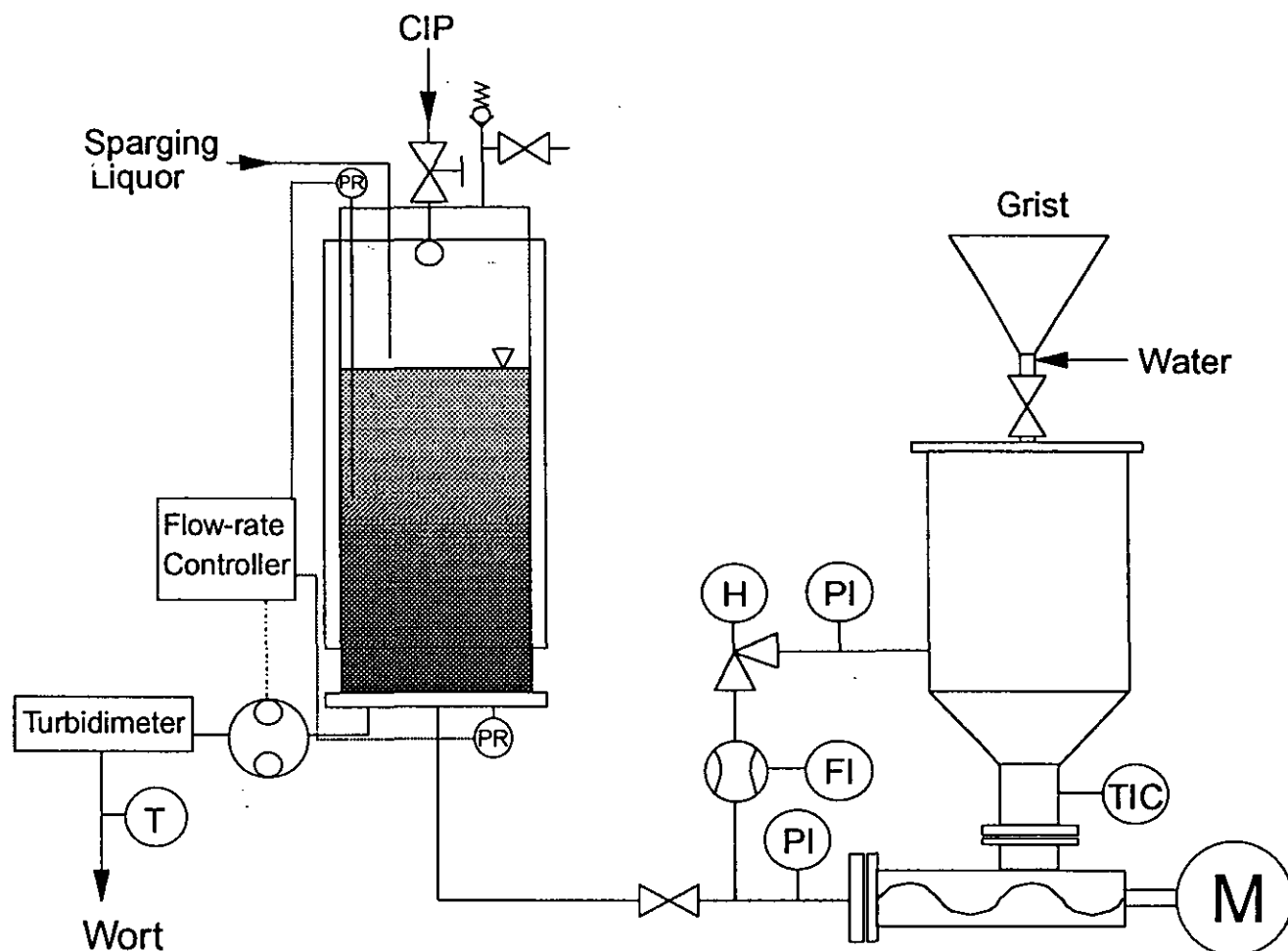


Figure 1: Pilot scale brewhouse comprising a mashing vessel designed for agitation trials and an automated lauter tun (scale: 15 litres of mash).

Results and Discussion

Temperature Effects

Aggregation of particles occurs with increasing final mash temperatures. Figure 2 shows the change in the particle size distributions of the fines, represented by the mean particle size (MPS) of the number distribution. The increase in MPS is caused by aggregation of fine particles, which is most likely due to precipitation of proteinaceous material in conjunction with polyphenols and other components [3], [4].

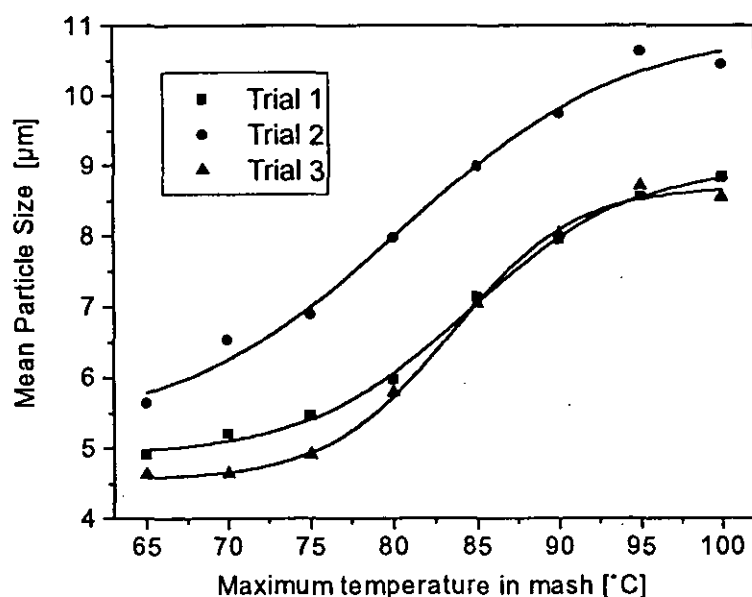


Figure 2: Particle size changes with increasing maximum temperature in mash.

Filterability of mash improves with increasing final mash temperatures (see Figure 3). Since filtration trials were carried out at constant temperature, the effect from viscosity could therefore be excluded. This demonstrates that particle aggregation is the predominant effect in improving run off rates with higher mashing-off temperatures. The optimum filterability is dependent on the extent of malt modification.

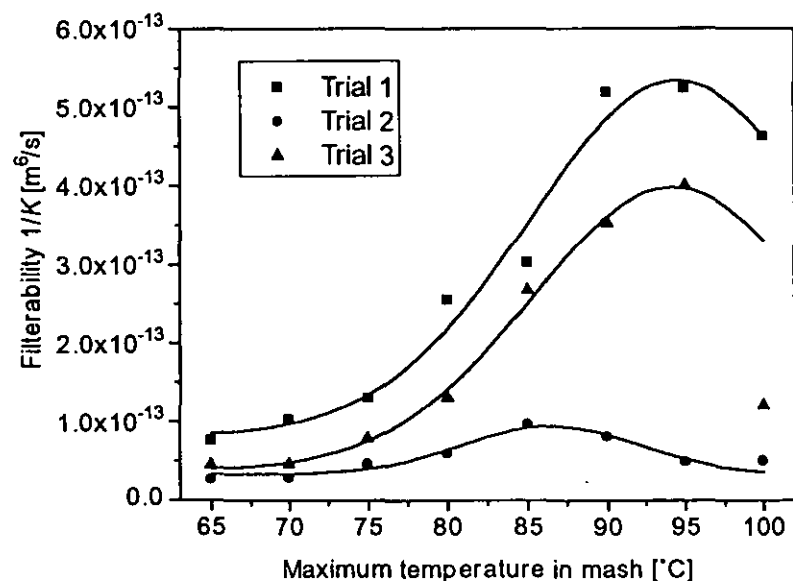


Figure 3: Filterability of mash, raised to different temperatures.

Figure 4 shows a very significant correlation between MPS and specific resistance. The change of specific cake resistance with respect to temperature over

the practical range of mashing-off temperatures, can be explained solely by MPS changes. Clearly, particle aggregation controls lautering performance.

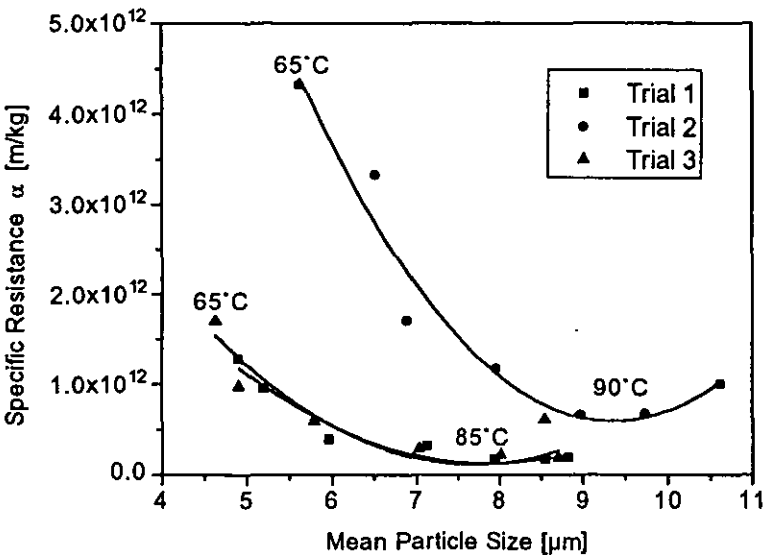


Figure 4: Specific resistance of mash filter cakes as a function of mean particle size.

Agitation Trials

Figure 5 shows that mechanical power dissipated in a mash causes particle attrition. This is demonstrated by the reduction of the mean particle size of the fines fraction: shear-sensitive material is broken up. Both pilot plant and laboratory scale trials showed this effect. Bench scale trials over the power input range used commercially revealed that damage occurs even with gentle stirring. Attrition cannot be avoided in any practical mashing procedure.

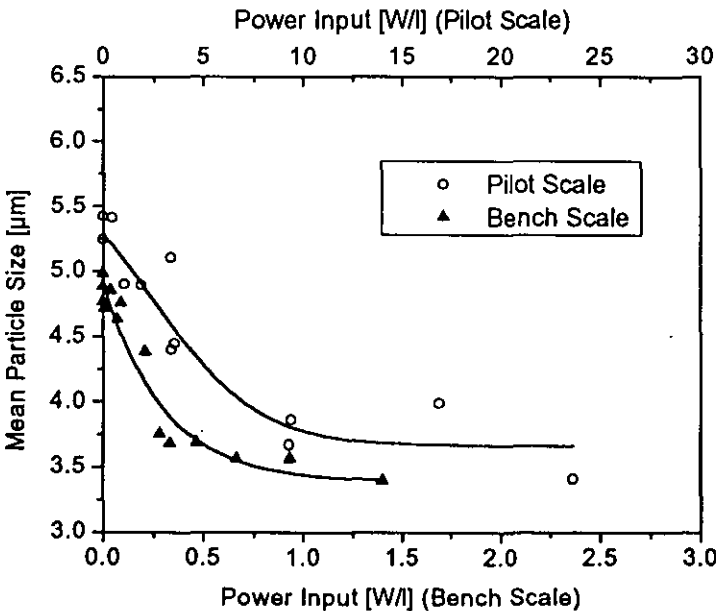


Figure 5: Particle attrition due to agitation (measured as specific mechanical power input in W/L).

Power input was determined in the pilot scale by measuring flow rate Q , and differential pressure loss Δp , in the flow loop (Equation 3). In order to give a range of power dissipation, the differential pressure alone was varied. The flow rate was kept constant to enable a constant mixing in the vessel with a quiescent liquid gas interface, thus avoiding variations in the extent of oxygen pick-up between experiments.

$$P = Q \Delta p \tag{3}$$

In laboratory scale trials a stirrer with torque meter was used to control the mechanical power input. Power input can be calculated using Equation 4.

$$P = \omega \tau \tag{4}$$

Where ω is the angular velocity and τ is the torque at the stirrer.

It can be shown that MPS affects mash filtration performance both in the lauter tun and in bench scale trials (see Figure 6). A reduction of the MPS (due to agitation) causes filterability to decrease. A reduction of the MPS by 2.93 μm resulted in an increase of the lautering time in the pilot lauter tun of 40 minutes.

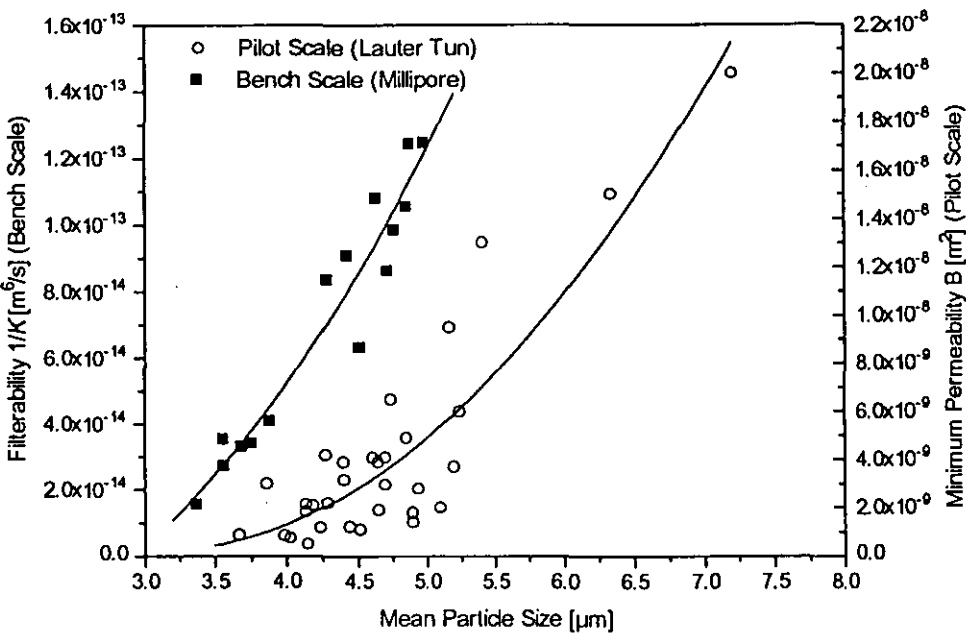


Figure 6: Filtration performance in the lauter tun and in bench scale in relation to mean particle size.

Conclusions and Practical Implications

Fine particles in a mash are aggregated by heat, which is beneficial for lautering. Particle size increase with higher mashing temperatures is the most important factor in the improvement of run off rates. This effect is permanent unlike changes of viscosity with temperature: this means that the peak temperature in the mash has a direct influence on lautering performance. Particle attrition caused by agitation can be minimised, but some particle attrition cannot be avoided in industrial scale application.

Particle attrition in the brewhouse can now be quantified, enabling measures to reduce it to be developed.

Reduction in filterability caused by particle attrition can be partially rectified by applying higher mash temperatures.

Nomenclature

A :	filter area	$[m^2]$
B :	permeability of the spent grains cake	$[m^2]$
c :	concentration of solids in the mash	$[kg/m^3]$
dV :	differential volume of filtered wort	$[m^3]$
dt :	differential time	$[s]$
L :	height of the cake	$[m]$
P :	mechanical power dissipated in mash	$[W]$
Q :	flow rate	$[m^3/s]$
V :	volume of filtrate (wort)	$[m^3]$
α :	specific resistance of the spent grains cake	$[m/kg]$
Δp :	differential pressure	$[Pa]$
η :	dynamic viscosity	$[Pa\ s]$
τ :	torque	$[Nm]$
ω :	angular velocity	$[s^{-1}]$

Acknowledgement

The Authors wish to thank the Director General of BRFI for the permission to publish this paper.

References

- [1] Leedham, P.A., Savage, D.J., Crabb, D., Morgan, G.T., Materials and methods of wort production that influence beer filtration, Proc. Eur. Brew. Conv., Cong. Nice, 1975, 201 - 216.
- [2] Hermia, J., Eyben, D., Considerations sur les procede de filtration en brasserie, Proc. Eur. Brew. Conv., Cong. London, 1983, 209 - 224.
- [3] Lewis, M.J., Oh, S.S., Influence of precipitation of malt proteins in lautering, MBAA Technical Quarterly, 1985, 108 - 111.
- [4] Lewis, M.J., Serbia, J.W., Aggregation of protein and precipitation by polyphenol in mashing, J. Am. Soc. Brew. Chem., 1984, 40 - 43.

Monatsschrift für **Brauwissenschaft**

Das wissenschaftliche Organ der
Fakultät für Brauwesen, Lebensmitteltechnologie und Milchwissenschaft, Weihenstephan,
Versuchs- und Lehranstalt für Brauerei in Berlin (VLB)
Wissenschaftlichen Station für Brauerei in München

**SONDERDRUCK
REPRINT
TIRÈ A PART**

BC 033 Flow injection analysis/ 201 rubbers, glucanes/ 214 dissolving features

This article describes the most common methods for the determination of the cytolytic dissolving of brewing malts in current usage. On the basis of malting tests and the study of trade malts, the authors assess the information provided from the friabilimeter and calcofluoride method and the determination of beta glucanes in the congress wort using flow injection. The benefits and drawbacks of the various methods are compared.

Wackerbauer, K., Hardt, R., et Hirse, U.: Evaluation des propriétés de désagréation des malts au moyen du Friabilimètre, méthode FIA indirecte au Calcofluor — Monatsschrift für Brauwissenschaft 49, No 7/8, 220 – 225, 1996

BC 033 Analyse par injection de flux/ 201 gommages, glucanes/ 214 propriétés de désagréation

Dans le présent travail on décrit les méthodes actuelles les plus utilisées pour la détermination de la désagréation cytolitiques du malt. A partir d'essais de maltage ainsi que de l'évaluation de malts industriels, on a déterminé la valeur d'expression de la méthode au Friabilimètre et du Calcofluor ainsi que du dosage des b β -glucanes solubles du moût du brassin conventionnel par analyse par injection de flux. Les avantages et les inconvénients des différentes méthodes sont confrontés.

6 Literatur

1. McCleary, B. V., und Glennie-Holmes, M.: „Enzymic Quantification of 1,3-1,4- β -D-Glucan in Barley and Malt“, J. Inst. Brew., 91, 285 – 295, 1985.
2. McCleary, B. V., und Nurthen, E.: „Measurement of 1,3-1,4-(-D-Glucan in Malt, Wort and Beer“, J. Inst. Brew., 92, 168 – 173, 1986.
3. Wood, P. J., und Fulcher, R. G.: „Interaction of some Dyes with Cereal β -Glucans“, Cereal Chem., 55, 952 – 966, 1978.
4. Aastrup, S., Gibbson, G. C., und Munck, L.: „A Rapid Method for Estimating the Degree of Modification in Barley Malt by Measurement of Cell Wall Breakdown“, Carlsberg Res. Commun., 46, 77 – 86, 1981.
5. Wackerbauer, K., Carnielo, M., und Hardt, R.: „Video/Image Analysis System for the Calcofluor Malt Modification Method“, Proceedings of the 24th Congress of the European Brewery Convention, 479 – 486, Oslo 1993.
6. Carnielo, M., Foucaut, M.-A., und Moll, M.: „Application of a Test for Modification in Green and Kilned Malts“, Brauwiss., 35, 168 – 170, 1982.
7. Aastrup, S.: „A Review of Quick, Reliable and Simple Check Methods for Barley and Malt Based on the Carlsberg Seed Fixation System“, ASBC Journal, 46, 37 – 43, 1988.
8. Aastrup, S., und Jorgensen, K. G.: „Application of the Calcofluor Flow Injection Analysis Method for Determination of β -Glucan in Barley, Malt, Wort and Beer“, ASBC Journal, 46, 76 – 81, 1988.
9. Baxter, E. D., und O'Farrell, D. D.: „Use of the Friabilimeter to Assess Homogeneity of Malt“, J. Inst. Brew., 89, 210 – 214, 1983.
10. Giarratano, C. E., und Thomas, D. A.: „Rapid Malt Modification Analyses in a Production Malt House: Friabilimeter and Calcofluor Methodologies“, ASBC Journal, 44, 95 – 97, 1986.
11. Jorgensen, K. G., und Aastrup, S.: „Analysis of β -Glucan in Wort“, EBC Monograph XI, Symposium on Wort Production, 262 – 271, Maffliers, France 1986.
12. Jorgensen, K. G., Jensen, S. A., Hartlev, P., und Munck, L.: „The Analysis of β -Glucan in Wort and Beer Using Calcofluor“, Proceedings of the 20th Congress of the European Brewery Convention, 403 – 410, Helsinki 1985.
13. Wackerbauer, K., Anger, H.-M., und Kölsch, J.: „Zur Aussagekraft des Friabilimeter“, Brauwelt, 125, 1758 – 1763, 1985.
14. Burbidge, M.: „Homogenität und Malzanalyse“, Monatsschr. f. Brauwiss., 37, 4 – 9, 1984.
15. Greif, P.: „Friabilimeterwerte nur abhängig von der Spelzenstärke?“, Tagesz. f. Brauerei, 77, 66, 1980.
16. Sarx, H. G., und Rath, F.: „Filtration Risk Analysis. New Method for Predicting Problems in Wort and Beer Filtration“, Proceedings of the 25th Congress of the European Brewery Convention, 615 – 620, Brussels 1995.

EUROPEAN BREWERY CONVENTION

MONOGRAPH XXIV

E.B.C. - SYMPOSIUM
IMMOBILIZED YEAST APPLICATIONS
IN THE BREWING INDUSTRY
ESPOO · FINLAND
OCTOBER 1995



**Fachbuch-
handlung
Hans Carl**

Postfach 99 01 53
90268 Nürnberg
Fax (0911) 9 52 85-47

**EUROPEAN BREWERY CONVENTION
MONOGRAPH XXIV**

**E.B.C. - Symposium - Immobilized Yeast Applications
in the Brewing Industry** Espoo · Finland / October 1995
XIV/260 Seiten, zahlreiche Abb. u. Tabellen DM 88,-
Best.-Nr. 749 (In englischer Sprache) zuzüglich
Versandkosten

FAX-BESTELLUNG: 0911 / 9 52 85-47

Name

Kunden-Nr.

Firma

USt.-Id.-Nr.

Straße

PLZ/Ort

Datum

Stempel/Unterschrift

T. M. Bühler, M. T. McKechnie and R. J. Wakeman

A model describing the lautering process

This article describes modelling of the wort separation procedure in a lauter tun. It has been shown that viscosity and particle size distribution in the fines are the main parameters determining lautering performance when other raw material conditions are constant. MPS and viscosity can be varied with conditions such as temperature of the mash or agitation. The background of how these two parameters influence the sedimentation, filtration performance and washing efficiency of the cake has been described. A computer model has been established which enables prediction of the main process parameters: wort run off rate, wort extract and height of the spent grains cake. It has been shown that the model predicts existing data with good accuracy.

BC202 Viscosity/222 Mashing intensity/223 Lautering procedure/ 223 Wort run-off/ 30 Modelling, models

(Descriptors EBC: Wort, wort production, lautering, mash filtration, mash separation conditions.

Deskriptoren EBC: Würze, Würzeherstellung, Abläutern, Maischefiltration, Würzetreibertrennungsparameter.)

1 Introduction

The lautering process is substantially influenced by raw materials and processing conditions. In this paper physical influences on lautering performance are described. A computer model of lautering has been established which is based on the results of pilot scale trials. The parameters influencing lautering performance were characterised and used as input variables.

In the literature mainly viscosity is reported as a key determinant of lautering rates (1, 2). Our previous report, however, (3) illustrates that particle size distribution within the fine fraction is a very important parameter determining lautering performance. Changes in mashing conditions, such as agitation rate and temperature can greatly affect this parameter.

The model described in this paper is based on both viscosity and particle size distribution in the fines. Other parameters such as malt quality or milling regimes have not yet been incorporated into the model, but their influence on lautering is likely to be via effects of viscosity and particle size.

2 Experimental

Trials were performed over a 10 – 50 litre range of pilot scale mashing and lautering. Different mean particle size (MPS) levels in the fines were created by means of agitation with a Mono pump and by heating of the mash. The lautering performance was analysed in a pilot scale jacketed glass column (see Fig. 1). The differential pressure measured across the cake controlled the speed of a peristaltic pump. The setting of the pump flow controller followed equation:

$$dV \cdot dt^{-1} = 1.65 \times 10^{-6} - 5.32 \times 10^{-10} \Delta p - 4.66 \times 10^{-14} \Delta p^2 \quad (1)$$

The lauter tun is filled from the bottom. After this the mash is allowed to settle for 10 minutes. Then wort was run off by the peristaltic pump until a total constant volume of 11 litres was collected. The removed wort was replaced by hot water, added on top of the liquid level. The design of the plant guaranteed the level to be constant.

Lautering performance was determined measuring filtrate volume over time, height of the cake, extract in the wort and the pressure across the cake. In addition, the turbidity of the mash was analysed in-line.

The particle size distribution in the fine fraction of the mash was measured using a Coulter Counter LS 130 Laser sizer with a sieve step at 106 µm. The viscosity in the liquid fraction of the mash was measured using a falling ball viscometer after filtration through a pleated filter paper. Extract in the wort was measured externally by refraction or hydrometer.

3 Basic relationships between input variables and parameters of the filter cake

3.1 Particle size changes

The mean particle size (MPS) of the fine fraction of mash grows with increasing temperature. Different malts may vary in their MPS level, however, the proportional change in MPS with temperature is similar for different malts. This basic correlation is shown in Figure 2. Different heating rates do not appear to influence this relationship. Trials 1 and 3 were carried out with the same malt, but

different mashing systems. Trials 2 and 4 used malt different from trials 1 and 3. The range from 72 to 95°C can be described with a linear fitting function.

As not only temperature influences MPS but also shear stress, it is necessary to measure the MPS for different malts and different brewhouse conditions before lautering.

3.2 Viscosity effects

Effects of temperature and extract concentration on viscosity have been reported in the literature by, amongst others, *Asselmeyer et al.* (4) and *Eyben and Huipe* (5). The viscosity change for water

and sugar solutions is documented by *Perry and Green* (6). Figure 3 shows this relationship.

Viscosity at 70°C can be calculated from a given laboratory analysis at 20°C using the equation:

$$\eta_{70^{\circ}\text{C}} = 0.180 + 0.254 \times \eta_{20^{\circ}\text{C}} \tag{2}$$

The following function was used to calculate the viscosity at lautering temperature (in the range 65 to 85°C) from the value at 70°C.

$$\eta_{\text{laut}} = \eta_0 + 0.0298 \times T_{\text{laut}} + 1.30 \times 10^{-4} \times T_{\text{laut}}^2 \tag{3}$$

η_0 can be calculated from the 70°C viscosity value.

The viscosity of the mash at 20°C needs to be measured for different malts and different brewhouse conditions as both factors can influence this parameter.

Viscosity also changes with sparging of the cake. Variation of viscosity with different extract levels was described by *Kolbach* (7). The following equation fits his data with an accuracy of $R = 0.99998$.

$$\eta = \eta_0 + 5.856 \times 10^{-2}E - 1.4188 \times 10^{-4}E^2 + 1.4646 \times 10^{-4}E^3 \tag{4}$$

This equation was used to describe the viscosity change during lautering as a function of extract concentration. The dilution of the extract concentration during washing causes the viscosity of the filtrate to decrease with filtrate volume. Hence the differential pressure across the cake decreases and, as filtrate flow-rate and pressure drop were linked by the experimental setup, the flow rate increases.

3.3 Cake sedimentation

Both cake formation and compaction of the cake are influenced by the MPS in the fines and by viscosity. Sedimentation of the cake in closed systems with a wide range of particle sizes and with high solids concentrations in the mash occurs in bands. Most of the particles settle to the slotted bottom leaving the fine particles behind. These fine particles settle on top of the main cake and form a separate band.

The sedimentation rate of these particles can be correlated to the square of the particle size. Figure 4 illustrates this correlation. The equation of the fitting function is:

$$dh \cdot dt^{-1} = 1.474 \times 10^{-4} - 1.4802 \times 10^{-5} \text{MPS}^2 \tag{5}$$

In the pilot scale lautering procedure, settling was limited to 10 minutes after which filtration was started. In addition to particle size, the height of the bed after the sedimentation stand depends on the filling level of mash, mash concentration and the packing density of the spent grains. All these additional parameters were kept constant in the trials and, hence, a constant minimal height of the bed after sedimentation of 42 cm was recorded. For slower settling (which occurred at MPS values below 5 μm), the bed height after the sedimentation stand did not reach this level, hence cake height was increased at the start of filtration.

3.4 Permeability of the cake and cake height

The final permeability of the cake, after collection of 8 litres of wort (during cake washing), reached a constant value. At this time the cake is sparged with hot water, with no additional compaction occurring. The final permeability value of the consolidated cake

Nomenclature		
$dV \cdot dt^{-1}$	differential flow rate	$\text{m}^3 \cdot \text{s}^{-1}$
Δp	differential pressure across the cake	Pa
$\eta_{20^{\circ}\text{C}}$	viscosity at 20°C	mPas
$\eta_{70^{\circ}\text{C}}$	viscosity at 70°C	mPas
$\eta_{0^{\circ}\text{C}}$	viscosity at 0°C	mPas
T_{laut}	lautering temperature	°C
E	extract content in the wort	°Plato
$dh \cdot dt^{-1}$	sedimentation rate	$\text{m} \cdot \text{s}^{-1}$
MPS	mean particle size of the number distribution	μm
B	permeability of the cake	m^2
ϵ	porosity of the cake	—
S_0	specific surface of particles in the cake	$\text{m}^2 \cdot \text{m}^{-3}$
K_0	Kozeny constant	—
L	total height of the bed	m
A	floor area of the lauter tun	m^2
L_{min}	minimum height of the cake	m
L_0	initial height of the cake before start of filtration	m
W	wash ratio	—
u	average velocity	$\text{m} \cdot \text{s}^{-1}$
D_L	axial diffusion coefficient	—
t_{decay}	decay constant	—
V_{void}	void volume	m^3
V_{cake}	cake volume	m^3
$V_{\text{particles}}$	particle volume	m^3
V_{wort}	wort volume	m^3
V_{total}	total wort collected	m^3
dX	width of the extract fitting function	m^3
X_c	centre of the extract fitting function (Boltzman function)	m^3

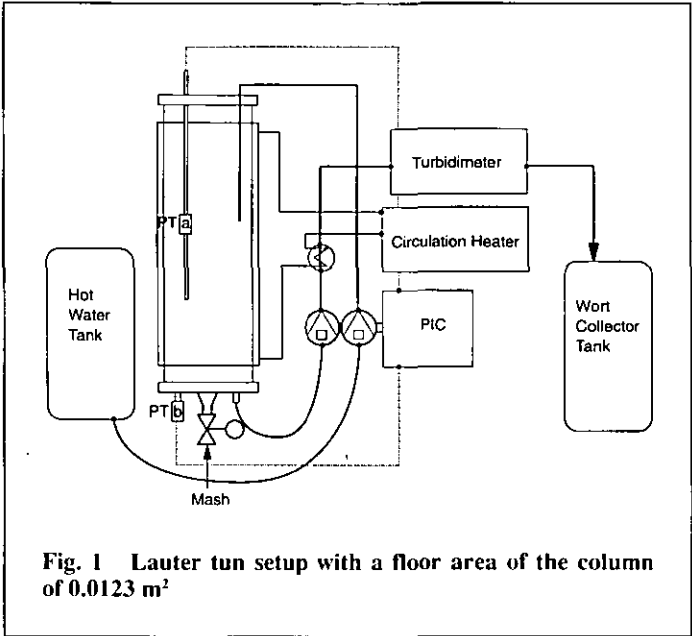


Fig. 1 Lauter tun setup with a floor area of the column of 0.0123 m²

also depends on the square of the MPS. The correlation is shown in Figure 5: the fitted line shows a distinct off-set on the x-axis from the origin. This is due to the characteristics of the laser sizer and the model used to calculate the size distribution. In the number distributions presented here, the limit of the MPS value was reached at approximately 3.6 μm.

The cake height in the lautertun is influenced by the differential pressure across the cake and the change of permeability with different particle size distributions in the fines. Small particles exert a higher resistance to flow, thus creating higher pressure drops leading, due to the compressibility of the cake, to greater compaction of the bed. Consequently, the lower part of the bed also compacts and overall permeability decreases again.

The effects of compaction and reduced porosity on permeability, B, of the cake can be described using the Kozeny equation (8):

$$B = \frac{\epsilon^2}{S_0^2 (1 - \epsilon)^2} K_0 \tag{6}$$

Since the total volume of solids is constant over filtration time, the porosity ε should solely be a function of cake height L.

$$B = f\left(\frac{\epsilon^3}{(1 - \epsilon)^2}\right) = f(L^3 \times L^2) = f(L^5) \tag{7}$$

This relationship was used to describe the change of porosity with height of the bed (Fig. 6). For the compacted cakes where porosity is lower (0.20 < ε < 0.55) than the initial porosities (ε_{init} ≈ 0.68), a good correlation with experimental data was found. Initial permeabilities cannot be described by the model, mainly because liquid drains from the lower layers of the cake during compaction. This liquid does not flow through the entire length of flow channels in the cake and therefore causes a lower pressure drop.

The final permeability of the consolidated cake at sparging is also linked to the minimal cake height. The correlation, shown in Figure 7 was fitted with the following equation:

$$B = 1.31 \times 10^{-8} \times L^{4.68} \tag{8}$$

In Darcy's law, flow of liquid through a bed of particles is described as a function of permeability, the height of the bed and pressure drop across the cake. If viscosity is included, Darcy's law can be written as follows:

$$\frac{1}{A} \frac{dV}{dt} = \frac{B \Delta p}{\eta L} \tag{9}$$

With this equation, the above correlations and the fixed relationship between pressure across the cake and flow rate, it is possible to calculate the cake height, L_{min}, which will develop at the end of filtration during cake washing. L_{min} will be affected by MPS, viscosity and the flow-rate pressure drop relationship. The height of the bed at sparging will represent an equilibrium between these parameters.

3.5 Cake compaction

The lautertun cake compacts as wort is run off from the lautertun. This compaction is influenced by two main factors. Firstly, wort drains from the different sections of the cake, secondly, the cake exerts a resistance to flow through the bed. As the top layer has the highest resistance, the bed is compressed and the overall resistance increases further.

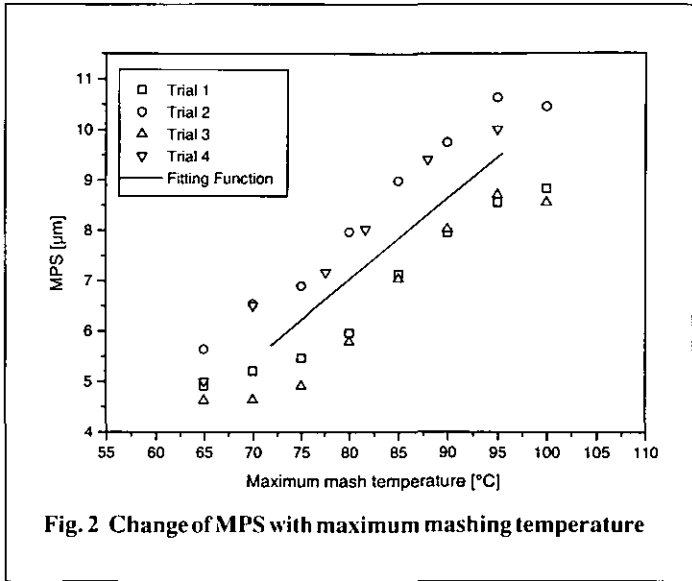


Fig. 2 Change of MPS with maximum mashing temperature

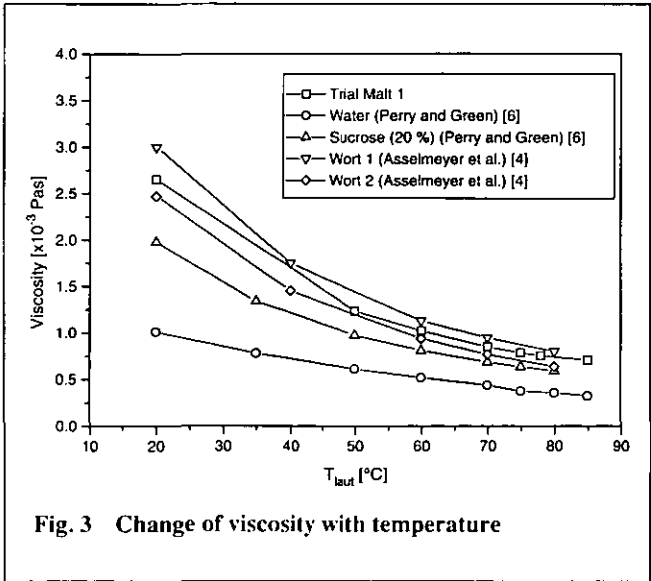


Fig. 3 Change of viscosity with temperature

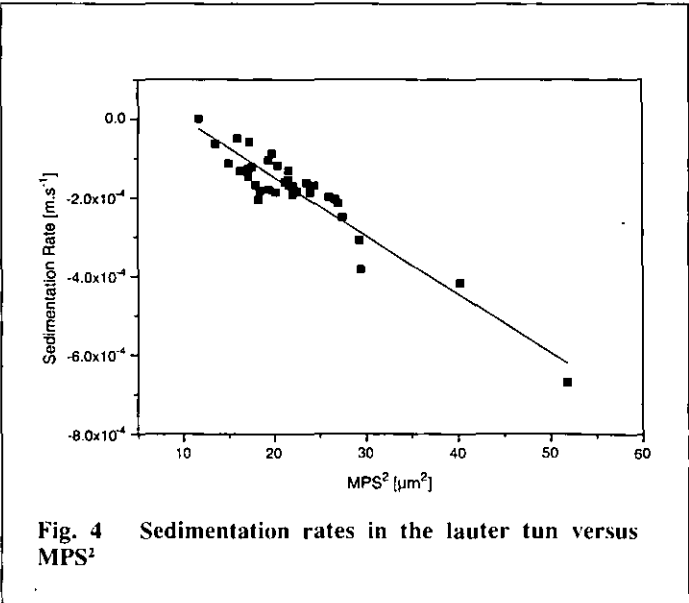


Fig. 4 Sedimentation rates in the lauter tun versus MPS²

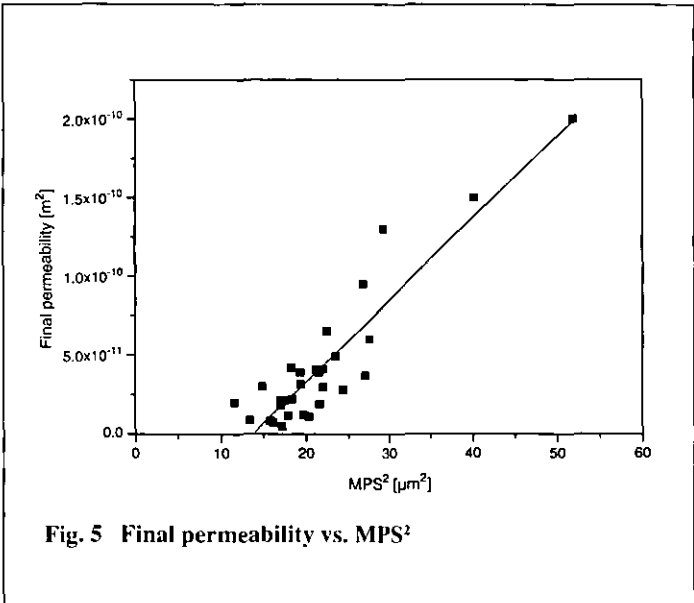


Fig. 5 Final permeability vs. MPS²

These effects influence cake height and permeability simultaneously and are combined in the model. The change of the cake height-difference (between the height at each volume of filtrate and the final height at cake washing) with volume of filtrate can be described using a first order exponential decay function. The function is shown in the following equation:

$$L = L_0 + \left\{ (L_0 - L_{min}) \times e^{\frac{-V}{V_{decay}}} \right\} \tag{10}$$

t has been described as a function of L_{min}:

$$t = 0.00247 - 0.00310 \times L_{min} - 0.00246 \times L_{min}^2 \tag{11}$$

3.6 Sparging – cake washing

Extract concentration in the lautered wort is dependent on mash concentration and the efficiency of filter cake washing. The lauter tun cake is washed by displacement washing (9): sparge liquor displaces residual wort as it flows through the pores. In displacement washing there are different modes of operation apparent (10). Initially the wort entrained in the pores is directly displaced by the sparge liquor. In the following stages extract is transferred from the pores of the cake and the malt grains into the hot water by different transfer processes.

Cake washing in lautering of hammer milled grist was described by Hermia and Rahier (9) with the so called dispersion model. For washing of spent grains with pure water, and because there are no sorption effects of the cake, the model was simplified to the following equation:

$$\frac{c}{c_0} = \frac{1}{2} \left[1 + \operatorname{erf} \left(\frac{1 - W}{2\sqrt{WL}} \right) \sqrt{\frac{uL}{D_L}} \right] \tag{12}$$

The suitability of this model has been tested using experimental data. For the comparison of these trials with the model, the total void volume of the cake was calculated to be 1.5 x 10⁻³ m³ for 9.5 x 10⁻³ m³ of mash. It can be anticipated that milling, concentration of the malt and even the malt quality influence the volume of the

solids in the cake. The void volume of the cake at sparging can be determined as:

$$V_{void} = V_{cake} - V_{particles} \tag{13}$$

The void volume of the spent grains cake can be calculated using the individual height of the cake after consolidation and the filtration area of the cake. With these figures it is now possible to determine the volumes of wash liquor used per void volume of the cake, W.

Washing of the cake starts when all supernatant wort is drawn into the cake. The total volume of wort to be filtered before washing occurs is calculated using the equation:

$$V_{wort} = V_{total} - [(H_0 - L_{min}) \times A_{filter}] \tag{14}$$

The extract content per volume of filtrate was normalised by the maximum extract content in the filtrate. Figure 8 shows the result of this fitting process. It can be seen that the axial dispersion

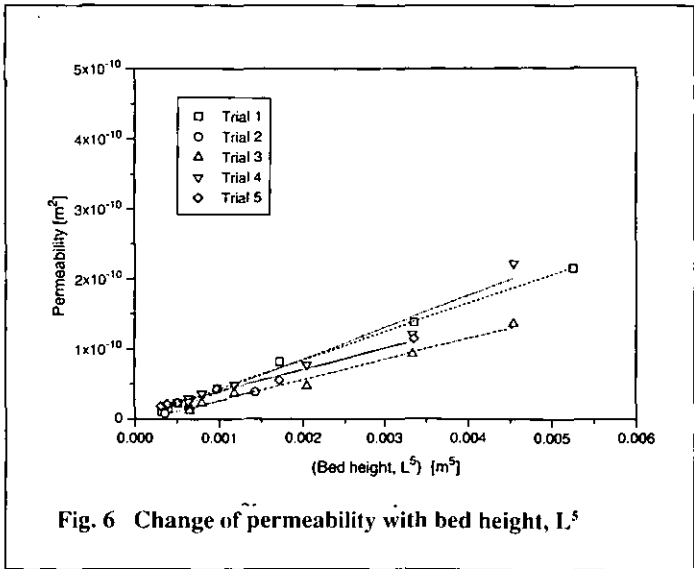


Fig. 6 Change of permeability with bed height, L⁵

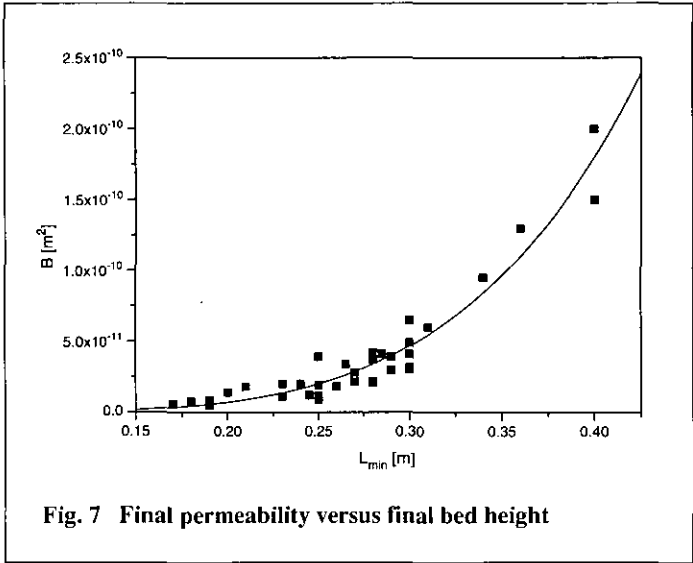


Fig. 7 Final permeability versus final bed height

model, with the assumptions mentioned above, describes the washing of the spent grains quite well.

In addition, it could be shown that extraction of the cake is also affected by the MPS of the fines (see Fig. 9).

There are two reasons for this effect:

- a bigger particle size in the fines could increase permeability of the cake. The tortuosity of channels in the bed would be increased, because less pores would be blocked. This effect reduces the axial dispersion coefficient, D_L , resulting in a better washing efficiency;
- another important effect which influences washing efficiency is the height of the consolidated bed. As described earlier, it is affected by the MPS of the fines. A higher bed level increases the last term in equation 12, with washing efficiency increasing.

These effects on extraction efficiency of the filter bed were incorporated into the mathematical model. To describe the extract

data over the filtrate volume directly, the following sigmoidal function was used.

$$E = \frac{E_{\max} - E_0}{1 + \exp \frac{V - X_c}{dX}} + E_0 \tag{15}$$

In the model dX was varied as a function of MPS to describe the change in the slope of the extract curve over volume of filtrate. The centre of the curve was set constant at $dX = 0.78 \times V_{\text{total}}$.

4 Computer model

In large scale lautering, run off rates are varied with differential pressure. This condition was also used in the experiments reported here. Because pressure and flow rate are variable, the required time to collect a pre-set volume of wort (here $V_{\text{total}} = 11$ litres) was calculated by iteration. This makes the model very flexible for upscaling to industrial equipment. The flowcharts in Figure 10 and 11) show the individual parts of the computer algorithm.

The initial calculations determine MPS and viscosity at lautering temperature. The next step of the programme calculates the height of the filter cake after sedimentation, before filtration starts. The initial height of the cake is affected by the sedimentation rate and reflects the size of the particles. Higher initial levels are related to smaller particle sizes. As smaller particles have lower permeability this also affects run off.

In the following calculation the final height of the bed after washing is determined. It was found in the experiments that the final height of the cake for the trials depends only on the change of the permeability of the cake. The permeability of the cake is dominated by the permeability of the fines. The most influential factor was MPS.

The main part of the algorithm is shown in Figure 11. This part calculates the main parameters for the course of the filtration and washing process. As both flow-rate and differential pressure are variable, the process was calculated by iteration. The relationships shown above were used in this algorithm.

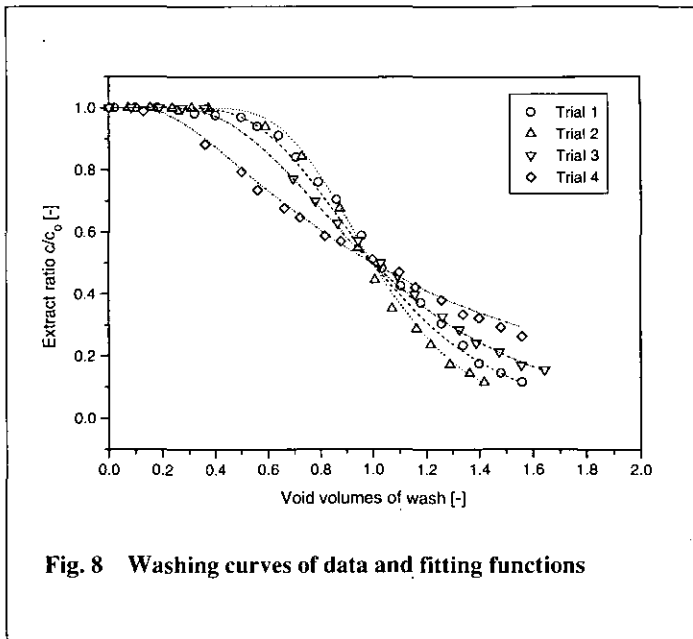


Fig. 8 Washing curves of data and fitting functions

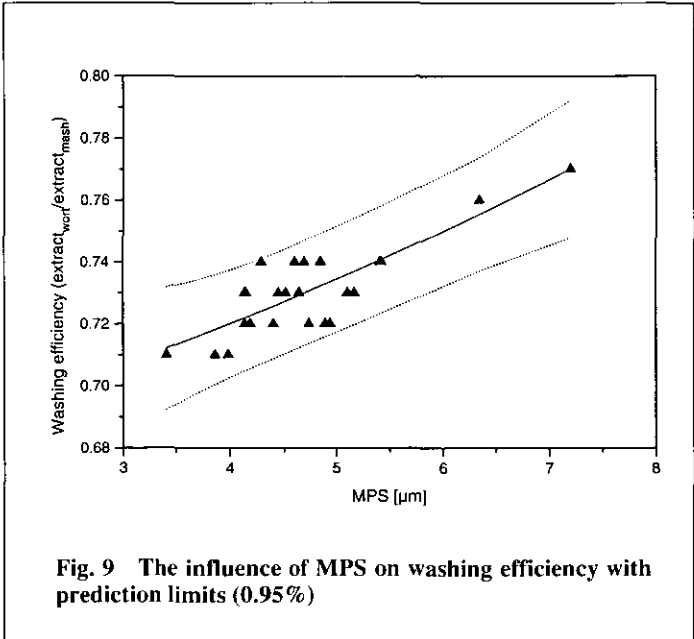


Fig. 9 The influence of MPS on washing efficiency with prediction limits (0.95%)

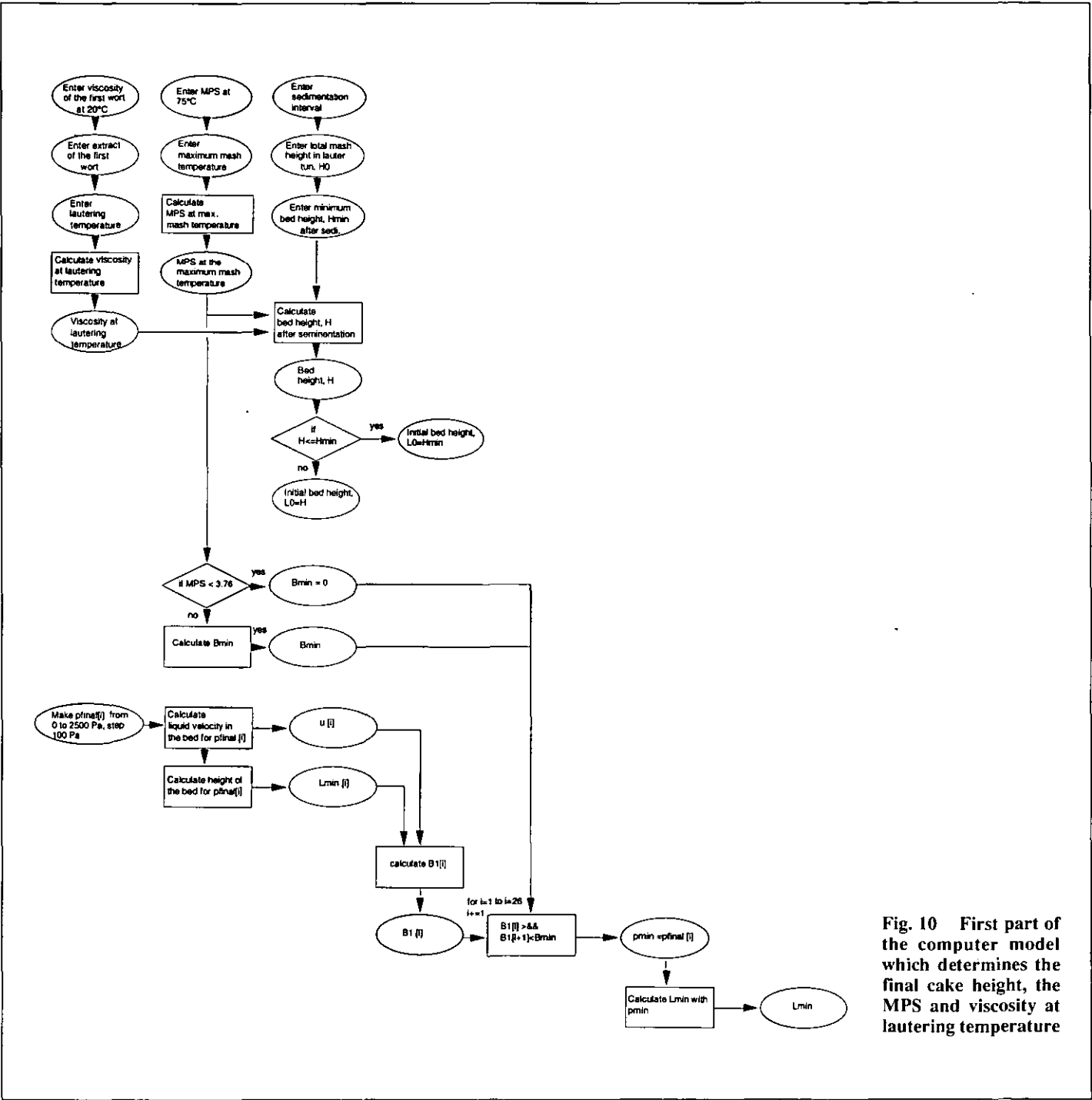


Fig. 10 First part of the computer model which determines the final cake height, the MPS and viscosity at lautering temperature

5 Prediction with the model

The model has been checked with existing data from the trials and with additional lautering data. In this article two comparisons of real and calculated data are presented (Figures 12 and 13). It can be seen that the model can predict the lautering process.

The lautering time observed in the trials was compared with data calculated from the model by varying MPS. Viscosity was set as constant. Figure 14 shows that the lautering time predicted from the model lies in the same range as the measured data.

The slope of the fitted curves with MPS are very similar. The relatively large variation in lautering time is mainly due to variations in viscosity.

Zusammenfassung

Bühler, T. M., McKechnie, M. T., und Wakemann, R. J.: Ein Modell zur Beschreibung des Abläuterprozesses – Monatsschrift für Brauwissenschaft 49, Nr. 7/8, 226 – 233, 1996

BC 202 Viskosität/ 222 Maischintensität/ 223 Läuterarbeit/ 223 Würzeablauf/ 30 Simulationen, Modelle

Dieser Artikel beschreibt ein Modellsystem für die Abläuterung im Läuterbottich. Es konnte gezeigt werden, daß Viskosität und Partikelgrößenverteilung in der Feinfraktion die beiden entscheidenden Parameter sind, wenn andere Bedingungen wie z.B. die Ausgangsmaterialien konstant gehalten werden. Die mittlere Partikelgröße und die Viskosität können durch Maischtemperatur oder durch das Rühren der Maische

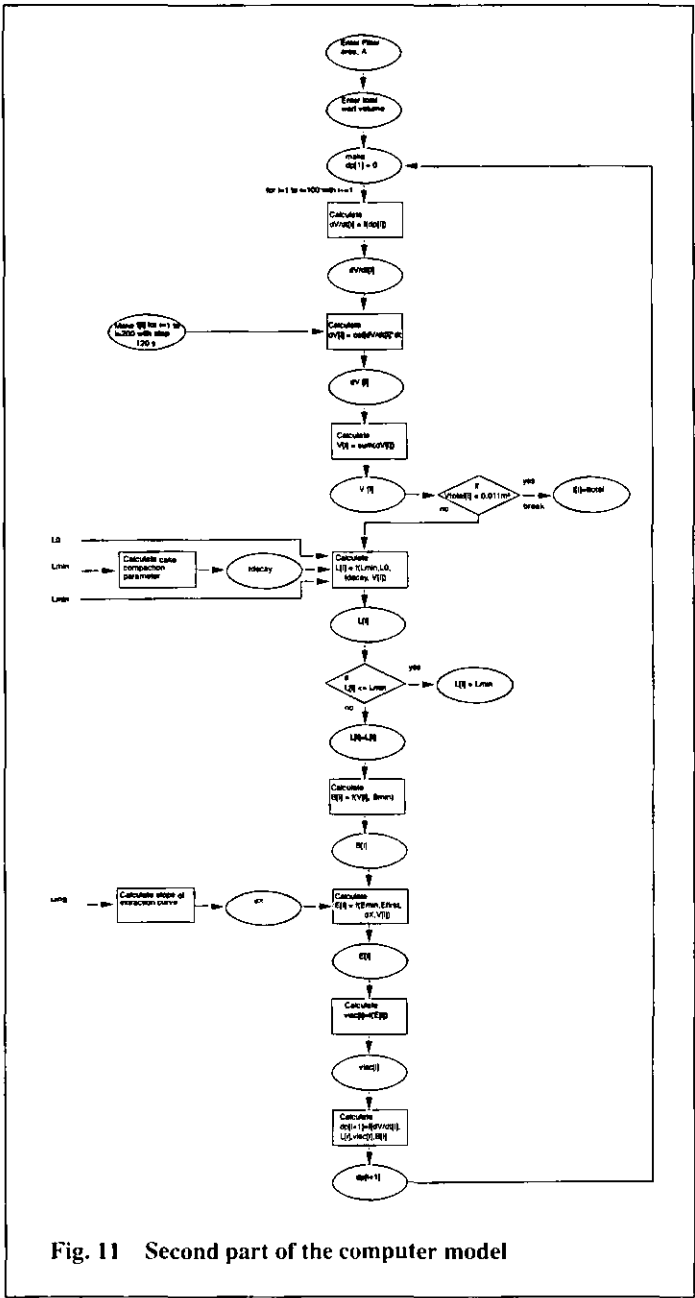


Fig. 11 Second part of the computer model

beeinflusst werden. Hier werden die Hintergründe beschrieben, wie die beiden Parameter die Sedimentation, den Durchsatz des Läuterbottichs und die Auswaschung des Filterkuchens beeinflussen. Es wurde ein Computerprogramm erstellt, mit dem eine Vorhersage der Hauptprozessparameter beim Abläutern ermöglicht wird. Beim Vergleich des Modells mit den experimentellen Daten wurde eine hohe Genauigkeit festgestellt.

Bühler, T. M., McKechnie, M. T., et Wakeman, R. J.: Un modèle de description du procédé de filtration de la maïs — Monatsschrift für Brauwissenschaft No 7/8, 226 – 233, 1996

BC 202 Viscosité/ 222 Intensité de brassage/ 223 Travail de la filtration de la maïs/ 225 Ecoulement du moût/ 30 Simulations, modèles

Cet article décrit une modélisation pour la filtration de la maïs en cuve filtre. Il a été démontré que la viscosité et la répartition de la taille des particules dans la fraction fine étaient les deux paramètres dominants, à condition de maintenir constants les matériaux de départ, par exemple. La taille moyenne des particules et la viscosité peuvent être influencées par l'agitation de la maïs ou sa température. On décrit les causes des deux paramètres qui influencent la sédimentation, le débit de la cuve filtre et le lavage du gâteau filtrant. Un logiciel permettant de prédire les paramètres clé de la filtration de la maïs a été élaboré. En comparant le modèle avec les valeurs expérimentales, on a pu constater une liaison étroite.

Acknowledgement

The authors thank the Director General of BRF International for the permission to publish this paper, Prof. Charlie Bamforth for reviewing this article and the staff of BRFI for their support during the experimental phase of this work.

6 Literature

- 1. Lüers, H.: Die wissenschaftlichen Grundlagen von Brauerei und Mälzerei, Verlag H. Carl, Nürnberg, 1950.

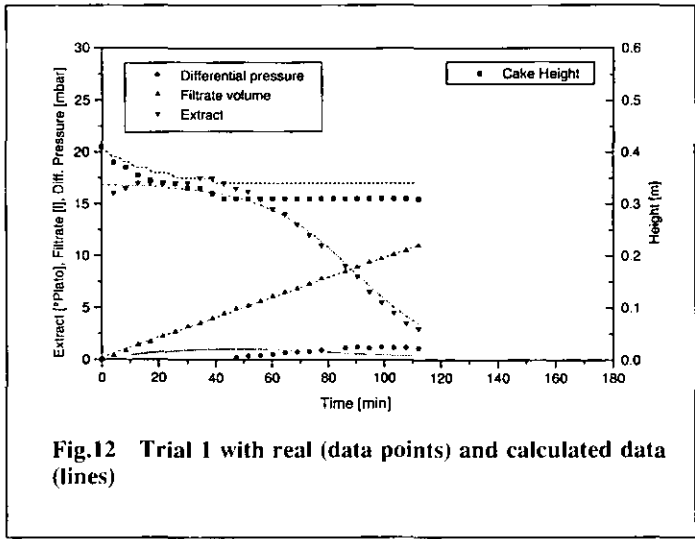


Fig.12 Trial 1 with real (data points) and calculated data (lines)

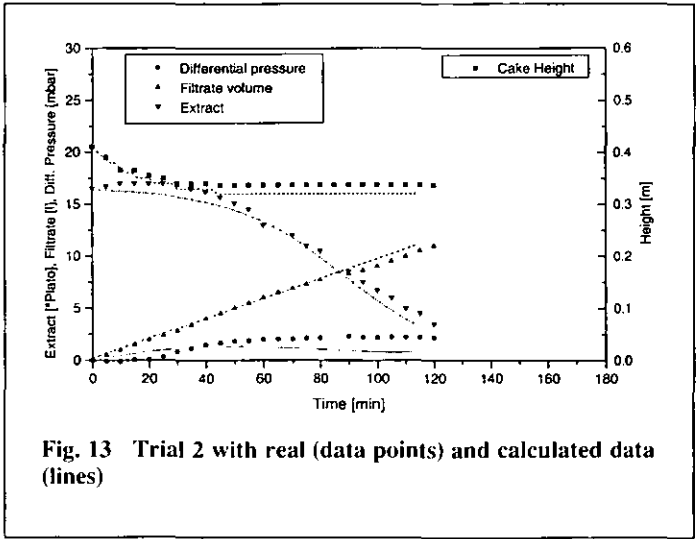


Fig. 13 Trial 2 with real (data points) and calculated data (lines)

- Narziß, L.: Die Bierbrauerei, Volume 2: Die Technologie der Würzebereitung, 6. Edition, Ferdinand Enke, Stuttgart, 1985.
- Bühler, T. M., Matzner, G., and McKechnie, M. T.: „Agitation in Mashing“, EBC Proceedings of the 25th Congress, Brussels, Oxford University Press, Oxford, 1995, 293 – 300.
- Asselmeyer, F., Höhn, K., and Issing, E.: „Die Temperaturabhängigkeit von Viskosität und Dichte bei Bieren, Ausschlag- und Vorderwürzen“, Brauwissenschaft 26, 4, 93 – 101, 1973.
- Eyben, D., and Hupe, J.: „Filterability of Wort and Beer and its Relationship with Viscosity“, EBC Symposium on the Relationship between Malt and Beer, Helsinki, Verlag H. Carl, Nürnberg, 1980, 201 – 212.
- Perry, R. H., and Green, D.: Chemical Engineers Handbook, McGraw-Hill, Singapore, 1985.
- Kolbach, P.: „Die Umrechnung von Würze und Bier auf einen bestimmten Extraktgehalt“, Monatsschrift für Brauerei 13, 21 - 25, 1960.
- Carman, P. C.: „Fluid Flow Through Granular Beds“, Transactions of the Institute of Chemical Engineers, 15, 150 – 166, 1937.
- Hermia, J., and Rahier, G.: „Designing a New Wort Filter“, Filtr. and Sep. 11/12, 421, 422, 424, 1990.
- Wakeman, R. J.: „Filtration Post-Treatment Processes“, Elsevier, Amsterdam, 1975.

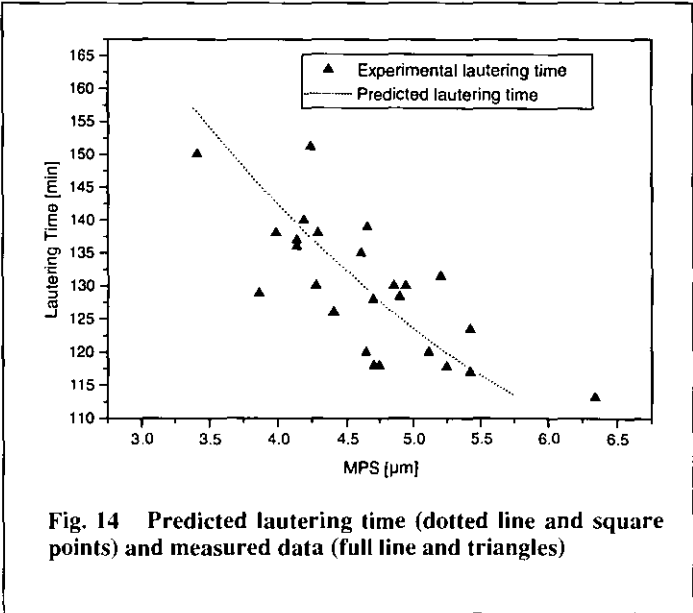


Fig. 14 Predicted lautering time (dotted line and square points) and measured data (full line and triangles)



European Brewery Convention
Manual of Good Practice

Brewery Utilities

Prepared by the EBC Technology and Engineering Forum
with the support of the European Union AIR Programme

Published by
Getränke-Fachverlag Hans Carl

IN VORBEREITUNG
MANUAL OF GOOD PRACTICE
Vol. 2: Brewery Utilities

*"Technology und Engineering Forum" of the
European Brewery Convention (Hg.)*
ca.150 Seiten, DIN A 4, 40 Abbildungen und
Diagramme. Price: DM 75,- (zuzüglich Versand-
kosten) Bestell-Nr.: 756

WEITERER TITEL:
Manual of Good Practice Vol. 1: Beer
Pasteurisation
148 Seiten., DIN A 4, zahlreiche Illustrationen
und Diagramme.
DM 75,- zuzügl. Versandkosten) Bestell-Nr.: 748

FAX-BESTELLUNG: 0911 / 9 52 85-47

.....Ex. Manual of Good Practice Vol. 2:
Brewery Utilities

.....Ex. Manual of Good Practice Vol. 1:
Beer Pasteurisation

Name	Kunden-Nr.
Firma	USt.-Id.-Nr.
Straße	PLZ/Ort
Datum	Stempel/Unterschrift



Fachbuch-
handlung
Hans Carl
Postfach 99 01 53
90268 Nürnberg
Fax (0911) 9 52 85-47

K.-J. Hutter und S. Müller

Biomonitoring der Betriebshefen in praxi mit fluoreszenzoptischen Verfahren

IV. Mitteilung: Zellzyklus und 3 β -Hydroxysterolgehalt

Zu den wesentlichen intrazellulären Parametern der *Saccharomyces*-Hefen zählen der DNS-Gehalt sowie die Gehalte an Neutrallipiden, Enzymen und membrangebundenen 3 β -Hydroxysterolen. Sie haben großen Einfluß auf die Physiologie der Betriebshefen. Ein Biomonitoring der Gärung und Reifung muß neben der Proliferations-Kontrolle auch die Funktionalität der Hefezellen einbeziehen. Die 3 β -Hydroxysterole übernehmen zwei Schlüsselfunktionen während des Wachstums und der Vermehrung der Hefe. Die „sparking function“ wird als das auslösende Moment für die Proliferation (Zellzyklus-initiierung) der Hefezellen angesehen. Die „bulk membrane function“ nimmt Einfluß auf die Permeabilität, Fluidität und Stabilität der Hefemembran. Das Zusammenspiel zwischen Umweltbedingungen und Signalübertragung durch die Hefezelle, ob die vorgegebenen Bedingungen ausreichen, einen Zellzyklus zu beginnen bzw. das Wachstum und die Vermehrung vorübergehend einzustellen, sind für den Ablauf der Gärung von großer Bedeutung. Mit fluoreszenzoptischen Analysen können die Zellzyklusphasen und die verschiedenen Zellzustände in einer Population während des Wachstums statistisch signifikant bestimmt werden.

BC 033 Fluoreszenzanalyse/ 41 Gärfähigkeit/ 41 Gärleistung/
43 Lebensfähigkeitsbestimmung

(Deskriptoren EBC: Hefe, Gärfähigkeit, Hefeanalyse (Methode zur), Gärkraft (Methode zur Bestimmung der).

Descriptors EBC: Yeast, yeast fermentative ability, yeast cell analysis, fermentability (method for determination of)).

1 Einleitung

Für das Monitoring biotechnischer Prozesse werden Methoden, wie etwa die Fluoreszenzmikroskopie mit ihren Weiterentwicklungen, z.B. der automatisierten Bildanalyse und der Laser Scanning Mikroskopie und darüber hinaus der Flußzytometrie, zur Charakterisierung des physiologischen Zustandes mikrobieller Populationen zunehmend unverzichtbar. Dies ist besonders im Hinblick auf die Gäraktivität und Gärgeschwindigkeit der Betriebshefen von Bedeutung, da es bisher keine zufriedenstellende Möglichkeit gibt, um die geschlossene, zylindrokonische Gärung beginnend mit der Propagation, der Gärung und Reifung und der Hefelagerung verfahrenstechnisch zu kontrollieren.

Von den Heferasen und Hefestämmen, die in biotechnologischen Prozessen verwendet werden, wird fast immer angenommen, daß die eingesäten Zellen sich alle im gleichen Zustand (Wachstums- und morphologischem Zustand) befinden. Daraus schließt man, daß diese Zellen auch die gleiche Leistung erbringen.

Während der Gärung wachsen und vermehren sich die Betriebshefen jedoch nicht unter synchronisierten Bedingungen, vielmehr führt jede Hefezelle ihren individuellen Zellzyklus durch. Dieses individuelle Wachstum, das jeweils mit der Geburt einer Tochterzelle (Sproßzelle) abgeschlossen wird, unterliegt einer variablen Abhängigkeit, die geprägt ist von den Nährstoffbedingungen, metabolischen Aktivitäten der Zellen, den Umweltbelastungen (z.B. Äthanolzunahme), den Temperaturbedingungen oder intrazellulären Zustandsformen der Makromoleküle (wie DNS-, RNS- und Proteingehalte, Enzyme, Reservestoffe, Hormone etc.) der Hefen (3, 4).

Das Zusammenspiel zwischen Umweltbedingungen und Signalübertragung durch die Hefezelle, ob die vorgegebenen Konditionen ausreichen, einen Zellzyklus zu initiieren, sind für einen Ablauf der Gärung von eminenter Bedeutung und können mit fluoreszenzoptischen Kontrollen erkannt werden. Die Fluoreszenzmikroskopie und die Flußzytometrie sind geeignet, verschiedene Zellzustände in der Population statistisch signifikant nachzuweisen (4, 12, 14).

Die Mischungsverhältnisse im ZGK sind oft sehr heterogen. Dies liegt einmal darin, daß Fehler beim Drauffassen des Zeugs gemacht werden, zum anderen keine Möglichkeit besteht, ohne größere Schaumbildung zu rühren. Somit können sich Subpopulationen bilden, die wiederum eigenen, zellkinetischen Abläufen unterliegen (1, 11).

Auf der Suche geeigneter Parameter für ein Biomonitoring der Betriebshefe wird in diesem Beitrag der flußzytometrische Nachweis der 3 β -Hydroxysterole beschrieben, die durch ihre Doppelfunktion in der Hefezelle zunächst eine „sparking function“ besitzen. Diese wird als auslösendes Moment für die Proliferation der Hefezellen angesehen. Zum zweiten haben die Sterole mit der „bulk membrane function“ einen Einfluß auf die Permeabilität, Fluidität und Stabilität der Hefemembranen. Zu den 3 β -Hydroxysterolen zählt das Ergosterol, welches unter den etwa 20 bekannten Sterolen der Hefe eine Schlüsselposition einnimmt.

TEMPERATURE INDUCED PARTICLE AGGREGATION IN MASHING AND ITS EFFECT ON FILTRATION PERFORMANCE

T. M. BÜHLER, M. T. McKECHNIE and R. J. WAKEMAN (FELLOW)*

BRF International, Redhill, Surrey.

**Department of Chemical Engineering, Loughborough University, UK*

This paper reports on changes in particle size distribution in a mash which occur with increasing temperature, and their effects on filtration. In large scale deep bed filtration, the mash slurry sediments in two phases. The fine particle fraction, in the range from sub micron to approximately 150 μm , forms a top layer which determines filtration performance. By measuring particle size distribution in this fine particle fraction of mash, it was possible to show that particles aggregate with increasing temperature and that this parameter is dominant in influencing filtration performance.

Keywords: brewing; brewhouse; mashing; temperature; lautering; filtration; particle sizing; viscosity

INTRODUCTION

In beer brewing, the mashing process is one of the initial operations in the brewhouse and has to solubilize the contents of malt in water. To enhance extraction, malt is crushed using a roller mill and mixed with hot water in a mash vessel. This slurry of malt and water is called the mash. During the solubilization process, a variety of different enzymes from the malt are active and the activity of each can be controlled by adjusting the temperature in the mash. Starch, the main constituent of malt, gelatinizes at mashing temperatures and is broken down by enzymes into mono-, di-, tri- and oligo-saccharides. α -amylase and β -amylase are the main enzymes involved in this conversion. Malt- α -amylase has the highest inactivation temperature of all starch degrading enzymes in the mash; it is active up to temperatures of 78°C and at 80°C a rapid decline in activity occurs¹.

In practice, temperatures close to the upper activity limit are employed, because mash filtration performance is found to improve with higher temperatures². Operations with temperatures above the limit have been proposed, but have not found widespread application. The only explanation for the improved filterability (defined as a shorter run time) given in the literature is the reduction of viscosity with increasing temperature^{3,4}. This article reports on the changes in particle size distribution in the fine particle fraction in mash that occur with increasing temperature and which are shown to be dominant in determining filtration performance.

MATERIALS AND METHODS

Mashing

A mash was prepared from different malts in pilot scale mash vessels (15–50ℓ), at water-to-ground-malt

ratios of 3.5 to 1 by mass, using a single incubation temperature of 65°C over a time period of 45 minutes. After this time, the entire mash was heated to 100°C. The heating rates for the entire mashes were 0.3 (Trial 1 and 2) and 1.0°C.min⁻¹ (Trial 3). During this heating, mash was sampled at 5°C intervals. Thus, individual samples were obtained at temperatures of 65, 70, 75, 80, 85, 90, 95 and 100°C. These samples were then analysed and the parameter investigated was described as, 'maximum mash temperature', referring to the maximum temperature of each individual sample.

Two different malt qualities were examined: Trials 1 and 3 employed highly modified malt in which most cell wall material (consisting of carbohydrates such as β -glucan, pentosan and dextrans) was broken down during the malting process of barley into oligosaccharides. Trial 2 used undermodified malt which still contained large amounts of undegraded, branched carbohydrates from cell walls—this malt had a much shorter germination period during malting compared with the well modified malt sample. These substrates are not broken down entirely during mashing at temperatures above 65°C, as suitable de-branching enzymes are not available. Table 1 shows that the milling of the undermodified malt creates coarser particles and that this malt has a higher viscosity after extraction in the laboratory. This reflects the presence of high molecular weight cell wall material.

Sample Analysis

The mash samples were analysed for all parameters affecting filtration performance. The following analyses were carried out:

- particle sizing was carried out by diffraction laser light scattering with a Coulter LS130 (Coulter Electronics). The sample was wet classified through a 106 μm sieve

Table 1. Comparison of key parameters of the two malt samples.

	Highly modified malt	Undermodified malt
Mean size after milling (0.75 mm gap setting, sieve analysis)	1151 μm	1344 μm
Viscosity (Laboratory standard analysis)	1.50 mPas	2.00 mPas

before analysis, in order to enhance the resolution in the small particle range of the mash. This was necessary because the overall particle range is very wide (up to 4000 μm) (see Table 1);

- particle concentrations in the sub-106 μm -sieve fraction were determined gravimetrically on a dry weight basis;
- density of the liquid phase of the mash (called wort) was determined using an automated U-tube densitometer;
- viscosity of the liquid phase of the mash was measured using an automated capillary suction viscometer;
- filtration tests were carried out at constant pressure in a 200 ml filter cell, driven by an air pressure of 10^4 Pa. Filtration temperature was 65°C. The filtrate flow was measured over a time of 10 minutes using a digital balance with printer. A Whatman GF/D filter disk was used as the filter medium.

Processing of Analysis Data

Cake filtration in the Millipore filter cell can be described using the basic filtration equation⁵:

$$\frac{1}{A} \frac{dV}{dt} = \frac{A \Delta p}{\eta(\alpha c V + AR_m)} \quad (1)$$

(AR_m) has been determined in pre-trials to be much smaller than ($\alpha c V$), hence the filter medium term is neglected. Thus, equation (1) can be simplified to:

$$\frac{dV}{dt} = \frac{A^2 \Delta p}{\eta \alpha c V} = \frac{1}{K} \frac{1}{V} \quad (2)$$

The filterability $1/K$ was determined from the slope of dt/dV versus V plots. If data deviated from the cake filtration law with time during filtration, only data in the linear range was fitted. If zero flowrate occurred during the filtration cycle, the maximum volume of filtrate achieved, before blockage occurred, was reported.

EXPERIMENTAL RESULTS AND DISCUSSION

Small particles in the mash (fines) which consist of large amounts of protein are known to affect the filterability of a mash considerably^{6,7}. The change of particle size distribution in the fine particle fraction (smaller than a 106 μm sieve size) with maximum mash temperature of the individual samples is shown in Figure 1 for Trial 1. It can be seen that the number distribution is shifted towards larger sizes with increasing

mash temperature, and the width of the size distribution is increased with temperature.

To describe this effect with only one number, the geometric mean particle size (*MPS*) of a number distribution has been calculated using:

$$MPS = \text{antilog} \left[\frac{\sum (n_c \times \log \bar{S}_c)}{\sum n_c} \right] \quad (3)$$

where:

\bar{S}_c = the median size of a channel (in total 100 channels are logarithmically spaced from 0.1 to 900 μm) and n_c = the percentage of particles in each channel.

Figure 2 shows the change of *MPS* with maximum temperature in the mash. It was possible to identify a significant change of the *MPS* for both malt qualities and with different heating rates. The two malt qualities show different initial sizes. However, the increase of *MPS* with temperature of the undermodified malt is similar to the well modified malt trials. This size change is caused by the aggregation of proteinaceous material in the presence of polyphenols at higher temperatures^{8,9,10}. Comparison of the results from Trials 1 and 3 suggests that the heating rate had little effect on the particle size distribution.

Concentration of Fine Particles

The analysis of particle size distributions by laser diffraction does not allow the determination of total particle concentrations, as the sample volume in the LS 130 is unknown. Therefore, particle concentrations were

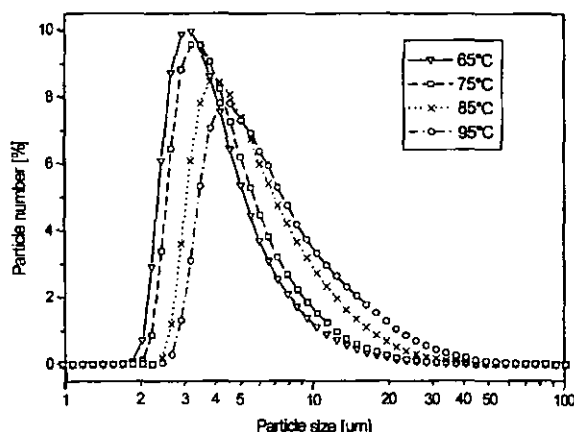


Figure 1. Effect of maximum mash temperature on particle size distribution (number) for Trial 1 (well modified malt, heating rate $0.3^\circ\text{C}.\text{min}^{-1}$) (each data point represents a size channel).

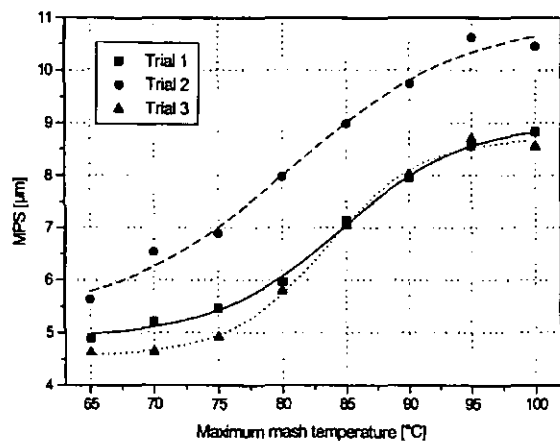


Figure 2. Change of MPS with maximum mash temperature of the sample.

determined separately as dry solids. This analysis indicated that the solids percentage does not change with increasing mash temperature (the concentration was $0.35 \text{ g dry solid } \ell^{-1}$ of mash for all trials). This suggests that no additional fine particles are created during the heating step from 65°C to the maximum temperature and that the change of the MPS with time is a true shift in the distribution, and not caused by the formation of new, larger particles from solution. The total concentration of mash solids (relative to the filtrate volume), including those above $106 \mu\text{m}$, was also constant over the temperature increase and did not vary between the trials. It was determined to be $132 \text{ kg wet solids } \text{m}^{-3}$.

Viscosity and Density of Mash

The viscosity of the liquid phase of mash has been measured for all samples at 65°C which was the same temperature used for the filterability trials. Figure 3 shows that for the highly modified malt (Trials 1 and 3), the viscosity does not change to a great extent. The different levels of Trials 1 and 3 are caused by different densities in the aqueous phase (see density analysis).

The viscosity of Trial 2, using undermodified malt, shows a strong increase with mashing temperature. As the density values are only slightly increasing (see Figure 4), it can be concluded that the drastic increase is due to

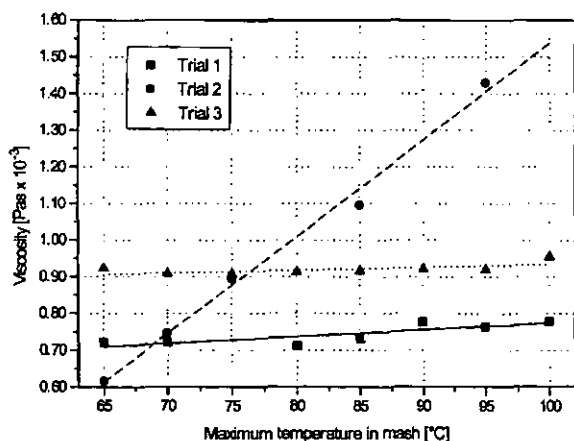


Figure 3. Change of viscosity in the liquid phase of mash, measured at 65°C , with maximum temperature.

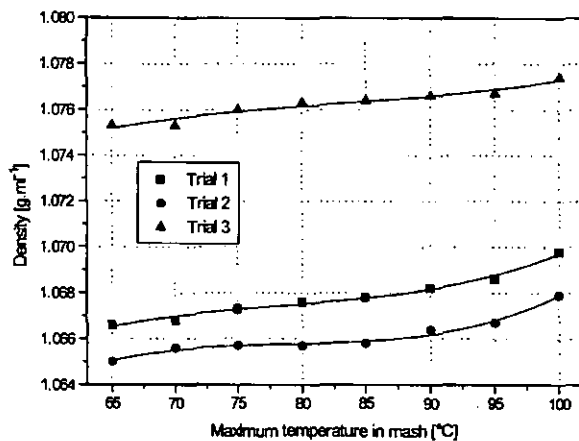


Figure 4. Density of mash liquid phase at 20°C with maximum temperature.

solubilization of higher molecular weight branched carbohydrates. These substances are leached out of the solids, and their concentration and chemical structure increases the suspension viscosity. As no enzymes are present to break these substances down, viscosity increases as these higher molecular weight carbohydrates are leached.

The density in the liquid phase of the mash samples was measured at 20°C (see Figure 4). Trials 1 and 3 were mashed at different ground malt/water ratios and the different amounts of soluble material caused the variation in the density levels. The undermodified malt in Trial 2 and the well modified malt release similar amounts of soluble material into the aqueous phase and the density increase with higher mashing temperature is similar for all trials. However, the properties of the materials released and their effect on viscosity are considerably different.

Filterability of Mash

Filterability was determined at 65°C . This temperature was chosen to avoid additional effects on particle aggregation by higher temperatures and 'cold trub' formation ('cold trub' are fine proteinaceous particles below $10 \mu\text{m}$ in diameter which precipitate at temperatures below 60°C).

Filterability $1/K$ was determined for each sample from the linear range of dt/dV vs V plots at the individual maximum mash temperatures. If filtration curves deviated from cake filtration laws in the later stages, the maximum volume filtered under conditions of cake filtration was noted for the data point.

The variation of filterability with temperature is displayed in Figure 5. It can be seen that filterability increases dramatically with the maximum temperature in the mash sample. The differences in malt quality are also visible: Trial 2 exhibits the lowest filterability level and the peak filterability is reached at a lower temperature. This can be explained by the higher wort viscosity for this malt, arising from the increasing carbohydrate leaching, which counteracts any improvement in filterability that might have otherwise been obtained with higher temperatures. Trials 1 and 3 show a very similar shape of curve: the curves are displaced relative to one another

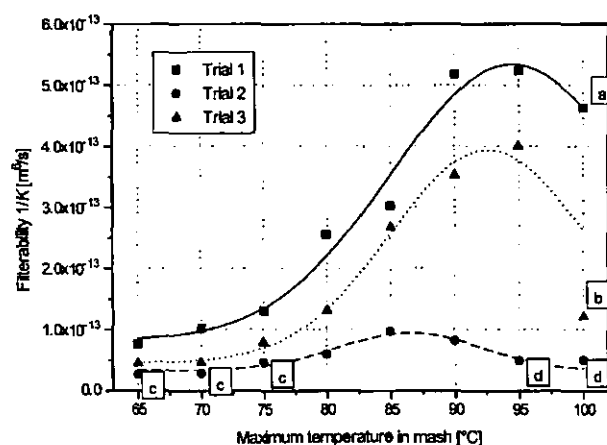


Figure 5. Filterability for different mashing temperatures (indices on data points indicate maximum volume filtered, per unit area, before filtration law deviated from cake filtration law: (a) $< 0.017 \text{ m}^3 \text{ m}^{-2}$, (b) $< 0.006 \text{ m}^3 \text{ m}^{-2}$, (c) $< 0.005 \text{ m}^3 \text{ m}^{-2}$, d $< 0.006 \text{ m}^3 \text{ m}^{-2}$, for data points without index, no blockage was observed).

by a fairly constant amount. This is largely accounted for by the different viscosity levels between Trials 1 and 3.

Specific Resistance of the Cake

To show that filtration properties of the cake change with increasing temperature, it is useful to investigate the variation of specific resistance of the cake with this parameter (see Figure 6). Trials 1 and 3 show no difference in specific resistance. The different incubation times up to the maximum temperatures (caused by the different heating rates) have no major effect on the specific resistance of the cake. The strong change in specific resistance with the maximum mashing temperature accounts for the changes in filterability: it is the predominant parameter which determines mash filtration performance.

Correlation Between Specific Resistance and Mean Particle Size

The specific resistance to filtration is mainly dependent on the square of the particle specific surface and the

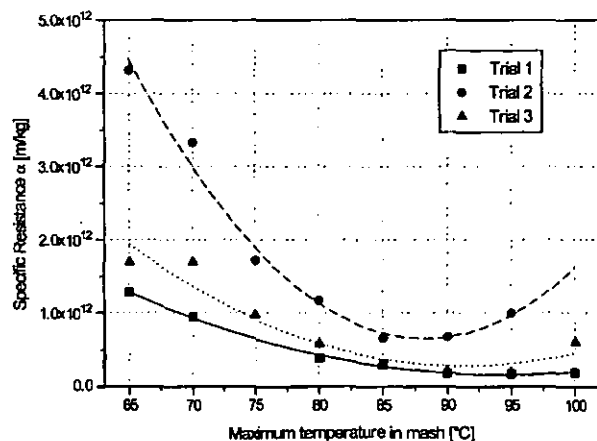


Figure 6. Specific resistance of the cake with maximum temperature in the mash.

packing density (β) function of the particles in the cake¹¹. Specific surface is indirectly proportional to the square of the mean particle size, and hence:

$$\alpha \propto \frac{f(\beta)}{MPS^2} \quad (4)$$

The change of the specific resistance of the cake can be plotted against the shift of the particle size distribution observed in this investigation. In such a plot of specific resistance vs MPS^{-2} , see Figure 7, it can be seen that the decrease in specific resistance is related almost linearly, with high significance ($R = 0.91$ to 0.95), to the change in MPS^{-2} .

The packing density function $f(\beta)$ also varies with the mashing temperature; this is shown in Figure 8 by plotting (αMPS^2) vs maximum mash temperature. The change of $f(\beta)$ with temperature suggests that there is a corresponding change in cake porosity as temperature is increased. However, this change is smaller than the changes in specific resistance α . The major factor controlling cake specific resistance during filtration is therefore the mean particle size. The changes in specific resistance α , filterability $1/K$ and (αMPS^2) are listed in Table 2.

It shows that:

- (i) α is a better filter scale-up parameter than $1/K$ since changes in α with process conditions are smaller,

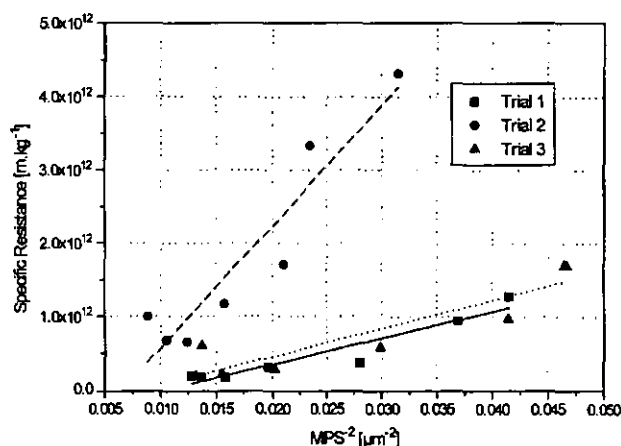


Figure 7. Correlation between specific resistance and MPS^{-2} .

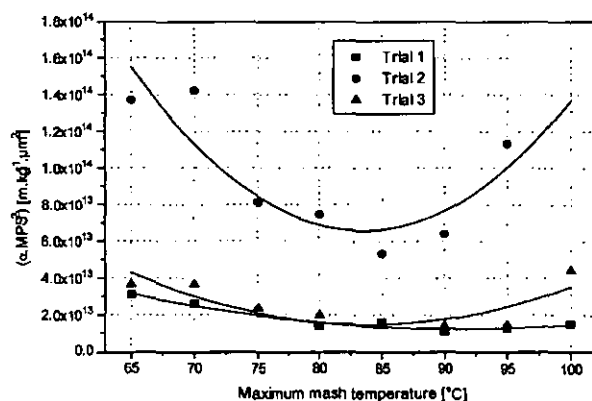


Figure 8. Plot of (αMPS^2) against maximum mash temperature.

Table 2. Maximum changes over the temperature range investigated.

	factor for filterability, $1/K$ - change	factor for resistance, α - change	factor for $(\alpha \cdot MPS^2)$ change
Trial 1	6.2	6.9	2.52
Trial 2	2.8	6.8	2.36
Trial 3	9.8	7.9	2.92

(ii) ($\alpha \cdot MPS^2$) is almost independent of the malt type,
 (iii) changes of $f(\beta)$ with temperature and malt type are smaller than changes in resistance and, hence, the particle packing density is little affected by these parameters.

CONCLUSION

This work shows that previous assumptions about the improvement of mash filterability with mash temperature have not taken the importance of the change of particle size distributions into account. In the brewing literature^{4,12,13}, the viscosity reduction due to temperature increase is given as the only explanation for improved lautering performance. In contrast with any viscosity changes with temperature, particle size changes due to the described temperature effect are permanent, which will have further implications on brewing technology.

The particle size distribution of the fines has been identified as the predominant parameter affecting mash filtration performance. It can now be used to predict specific resistance of the filter cake and anticipate the filtration performance of the mash.

NOMENCLATURE

dV	differential volume, m^3
dt	differential time, s
V	volume, m^3
A	area, m^2
Δp	pressure difference, Pa
c	concentration of solids, per unit volume of filtrate, $kg\ m^{-3}$
η	viscosity, $\times 10^{-3}$ Pas
V	volume of filtrate, m^3
R_m	resistance of the filter medium, m^{-1}
$1/K$	filterability, $m^6\ s^{-1}$

α	specific resistance, $kg\ m^{-1}$
β	packing density, —
\bar{S}_c	median size of a channel, μm
n_c	percentage of particles in each channel, %

REFERENCES

1. Moll, M. and de Blauwe, J.J. 1994, *Beers and Coolers*, (Intersept, Andover).
2. Briggs, D. E., Hough, J. S., Stevens, R. and Young, T. W., 1986, *Malting and Brewing Science, Vol 1, Malt and Sweet Wort* (Chapman & Hall, New York).
3. Schaus, O. O., 1972, Elevated temperature lautering, *Master Brew Assoc of the Americas, Tech Quart*, 9, (4): 192–194.
4. Lüers, H., 1950, *Die wissenschaftlichen Grundlagen von Mälzerei und Brauerei* (Hans Carl, Nürnberg).
5. Ruth, B. F., 1946, Correlating filtration theory with practice, *Ind Eng Chem*, 38: 564.
6. Muts, G. C. J. and Pesman, L., 1986, The influence of raw materials and brewing process on lautertun filtration, *EBC Monograph XI, Maffler*, 25–35 (Hans Carl, Nürnberg).
7. Webster, R. D. J. and Portno, A. D., 1981, Analytical prediction of lautering performance, *Proc Eur Brew Conv, Copenhagen*, 153–160 (Hans Carl, Nürnberg).
8. Lewis, M. J. and Nelson-Wahnon, N., 1984, Precipitation of protein during mashing: evaluation of the role of calcium, phosphate, and mash pH, *Am Soc Brew Chem*, 42 (4): 159–163.
9. Lewis, M. J. and Oh, S. S., 1985, Influence of precipitation of malt proteins in lautering, *Master Brew Assoc of the Americas, Tech Quart*, 22 (3): 108–111.
10. Lewis, M. J. and Serbia, J. W., 1984, Aggregation of protein and precipitation by polyphenol in mashing, *Am Soc Brew Chem*, 42 (1): 40–43.
11. Coulson, J. M., Richardson, J. F., Backhurst, J. R. and Harker, J. H., 1978, *Chemical Engineering Volume 2*, (Pergamon, London).
12. Narziß, L., 1985, *Die Bierbrauerei, Volume 2: Die Technologie der Würzebereitung*, 6th edition (Ferdinand Enke, Stuttgart).
13. Schaus, O. O., 1972, Elevated temperature lautering, *MBAA Tech Quart*, 9 (4): 192–194.

ACKNOWLEDGEMENT

The authors acknowledge the Director of BRF International for permission to publish this paper.

ADDRESS

Correspondence concerning this paper should be addressed to Mr T. Bühler, Bergfriedstrasse 8, D-91207 Lauf, Germany.

The manuscript was received 29 December 1995 and accepted for publication after revision 19 August 1996.

